Taxonomy and phylogenetics of the genus Ulonemia Drake and Poor, 1937 (Heteroptera: Tingidae), with an emphasis on the population genetics of a pestiferous species

Author:
Shofner, Ryan

Publication Date:
2018

DOI:
https://doi.org/10.26190/unsworks/21243

TAXONOMY AND PHYLOGENETICS OF THE GENUS *ULONEMIA* DRAKE AND POOR, 1937 (HETEROPTERA: TINGIDAE), WITH AN EMPHASIS ON THE POPULATION GENETICS OF A PESTIFEROUS SPECIES

Ryan M. Shofner

A thesis in fulfilment of the requirements for the degree of

Doctor of Philosophy

School of Biological, Earth and Environmental Sciences

Faculty of Science

August 2018

Thesis/Dissertation Sheet

Surname/Family Name	:	**Shofner**
Given Name/s	:	**Ryan Michael**
Abbreviation for degree as give in the University calendar	:	**PhD**
Faculty	:	**Science**
School	:	**Biological, Earth, and Environmental Sciences**
Thesis Title	:	**Taxonomy and phylogenetics of the genus *Ulonemia* Drake and Poor, 1937 (Heteroptera: Tingidae), with an emphasis on the population genetics of a pestiferous species**

Abstract 350 words maximum: (PLEASE TYPE)

Agricultural systems are increasingly faced with the emergence of novel pests. Within the last decade, the macadamia lace bug, *Ulonemia decoris* Drake, 1942, became established in macadamia orchards in northern New South Wales and southern Queensland. This study provides the first comprehensive overview of the genus and its status in Australia. This study had three broad goals: 1) to describe the relationship between *Ulonemia* and other tingids in Australia using genetics; 2) to redefine the genus *Ulonemia* using the results from part 1; 3) to examine the population genomics of *U. decoris* to determine the dispersal rate of individuals between populations. Analysis of four genes (two mitochondrial and two nuclear) by Maximum Likelihood and Bayesian estimation returned a paraphyletic *Ulonemia* with three strongly supported clades; a combined morphological and molecular analysis with parsimony failed to resolve any relationships. Two new genera and five new species, *Cercotingis* (*C. croajingolong* sp. nov., *C. namadgi* sp. nov., *C. tasmaniensis* sp. nov.) and *Proteatingis* (*P. astibosetes* sp. nov., *P. howardi* sp. nov.), are described to account for the observed molecular phylogenies. One species of *Tingis* and *U. decoris* were transferred into *Cercotingis*, and three species of *Ulonemia* were transferred to *Proteatingis*. The capability of lace bugs to disperse between orchards is critical in developing better control methods, because determining dispersal ability can provide valuable information on the geographic extent over which control must be coordinated. Single-nucleotide polymorphism (SNP) data were obtained for *C. decoris* for 204 individuals over 7 localities in northern NSW. Each sample locality had an excess of homozygous individuals and there was minimal genetic differentiation over geographic distance. This evidence points to selection against heterozygotes, recent extensive mixing, non-random mating, parthenogenesis, or cryptic species within *C. decoris*. The high dispersal and possible rapid reproduction due to parthenogenesis would make *C. decoris* difficult to manage. There is also a need to monitor for other emergent pest species, because there are multiple lace bug lineages on the Proteaceae, with three of these lineages containing verified pests. In summary, optimal management of the species will likely require region-wide coordination.

FOR OFFICE USE ONLY Date of completion of requirements for Award:

ORIGINALITY STATEMENT

'I hereby declare that this submission is my own work and to the best of my knowledge it contains no materials previously published or written by another person, or substantial proportions of material which have been accepted for the award of any other degree or diploma at UNSW or any other educational institution, except where due acknowledgement is made in the thesis. Any contribution made to the research by others, with whom I have worked at UNSW or elsewhere, is explicitly acknowledged in the thesis. I also declare that the intellectual content of this thesis is the product of my own work, except to the extent that assistance from others in the project's design and conception or in style, presentation and linguistic expression is acknowledged.'

Signed ……..

Date ……..

INCLUSION OF PUBLICATIONS STATEMENT

UNSW is supportive of candidates publishing their research results during their candidature as detailed in the UNSW Thesis Examination Procedure.

Publications can be used in their thesis in lieu of a Chapter if:

- The student contributed greater than 50% of the content in the publication and is the "primary author", ie. the student was responsible primarily for the planning, execution and preparation of the work for publication
- The student has approval to include the publication in their thesis in lieu of a Chapter from their supervisor and Postgraduate Coordinator.
- The publication is not subject to any obligations or contractual agreements with a third party that would constrain its inclusion in the thesis

Please indicate whether this thesis contains published material or not.

☒ *This thesis contains no publications, either published or submitted for publication*

☐ *Some of the work described in this thesis has been published and it has been documented in the relevant Chapters with acknowledgement*

☐ *This thesis has publications (either published or submitted for publication) incorporated into it in lieu of a chapter and the details are presented below*

CANDIDATE'S DECLARATION

I declare that:

- I have complied with the Thesis Examination Procedure
- where I have used a publication in lieu of a Chapter, the listed publication(s) below meet(s) the requirements to be included in the thesis.

Name	Signature	Date (dd/mm/yy)

Postgraduate Coordinator's Declaration (to be filled in where publications are used in lieu of Chapters)

I declare that:

- the information below is accurate
- where listed publication(s) have been used in lieu of Chapter(s), their use complies with the Thesis Examination Procedure
- the minimum requirements for the format of the thesis have been met.

PGC's Name	PGC's Signature	Date (dd/mm/yy)

ACKNOWLEDGEMENTS

This thesis was a long journey, possible only through the endless contributions of numerous wonderful people. I was fortunate to cover vast expanses of Australia in my quest for knowledge on lace bugs, and I have lost count of how many truly helpful and inspiring people I've met along the way. They have all contributed, in a small part at least, to this thesis, and all have earned my gratitude and thanks. First and foremost, I thank my supervisors, Gerry Cassis and Bill Sherwin, without whom this project would not have happened at all. They endured countless hours of questions as well as rebuttals when I thought I knew better. Without fail, they put be back on the correct track. I thank my committee Russell Bonduriansky, Shaun Laffin, and Terry Ord for the help and guidance they provided throughout my candidature.

I thank Marina Cheng, without whom the project, and myself, would have fallen into a completely disorganised mess. From providing lab training, support, and logistics, or helping me in the field, to making sure I and everyone in the lab have plenty of homemade cookies to snack on, Marina has been invaluable to me. I also thank her parents, George and Lin, who took it upon themselves to ensure I had three square meals a day. Without them, I assuredly would have wasted away from starvation.

This project relied on funding and support from macadamia growers, pest scouts, consultants, and organisations. I thank Bob and Judy Howard for not only allowing me to gather samples on their property, but also for their amazing hospitality while I conducted field work, serving as a literal "home base" for me in the Northern Rivers. Bob's passion for knowing his enemy, the macadamia lace bugs, and his drive for developing new orchard and pest management strategies directly led to the formation of this project. I thank Ken Dorey for his invaluable assistance in locating wild macadamias,

his insight into the macadamia industry, and for allowing me access to his orchard to collect samples. I thank Peter and Karen Norman for their wonderful hospitality and allowing me to tromp through their woods in pursuit of wild macadamias and their lace bug denizens. I thank Gavin Arthur, Peter Fraser, Will Kent, Colin Rijks, Peter Schoultz, Greg Woods, and Pam Woods for allowing me access to their properties and collecting samples. I thank Tom and Marty Inderbitzin for access to their orchard and providing insights to macadamia lace bugs in the Atherton Tablelands. I thank Jarrah Cotes for his invaluable help by sharing his knowledge about lace bugs, particularly their peak times of emergence and locations where they were common. Jarrah also helped immensely by arranging access to properties, and sending me samples from all over the region. Likewise, I thank Steve McLean and Scott Hill for providing me information on lace bugs, providing specimens, and for taking me around to various orchards. I thank Terri Irwin and Australia Zoo for providing access to their extensive macadamia orchards to collect lace bug specimens, and I thank the Australia Zoo staff, especially Amanda Cole for arranging access and Stuart Gudgeon for working with me on the property. I thank Ruth Huwer and Craig Maddox from the New South Wales Department of Primary Industries for their immense body of knowledge on macadamia lace bugs, for providing samples, and for contributing to the research in this study. I thank Robbie Commens, Jolyon Burnett, and the Australian Macadamia Society for supporting this study and coordinating the flow of information between researchers, growers, and consultants. I thank Brenda Kranz at Hort Innovation for her oversight of the project and her efforts to ensure the entire research process ran smoothly. I thank Hort Innovation for funding this project through the macadamia research development levy and funds from the Australian government. I thank UNSW Sydney for providing research and tuition funding for my PhD candidature.

It cannot be overstated how important contributions and moral support provided by friends and fellow researchers have helped this project. I thank Shaun Cullerton for his help in the field, and for his help as a sounding board for ideas and questions relating to lace bugs and research in general. I thank Hannah Mathews for her excellent skills as an illustrator and bug bits disassembler, and for being our unofficial lab morale officer. I thank Celia Symonds with her extensive help on lace bugs and providing crucial knowledge on the group that formed an important foundation for this study. I thank Alex Sentinella for his expert help with scripting in R and research workflows and providing critical feedback on methods. I thank the Cassis Lab group: Cynthia Chan; Ivy Chin; Steven Chu; Michael Elias; Serena Lam; Arlee McMah; Anna Namyatova; Cristiano Schwertner; Christian Sherlock; Jayden Streatfeild; and Luciana Weiler; the Sherwin Lab group: Claire Bradenburger; Jules Byrnes; Marianne Frommer; Marie Kidd; Oliver Manlik; Gabe O'Reilly; and John Sved; as well as Lee Ann Rollins and Dan Selechnik for all of their input, feedback, and support with all aspects of the project and postgraduate life in general.

Fieldwork was critical to this research, as our collections and knowledge of lace bugs are incomplete. The species discovery program Bush Blitz, run by the Australian Biological Resources Study was invaluable in providing opportunities for field work in remote corners of Australia. I thank Jo Harding, Kate Gillespie, Mim Jambrecina, Brian Hawkins, and all the other Bush Blitz staff for all the hard work they put into organising and running their wonderful biological surveys. I thank the traditional owners of the land here in Australia, especially those that I had the wonderful privilege to work with directly through Bush Blitz: The Olkola Aboriginal Corporation, The Laura Rangers, the Tjamu Tjamu Aboriginal Corporation, and the Western Yalanji Aboriginal Corporation.

I would not have made it far without a strong academic foundation to build on. The diverse knowledge provided to me by my previous professors and mentors proved invaluable in my research, from identifying host plants, pinning insects and curating collections, to understanding the nuances of statistical analysis. For these things and more, I thank Richard Packauskas, Joseph Thomasson, Rob Channell, Greg Farley, William Stark, Jordge LaFantasie, Chris Bennett, Sam Zwenger, Mark Eberle, Elmer Finck, Curtis Schmidt, Reese Barrick, and the late John Heinrichs.

Last, but certainly not the least, I thank my family: John and Diane Shofner, Scott and Christine Plohocky, my brothers David and Wesley, and my sisters Molly and Lauren, whose love and support and acceptance of the miles between us has sustained me through this endeavour. And I thank Peter and Barbara May for taking me in as family on my arrival in Australia and providing me a starting place for my long journey here.

TABLE OF CONTENTS

LIST OF TABLES

LIST OF FIGURES

CHAPTER 1: GENERAL INTRODUCTION

Agricultural systems increasingly face the emergence of novel pests (Crowl et al. 2008). These pests are often the result of invasions by alien species that have been either transported deliberately or accidentally introduced into a new area (Pimentel et al. 2001). However, there is an increasing number of species that have become pestiferous within their native range (Webber and Scott 2012). In Australia, there are several native taxa within the hemipteran sub-order Heteroptera that have become pests of various crops. Heteroptera feed by piercing plant tissues with their mouthparts and sucking sap from the phloem or ingesting the contents of sub-epidermal cells (Stonedahl, Dolling, and duHeaume 1992); these interactions can be damaging to the plant host through mechanical damage from feeding and/or the spread of plant pathogens (Smith 1926, Storey 1939, Pollard 1973, Kabrick and Backus 1990, Nault 1997). With sufficient numbers, heteropterans that feed on commercial crop species can cause significant economic losses if not controlled.

One heteropteran group of economic importance is the family Tingidae; over 35 species have been recorded as pests of agricultural or horticultural systems (Stonedahl, Dolling, and duHeaume 1992). The Tingidae is a family of cimicomorphan bugs that comprise 260 genera and 2,124 species worldwide, with 56 genera and 147 species within Australia (Henry 2009); subsequent authors (Moir 2009, Guilbert and Moir 2010, Cassis and Symonds 2011, Moir and Lis 2012, Moir and Guilbert 2012, Symonds and Cassis 2013, Symonds and Cassis 2014, Cassis et al. 2017, Cassis, Symonds, and Branson, *in press*) have expanded the total for Australia to 58 genera and 214 species. The majority of supraspecific and specific taxa were described by the American heteropterist Carl Drake, who described >50% of all known Australian taxa.

Tingids are generally phytophagous; and many have high fidelity to their host taxa, with species generally restricted to closely-related host taxa, or even a single host species, while a smaller number of species are polyphagous and occur across a broader range of host taxa (Drake and Ruhoff 1965, Stonedahl, Dolling, and duHeaume 1992).

Within Australia, several species of tingid have become agricultural pests, one of which is the macadamia lace bug, currently known as *Ulonemia decoris* Drake, 1942. This species is an emerging pest in macadamia orchards in northern New South Wales and southern Queensland. Within the last decade, *U. decoris* has caused major economic losses in the macadamia nut industry (Huwer and Maddox 2007, Commens 2013); the lace bug feeds on and damages the macadamia flowers, which prevents the development of the nuts.

As the impacts of *U. decoris* grew, so did interest in the species. Preserved tingid specimens from across Australia were examined for this study to determine the geographic extent and breadth of host plant taxa used by *U. decoris*. During this process, several undescribed tingid species that bore morphological resemblance to *Ulonemia* were discovered, and were putatively assigned to this genus. Each of these species were collected in association with members of the plant family Proteaceae, of which *Macadamia* F. Muell. is a member. In addition, two other species of tingid were found during this study to be pestiferous on *Macadamia*: *U. leai* from far north Queensland, and an undescribed species from northern New South Wales and southern Queensland. This undescribed species bore resemblance to some members of *Ulonemia*, though it possessed some intricate cells on the costal margin and a dark overall colour that made it distinct from any other members of the genus. In addition, the range of this species overlaps with that of *U. decoris* almost completely, and even occur on the same flower (pers. obs.).

Other genera of tingids were found that had species associated with proteaceous hosts, though they also had members that were associated with host plants of other families. Many of these genera are also poorly diagnosed, and placing new species into an appropriate genus can be difficult. However, as many tingids are host-specific—with some species occurring on several closely-related host taxa (Drake and Ruhoff 1965, Stonedahl, Dolling, and duHeaume 1992)—there exists a potential for tingid species that feed on Proteaceae to switch onto *Macadamia*, even if they have not yet been recorded from *Macadamia*.

The growing concern over the economic losses to lace bug damage in the macadamia nut industry (Huwer and Maddox 2007, Commens 2013), coupled with the lack of knowledge of tingid taxonomy and classification within Australia demonstrated the necessity for an in-depth investigation of Australian tingids, in particular *Ulonemia* and allied taxa. To date, there has been little research into the genus *Ulonemia*, and the entire body of literature constitutes taxonomic works describing new species, with no research into the phylogenetic relationships between *Ulonemia* and other genera (Drake and Poor 1937, Drake 1942, Péricart 1992, Dang et al. 2014). This study will provide the first comprehensive overview of the genus and its status in Australia. To that end, this study has three broad goals:

1) to describe the relationship between *Ulonemia* and other morphologically-simplified tingids in Australia, especially those that utilise proteaceous species as hosts;
2) to redefine the genus *Ulonemia* using the results from part 1, including erecting new genera and species as appropriate and provide keys to their identification, to better inform macadamia orchard managers on the identity of their pests;

3) to examine the population genetics of the foremost pestiferous species, *Ulonemia decoris*, to determine the dispersal rate of individuals between populations in order to provide orchard managers guidance on control methods.

CHAPTER 2: PHYLOGENETICS OF THE GENUS *ULONEMIA* DRAKE AND DAVIS, 1937 (HEMIPTERA: HETEROPTERA: TINGIDAE)

ABSTRACT

Tingid classification has been problematic since the recognition of the family. The unique and often exaggerated ornamentation of tingids has led to confusion in morphology-based phylogenies due to convergence of characters. However, some genera do not have highly exaggerated structures and their identifications rely on reduced morphology as diagnosable characters, in which case distinguishing between taxa becomes difficult. Other features that are important in the classification of the tingids' sister group Miridae, such as the structure of male genitalia, are simplistic in the tingids and provide little information for classification. This can cause taxonomic confusion when describing new species. In Australia, this includes genera such as *Eritingis*, *Epimixia*, *Ischnotingis*, *Malandiola*, *Nethersia*, and *Ulonemia*. The relationship between these genera is of great interest, as several species of *Ulonemia* have recently become pests of *Macadamia*, and many of these genera have members which can be found on the Proteaceae.

To determine the relationships of these genera, four genes were amplified: a fragment of the 16S rRNA gene, a fragment of the cytochrome *c* oxidase subunit I (COI) mtDNA gene, a fragment of the 18S rRNA gene, and a fragment of the 28S ribosomal DNA (rDNA) gene. These genes were analysed using Maximum Likelihood (ML) and Bayesian phylogenetic inferences. In addition, a combined molecular and morphological dataset was analysed using parsimony. The parsimony analysis yielded numerous morphological homoplasies, and most deep clades lacked support. The ML and Bayesian analyses had strong support, and returned a paraphyletic *Ulonemia* with three strongly

supported clades. Two new genera are recognised to account for the observed phylogenies.

INTRODUCTION

Classification of the Tingidae

The classification of the Tingidae has posed a challenge since the recognition of the family (Drake and Davis 1960, Schuh et al. 2006). Members of this family are known for their unique and often extravagant ornamentation, especially on the pronotum and the hemelytra. Earlier authors (Drake and Davis 1960, Froeschner 1996) recognised the value of these diverse structures for identifying and defining species but noted that these same characters offered limited value in constructing the phylogeny of the Tingidae. Regardless, most studies to date have used morphological approaches in the evaluation of tingid classification (Lis 1999, Guilbert 2001, Guilbert 2004, Schuh et al. 2006).

The first comprehensive attempt at classifying the Tingidae was by Stål (1873), who divided the family into three subfamilies: Tinginae, Cantacaderinae, and Agrammatinae. Drake and Davis (1960) synonymised Agrammatinae with Tinginae, incorporated the family Vianaididae as a subfamily within Tingidae, and erected two tribes within Cantacaderinae: Cantacaderini and Phatnomatini. The taxonomy proposed by Drake and Davis (1960) forms the basis of the current arrangement of the Tingidae, and our understanding has changed little since then. Subsequent authors have proposed changes to this arrangement based on morphological characters. For example, Froeschner (1968) found morphological support based on the stenocostal area for the two tribes in Cantacaderinae. Lee (1969) examined male genitalia and larval morphological characters and determined that Cantacaderinae possessed characters not found outside of that subfamily, but found the Tinginae highly variable, even within genera (e.g. *Stephanitis*

Stål, 1873). Froeschner (1996) removed the subfamily Vianaidinae from Tingidae and elevated it to its own family.

The turn of the current century marked the start of more intensive studies on tingid phylogenetics. Based on a cladistic analysis using morphological characters, Lis (1999) also recognised Vianaidinae as its own family, and further elevated Cantacaderinae to family status. In addition, Lis elevated the Phatnomatini to subfamily status within Tingidae. These arrangements represented the first significant departure from Drake and Davis (1960). The first attempt to study the evolution of tingid external morphology was conducted by Guilbert (2001), who found a paraphyletic Tingidae with Cantacaderinae—again considered as a subfamily of Tingidae—placed in the middle of the clade, and the return of Phatnomatini as a tribe within Cantacaderinae. The arrangement and phylogenetic support of tribes between Lis (1999) and Guilbert (2001) was strikingly different, though based on different taxa and characters, and Guilbert noted that many groups within Tinginae were poorly defined and potentially paraphyletic, in particular the Ypsotingini and Litadeini. The limits of cladistic analysis using morphological characters were evident in the phylogenies constructed by Guilbert (2001), as many characters were found to be homoplasious. Guilbert (2001) concluded that tingid morphological traits evolved in the direction of simple to complex (or exaggerated) and did so at least three times independently. A later study by Guilbert (2004) of the morphological characters of tingid nymphs for the most part resurrected the classifications of Drake and Davis (1960), concluding that taxonomic under-sampling by previous authors led to problems in constructing informative phylogenies.

Another problem in constructing the phylogenies of Tingidae was outgroup selection, as highlighted by Schuh et al. (2006). They found that the use of Vianaididae as an outgroup obscured the relationship of that family to the rest of Tingidae. They

recovered a monophyletic Tingidae with Vianaidinae and Cantacaderinae as subfamilies, with Miridae as the sister to the Tingidae, and indicated that DNA would be an important factor in further analyses, and additionally provided support for their phylogenetic determinations.

Molecular markers were first used to examine relationships within the Tingidae by Guilbert et al. (2014), who noted that phylogenies constructed with morphological characters lacked support due to high levels of homoplasy. They concluded that the Phatnomatini should be placed as a tribe within Tinginae as sister to Tingini, and that Ypsotingini and Litadeini are invalid tribes, which were synonymised with Tingini. They further supported the conclusion of Schuh et al. (2006) that Vianaidinae and Cantacaderinae are subfamilies within Tingidae.

Generic concepts in the Tingidae

Many tingid genera are defined by characters of the external morphology, which in many tingid taxa comprises exaggerated projections of the dorsum, particularly of the pronotum and hemelytra, coupled with spines of the dorsal face of the head, and lacelike texture that can vary size in shape. Unlike the Miridae, which is considered the sister group to the Tingidae, the genitalia of Tingidae are generally uninformative as phylogenetic characters. They are relatively simple in comparison to the diverse forms of Miridae genitalia, and as such there are few characters which can be used to infer relationships.

Although exaggerated external morphology can be species specific, exaggerated traits are common in the diagnoses of numerous tingid genera. However, some genera that do not have highly exaggerated structures often rely on reduced morphology as diagnosable characters. This can cause taxonomic confusion when describing new species, as the original diagnoses of these genera are often lacking sufficient detail for effective identification. In the Australian context, these include genera such as *Eritingis*

Drake and Ruhoff, 1962, *Epimixia* Kirkaldy, 1908, *Ischnotingis* Horváth, 1925, *Malandiola* Horváth, 1925, *Nethersia* Horváth, 1925, and the subject of this thesis, *Ulonemia* Drake and Poor, 1937. The taxonomic history and diversity of *Ulonemia* are covered in chapter 2.

Plant association of Australian Tingidae

Tingids have been recorded as having high specificity to host plant taxa, with tingid species often restricted to a single host species or closely related groups (Drake and Ruhoff 1965, Stonedahl, Dolling, and duHeaume 1992). Cassis and Symonds (2008, 2011), Cassis et al. (2017), and Symonds and Cassis (2018) found that in groups with high host plant specificity (Miridae, Tingidae), the host taxa can be phylogenetically informative. *Ulonemia* spp. are restricted to the Proteaceae (see chapter 2); additionally, several other genera (e.g. *Cysteochila*, Stål, 1873, *Euaulana* Drake, 1945) have taxa that feed on Proteaceae, and the phylogenetic relationships between these taxa are unclear.

Aim and objectives

The aim of this chapter was to establish a phylogenetic framework for this thesis and to enable a robust and predictive classification the proteaceous-feeding genus *Ulonemia* sensu lato. To achieve this goal, this chapter has the following objectives:

1) to assess the monophyly of *Ulonemia* using morphological characters combined with mitochondrial and nuclear gene markers;
2) to assess the monophyly of *Ulonemia* using only mitochondrial and nuclear gene markers; and,
3) to determine monophyletic groups within a putatively related tingids associated with the plant family Proteaceae and allied lace bug taxa with simplified morphology.

METHODS AND MATERIALS

Taxon sampling

Specimens were collected in conjunction with a variety of projects, including the Australian Biological Resources Study (ABRS) Bush Blitz species discovery program (http://www.bushblitz.org) and the Hort Innovation Macadamia Fund. Specimens to be sequenced were stored in ethanol after collection, while those used for morphological analysis were mounted on paper points attached to an entomological pin. Species of *Ulonemia* sensu lato were specifically targeted for collection to cover the highest number of species as possible within that genus. Other taxa were collected opportunistically, with the goal of sampling a cross-section of Australian tingid diversity. Specimens were assigned a unique specimen identifier (USI) code and recorded in the Planetary Biodiversity Inventory (PBI) database. Further data associated with these specimens can be accessed at http://research.amnh.org/pbi/heteropteraspeciespage/. Additional tingid taxa from Guilbert et al. (2014) were exported from GenBank (https://www.ncbi.nlm.nih.gov/genbank/); the taxa selected for this analysis all had three genes used in their study, while those missing one or more genes were excluded. Six genera and seven species of Miridae from Cheng (2017 PhD thesis) were used as outgroup taxa for the molecular analyses. See Table 2.1 for the full list of specimens, GenBank codes, and USI numbers. In the morphological + molecular parsimony analysis, species of *Ulonemia* for which no specimens were available were coded based on original descriptions and habitus images of holotypes. Outgroup and ingroup taxa plus GenBank codes are included in Table 2.2.

Two new genera, *Cercotingis* gen. nov. and *Proteatingis* gen. nov. are described in this work; they are used in this chapter as a consequence of the phylogenetic analyses, with their formal description given in chapter 3. New taxonomic arrangements are

indicated where appropriate with either stat. nov. (new combination), sp. nov. (new species), or incertae sedis (uncertain taxonomic placement).

DNA extraction and amplification

Extraction of DNA from specimens stored in ethanol followed the following protocol. Abdomens were removed from specimens and placed in separate 2 ml microcentrifuge tubes. Abdomens were macerated using a plastic pestle in each tube. A Qiagen DNeasy kit was used for extraction of DNA products, following the Purification of Total DNA from Animal Tissues protocol (http://diagnostics1.com/MANUAL/General_Qiagen.pdf) specific to that kit. Tissue digestion was accomplished by incubating the abdominal tissue in a solution of ATL Buffer and Proteinase K in a BioSan TS-100 thermoshaker at 56 ˚C for >6 hours, depending on specimen quality. DNA products were stored at -20 ˚C.

The polymerase chain reaction (PCR) of gene fragments was prepared using Promega GoTaq Green as a master mix, with 12.5 µl master mix volume, 1 µl forward primer, 1 µl reverse primer, 2 µl DNA template, and 8.5 µl nuclease-free water for a total volume of 25 µl per reaction. Four genes—two mitochondrial and two nuclear—were amplified: a fragment of the mitochondrial 16S rRNA gene (~425 – 435 base pairs (bp)), a fragment of the mitochondrial cytochrome *c* oxidase subunit I (COI) mtDNA gene (~822 bp), a fragment of the nuclear 18S rRNA gene (~642 bp), and a fragment of the nuclear 28S ribosomal DNA (rDNA) gene (~1,250 – 1,520 bp). Primers used for amplification, their sequences, and accompanying references are listed in Table 2.3.

Amplification of PCR products was done using a BioRad T1000 Thermal Cycler or Eppendorf PCR machine. PCR programs for each gene are listed in Table 2.4. PCR products were visualized by placing 2 µl of product in 1% agarose gel and running the gel in a Bio-rad gel tank at 100 V for 20 minutes. Product purification to degrade any excess primers was performed by adding 2 µl of ExoSAP-IT to the PCR product and

incubating in a thermal cycler at 37 ˚C for 15 minutes, then at 80 ˚C for 30 minutes. Final PCR products were sent to Macrogen Inc in South Korea for sequencing.

Sequence alignment

Raw sequence data in ab1 format were imported into Geneious 8.1.8 for trimming and alignment. Sequence pairs were aligned using De Novo Assemble. Primer sequences were manually added to Geneious, and mapped to each aligned sequence pair. The product between primer pairs was retained, and the primer sequences and other extraneous base pairs outside the region of interest were removed. Ambiguities in the final sequences were called by using the highest peak in the chromatogram for that location. Additionally, edited base pairs were compared against sequences from either the same species or another closely-related taxon for continuity, or for change in the coded amino acid in the case of COI. Gaps resulting from poor read quality in either the forward or reverse sequence were removed. For the protein-coding gene COI, the sequences were checked for stop codons by examining all reading frames; once the correct reading frame was found, the sequence had one or two base pairs trimmed from the start to force all sequences to begin in reading frame 1. Multiple alignments for each gene were performed using MUSCLE with the default options in Geneious. The final concatenated sequence for the combined morphological + molecular parsimony analysis was 3,572 bp with 19 terminal taxa. The final concatenated sequence for the molecular phylogenetic analyses was 3,689 bp with 83 terminal taxa; the sequences were exported in Nexus and Phylip formats for analysis.

Morphological characters and parsimony analysis

Fifty morphological characters (Table 2.5) were coded for 18 ingroup taxa and 13 outgroup taxa (Table 2.6) using Mesquite 3.40 (Maddison and Maddison 2017). The root taxon for the resulting tree was *Cantacader quinquecostatus* (Fieber, 1844). Taxa with

missing molecular sequences are *Ceratocader armatus* (Hacker, 1928), *Epimixia vulturna* (Kirkaldy, 1908), *Eritingis exalla* (Drake, 1961), *Nethersia absimilis* Drake, 1944, *Tingis impensa* Drake, 1947, *Ulonemia angusta* Dang et al., 2014, *U. assamensis* (Distant, 1903), *U. concava* Drake, 1947, *U. dignata* Drake and Poor, 1937, *U. jingae* Dang et al., 2014, *U. magna* Dang et al., 2014, and *U. plesia* Drake and Ruhoff, 1961. Molecular data were coded as multi-state characters, with gaps treated as missing, and concatenated with the morphological data in Mesquite. A parsimony analysis using equal weights, tree-bisection-reconnection (TBR) branch swapping, a maximum of 500 trees, and 1,000 bootstrap replicates was run using PAUP* 4.0a162 (Swofford 2004). Bootstrap support values were mapped to the strict consensus tree. Morphological character optimisation to the consensus tree was done using WinClada (Nixon 2002).

Molecular phylogenetic analyses

The finalised sequence alignment was imported into PartitionFinder 2, with separate subsets for 16S, 18S, 28S, and each codon position of COI. Model parameters were: linked branch lengths, model selection based on the corrected Akaike Information Criterion (AICc), and greedy search (Guindon et al. 2010, Lanfear et al. 2012, 2017). The best scheme data block was added to Phylip file for RAxML, while the best scheme for MrBayes was set to nst = 6 and rates = invgamma for all subsets.

A Bayesian estimation of phylogeny was conducted using MrBayes 3.2.6 with Open MPI 1.10.2. The number of generations was 250,000,000 with 3 runs and 2 chains (one heated, one cold) and a temperature of 0.1 for the heated chain, the burn-in fraction was set to 30%, and the sample frequency was every 20,000 generations; all other settings were left at their default values. The outgroup for the analysis was *Naranjakotta chinnocki* Cassis and Symonds, 2016. Support values were mapped to the branches of the consensus tree.

Maximum Likelihood (ML) estimation of phylogeny was conducted using RAxML-NG 0.6.0 (Kozlov et al. 2018) with *N. chinnocki* as the outgroup. The number of bootstraps was determined using the autoMRE bootstrap convergence test; convergence was reached after 1,350 replicates. Missing values were treated as missing and not as a fifth state. Bootstrap support values were mapped to the branches of the best tree.

RESULTS

Parsimony analysis

The total number of rearrangements tried was 1,412,784, with 100 equally parsimonious trees retained. The strict consensus tree with optimised morphological characters and bootstrap support values is presented in Figure 2.1. The Tingini can be defined here by lacking a porrect frons (9), the presence of a posterior projection on the pronotum (16), possessing one areola in the costal area anterior to the discoidal midline (27), possessing one areola in the costal area posterior to the discoidal midline (28), and differently sized areolae in the sutural area compared to the discoidal and subcostal areas.

Maximum likelihood estimation

PartitionFinder 2 found four subsets in the data: subset 1, 16S; subset 2, COI (all codon positions); subset 3, 18S; subset 4, 28S. The best models were: GTR+I+G for 16S and 28S; TIM+I+G for 18S; TVMEF+I+G for all COI codon positions. These evolution models were used for the ML analysis in RAxML-NG. The evolutionary models are more limited in MrBayes; the most appropriate model for all sites, as determined by PartitionFinder 2, was GTR+I+G.

The final ML optimisation likelihood produced by RAxML was -30,382.899232 for the best tree (Figure 2.2). *Cantacader* Amyot and Serville, 1843 forms a clade and is sister to the remainder of the tingids, including *Phatnoma* Fieber, 1944, with strong

support (100). *Phatnoma* is sister to the Tingini + Ypsotingini with strong support (89). Ypsotingini, here represented by *Dictyonota strichnocera* Fieber, 1944 and *Kalama tricornis* (Schrank, 1801), is paraphyletic with respect to the Tingini, but weakly supported (16); *Corythucha cydoniae* (Fitch, 1861) (Tingini) is basal to Ypsotingini with strong support (89). The remainder of Tingini is placed sister to Ypsotingini with weak support (4). *Leptobyrsa decora* Drake, 1922, *Stephanitis subfasciata* Horváth, 1912, *Leptopharsa firma* Drake and Hambleton, 1938, and *Gargaphia* Stål, 1862 form a clade with weak support (38). *Copium teucrii* (Host, 1788), *Catoplatus carthusianus* (Goeze, 1778), and *Elasmotropis testacea* (Herrich-Schaeffer, 1830) form a clade with low support (2). *Radinacantha reticulata* Hacker, 1929, *Epimixia aboccidente* Cassis, Symonds, and Branson, 2018, *Lasiacantha* Stål, 1873, and *Inoma* Hacker, 1927 form a clade with moderate support (61). *Diplocysta trilobata* Drake and Poor, 1939 and *Tingis* Fabricius, 1803 sp. 1 form a clade with low support (30) and is sister to a clade containing *Ulonemia*, *Cysteochila*, *Euaulana*, *Ischnotingis horvathi* Drake, 1954, *Eritingis*, *Nethersia*, *Onchochila simplex* (Herrich-Schaeffer, 1830), *Cercotingis* gen. nov., and *Proteatingis* gen. nov. *Ulonemia* sensu lato is paraphyletic; *U. leai* forms a clade sister to *Cysteochila* + *Euaulana* + (*Ischnotingis* + *Eritingis* + *Nethersia*) + ((*Cercotingis* + *Onchophysa*) + *Proteatingis*) with moderate support (69). *Ischnotingis* + *Eritingis* + *Nethersia* is sister to all remaining *Ulonemia* sensu lato (i.e., *Cercotingis* and *Proteatingis*) from Australia, plus *Onchochila simplex*. *Onchochila simplex* forms a weakly supported clade (28) with *Cercotingis*. *Cercotingis decoris* (Drake, 1942) stat. nov., *C. croajingolong* sp. nov., *C. namadgi* sp. nov., and *C. tasmaniensis* sp. nov. form a strongly supported clade (99) and constitute a new genus. *Cercotingis* + *Onchochila simplex* is sister to *Proteatingis* gen. nov., though the support is weak (7). *Proteatingis astibosetes* sp. nov., *P. mjobergi* stat. nov., *P. howardi* sp. nov., *P. burckhardti* stat. nov.,

and *P. minuta* sp. nov. form a clade with moderate support (69) and constitute a new genus.

Bayesian estimation of phylogeny

The average standard deviation of split frequencies was 0.041357, the harmonic mean for run 1 was -29873.56, run 2 was -29846.18, run 3 was -29879.48, with -29878.39 as the total harmonic mean among the three runs. The topologies of the tree produced by MrBayes (Figure 2.3) and RAxML (Figure 2.2) are very similar, with the differences between the two analyses highlighted here.

Dulinius conchatus Distant, 1903 (Tingini) is placed basal to Ypsotingini with strong support (100), while *Corythucha cydoniae* is placed in an unresolved polytomy with a clade comprised of *Leptobyrsa decora* + *Leptopharsa firma* + *Stephanitis subfasciata* + *Gargaphia*, and the remainder of the Tingini. The placement of *Diplocysta trilobata* changed from sister to *Tingis* sp. 1 with weak support (30) in the RAxML analysis to *Diplocysta trilobata* as sister to *Catoplatus carthusianus* + *Elasmotropis testacea* with moderate support (54) in the MrBayes analysis. Clade A in RAxML has *Ratinacantha* + *Epimixia* + *Lasiacantha* + *Inoma* as sister to clade B with poor support (15), but in the Bayesian analysis, this clade was placed within clade B, with *Tingis* placed in clade A as sister to clade B with moderate support (54). The RAxML clade C contains all of *Ulonemia* sensu lato with moderate support (69), with *U. leai* as sister to *Cysteochila* + *Euaulana* + clade D, while the Bayesian analysis clade C is collapsed into a polytomy between *Cysteochila*, *U. leai* and clade D. The RAxML clade D consists of (*Ischnotingis* + *Eritingis* + *Nethersia*) + (*Cercotingis* + *Onchophysa*) + *Proteatingis* with weak support (19), while the same clade from MrBayes has higher support (50) and includes *Euaulana* with *Onchochila* as sister to *Cercotingis* with moderate support (51)

and also places (*Ischnotingis* + *Eritingis* + *Nethersia*) as sister to *Proteatingis* with moderate support (54).

DISCUSSION

The status of Cantacaderinae as sister to Tinginae within the Tingidae is supported by molecular analyses using both RAxML and MrBayes. The classification proposed by Guilbert et al. (2014)—the inclusion of Phatnomatini within the Tinginae as sister to Tingini and the invalidation of Ypsotingini as a tribe—is supported by the current analysis, though increased taxonomic sampling of the Ypsotingini and inclusion of the Litadeini is necessary to draw stronger conclusions about the tribal and subfamilial classifications of the Tingidae.

Parsimony analysis of molecular and morphological data yielded numerous morphological homoplasies (Figure 2.1). Most deep clades lacked support, with many collapsed to unresolved polytomies. Guilbert et al. (2014) also had high levels of homoplasious morphological character in their analysis, albeit with more phylogenetic resolution. In the current study, only *Epimixia* and *Nethersia* had greater than 50% support at the generic level, and are definable by morphological characters. The genus *Ulonemia* is highly unresolved in relation to *Eritingis* + *Nethersia* and *Tingis*. It is also unresolved in relation to several undescribed species that had putatively been assigned to new genera. As such, *Ulonemia* sensu lato does not have any morphological characters that unify the genus.

Currently, *Ulonemia* contains 16 species, 6 of which occur in Australia: *U. burckhardti*, *U. concava*, *U. decoris*, *U. leai*, *U. mjobergi*, and *U. plesia*. Only two species were excluded from the molecular analysis: *U. concava*, which has not been seen since 1967, and *U. plesia*, as no specimens were available for sequencing. *Ulonemia* sensu lato is paraphyletic in both RAxML and MrBayes phylogenies. In the RAxML tree, *U. leai*

was sister to *Cysteochila* + *Euaulana* + clade D, which contains the remaining *Ulonemia* as well as *Onchochila*, *Ischnotingis*, *Eritingis*, and *Nethersia* (Figure 2.2). The support for this arrangement is weak, and in the MrBayes analysis, the relationship is collapsed into a polytomy with strong support (90) with *Cysteochila*, *U. leai*, and clade D (Figure 2.3).

Clade E contains *U. decoris*, plus three new species, all of which bear superficial resemblance to *U. decoris*. This clade has strong support in both RAxML (99) and MrBayes (100) analyses (Figures 2.2, 2.3). The sister to clade E is *Onchochila* with low support (28) in RAxML (Figure 2.2); in MrBayes, clade E is sister to *Onchochila* + *Euaulana* with moderate support (58) (Figure 2.3). Clade F contains *U. burckhardti* and *U. mjobergi*, plus three currently undescribed species. Clade F is sister to Onchochila + clade E with weak support (7) in the RAxML analysis (Figure 2.2), but is sister to *Ischnotingis* + *Eritingis* + *Nethersia* with moderate support in MrBayes (54) (Figure 2.3). *Ulonemia leai* forms its own clade, with strong support in RAxML (100) and MrBayes (100). These relationships indicate that *Ulonemia*, as currently described, contains members from at least three different genera. *Ulonemia leai* should be treated as its own genus, with clades E and F each forming a new genus. Two new genera are erected in chapter 3 to address the taxonomic implications of this study.

Of additional interest are the positions of *Epimixia*, *Inoma*, and *Lasiacantha*. Cassis and Symonds (2008, 2011) previously explored the phylogenetic relationships of these taxa, and concluded that they were sister taxa with several morphological characters to distinguish the two genera. Though based on only two species for each genus, both ML and Bayesian analyses place *Inoma* and *Lasiacantha* in a single clade with strong support. The position of *Epimixia* as sister to *Inoma* + *Lasiacantha* is surprising, given the stark differences in the morphology between the two groups. *Epimixia* has highly simplified

morphology, whereas both *Inoma* and *Lasiacantha* have highly exaggerated morphology, especially of the pronotal carinae and paranota (which are reduced and lacking in *Epimixia*, respectively). The sample size here is too small to draw taxonomic conclusions, and more work should be done on these groups to resolve their relationships.

Ischnotingis, *Eritingis*, and *Nethersia* form a strongly supported clade (87) in MrBayes, but have weak support (24) in RAxML. These three genera have highly reduced morphologies, especially of the pronotal carinae, paranota, costal margins, and cephalic spination. Various authors (Drake and Ruhoff 1965, Cassis and Gross 1995) have transferred species between *Eritingis* and *Nethersia*, and the two genera are difficult to diagnose. Their relationship has been reaffirmed here, though the sample size is too low to draw taxonomic conclusions. However, the hypothesised close relationship between *Epimixia* and *Eritingis* + *Nethersia* (Cassis et al. 2017) is demonstrably false, as the molecular phylogenies indicate that they are genetically distant, belying their similar simplified morphologies.

It is apparent that the phylogenetic relationships of the Tingidae are obscured by their morphology. The unique ornamentation of many members of the family appear to arise multiple times independently. Inferring phylogenies through analysis of molecular data should be the recommended approach for the Tingidae. Molecular studies of this family are in their infancy, and much work needs to be done to fully understand the evolution of tingids' fascinating structure.

Table 2.1. List of taxa used for RAxML and MrBayes analyses. PBI USI codes are for specimens which have been accessioned into the AMNH PBI database. 16S, COI, 18S, and 28S codes are GenBank accession numbers. * From Cheng (2017); ** from Guilbert et al., (2014); *** sequences provided by Shaun Cullerton as a courtesy and will be submitted to GenBank with his later publication.

Species	Outgroup	PBI USI Code	16S	COI	18S	28S
Miridae: Orthotylinae: Austromirini						
Lattinova jacki Cassis, 2008	X	AMNH_PBI 00401044	KY797840*	KY797936*	KY776808*	KY776970*
Zanessa pictulifer (Walker, 1873)	X	AMNH_PBI 00401028	KY797841*	KY797937*		KY776971*
Miridae: Orthotylinae: Orthotylini						
Erysivena sp.	X		KY777131*	KY777084*	KY776792*	KY776955*
Myrtlemiris rubrocuneatus Cheng, Mututantri, and Cassis, 2012	X	AMNH_PBI 00023921	KY777086*	KY777031*	KY776707*	KY776871*
Naranjakotta chinnocki Cassis and Symonds, 2016	X	AMNH_PBI 00400947	KR610453*	KX619636*		KX619626*
Naranjakotta macfarlanei Cassis and Symonds, 2016	X	AMNH_PBI 00023485	KY816759*	KY816782*		KY816769*
Pseudoloxops sp.	X	AMNH_PBI 00401063	KY797869*	KY797969*	KY776842*	KY777005*
Tingidae: Cantacaderinae: Cantacaderini						
Cantacader lethierryi Scott, 1874			KF661777**	KF661844**		KF661837*
Cantacader quinquecostatus (Germar and Berendt, 1856)			KF661778**	KF661863**		KF661838**
Tingidae: Tinginae: Phatnomatini						
Phatnoma natensis Guilbert, 2007			KF661772**	KF661871**		KF661832**
Tingidae: Tinginae: Tingini						
Catoplatus carthusianus (Goeze, 1778)			KF661740**	KF661856**		KF661800**
Cercotingis croajingolong sp. nov.		UNSW_ENT 00050540	MH796856	MH802526	MH796801	MH796914
Cercotingis croajingolong sp. nov.		UNSW_ENT 00050569	MH796857	MH802527	MH796802	MH796915
Cercotingis croajingolong sp. nov.		UNSW_ENT 00050599	MH796858	MH802528	MH796803	MH796916

Table 2.1 continued, next page.

Table 2.1, cont.

Species	Outgroup	PBI USI Code	16S	COI	18S	28S
Tingidae: Tinginae: Tingini						
Cercotingis croajingolong sp. nov.		UNSW_ENT 00050616	MH796859	MH802529	MH796804	MH796917
Cercotingis decoris (Drake, 1942)		AMNH_PBI 00404708	MH796860	MH802530	MH796805	MH796918
Cercotingis decoris (Drake, 1942)		AMNH_PBI 00404751	MH796861	MH802531	MH796806	MH796919
Cercotingis decoris (Drake, 1942)		AMNH_PBI 00404749	MH796862	MH802532	MH796807	MH796920
Cercotingis decoris (Drake, 1942)		AMNH_PBI 00404791	MH796863	MH802533	MH796808	MH796921
Cercotingis namadgi sp. nov.		UNSW_ENT 00050542	MH796864	MH802534	MH796809	MH796922
Cercotingis namadgi sp. nov.		UNSW_ENT 00050548	MH796865	MH802535	MH796810	MH796923
Cercotingis namadgi sp. nov.		UNSW_ENT 00050555	MH796866	MH802536	MH796811	MH796924
Cercotingis namadgi sp. nov.		UNSW_ENT 00050571	MH796867	MH802537	MH796812	MH796925
Cercotingis tasmaniensis sp. nov.		UNSW_ENT 00050632	MH796868	MH802538	MH796813	MH796926
Cercotingis tasmaniensis sp. nov.		UNSW_ENT 00050608	MH796869	MH802539	MH796814	MH796927
Cercotingis tasmaniensis sp. nov.		UNSW_ENT 00050583	MH796870	MH802540	MH796815	MH796928
Cercotingis tasmaniensis sp. nov.		UNSW_ENT 00050566	MH796871	MH802541	MH796816	MH796929
Copium teucrii (Host, 1788)			KF661755**	KF661845**		KF661815**
Corythucha cydoniae Fitch, 1861			KF661727**	KF661842**		KF661787**
Cysteochila sp.		UNSW_ENT 00050823	MH796872		MH796817	MH796930
Cysteochila sp.		UNSW_ENT 00050824	MH796873		MH796818	MH796931
Dictyonota strichnocera Fieber, 1844			KF661739**	KF661862**		KF661799**
Diplocysta trilobata Drake and Poor, 1939		UNSW_ENT 00050827		MH802542	MH796819	MH796932
Dulinius conchatus Distant 1903			KF661757**	KF661873**		KF661817**

Table 2.1 continued, next page.

Table 2.1, cont.

Species	Outgroup	PBI USI Code	16S	COI	18S	28S
Tingidae: Tinginae: Tingini						
Elasmotropis testacea (Herrich-Schaeffer, 1830)			KF661741**	KF661870**		KF661801**
Epimixia aboccidente Cassis, Symonds, and Branson, 2018		UNSW_ENT 00050825	MH796874	MH802543	MH796820	MH796933
Epimixia aboccidente Cassis, Symonds, and Branson, 2019		UNSW_ENT 00050826	MH796875	MH802544	MH796821	MH796934
Eritingis trivirgata (Horváth, 1908)		AMNH_PBI 00404785	MH796878	MH802545	MH796822	MH796935
Eritingis trivirgata (Horváth, 1908)		UNSW_ENT 00051328	MH796880	MH802546	MH796823	MH796936
Eritingis trivirgata (Horváth, 1908)		UNSW_ENT 00051329	MH796881	MH802547	MH796824	MH796937
Euaulana tasmaniae Drake, 1945		UNSW_ENT 00050658	MH796882	MH802548	MH796825	MH796938
Euaulana tasmaniae Drake, 1946		UNSW_ENT 00050671	MH796883	MH802549	MH796826	MH796939
Euaulana tasmaniae Drake, 1947		UNSW_ENT 00050677	MH796884	MH802550	MH796827	MH796940
Gargaphia arizonica Drake and Carvalho, 1944			KF661738**	KF661849**		KF661798**
Gargaphia solani Heidemann, 1914			KF661744**	KF661859**		KF661804**
Inoma sp. 1			***	***	***	***
Inoma sp. 2			***	***	***	***
Ischnotingis horvathi Drake, 1954		UNSW_ENT 00050661	MH796885	MH802551	MH796828	MH796941
Ischnotingis horvathi Drake, 1955		UNSW_ENT 00050668	MH796886	MH802552	MH796829	MH796942
Ischnotingis horvathi Drake, 1956		UNSW_ENT 00050696		MH802553	MH796830	MH796943
Kalama tricornis (Schrank, 1801)			KF661750**	KF661846**		KF661810**
Lasiacantha caneriverensis Cassis and Symonds, 2013			***	***	***	***
Lasiacantha pilbara Cassis and Symonds, 2011			***	***	***	***
Leptobyrsa decora Drake, 1922			KF661728**	KF661874**		KF661788**

Table 2.1 continued, next page.

Table 2.1, cont.

Species	Outgroup	PBI USI Code	16S	COI	18S	28S
Tingidae: Tinginae: Tingini						
Leptopharsa firma Drake and Hambleton, 1938			KF661742**	KF661843**		KF661802**
Nethersia chazeaui (Guilbert, 1997)			KF661762**	KF661854**		KF661822**
Nethersia sp.		UNSW_ENT 00051402	MH796879	MH802554	MH796831	MH796944
Nethersia sp.		UNSW_ENT 00050610	MH796876	MH802555	MH796832	MH796945
Nethersia sp.		UNSW_ENT 00050670	MH796877	MH802556	MH796833	MH796946
Onchochila simplex (Herrich-Schaeffer, 1830)			KF661760 **	KF661857**		KF661820**
Proteatingis astibosetes sp. nov.		UNSW_ENT 00050822	MH796887	MH802557	MH796834	MH796947
Proteatingis burckhardti (Péricart, 1992)		UNSW_ENT 00050818		MH802558	MH796835	MH796948
Proteatingis burckhardti (Péricart, 1992)		UNSW_ENT 00050820		MH802559	MH796836	MH796949
Proteatingis howardi sp. nov.		AMNH_PBI 00400703	MH796888	MH802560	MH796837	MH796950
Proteatingis howardi sp. nov.		UNSW_ENT 00051337	MH796889	MH802561	MH796838	MH796951
Proteatingis howardi sp. nov.		UNSW_ENT 00051376	MH796890	MH802562	MH796839	MH796952
Proteatingis howardi sp. nov.		UNSW_ENT 00051415	MH796891	MH802563	MH796840	MH796953
Proteatingis minuta sp. nov.		UNSW_ENT 00050549	MH796892		MH796841	MH796954
Proteatingis minuta sp. nov.		UNSW_ENT 00050560	MH796893	MH802564	MH796842	MH796955
Proteatingis minuta sp. nov.		UNSW_ENT 00050562		MH802565	MH796843	MH796956
Proteatingis mjobergi (Horváth, 1925)		UNSW_ENT 00050570	MH796894	MH802566	MH796844	MH796957
Proteatingis mjobergi (Horváth, 1925)		UNSW_ENT 00050578	MH796895	MH802567	MH796845	MH796958
Proteatingis mjobergi (Horváth, 1925)		UNSW_ENT 00050586	MH796896	MH802568	MH796846	MH796959
Proteatingis mjobergi (Horváth, 1925)		UNSW_ENT 00050588	MH796897	MH802569	MH796847	MH796960

Table 2.1 continued, next page.

Table 2.1, cont.

Species	Outgroup	PBI USI Code	16S	COI	18S	28S
Tingidae: Tinginae: Tingini						
Radinacantha reticulata Hacker, 1929		UNSW_ENT 00050828	MH796898	MH802570	MH796848	MH796961
Stephanitis subfasciata Horváth, 1912			KF661770**	KF661872**		KF661830**
Tingis sp.		UNSW_ENT 00050651	MH796899	MH802571	MH796849	MH796962
Tingis sp.		UNSW_ENT 00050630	MH796900	MH802572	MH796850	MH796963
Tingis sp.		UNSW_ENT 00050582	MH796901	MH802573	MH796851	MH796964
Tingis sp.		UNSW_ENT 00050678	MH796902	MH802574	MH796852	MH796965
Ulonemia leai Drake, 1942		AMNH_PBI 00404774		MH802575	MH796853	MH796966
Ulonemia leai Drake, 1943		UNSW_ENT 00050665		MH802576	MH796854	MH796967
Ulonemia leai Drake, 1944		UNSW_ENT 00050575	MH796903	MH802577	MH796855	MH796968

Table 2.2. List of taxa used for the parsimony analysis. 16S, COI, 18S, and 28S codes are GenBank accession numbers. * From Guilbert et al., (2014); ** sequences provided by Shaun Cullerton as a courtesy and will be submitted to GenBank with his later publication.

Species	Outgroup	16S	COI	18S	28S
Tingidae: Cantacaderinae: Cantacaderini					
Cantacader quinquecostatus (Germar and Berendt, 1856)	X	KF661778*	KF661863*		KF661838*
Ceratocader armatus (Hacker, 1928)	X				
Tingidae: Tinginae: Tingini					
Cercotingis croajingolong sp. nov.		MH796856	MH802526	MH796801	MH796914
Cercotingis decoris (Drake, 1942)		MH796860	MH802530	MH796805	MH796918
Cercotingis impensa (Drake, 1942)					
Cercotingis namadgi sp. nov.		MH796864	MH802534	MH796809	MH796922
Cercotingis tasmaniensis sp. nov.		MH796868	MH802538	MH796813	MH796926
Epimixia aboccidente Cassis, Symonds, and Branson, 2019	X	MH796874	MH802543	MH796820	MH796933
Epimixia vulturna (Kirkaldy, 1908)	X				
Eritingis exalla (Drake, 1961)	X				
Eritingis trivirgata (Horváth, 1908)	X	MH796878	MH802545	MH796822	MH796935
Inoma sp. 1	X	*	*	*	*
Inoma sp. 2	X	*	*	*	*
Lasiacantha sp. 1	X	*	*	*	*
Lasiacantha sp. 2	X	*	*	*	*
Nethersia absimilis Drake, 1944	X				
Nethersia sp.	X	MH796879	MH802554	MH796831	MH796944

Table 2.2 continued, next page.

Table 2.2, cont.

Species	Outgroup	16S	COI	18S	28S
Tingidae: Cantacaderinae: Cantacaderini					
Proteatingis astibosetes sp. nov.		MH796887	MH802557	MH796834	MH796947
Proteatingis burckhardti (Péricart, 1992)			MH802558	MH796835	MH796948
Proteatingis howardi sp. nov.		MH796888	MH802560	MH796837	MH796950
Proteatingis minuta sp. nov.		MH796893	MH802564	MH796842	MH796955
Proteatingis mjobergi (Horváth, 1925)		MH796894	MH802566	MH796844	MH796957
Proteatingis plesia (Drake and Ruhoff, 1961)					
Tingis cardui (Linnaeus, 1758)	X	NC_037836	NC_037836		
Ulonemia angusta Dang et al., 2014					
Ulonemia assamensis (Distant, 1903)					
Ulonemia concava Drake, 1942					
Ulonemia dignata (Drake and Poor, 1937)					
Ulonemia jingae Dang et al., 2014					
Ulonemia leai Drake, 1942					
Ulonemia magna Dang et al., 2014					

Table 2.3. Primer names, direction, amplified gene, primer sequence, and reference for each primer used.

Primer Name	Direction	Gene	Sequence	Reference
16sA	Forward	16S	CGCCTGTTTAACAAAAACAT	Simon et al. 1994
16sB2	Reverse	16S	TTTAATCCAACATCGAGG	Cognato and Vogler 2001
C1-J-2183	Forward	COI	CAACATTTATTTTGATTTTTTGG	Damgaard and Sperling 2001
TL2-N-3014	Reverse	COI	TCCAATGCACTATCTGCCATATTA	Simon et al. 1994
18s3F	Forward	18S	GTTCGATTCCGGAGAGGGA	Giribet et al. 1996
18s5R	Reverse	18S	CTTGGCAATGCTTTCGC	Giribet et al. 1996
28sRD1A	Forward	28S-PP1	CCCSCGTAAYTTAGGCATAT	Menard et al. 2014
28sRD4B	Reverse	28S-PP1	CCTTGGTCCGTGTTTCAAGAC	Menard et al. 2014
28sRD3.2a	Forward	28S-PP2	AGTACGTGAAACGCTTCASGGGT	Menard et al. 2014
28sB	Reverse	28S-PP2	TCGGAAGGAACCAGCTACTA	Menard et al. 2014
28sA	Forward	28S-PP3	GACCCGTCTTGAAGCACG	Menard et al. 2014
28sBout	Reverse	28S-PP3	CCCACAGCGCCACTTCTGCTTACC	Menard et al. 2014

Table 2.4. Polymerase chain reaction (PCR) protocols used for each primer set/gene.

PCR Program 16S	
95 ˚C/3 min	1 cycle
95 ˚C/35 sec 38 ˚C/40 sec 72 ˚C/60 sec	15 cycles
95 ˚C/35 sec 50 ˚C/40 sec 72 ˚C/60 sec	25 cycles
72 ˚C/2 min	1 cycle
HOLD	4 ˚C

PCR Program COI	
95 ˚C/3 min	1 cycle
95 ˚C/30 sec 40 ˚C/45 sec 72 ˚C/60 sec	15 cycles
95 ˚C/30 sec 50 ˚C/40 sec 72 ˚C/60 sec	25 cycles
72 ˚C/2 min	1 cycle
HOLD	4 ˚C

PCR Program 18S	
95 ˚C/3 min	1 cycle
95 ˚C/30 sec 55 ˚C/45 sec 72 ˚C/60 sec	10 cycles
95 ˚C/30 sec 50 ˚C/40 sec 72 ˚C/60 sec	32 cycles
72 ˚C/2 min	1 cycle
HOLD	4 ˚C

PCR Program 28S	
95 ˚C/3 min	1 cycle
95 ˚C/30 sec 55 ˚C/45 sec 72 ˚C/60 sec	15 cycles
95 ˚C/30 sec 50 ˚C/40 sec 72 ˚C/60 sec	25 cycles
72 ˚C/2 min	1 cycle
HOLD	4 ˚C

Table 2.5. Morphological characters and character states for the parsimony phylogenetic estimation.

Num	Character
1)	*Dorsum ornamentation* : **(0)** without exaggerated processes; **(1)** with exaggerated processes on pronotum and hemelytra.
2)	*Frontal spines - length* : **(0)** minute (just protruding from frons); **(1)** shorter in length than AI; **(2)** subequal to equal in length to AI; **(3)** longer in length than AI.
3)	*Frontal spines* - base : **(0)** separated basally by distance greater than frontal spine; **(1)** subcontiguous.
4)	*Medial spine* : **(0)** absent; **(1)** present.
5)	*Medial spine - shape* : **(0)** conical; **(1)** ovate; **(2)** obtuse; **(3)** bifurcated.
6)	*Occipital spines - aspect* : **(0)** flattened to vertex; **(1)** projecting above vertex; **(2)** absent.
7)	*Occipital spines - length* : **(0)** minute (barely visable); **(1)** just reaching posterior margin of eye; **(2)** reaching midpoint of eye; **(3)** reaching anterior margin of eye.
8)	*Occipital spines - orientation* : **(0)** incurved; **(1)** parallel; **(2)** divergent.
9)	*Antennal segment 4 - shape* : **(0)** subfusiform; **(1)** clavate.
10)	*Frons -porrect* : **(0)** absent; **(1)** present.
11)	*Bucculae - structure* : **(0)** areolate; **(1)** punctate.
12)	*Bucculae - height* : **(0)** short; **(1)** tall.
13)	*Bucculae - posterior margin equal to supracoxal lobes* : **(0)** absent; **(1)** present.
14)	*Collum - hood* : **(0)** absent; **(1)** present.
15)	*Collum - hood height vs. pronotal disc* : **(0)** shorter; **(1)** subequal; **(2)** exceeds.
16)	*Medial pronotal carina - height* : **(0)** decumbent; **(1)** raised; **(2)** greatly raised; **(3)** fused; **(4)** absent.
17)	*Pronotum - posterior projection* : **(0)** absent; **(1)** present.
18)	*Paranota* : **(0)** absent; **(1)** Incomplete/reduced beyond humeral angles; **(2)** complete.
19)	*Paranota - shape* : **(0)** expanded; **(1)** expanded and curved upwards; **(2)** carina-like.
20)	*Paranota - areolae at humeral angles* : **(0)** one; **(1)** two.
21)	*Mesosternal carinae - anterior margin reaches procoxae midline* : **(0)** absent; **(1)** present.
22)	*Mesosternal carinae - shape* : **(0)** cordiform/subcordiform; **(1)** parallel.
23)	*Mesosternal carinae - width* : **(0)** narrow, barely wider than rostrum; **(1)** wide, 2x or greater than rostrum.
24)	*Metasternal carinae - shape* : **(0)** cordiform/subcordiform/ovoid; **(1)** parallel.
25)	*Metasternal carinae - width* : **(0)** equal to mesosternal carinae; **(1)** wider than mesosternal carinae.
26)	*Peritreme* : **(0)** absent; **(1)** present.
27)	*Costal area* : **(0)** carinate or obsolete; **(1)** areolate, at least in part.

Table 2.5 continued, next page.

Table 2.5, cont.

Num	Character
28)	*Costal margin - areolae number anterior to discoidal midline* : **(0)** 1; **(1)** 2; **(2)** 3 or more.
29)	*Costal margin - areolae number posterior to discoidal midline* : **(0)** 1; **(1)** 2; **(2)** 3 or more.
30)	*Discoidal and sutural with cross veins* : **(0)** absent; **(1)** present.
31)	*Hemelytra - disposition* : **(0)** contiguous at midline; **(1)** overlapping.
32)	*Hemelytra - relative size of areolae* : **(0)** all subequal; **(1)** larger in sutural area than discoidal and subcostal areas.
33)	*Hemelytra - length* : **(0)** ending in line with apex of abdomen; **(1)** extending beyond end of abdomen.
34)	*Hemelytra - veins* : **(0)** raised; **(1)** flat to obsolete.
35)	*Vestiture - bucculae dorsal margin* : **(0)** near glabrous or with fine setae; **(1)** waxlike setae; **(2)** hairlike setae; **(3)** hairlike and waxlike setae.
36)	*Vestiture - wax in calli* : **(0)** absent; **(1)** present.
37)	*Vestiture - seteiferous tubricles on anterior margin of collum* : **(0)** absent; **(1)** present.
38)	V*estiture - pronotal disc setae* : **(0)** absent; **(1)** scalelike; **(2)** hairlike; **(3)** long, wooly.
39)	*Vestiture - pronotal carinae seteiferous tubricles* : **(0)** absent; **(1)** present.
40)	*Vestiture - hemelytra setae* : **(0)** absent; **(1)** hairlike; **(2)** wooly; **(3)** short.
41)	*Vestiture - costal margin seteiferous tubricles* : **(0)** absent; **(1)** present.
42)	*Vestiture - scale-like setae on abdomen* : **(0)** absent; **(1)** present.
43)	*Vestiture - trochanter* : **(0)** without tuft of setae; **(1)** with patch/tuft of adpressed or erect scalelike setae.
44)	*Vestiture - long, erect setae on femora* : **(0)** absent; **(1)** present.
45)	*Trochanter* : **(0)** contiguous with femur; **(1)** differentiated from femur.
46)	*Male genitalia - paired pygophoral processes* : **(0)** absent; **(1)** present.
47)	*Male genitalia - endosomal lobal sclerites* : **(0)** absent; **(1)** present.
48)	*Male genitalia - endosomal lobal sclerites size* : **(0)** reduced; **(1)** enlarged.
49)	*Male genetalia - endosomal lobal sclerites texture* : **(0)** smooth; **(1)** spinulate.
50)	*Male genitalia - endosomal spinulation medially* : **(0)** absent; **(1)** present.

Table 2.6. Morphological character states for the taxa included in the parsimony phylogenetic estimation. For character and state descriptions, see Table 2.5.

Taxa	Character states																												
	1	2	3	4	5	6	7	8	9	10	11	12	13	14	15	16	17	18	19	20	21	22	23	24	25	26	27	28	29
Cantacader quinquecostatus	0	3	1	0	-	0	3	1	1	1	0	0	0	0	-	1	0	2	1	2	0	1	0	1	0	1	1	2	2
Ceratocader armatus	0	3	1	0	-	1	3	2	1	1	1	0	0	1	2	2	0	2	0	2	0	1	0	1	0	0	1	2	2
Cercotingis croajingolong	0	1	1	1	0	0	1	1	1	0	0	0	0	0	-	2	1	2	1	2	0	1	0	1	0	1	1	1	0
Cercotingis decoris	0	1	1	1	0	0	1	1	1	0	0	0	0	0	-	0	1	2	1	2	0	1	0	0	1	1	1	1	0
Cercotingis impensa	0	2	1	1	0	1	1	2	1	0	0	0	0	0	-	2	1	2	1	2	0	1	1	1	0	1	1	1	0
Cercotingis namadgi	0	1	1	1	0	0	1	1	1	0	0	0	0	0	-	1	1	2	1	1	0	1	0	1	0	1	1	1	0
Cercotingis tasmaniensis	0	1	1	1	0	0	1	1	1	0	0	0	0	0	-	0	1	2	1	2	0	1	0	1	0	1	1	1	0
Epimixia aboccidente	0	0	0	0	-	0	0	2	0	0	1	1	1	0	-	3	1	1	2	3	1	1	0	0	1	1	1	0	0
Epimixia vulturna	0	0	0	0	-	0	0	1	1	0	1	1	1	0	-	3	1	1	2	3	1	1	0	0	1	1	0	-	-
Eritingis exalla	0	1	1	1	0	0	1	1	1	0	1	1	1	0	-	3	1	1	2	3	0	0	1	0	1	1	0	-	-
Eritingis trivirgata	0	1	1	1	0	0	1	1	1	0	1	1	0	0	-	0	1	1	1	0	0	0	1	0	1	1	1	0	0
Inoma sp. 1	1	3	1	1	0	1	3	2	1	0	0	1	1	1	0	1	1	2	0	1	0	1	1	1	0	0	1	1	1
Inoma sp. 2	1	3	1	1	0	1	3	2	1	0	1	1	1	1	0	1	1	2	0	0	0	1	1	1	1	0	1	0	1
Lasiacantha sp. 1	1	3	1	1	3	1	3	2	1	0	1	1	1	1	2	2	1	2	0	2	0	1	1	1	0	0	1	2	2
Lasiacantha sp. 2	1	3	1	1	0	1	3	2	1	0	1	1	1	1	1	2	1	2	0	1	0	1	1	0	0	0	1	1	1
Nethersia absimilis	0	2	1	0	-	0	3	0	1	0	1	1	0	0	-	3	1	1	2	3	0	1	1	0	0	0	0	-	-
Nethersia sp.	0	3	1	0	-	0	1	0	1	0	1	1	0	0	-	3	1	1	2	3	0	0	1	0	0	1	0	-	-
Proteatingis astibosetes	0	1	1	1	0	0	1	1	1	0	0	0	0	1	0	1	1	1	2	0	0	1	0	1	1	1	1	0	0
Proteatingis burckhardti	0	1	1	1	0	0	1	1	1	0	0	0	0	1	1	1	1	2	0	0	0	1	0	1	0	1	1	0	0

Table 2.6 continued, next page.

Table 2.6, continued.

Taxa	Character states																				
	30	31	32	33	34	35	36	37	38	39	40	41	42	43	44	45	46	47	48	49	50
Cantacader quinquecostatus	0	1	0	1	0	0	0	0	0	0	0	0	0	0	0	0	?	?	?	?	?
Ceratocader armatus	1	0	0	1	0	0	0	0	0	0	0	0	0	0	0	0	?	?	?	?	?
Cercotingis croajingolong	0	1	1	1	0	1	1	0	1	0	0	0	1	0	0	1	1	1	1	1	0
Cercotingis decoris	0	1	1	1	0	1	1	0	1	0	0	0	1	0	0	1	1	1	1	1	0
Cercotingis impensa	0	1	1	1	0	0	0	0	0	0	0	0	1	0	0	1	1	1	0	0	0
Cercotingis namadgi	0	1	1	1	0	1	1	0	1	0	0	0	1	0	0	1	0	1	1	1	1
Cercotingis tasmaniensis	0	1	1	1	0	1	1	0	1	0	0	0	1	0	0	1	?	?	?	?	?
Epimixia aboccidente	0	1	1	1	1	0	0	0	0	0	0	0	0	0	0	0	0	1	1	0	0
Epimixia vulturna	0	1	1	1	1	0	0	0	0	0	0	0	0	0	0	0	0	1	1	0	0
Eritingis exalla	0	1	1	1	0	1	0	0	0	0	0	0	1	0	0	1	?	?	?	?	?
Eritingis trivirgata	0	1	1	1	0	1	1	0	0	0	0	0	1	0	0	1	?	?	?	?	?
Inoma sp. 1	0	1	1	1	0	3	0	1	2	1	1	1	1	0	1	1	0	1	1	0	0
Inoma sp. 2	0	1	1	1	0	2	0	1	2	1	1	1	0	0	1	1	0	0	-	-	0
Lasiacantha sp. 1	0	1	0	1	0	2	0	0	3	0	1	1	1	0	1	1	0	0	-	-	0
Lasiacantha sp. 2	0	1	1	1	0	3	0	1	2	1	1	1	1	0	1	1	0	0	-	-	0
Nethersia absimilis	0	1	0	0	0	3	1	0	2	0	3	0	1	1	1	1	0	0	-	-	0
Nethersia sp.	0	1	1	0	0	3	1	0	2	0	3	0	1	1	1	1	0	0	-	-	0
Proteatingis astibosetes	0	1	1	1	0	1	1	0	1	0	0	0	1	0	0	1	0	1	1	0	1
Proteatingis burckhardti	0	1	1	1	0	1	1	0	1	0	0	0	1	0	0	1	1	1	1	0	1

Table 2.6 continued, next page.

Table 2.6, continued.

Taxa	Character states																											
	1	2	3	4	5	6	7	8	9	10	11	12	13	14	15	16	17	18	19	20	21	22	23	24	25	26	27	28	29
Proteatingis howardi	0	1	1	1	0	0	1	1	1	0	0	0	0	1	0	1	1	2	0	0	0	1	0	0	1	1	1	0	0
Proteatingis minuta	0	1	1	1	0	0	1	1	1	0	0	0	0	1	2	1	1	2	0	0	0	1	0	1	0	1	1	0	0
Proteatingis mjobergi	0	1	1	1	0	0	1	1	1	0	0	0	0	1	1	1	1	2	0	0	0	1	0	0	1	1	1	0	0
Proteatingis plesia	0	1	1	1	0	0	1	1	1	0	0	0	0	1	1	0	1	2	0	0	0	1	0	0	1	1	1	0	0
Tingis cardui	0	1	1	1	0	0	0	1	1	0	0	0	0	1	0	0	1	2	0	2	0	1	0	0	1	1	1	2	2
Ulonemia angusta	0	1	1	1	0	0	1	1	1	0	0	0	0	1	1	0	1	2	1	1	0	1	0	0	1	1	1	0	0
Ulonemia assamensis	0	1	1	1	0	0	1	1	0	0	0	0	0	1	1	0	1	1	2	0	0	1	0	0	0	1	1	0	0
Ulonemia concava	0	1	1	1	0	0	1	1	1	0	0	0	0	0	-	0	1	1	2	0	0	1	0	0	0	1	1	1	0
Ulonemia dignata	0	1	1	1	0	0	1	1	0	0	?	?	?	1	?	0	1	2	0	0	?	1	0	0	1	1	1	0	0
Ulonemia jingae	0	1	1	1	0	0	1	1	0	0	0	0	0	1	2	1	1	2	1	1	0	1	0	0	0	1	1	0	0
Ulonemia leai	0	1	1	1	0	0	1	1	1	0	0	0	0	0	-	0	1	1	2	0	0	1	0	0	1	1	1	0	0
Ulonemia magna	0	1	1	1	0	0	1	1	0	0	0	0	0	1	2	1	1	2	1	1	0	1	0	0	0	1	1	0	0

Table 2.6 continued, next page.

Table 2.6, continued.

Taxa	Character states																				
	30	31	32	33	34	35	36	37	38	39	40	41	42	43	44	45	46	47	48	49	50
Proteatingis howardi	0	1	1	1	0	1	1	0	1	0	0	0	1	0	0	1	1	1	1	1	1
Proteatingis minuta	0	1	1	1	0	1	1	0	1	0	0	0	1	0	0	1	0	1	1	0	1
Proteatingis mjobergi	0	1	1	1	0	1	1	0	1	0	0	0	1	0	0	1	1	1	1	0	1
Proteatingis plesia	0	1	1	1	0	1	1	0	1	0	0	0	1	0	0	1	1	1	1	0	1
Tingis cardui	0	1	0	1	0	2	0	0	2	0	1	0	1	0	0	1	0	0	-	-	1
Ulonemia angusta	0	1	1	1	0	1	1	0	1	0	0	0	1	0	0	1	?	?	?	?	?
Ulonemia assamensis	0	1	1	1	0	1	1	0	1	0	0	0	1	0	0	1	?	?	?	?	?
Ulonemia concava	0	1	1	1	0	1	1	0	1	0	0	0	1	0	0	1	1	1	1	0	1
Ulonemia dignata	0	1	1	1	0	1	1	0	0	0	0	0	?	0	0	1	?	?	?	?	?
Ulonemia jingae	0	1	1	1	0	1	1	0	1	0	0	0	1	0	0	1	?	?	?	?	?
Ulonemia leai	0	1	1	1	0	1	1	0	1	0	0	0	1	0	0	1	1	1	0	0	0
Ulonemia magna	0	1	1	1	0	1	1	0	0	0	0	0	1	0	0	1	?	?	?	?	?

Figure 2.1. Strict consensus of 100 Parsimony trees based on 50 morphological characters and 4 molecular markers. The tree is rooted with *Cantacader quinquecostatus*. Morphological characters are optimized onto the tree; closed circles on branches are synapomorphies, open circles on branches are homoplasious synapomorphies. Values in grey squares are bootstrap supports for the node. New taxonomic arrangements indicated by stat. nov., sp. nov., and incertae sedis. All stat. nov. taxa were previously assigned to *Ulonemia*.

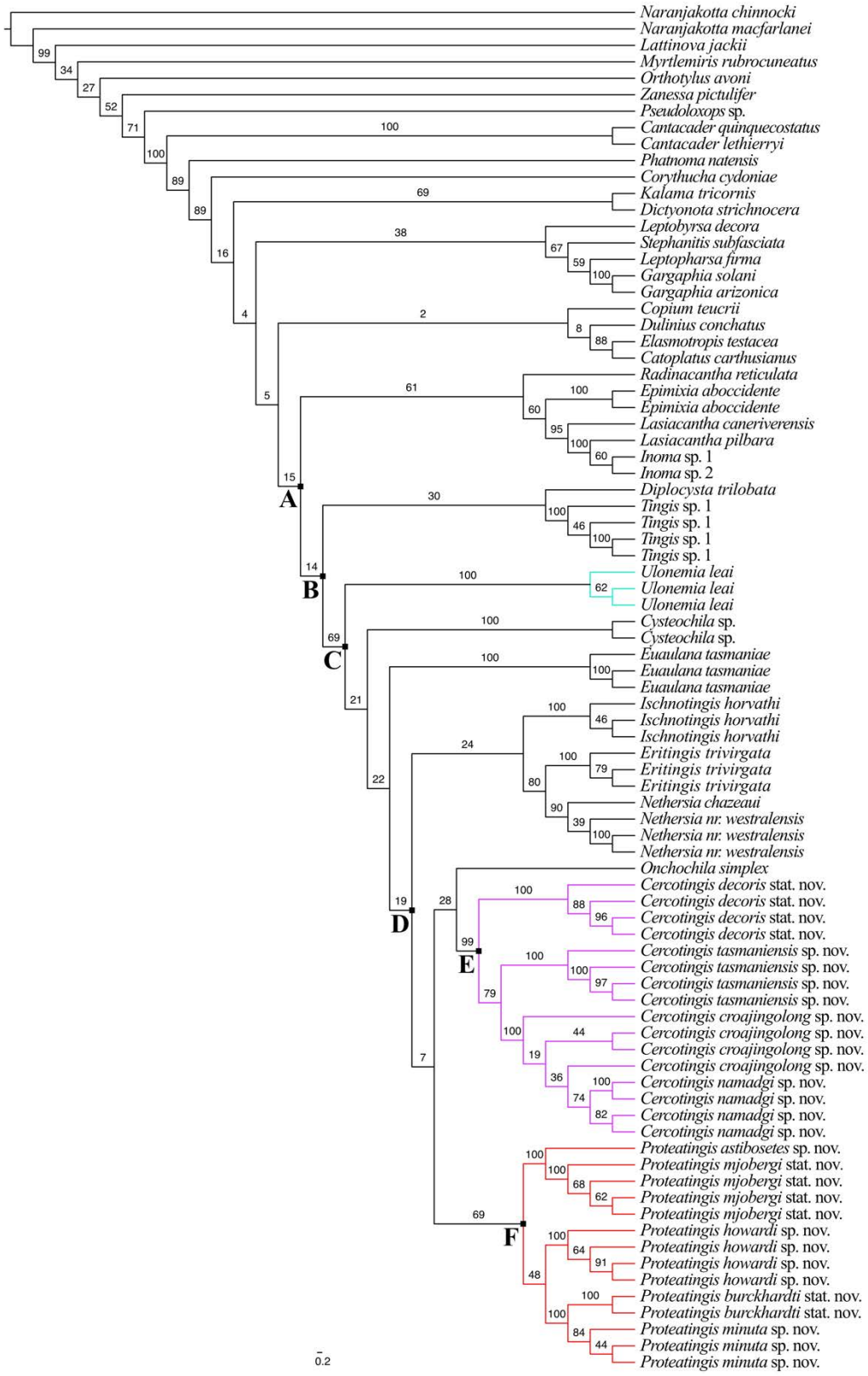

Figure 2.2. Maximum Likelihood tree produced by RAxML based on 4 molecular markers. Bootstrap supports are provided for each node. Letters indicate clades of interest; see Discussion. Coloured branches indicate *Ulonemia* sensu lato. New taxonomic arrangements indicated by stat. nov., sp. nov., and incertae sedis. All stat. nov. taxa were previously assigned to *Ulonemia*.

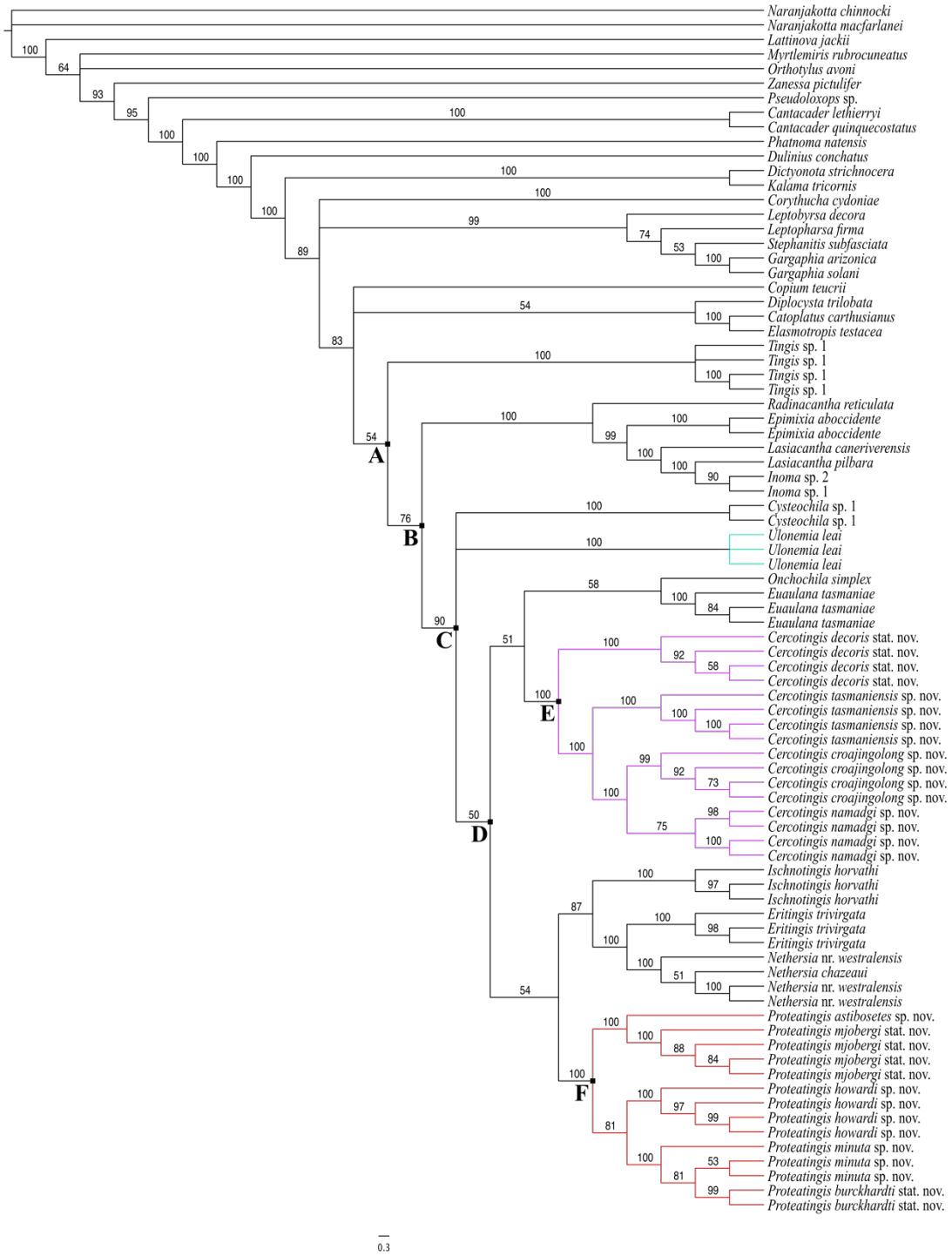

Figure 2.3. Bayesian phylogenetic inference tree produced by MrBayes based on 4 molecular markers. Bootstrap supports are provided for each node. Letters indicate clades of interest; see Discussion. Coloured branches indicate *Ulonemia* sensu lato. New taxonomic arrangements indicated by stat. nov., sp. nov., and incertae sedis. All stat. nov. taxa were previously assigned to *Ulonemia*.

CHAPTER 3. RECLASSIFICATION AND TAXONOMY OF THE GENUS *ULONEMIA* DRAKE AND POOR, 1937 AND DESCRIPTION OF NEW PROTEACEOUS-INHABITING LACE BUG TAXA (INSECTA: HETEROPTERA: TINGIDAE)

ABSTRACT

The genus *Ulonemia* Drake and Poor, 1937 is paraphyletic with respect to other Australian tingid genera with simplified morphology. Three genus-group taxa were recovered from *Ulonemia* that are specialised on the Proteaceae. Two of these groups are erected as new genera, *Cercotingis* gen. nov. and *Proteatingis* gen. nov., with *Ulonemia* redescribed as the third group. Additional genera were found that include one to several species associated with the Proteaceae, but are not exclusively associated with the family. A key to the tingid genera that occur on the Proteaceae is provided to aid identification of these groups. Three new species of *Cercotingis* (*C. croajingolong* sp. nov., *C. namadgi* sp. nov., *C. tasmaniensis* sp. nov.) and two new species of *Proteatingis* (*P. astibosetes* sp. nov., *P. howardi* sp. nov.) are described, with keys to their identification provided.

INTRODUCTION

The family Tingidae is a diverse group of heteropteran insects, with over 200 described species in Australia (Henry 2009, pers. obs.), and is known for the extravagant ornamentation of many of its members. The diverse array of morphology present in the Tingidae has often caused taxonomic confusion, especially among species with simplified features; the morphology that has defined many genera has been shown to be homoplasious (Guilbert et al. 2014), with the result that many genera are now poorly diagnosed. As demonstrated in chapter 2, some of these previously recognised genera, such as *Eritingis* Drake and Ruhoff, 1962, *Lasiacantha* Stål, 1873, *Nethersia* Horváth,

1925, *Tingis* Fabricius, 1803, and *Ulonemia* Drake and Poor, 1937, are paraphyletic. As such, their taxonomy needs to be rectified to reflect these relationships. This work focuses on the genus *Ulonemia* sensu lato, of which several species have become important economically due to their impacts on the Australian macadamia nut industry.

The Australasian tingid genus *Ulonemia* was described by Drake and Poor (1937) as a subgenus of *Perissonemia* Drake and Poor, 1937. The subgenus initially included five species, with three species (including the type species) from the Philippines, one from Borneo, and one from Singapore. Drake (1942) elevated *Ulonemia* to a genus and described three species from Australia: *U. concava*, *U. decoris*, and *U. leai*. The 1960s saw many additions to the genus, with *U. aptata* Drake, 1960 described from New Guinea, while *Perissonemia electa* Drake and Poor, 1937, *P. dignata* Drake and Poor, 1937, *P. malaccae* Drake, 1942, *Tingis assamensis* Distant, 1903, and *T. mjobergi* Horváth, 1925 were transferred to *Ulonemia* by Drake and Ruhoff (1960a). A year later, another Australian species, *U. plesia* Drake and Ruhoff, 1961, was described from Western Australia (WA). Drake and Ruhoff (1962) removed *U. recentis* and placed it in the newly erected genus *Eritingis*. In their world catalogue of Tingidae, Drake and Ruhoff (1965) transferred *U. borneenis* to *Perissonemia*, and listed 10 species within *Ulonemia*. The next work on the genus was the description of *U. burckhardti* Péricart, 1992 from New South Wales. Dang et al. (2014) redescribed *Ulonemia* and *U. assamensis*, and added three oriental species, *U. angusta* Dang et al., 2014, *U. jingae* Dang et al., 2014, and *U. magna* Dang et al., 2014, bringing the total to 13 described species in the genus, distributed in Australia, Borneo, China, India, Malaysia, New Guinea, Philippines, Taiwan, and Vietnam.

Ulonemia sensu lato has great economic importance, with several species—including one that was hitherto undescribed—causing severe damage to *Macadamia* nut

crops in eastern Australia (Huwer and Maddox 2007, Commens 2013). The rapid onset of outbreaks and sheer scale of the damage caused by *Ulonemia* spp. over the last 10 years highlights the dearth of knowledge on the genus within Australia. In addition, initial surveys of the lace bug outbreaks misidentified one species and failed to detect the other; this had real-world management implications via incorrect pesticide application permits.

The only previous mention of *Ulonemia* host plant associations was by Tomokuni (2007), who reported *U. assamensis* from Taiwan on *Helicia formosana* Hemsl., a species of Proteaceae. The presence of these tingids on proteaceous species led to an investigation of collection records to determine if any additional tingid taxa occurred on the family. Of particular interest were any species that were related to the two known *Macadamia* pests assigned to *Ulonemia*, as these could potentially cross from related host species onto *Macadamia*. Their proper identification is critical to not only detect potential pest species in *Macadamia* orchards but also formulate effective control strategies.

In this chapter, the taxonomy of *Ulonemia* sensu lato is addressed; this includes erecting two new genera and several new species, and recording the host plants for each taxon. Keys to differentiate Australian tingid genera with known associations with the Proteaceae are included, as well as keys to the species of *Cercotingis* gen. nov. and *Proteatingis* gen. nov., which incorporate species previously assigned to *Ulonemia*.

MATERIALS AND METHODS

Material examined

Over 700 specimens of *Ulonemia* sensu lato were examined, many of which were collected during Bush Blitz (http://www.bushblitz.org), a species discovery program run by the Australian Biological Resources Study (ABRS). I also examined habitus photographs of holotypes for *Tingis impensa* Drake, 1947, *U. angusta*, *U. concava*, *U. decoris*, *U. dignata*, *U. jingae*, *U. leai*, *U. magna*, and *U. plesia*. All specimens that I

physically examined were added to the Planetary Biodiversity Inventory Plant Bug (PBI) database; each specimen was labelled with a unique specimen identifier (USI) code, which are denoted in brackets after specimen details in each species description. Data associated with these specimens that is stored in the PBI database can be accessed at http://research.amnh.org/pbi/heteropteraspeciespage/. A list of tingid species associated with the Proteaceae was pulled from the PBI database to construct a key of Proteaceae-associated tingid genera (Appendix A).

Acronyms representing institutional provenance of the examined insect specimens are as follows:

AM—Australian Museum (Sydney, Australia);

AMNH—American Museum of Natural History (New York, U.S.A.);

ANIC—Australian National Insect Collection (Canberra, Australia);

ASCU—Agricultural Scientific Collections Unit, New South Wales Department of Primary Industries (Orange, NSW, Australia)

BPBM—Bernice Pauahi Bishop Museum (Honolulu, Hawai'i, U.S.A);

QDPI—Queensland Primary Industries Insect Collection (Brisbane, Australia);

QM—Queensland Museum (Brisbane, Australia);

SAMA—South Australian Museum (Adelaide, Australia);

TDAH—Tasmanian Department of Agriculture (Hobart, Australia);

TMAG—Tasmanian Museum and Art Gallery (Hobart, Australia); and

UNSW—University of New South Wales Insect Collection (Sydney, Australia).

Morphometric characters

Thirteen morphometric characters for all species of *Cercotingis* and *Proteatingis* plus *U. leai* were recorded taxa using a Leica M205C stereomicroscope with an attached Leica MC170 camera and a calibrated digital micrometre via the Leica Application Suite v4.2.

The character list includes: total body length; head length; head width; interocular distance; length of antennal segments 1 (AI), 2 (AII), 3 (AIII), and 4 (AIV); pronotal length; pronotal width; length of hemelytra; length of discoidal area; and length of the sutural area.

Genitalic dissections

Drawings of male genitalia for all species of *Cercotingis* (except *C. tasmaniensis* due to scarcity of male specimens), *Proteatingis*, and *U. leai* were included to provide diagnostic characters. The pygophore was removed from the abdomen and macerated in 10% KOH for 10 minutes to soften and clear the structures. The pygophore was then rinsed in distilled H_2O for 30 minutes and placed in glycerol for observation. The pygophore was drawn using a camera lucida attached to a Leica DM500B compound microscope. The parameres and aedeagus were removed and drawn separately after work with the pygophore was complete.

Imaging

Habitus images are provided for each species, with additional photographs of nymphs and intraspecific morphs where known. Specimens were cleaned with a small paintbrush prior to photography to remove excess debris. Images were acquired with a Canon 5D mk II DSLR and Canon MP-E 65 mm 1–5x macro lens mounted to a Visionary Digital P-51 CamLift focus system. Two Canon 430EX II speedlites were used for illumination. The camera settings for images were 1/100 seconds, f/4.5, ISO 100, at 5x magnification (except for *U. minuta*, which were taken at 7x magnification with the addition of a Canon 1.4x teleconverter), and images were recorded in RAW format. Polarisation filters were attached to the flash heads and the camera lens for cross-polarisation to eliminate any glare. Images were bracketed using the CamLift software, imported into Adobe Lightroom 5 for conversion from RAW to TIFF and for sharpening. Images were then

exported to HeliconFocus and combined into a single focus stack image using method C. The image went through final editing in Adobe Photoshop CS4; background colour was adjusted to white, and debris (dust, fibres, etc.) and mounting materials were removed.

Specimens were prepared for scanning electron micrograph (SEM) imaging by removing surface debris with a small paintbrush, then attaching the specimen, point, and pin to a small clamp-like mount. Specimens were not coated with a conductive metal, but were placed directly into the imaging chamber. Scanning electron micrographs were acquired with a Hitachi TM3000 Tabletop Microscope. Observation conditions were as follows: 15 kV accelerating voltage, charge-up reduction mode, and COMPO image observation mode. Images were adjusted for brightness and contrast, and were cropped in Adobe Photoshop CS4.

RESULTS

Tingidae genera associated with the Proteaceae

Tingid clades are often specialised with particular plant genera (Cassis and Symonds 2011, Cassis et al. 2017). Based on recent surveys (Cassis et al. 2007) numerous tingid taxa are associated with the plant family Proteaceae. Host records from the PBI database were harvested for a list of tingid taxa associated with Proteaceae (Appendix 1), including taxa putatively assigned to *Ulonemia*, as analysed in chapter 2. Three genus-group taxa were recovered from the analyses in chapter 2 that are specialised on the Proteaceae. In addition, there are several genera that have one to several species associated with the Proteaceae, but are not exclusively associated with the family. The following key accounts for all genera that have at least one species that are associated with the Proteaceae.

Key to Tingidae associated with Proteaceae

1. Paranota highly modified, extending dorsally onto pronotal disc and exceeding lateral carinae, inflated to produce paired bulbous structures (Figure 3.1a, b, *para*) 2

1'. Paranota not as above 3

2. Frons porrect, extending beyond antenniferous tubercles (Figure 3.1a, b, *frn*) .... *Cysteochila* Stål, 1873

2'. Frons flattened to slightly protruding, but never exceeding antenniferous tubercles (Figure 3.1g, *frn*) ..... *Oncophysa* Stål, 1873

3. Pair of spines present on collum, their bases proximal to medial carina (Figure 3.1c, *pdsp*) ..... *Engynoma* Drake, 1942

3'. Collum without spines 4

4. Frons porrect, extending beyond antenniferous tubercles 5

4'. Frons flattened to slightly protruding, but never exceeding antenniferous tubercles 6

5. Subcostal area 4 areolae wide; dorsal surface of pronotum and hemelytra glabrous ..... *Chorotingis* Drake, 1961

5'. Subcostal area 3 or 4 areolae wide, if 4 then dorsal surface of pronotum and hemelytra with short hairs ..... *Euaulana* Drake, 1945

6. Trochanters fused to femurs (Figure 3.1d) ..... *Epimixia* Kirkaldy, 1908

6'. Trochanters differentiated from femurs (Figure 3.1e) 7

7. Paranota absent or reduced to carina-like structure on pronotal disc; if present anteriorly, upturned and adpressed to collum (Figure 3.1f, g, *para*) 8

7'. Paranota present, areolate over entire length; if reduced posteriorly on pronotal disc, paranota never adpressed to collum (Figure 3.2a, b, e, f, *para*) 10

8. Peritreme of metathoracic gland present (Figure 3.1g); medial spine present (Figure 3.1f, g); costal area areolate..... *Eritingis* Drake and Ruhoff, 1962

8'. Peritreme of metathoracic gland absent (Figure 3.2d); medial spine absent or greatly reduced in size (Figure 3.2c, d); if medial spine present, costal area reduced to carina-like structure..... 9

9. Costal area areolate for at least portion of length; mesosternal and metasternal carinae straight, forming narrow rostral channel; dorsal surface of pronotum and hemelytra glabrous ..... *Malandiola* Horváth, 1925

9'. Costal area reduced to carina-like structure, lacking areolae; mesosternal and metasternal carinae curved, forming broad rostral channel; dorsal surface of pronotum and hemelytra usually with setae or hairs..... *Nethersia* Horváth, 1925

10. Collum raised anteriorly, forming hood (Figure 3.2b, *hd*); paranota never more than 2 areolae wide anteriorly, 1 areola wide at humeral angles (Figure 3.2a); costal area 1 areolae wide over entire length.....*Proteatingis* gen. nov.

10'. Collum flattened, or if raised, only posteriorly, never forming hood; paranota 2 or more areolae wide, 1 - 3 areolae wide at humeral angles or carina-like; costal area 1 - 2 areolae wide, at least partially..... 11

11. Costal area 1 areolae wide over entire length; dorsal surface of pronotum glabrous ..... *Ulonemia* Drake and Poor, 1937

11'. Costal area 2 areolae wide anteriorly; dorsal surface of pronotum with scale-like setae .....*Cercotingis* gen. nov.

Taxonomy

The following taxon descriptions are restricted to the genera *Cercotingis*, *Proteatingis* and *Ulonemia*; these taxa include species that are: 1) previously or were provisionally assigned to *Ulonemia* at the commencement of this study; 2) Proteaceae specialists; and 3) with at least one species with *Macadamia* as a host.

***Cercotingis* gen. nov.**

(Figures 3.2e, f, 3.3 – 3.10)

Type species

Ulonemia decoris Drake, 1942, by original designation.

Diagnosis

Cercotingis is recognised by the following combination of characters: body elongate, oblong to almost parallel-sided, hemelytra exceeding abdomen; five cephalic spines present; bucculae narrow, areolate; antennae long, slender, AI – AIII with short setae, AIV with aciculate setae; AI and AII short, AIII long, length subequal to exceeding distance between humeral angles; AIV weakly clavate; pronotum convex, tricarinate, with numerous punctures, these with 6-8 triangular tuberculate processes distributed evenly around internal rim; collum mostly flattened, lacking hood, anterior margin nearly straight to slightly concave; paranota areolate, with deeply impressed calli, mostly three areolae wide; costal area biseriate anteriorly, uniseriate for posterior 2/3; subcostal area biseriate; peritreme of metathoracic gland large, loop-like.

Male

Macropterous, 2.6 mm – 3.8 mm (Table 3.1). COLOURATION. Ground colour brown, golden brown, dark brown; calli dark brown to black; head brown, reddish brown, or dark brown; thoracic sternites usually same colour as head; abdomen similar to ground colour

but usually darker. VESTITURE. *Head*: setae in bands from antennal tubercles to frontal spines, from frontal spines along either side of medial spine to posterior margin of head, and from antennal tubercles along dorsal margin of eye; bucculae with arcuate or aciculate setae and ciliate punctures; waxy deposits often encircling eyes and from frons to antennal tubercles to apex. *Antennae*: AI-AIII with white to stramineous decumbent setae, AIV with stramineous semi-erect to erect aciculate setae; distal end of AII and AIII with dense ring of microtrichia. *Pronotum*: disc with sparse distribution of minute setae; waxy exudate deposited in calli. *Thoracic pleura and sterna*: proepisternum with anterior minute setae and numerous punctures, these with 6-8 triangular tuberculate processes distributed evenly around internal rim; posterior projection areolate, lacking punctures; proepimeron and supracoxal lobes with minute setae and tuberculate punctures; mesepisternum with minute setae; mesepimeron and supracoxal lobes with minute setae and tuberculate punctures posteriorly; metepisternum with minute setae and tuberculate punctures. *Legs*: sparse distribution of minute setae on femora and tibiae; distal end of tibiae with slightly longer setae and denser distribution. *Hemelytra*: glabrous, except R+M and cubitus veins occasionally with sparse distribution of scalelike setae. *Abdominal venter*: sparse to moderate distribution of scalelike setae. STRUCTURE. *Head*: five cephalic spines present, unbranched; frontal spines parallel or convergent. *Antennae*: AI and AII short, AII 1/2 to subequal length of AI; AIII usually longer than distance between humeral angles; AIV weakly clavate, length subequal to AI + AII. *Labium*: moderate length, extending to anterior or posterior end of metasternum. *Pronotum*: strongly convex, collum flattened, lacking hood, anterior margin nearly straight to slightly concave; tricarinate, these extending from posterior margin of collum to posterior projection of pronotum; medial and lateral carinae equal width; lateral carinae slightly to moderately divaricating anteriorly; paranota extending from anterior margin

of collum to posterior edge of disc, curved, following shape of disc; paranota areolate, with deeply impressed calli, mostly three areolae wide. *Thoracic pleura and sterna*: peritreme of the metathoracic gland loop-like, often with dorsal extension reaching margin of hemelytra. Sternal carinae elevated, uniseriate, areolae rectangular to slightly rounded; prosternal carinae straight, parallel; mesosternal carinae straight to slightly divaricating anteriorly and slightly converging posteriorly; metasternal carinae vary from straight and parallel, equal in width to mesosternal carinae, to divaricating, wider than width of mesosternal carinae. *Hemelytra*: areolae small, irregular, nearly uniform in size in discoidal and subcostal areas; sutural area areolae anteriorly similar in size to discoidal areolae, increasing in size posteriorly; subcostal area biseriate with regular arrangement of areolae; costal area biseriate anteriorly, uniseriate for posterior 2/3. *Male genitalia*: pygophore boxlike, with lateral margins tumose, occasionally with pair of basal spurs near posterior margin of genital opening; parameres C-shaped with apophysis moderately tapered distally; aedeagus with Y or U-shaped dorsal plate; endosomal membrane not spinulate; pair of elongate, spinulate lobal sclerites.

Female

Macropterous. Body 2.6 mm – 4.2 mm, usually slightly larger and wider than male. COLOURATION. As in male. VESTITURE. As in male. STRUCTURE. As in male.

Distribution

Australia, Borneo, China, India, Malaysia, New Guinea, Philippines, Taiwan, Vietnam (Drake and Ruhoff 1965, Cassis and Gross 1995, Péricart and Golub 1996, Dang et al. 2014).

Etymology

Cerco- (Greek): the tail; tingis: in relation to *Tingis*. This genus is named for the posteriorly projecting hemelytra in some species, which has been described colloquially

among entomological workers in the macadamia industry as a “fish tail” due to its shape. Noun in apposition.

Remarks

Cercotingis is morphologically similar to several other genera; there is no single character that distinguishes it, though this is true for many lace bug genera, especially among the Tingini with reduced characters. *Cercotingis* can be distinguished from *Perissonemia* by the presence of lateral carinae on the pronotum (*Perissonemia* either lacks these carinae or they are weakly developed) and the well-developed paranota (lacking in *Perissonemia*). The triseriate paranota and biseriate anterior portion of the costal area set *Cercotingis* apart from both *Proteatingis* and *Ulonemia*, as well as other similar genera such as *Eritingis* and *Nethersia*.

Checklist of Cercotingis

C. croajingolong sp. nov..... New South Wales, Victoria

C. decoris (Drake, 1942)..... New South Wales, Queensland

C. impensa (Drake, 1947) .....Tasmania

C. namadgi sp. nov. ..... Australian Capital Territory

C. tasmaniensis sp. nov.....Tasmania

Key to the species of Cercotingis

1. Metasternal carinae curved, pyriform, width greater than mesosternal carinae; posterior half of medial carina black, changing to white at apex of posterior projection of pronotum (Figure 3.3)..... *C. decoris* (Drake, 1942)

1’. Metasternal carinae straight, parallel, width equal to mesosternal carinae; posterior half of medial carina golden brown, brown, or stramineous..... 2

2. Areolae of carinae small, obscure, carinae nearly contiguous with pronotal disc (Figure 3.5)..... *C. tasmaniensis* sp. nov.

2’. Areolae of carinae large, easily seen, carinae noticeably raised above pronotal disc, not contiguous with pronotal disc 3

3. Medial and occipital spines long, exceeding height of pronotal disc; frontal spines half of length of medial spine; medial carina greatly raised, exceeding 2x height of medial carinae, biseriate, areolae fused at apex, forming a thickened mass (Figure 3.4).....*C. impensa* (Drake, 1947)

3’. Medial and occipital spines medium to short, less than height of pronotal disc; frontal spines subequal in length to medial spine; medial carina raised, less than 2x height of lateral carinae, uniseriate to biseriate, areolae not fused at apex, easily distinguished and not forming a thickened mass..... 4

4. Lateral margin of paranota free from pronotal disc, paranotal areolae laterad to pronotal disc often visible from dorsal view (Figure 3.3)..... ..... *C. croajingolong* sp. nov.

4’. Lateral margin of paranota adpressed to pronotal disc, paranotal areolae laterad to pronotal disc obscured and not visible from dorsal view (Figure 3.4)..... .....*C. namadgi* sp. nov.

***Cercotingis croajingolong* sp. nov.**

(Figures 3.3, 3.6, 3.7)

Type material

HOLOTYPE: AUSTRALIA: New South Wales: Nerriga, 35.07°S 150.05°E, Sep 1979, P. vanderDuys, *Hakea sericea* Schrad. & J. C. Wendl (Proteaceae), 1 ♂ (UNSW_ENT 00046505) (ANIC).

PARATYPES: AUSTRALIA: New South Wales: McPherson State Forest, 33.21667°S 151.13333°E, 07 Oct 1990, Tom Gush, 1 ♀ (UNSW_ENT 00046526) (ANIC). Nerriga, 35.07°S 150.05°E, Sep 1979, P. vanderDuys, *Hakea sericea* Schrad. & J. C. Wendl (Proteaceae), 2 ♂ (UNSW_ENT 00046504, UNSW_ENT 00046506), 3 ♀ (UNSW_ENT 00046507, UNSW_ENT 00046508, UNSW_ENT 00046523) (ANIC). Terrigal, 33.449°S 151.443°E, Oct 1933, RRS, 1 ♂ (UNSW_ENT 00046525) (AM). Wedderburn, 34.1485°S 150.8179°E, 18 Oct 1959, C. E. Chadwick, *Grevillea* sp. (Proteaceae), 1 ♂ (UNSW_ENT 00046524) (ASCU). Victoria**:** 5 km E of Cann River, Reedy Creek, 37.5681°S 149.2036°E, 70 m, 19 Nov 2002, Cassis, Schuh, Schwartz, Silveira, *Hakea teretifolia* (Salisb.) Britten subsp. *hirsuta* (Proteaceae), det. NSW staff NSW658194, 1 ♀ (UNSW_ENT 00046510) (AM). Coastal forest nr Mallacoota Foreshore Holiday Park, 37.56014°S 149.7588°E, 11 m, 07 Nov 2016, R. Shofner, *Hakea* sp. (Proteaceae), det. Val Stajsic & Daniel Ohlsen RBGV, 5 ♂ (UNSW_ENT 00027773-UNSW_ENT 00027777), 4 ♀ (UNSW_ENT 00027778-UNSW_ENT 00027781) (UNSW).

Other material examined

AUSTRALIA: New South Wales: Nerriga, 35.07°S 150.05°E, 19 Sep 1979, P. vanderDuys, *Hakea sericea* Schrad. & J. C. Wendl (Proteaceae), 10 mixed sex (UNSW_ENT 00046509) (ANIC).

Diagnosis

Cercotingis croajingolong is recognised by the following combination of characters: frontal and occipital spines not exceeding height of pronotal disc; lateral margin of paranota free from pronotal disc, paranotal areolae laterad to pronotal disc often visible from dorsal view; pronotal carinae elevated from pronotal disc, areolate; anterior portion

of costal margin biseriate; metasternal carinae straight, parallel, equal to width of mesosternal carinae.

Male

Macropterous; large morph 3.58 mm ± 0.10 mm (n = 5), small morph 3.14 mm (n = 1) (Table 3.1). COLOURATION (LIGHT MORPH). Brown to stramineous. *Head*: dark brown; medial spine dark brown, golden brown distally; frontal and occipital spines golden brown to stramineous; bucculae stramineous, clypeus dark brown, genae dark brown; eyes black to reddish-black. *Antennae*: AI-AII dark reddish brown, AIII golden brown, AIV golden brown proximally to dark brown distally. *Labium*: mottled stramineous and dark brown, LIV black distally. *Pronotum*: disc golden brown, golden brown to stramineous on posterior projection; calli dark brown; collum brown, paranota light brown anteriorly, dark brown posteriorly, cells translucent; lateral carinae stramineous anteriorly, brown across disc, stramineous posteriorly; medial carina stramineous anteriorly, brown across disc with black macula at apex of disc, stramineous on the posterior projection. *Thoracic pleura and sterna*: proepisternum golden brown anteriorly, dark reddish brown posteriorly, proepimeron and supracoxal lobes golden brown; mesepisternum mostly dark reddish brown, mesepimeron and supracoxal lobes golden brown; metepisternum golden brown; peritreme of metathoracic gland stramineous; prosternum and mesosternum brown, metasternum golden brown; sternal carinae stramineous. *Hemelytra*: discoidal area stramineous anteriorly, golden brown to brown medially, posterior 1 – 3 cells stramineous; costal and subcostal areas brown medially, stramineous to light brown anteriorly and posteriorly; cubitus vein with two dark brown bands; R+M vein with stramineous, golden brown, and brown bands. *Legs*: tarsi brown to dark brown, tarsal claws golden brown; tibiae golden brown; femora dark brown; trochanter golden brown; coxae dark brown. *Abdominal venter*: golden brown;

abdominal sterna mostly golden brown, darkening dorsally; spiracles dark brown; pygophore brown. COLOURATION (DARK MORPH). Dark brown with stramineous patches. *Head*: dark brown to black; medial and frontal spines dark brown to black, occipital spines dark brown; bucculae stramineous, clypeus dark brown to black, genae dark brown to black; eyes black to reddish-black. *Antennae*: AI-AII dark brown, AIII golden brown, AIV dark brown. *Labium*: golden brown, LIII and LIV dark brown to black. *Pronotum*: disc dark brown; calli dark brown to black; collum dark brown; paranota dark brown, stramineous anteriorly, cells translucent; lateral carinae stramineous, dark brown at apex of disc, stramineous to white on posterior projection; medial carina stramineous to brown, with black macula at apex of disc, stramineous to white on posterior projection. *Thoracic pleura and sterna*: proepisternum dark brown anteriorly, black posteriorly, proepimeron and supracoxal lobes brown to golden brown; mesepisternum mostly dark brown, mesepimeron and supracoxal lobes brown to golden brown; metepisternum brown to golden brown; peritreme of metathoracic gland brown; prosternum and mesosternum dark brown to black, metasternum dark brown; sternal carinae stramineous. *Hemelytra*: discoidal area stramineous anteriorly, dark brown medially, posterior 1 – 3 cells stramineous to white; costal and subcostal areas dark brown medially, stramineous to light brown anteriorly and posteriorly; cubitus vein with two black bands; R+M vein with stramineous and black bands. *Legs*: tarsi dark brown, tarsal claws golden brown; tibiae golden brown; femora brown; trochanter brown; coxae dark brown. *Abdominal venter*: dark reddish brown; spiracles dark brown to black; pygophore dark reddish brown. VESTITURE. *Head*: white decumbent setae in bands from antennal tubercles to occipital spines and from frontal spines along either side of medial spine to back of head; bucculae with short white setae; dense globules of wax covering bucculae, gena, frons, encircling eye and from frons to apex. Occipital and medial spines with white

decumbent setae. *Antennae*: AI-AIII with white to stramineous decumbent setae, AIV with stramineous semi-erect to erect aciculate setae; distal end of AII and AIII with dense ring of microtrichia. *Pronotum*: anterior margin glabrous, rarely with short setae; paranotal margins, medial and lateral carinae, and disc with short setae; disc with numerous punctures with 6-8 triangular tuberculate processes distributed evenly around internal rim; calli glabrous, globules of wax often covering calli. *Thoracic pleura and sterna*: anterior portion of proepisternum, proepimeron, posterior portion of mesepisternum, mesepimeron, and metepisternum with moderate distribution of short white setae and tubercle-lined punctures as on pronotal disc; anterior portion of pro- and mesepisternum glabrous; sternal carinae with sparse distribution of arcuate setae; all surfaces covered with small globules of wax, propluron heavily coated with wax. *Legs*: coxae to tibiae with white short setae; ventral surface of tarsi with semi-erect aciculate setae; coxae covered with wax. *Hemelytra*: costal margins glabrous or rarely sparsely covered with short setae; subcostal, discoidal, and sutural area veins glabrous; cuboidal and R+M veins with sparse distribution of white to stramineous short setae. *Abdominal venter*: moderate distribution of decumbent arcuate setae, with white wax coating entire abdomen. STRUCTURE. *Head*: spines rounded apically; frontal spines upright, parallel or convergent distally, less than half the length of AI; medial spine conical, stout, length slightly exceeding that of frontal spines, width about ½ of length; occipital spines straight, entirely protruding beyond collum or with only base of spine hidden. *Antennae*: AI and AII short, AI 2x longer than AII; AIII longer than the pronotal width across humeral angles, AIV weakly clavate. *Labium*: moderate length, exceeding anterior margin of metasternum. *Pronotum*: strongly convex; collum apex inflated to subglobose, height ½ of disc; medial and lateral carinae raised, uniseriate; medial and lateral carinae equal width, lateral carinae slightly divaricating; paranota curved, adpressed to disc medially,

upturned and erect posteriorly, two to three areolae wide, exceeding height of hemelytra, ½ height of disc. *Thoracic sterna*: mesosternal and metasternal carinae elevated, uniseriate, areolae rectangular; mesosternal carinae straight, parallel; metasternal carinae curved, convergent posteriorly. *Legs*: legs thin; femora tapered proximally. *Thoracic pleura*: peritreme large, loop-like, strongly depressed medially, with dorsal extension reaching hemelytral margin. *Hemelytra*: areolae small and uniform size in discoidal and subcostal areas; sutural area areolae similar to discoidal area proximally, increasing in size 5x to 8x distally; costal areolae large, rectangular; costal area uniseriate, subcostal area mostly biseriate, discoidal increasing from one to six areolae wide, sutural area one to eight areolae wide. *Male genitalia*: pygophore (Figure 3.6a, b); parameres (Figure 3.6c - e); aedeagus with Y-shaped dorsal plate (Figure 3.6f); endosomal membrane not spinulate (Figure 3.6f – h); pair of elongate, medium-sized, spinulate endosomal lobal sclerites (Figure 3.6f – h).

Female

Macropterous; large morph 3.66 mm ± 0.12 mm (n = 7), small morph 3.23 mm (n = 1) (Table 3.1). COLOURATION. Overall lighter than male with more pronounced patterning, stramineous to golden brown. VESTITURE. As in male. STRUCTURE. As in male.

Host plants

Recorded from the Proteaceae and the following two genera: *Grevillea* sp., 1 specimen; *Hakea sericea*, 16 specimens, *H. teretifolia*, 1 specimen; *Hakea* sp., 9 specimens.

Distribution

Known from south-eastern NSW and far north-eastern Victoria (Figure 3.7).

Etymology

Croajingolong is a derivation of the Guani word Krauatungalung, which means "belonging to the east." *Cercotingis croajingolong* takes its name both from this meaning, and from the region where many specimens were collected—near Croajingolong National Park in Victoria.

Remarks

This species has two size classes, and two colour morphs; both colour morphs are present in both size classes. Specimens of differing morphs can occur in a single population; all size class and colour morph combinations have been collected off a single shrub. This species and *C. namadgi* are very similar, but is distinguished by the free paranota (vs. adpressed to the disc on *C. namadgi*).

***Cercotingis decoris* (Drake, 1942), comb. nov.**

(Figures 3.3, 3.7, 3.8)

Ulonemia decoris Drake, 1942: 360 (original description); Drake and Ruhoff (1965: 420) (world catalogue); Cassis and Gross (1995: 437) (Australian catalogue); Dang et al. (2014: 49).

Cercotingis decoris: new combination, this work.

Type material

HOLOTYPE. ♂, AUSTRALIA: Queensland: Mt. Glorious, Jan 5 1928, H. Hacker (USNM C. J. Drake Collection 1956). Type photo examined.

Other material examined

AUSTRALIA: New South Wales: 10 mi from Dorrigo on Ebor Rd, 30.36591°S 152.6233°E, 30 Aug 1961, C. N. Smithers & A.S. Smithers, 1 ♀ (UNSW_ENT 00046464) (AM). Old Byron Bay Road, 1.4 km SE of Newrybar, 28.72962°S

153.54184°E, 111 m, Aug 2014, B. Howard, *Macadamia* sp. (Proteaceae), det. G. Cassis, 4 ♂ (UNSW_ENT 00046665-UNSW_ENT 00046668), 9 ♀ (UNSW_ENT 00046669-UNSW_ENT 00046677) (UNSW). Old Byron Bay Road, 1.6 km SE Newrybar, 28.73009°S 153.54454°E, 132 m, 14 Apr 2015, R. Shofner, G. Cassis, & W. Sherwin, *Macadamia* sp. (Proteaceae), det. G. Cassis, 6 ♂ (UNSW_ENT 00046637, UNSW_ENT 00046659-UNSW_ENT 00046663), 1 ♀ (UNSW_ENT 00046664) (UNSW). Old Byron Bay Road, 1.8 km SE of Newrybar, 28.73213°S 153.54451°E, 130 m, 02 Oct 2017, R. Shofner, *Macadamia* sp. (Proteaceae), det. R. Shofner, 1 ♂ (UNSW_ENT 00046607), 1 ♀ (UNSW_ENT 00046608) (UNSW). Queensland: Australia Zoo, 2.25 km N of Beerwah, 26.83752°S 152.96146°E, 55 m, 04 Oct 2017, R. Shofner, *Macadamia* sp. (Proteaceae), det. R. Shofner, 7 ♂ (UNSW_ENT 00046597-UNSW_ENT 00046601, UNSW_ENT 00046605, UNSW_ENT 00046606), 3 ♀ (UNSW_ENT 00046602-UNSW_ENT 00046604) (UNSW). Blackall Range, 26.7°S 152.883°E, 25 May 1966, D. A. I., *Macadamia integrifolia* Maiden & Betche (Proteaceae), 1 ♀ (UNSW_ENT 00046433), 1 ♂ (UNSW_ENT 00046434) (QDPI). Maleny, 26.767°S 152.85°E, 02 Aug 1966, D. A. I., *Macadamia integrifolia* Maiden & Betche (Proteaceae), 2 ♀ (UNSW_ENT 00046429) (QDPI); 14 Apr 1966, D. A. I., *Macadamia integrifolia* Maiden & Betche (Proteaceae), 1 ♀ (UNSW_ENT 00046430), 1 ♂ (UNSW_ENT 00046431) (QDPI). Montville, 26.69°S 152.893°E, 09 May 1967, D. A. I., *Macadamia integrifolia* Maiden & Betche (Proteaceae), 1 ♀ (UNSW_ENT 00046435) (QDPI); 24 Jun 1966, D. A. I., *Macadamia integrifolia* Maiden & Betche (Proteaceae), 1 ♀ (UNSW_ENT 00046436) (QDPI). Tamborine, 27.8809°S 153.13023°E, 30 Mar 1948, A. R. B., 3 mixed sexes (UNSW_ENT 00046432) (QDPI).

Diagnosis

Cercotingis decoris is recognised by the following combination of characters: golden brown coloration with two dark brown maculae medially on cubitus and dark brown to black inverted cordate marking covering distal end of sutural area; posterior half of medial carina black, changing to white at apex of posterior projection of pronotum; pronotal carina ridge-like, lacking areolae; paranota upturned obliquely with 2-3 rows of uniform rounded areolae; anterior portion of costal margin biseriate; distinct constriction of hemelytra at posterior edge of discoidal area; metasternal carinae curved, pyriform, width greater than mesosternal carinae; posterior half of medial carina black, changing to white at apex of posterior projection of pronotum.

Male

Macropterous; 3.27 mm ± 0.08 mm (n = 10) (Table 3.1). COLOURATION. Golden brown, with two dark brown maculae medially on cubitus and dark brown to black inverted cordate marking covering distal end of sutural area. *Head*: brown to golden brown; spines golden brown, unicolorous; bucculae stramineous, darkening to brown proximally; eyes red dorsally, fading to reddish-black ventrally. *Antennae*: AI-AIII golden brown, AIII occasionally marginally lighter; AIV brown distally, transitioning to golden brown proximally. *Rostrum*: stramineous with brown apex. *Pronotum*: disc brown centrally, fading to golden brown towards edges; calli dark brown to black; collum and paranota stramineous; lateral carinae stramineous, occasionally darker posteriorly; medial carina stramineous anteriorly, dark brown to black on the posterior projection. *Thoracic pleura and sterna*: proepisternum stramineous anteriorly, mostly orange brown posteriorly, proepimeron and supracoxal lobes stramineous; mesepisternum mostly orange brown, mesepimeron and supracoxal lobes stramineous; metepisternum golden brown to stramineous; peritreme of metathoracic gland stramineous; pro-, meso-, and

metasternum golden brown; sternal carinae stramineous. *Hemelytra*: discoidal area light brown medially, fading to stramineous at edges; costal area stramineous, except brown medially and dark brown to black distally; R+M vein with 1-2 dark brown maculae; Cubitus vein with dark brown macula medially; apex of hemelytra stramineous, with inverted cordate dark brown to black field covering distal end of sutural area, interior of cordate dark field with cordate to triangular pale blotch. *Legs*: mostly golden brown, coxae brown. *Abdominal venter*: golden brown; posterior edge of sternites II-VIII dark brown across length, sternites II-VII with black macula medially along posterior edge; spiracles dark brown. VESTITURE. *Head*: sparse distribution of golden brown aciculate setae in bands from base of AI to occipital spines and from frontal spines along either side of medial spine, to back of head. Occipital and medial spines with golden brown short aciculate to hooked setae. *Antennae*: AI-AII with golden brown sparse, aciculate arcuate setae; AIII-A-IV with golden brown aciculate decumbent setae; distal end of AII and AIII with dense ring of microtrichia. *Pronotum*: paranotal and anterior margins with arcuate aciculate setae, these continuing posteriorly on medial and lateral carinae; disc with minute setae and numerous punctures with 6-8 cilia distributed evenly around internal rim of punctures. *Thoracic pleura and sterna*: prosternum, metasternum, and mesepimeron with arcuate aciculate setae and ciliate punctures as on pronotal disc; anterior portion of mesepisternum glabrous, with arcuate aciculate setae and ciliate punctures posteriorly. *Legs*: trochanter to tibia with golden brown aciculate setae; coxae glabrous. *Hemelytra*: costal margins sparsely covered with arcuate aciculate setae; veins glabrous. *Abdominal venter*: sparse aciculate setae laterally and anteriorly, transitioning to glabrous medially and posteriorly. STRUCTURE. *Head*: spines truncate; frontal spines parallel to slightly divergent, less than half the length of AI; medial spine straight, stout, height equal to frontal spines, width about half of height; occipital spines straight, often

barely protruding beyond collum. *Antennae*: AI and AII short, AII subequal in length to AI; AIV weakly clavate. *Labium*: moderate length, extending to anterior margin of metasternum. *Pronotum*: strongly convex; collum apex inflated to subglobose, height 2/3 to subequal of disc; carinae decurrent to disc and lacking areolae, medial and lateral carinae equal width, lateral carinae divaricating; paranota curved, following disc, upturned obliquely, 2-3 areolae wide. *Thoracic sterna*: mesosternal and metasternal carinae elevated, one areole wide, areolae rectangular; mesosternal carinae straight, parallel, metasternal carinae curved, pyriform. *Hemelytra*: areolae small and uniform size in discoidal and subcostal areas; sutural area areolae similar to discoidal area proximally, increasing in size to 10x distally; costal areolae small, rectangular; costal area one areole wide, subcostal area two areolae wide, discoidal increasing from one to six areolae wide, sutural area six to nine areolae wide. *Male genitalia*: pygophore (Figure 3.8a, b); parameres (Figure 3.8c - e); aedeagus with U-shaped dorsal plate (Figure 3.8f); endosomal membrane not spinulate (Figure 3.8f – h); pair of elongate, spinulate lobal sclerites (Figure 3.8f – h).

Female

Macropterous; 3.51 mm ± 0.09 mm (n = 10) (Table 3.1). COLOURATION. As in male. VESTITURE. As in male. STRUCTURE. As in male.

Host plants

Recorded from the proteaceous genus *Macadamia*, as follows: *M. integrifolia*, 8 specimens; and *Macadamia*. sp., 32 specimens.

Distribution

Known from Mt. Glorious, Maleny, North Tamborine, and Blackall Range, Queensland, Nambucca and the Northern Rivers region of New South Wales; additionally listed in Drake (1942) from “Cornbiey,” South Australia (Figure 3.7).

Remarks

The record from “Cornbiey” was unable to be located or verified. Currently, this represents the only known *Cercotingis* from South Australia, and is geographically disjunct from other records of this species. It is possible that this record is a misidentification, an introduction, or represents a significant gap in the knowledge of this species’ range.

Cercotingis decoris is a major pest of macadamia nut crops. It has caused significant economic losses by feeding on macadamia flowers, which wilt and fail to produce nuts.

***Cercotingis impensa* (Drake, 1947), comb. nov.**

(Figures 3.4, 3.7, 3.9)

Tingis impensa Drake, 1947 (original description); Drake and Ruhoff, (1965: 400) (catalogue); Cassis and Gross, (1995: 436) (catalogue).

Cercotingis impensa: new combination, this work.

Type material

HOLOTYPE. ♂, AUSTRALIA: Tasmania, J. W. Evans (USNM C. J. Drake Collection 1956). Type photo examined.

Other material examined

AUSTRALIA: Tasmania: 1.63 km E of Marlborough Hwy on Serpentine Rd, 42.05055°S 146.55407°E, 950 m, 21 Feb 2014, G. Cassis and J. Karras, *Hakea microcarpa* R.Br. (Proteaceae), det. Miguel De Salas & Matthew Baker TMAG, 1 ♀ (UNSW_ENT 00046286) (UNSW). 3.4 km E of Marlborough Hwy on Top Marsh Conservation Rd, 42.0307°S 146.62185°E, 1050 m, 20 Feb 2014, G. Cassis and J. Karras, *Hakea microcarpa* R.Br. (Proteaceae), det. Miguel De Salas & Matthew Baker TMAG, 2 ♀

(UNSW_ENT 00046281, UNSW_ENT 00046282), 1 ♂ (UNSW_ENT 00046280) (UNSW). 4.2 km W of Marlborough Hwy on Pine Tier Lagoon Rd, 42.09188°S 146.48858°E, 727 m, 22 Feb 2014, G. Cassis and J. Karras, *Hakea microcarpa* R.Br. (Proteaceae), det. Miguel De Salas & Matthew Baker TMAG, 2 ♀ (UNSW_ENT 00046287, UNSW_ENT 00046288) (UNSW). 4.2 km W of Marlborough Rd on Pine Tier Lagoon Rd, 42.09556°S 146.4904°E, 739 m, 19 Feb 2014, G. Cassis and J. Karras, *Hakea microcarpa* R.Br. (Proteaceae), det. Miguel De Salas & Matthew Baker TMAG, 3 ♀ (UNSW_ENT 00046283-UNSW_ENT 00046285) (UNSW). Bronte Park, 7.8 km E of Marlborough Hwy on Serpentine Rd, 42.08998°S 146.5667°E, 972 m, 23 Feb 2014, G. Cassis and J. Karras, *Hakea microcarpa* R.Br. (Proteaceae), det. Miguel De Salas & Matthew Baker TMAG, 2 ♂ (UNSW_ENT 00046289, UNSW_ENT 00046290), 4 ♀ (UNSW_ENT 00046291-UNSW_ENT 00046294) (UNSW). Central Plateau, St Patricks Plains, 42.067°S 146.85°E, 20 Jan 1988, P. B. McQuillan, 1 ♀ (UNSW_ENT 00046528) (TDAH). Mt. Barrow Road, 41.37432°S 147.42551°E, 1140 m, 16 Feb 1980, A. Newton & M. Thayer, *Leptospermum* sp. (Myrtaceae), 1 ♀ (UNSW_ENT 00046527) (AMNH). Skullbone Plains, 50m N of end of track on NW corner of reserve, 42.01261°S 146.36202°E, 936 m, 27 Feb 2012, M. Cheng, 1 ♂ (UNSW_ENT 00045222) (TMAG); 01 Mar 2012, M. Cheng, 2 ♂ (UNSW_ENT 00045224, UNSW_ENT 00045225) (UNSW). Skullbone Plains, 193m N of end of track on NW corner of reserve, 42.011°S 146.36291°E, 947 m, 27 Feb 2012, M. Cheng, 1 ♂ (UNSW_ENT 00045223) (TMAG). Skullbone Plains, 366m N of end of track on NW corner of reserve, 42.00938°S 146.36302°E, 916 m, 27 Feb 2012, M. Cheng, 1 ♀ (UNSW_ENT 00045226) (UNSW). Top Marsh Conservation Area, 2.7 km SE of Marlborough Rd, 42.02773°S 146.61508°E, 1059 m, 19 Feb 2014, G. Cassis and J. Karras, *Hakea microcarpa* R.Br. (Proteaceae), det.

Miguel De Salas & Matthew Baker TMAG, 2 ♂ (UNSW_ENT 00046271, UNSW_ENT 00046272), 7 ♀ (UNSW_ENT 00046273-UNSW_ENT 00046279) (UNSW).

Diagnosis

Cercotingis impensa is recognised by the following combination of characters: medial and occipital spines long, exceeding height of pronotal disc; frontal spines half of length of medial spine; medial carina greatly raised, exceeding 2x height of medial carinae, biseriate, areolae fused at apex, forming a thickened mass; anterior portion of costal margin biseriate; metasternal carinae straight, parallel, width equal to mesosternal carinae.

Male

Macropterous; 2.66 mm ± 0.03 mm (n = 2) (Table 3.1). COLOURATION. Brown, pronotal disc brown to dark brown. *Head*: dark brown to black; medial and frontal spines dark brown; occipital spines brown proximally, darkening to dark brown distally; bucculae stramineous, clypeus dark brown, genae dark brown; eyes black. *Antennae*: dark brown. *Labium*: mottled brown and black, with LIV darkening to black. *Pronotum*: disc brown; calli black; collum and paranota brown, cells translucent; lateral carinae light brown anteriorly, brown across apex of disc, light brown posteriorly; medial carina light brown anteriorly, dark brown to blackish at carinal apex, brown on the posterior projection. *Thoracic pleura and sterna*: proepisternum brown anteriorly, dark brown posteriorly, proepimeron and supracoxal lobes brown; mesepisternum mostly dark brown, mesepimeron and supracoxal lobes brown; metepisternum brown on supracoxal lobes; peritreme of metathoracic gland brown; pro-, meso-, and metasternum dark brown; sternal carinae stramineous. *Hemelytra*: discoidal, sutural, costal, and subcostal areas brown; cubitus vein light brown with brown band medially; R+M vein light brown with brown band medially, brown posterior to juncture with cubitus vein. *Legs*: tarsi brown,

tarsal claws brown; tibiae, femora, and coxae brown. *Abdominal venter*: brown; spiracles dark brown; pygophore brown. VESTITURE. *Head*: robust white setae in bands from antennal tubercles to frontal spines, aciculate white setae in bands from frontal spines along either side of medial spine to back of head; bucculae with arcuate setae; occipital and medial spines with sparse distribution of white setae. *Antennae*: AI-AIII with sparse distribution of white setae, AIV with white semi-erect to erect aciculate setae; distal end of AII and AIII with dense ring of microtrichia. *Pronotum*: anterior margin glabrous; paranotal margins, medial and lateral carinae, collum, calli, and disc with sparse distribution of arcuate setae, posterior projection glabrous; disc with numerous punctures with 6-8 triangular tuberculate processes distributed evenly around internal rim. *Thoracic pleura and sterna*: anterior portion of proepisternum, proepimeron, posterior portion of mesepisternum, mesepimeron, and metepisternum with arcuate setae and tubercle-lined punctures as on pronotal disc; anterior portion of pro- and mesepisternum with arcuate setae. *Legs*: coxae to tibiae with arcuate setae; tarsi with arcuate setae proximally and semi-erect aciculate setae distally; sternal carinae with sparse distribution of arcuate setae. *Hemelytra*: costal margins, R+M vein, and cubitus vein with sparse distribution of arcuate setae; discoidal area with scattered setae, otherwise glabrous; sutural areas glabrous. *Abdominal venter*: moderate distribution of arcuate setae. STRUCTURE. *Head*: frontal spines upright, cylindro-conical, convergent distally, subequal to AI; medial and occipital spines long, conico-acuminate, height ≥2x that of frontal spines, width less than 1/6 height; occipital spines upright, fully protruding beyond collum, subequal to height of pronotal disc. *Antennae*: AI and AII short, AI 2x longer than AII; AIII longer than the pronotal width across humeral angles, AIV weakly clavate. *Labium*: moderate length, reaching posterior margin of metasternum. *Pronotum*: strongly convex; collum flattened, apex only marginally inflated, height less than 1/2 of disc; medial carina greatly raised,

triangular in profile, mostly uniseriate, biseriate or occasionally triseriate towards apex, with veins thickened and fused into single mass at apex; lateral carinae raised, uniseriate; medial and lateral carinae equal width posterior to apex of disc, lateral carinae slightly divaricating; paranota upright, curved, pterygoid, two to four areolae wide, height 1/2 of disc. *Thoracic sterna*: mesosternal and metasternal carinae elevated, uniseriate, areolae rectangular; mesosternal carinae straight, parallel, metasternal carinae straight, parallel, width equal to mesosternal carinae. *Legs*: legs thin; femora tapered proximally. *Thoracic pleura*: peritreme large, loop-like, with short dorsal extension reaching hemelytral margin. *Hemelytra*: areolae small and uniform size in discoidal and subcostal areas, increasing in size in subcostal area posterior from juncture of R+M and cubitus veins; sutural area areolae similar to discoidal area proximally, increasing in size to 5x - 7x distally; costal areolae large, irregular anteriorly, rectangular posteriorly; costal area biseriate for anterior half, uniseriate for posterior half; subcostal area mostly biseriate, discoidal increasing from one to six or seven areolae wide; sutural area one to eight areolae wide. *Male genitalia*: pygophore (Figure 3.9a, b); parameres (Figure 3.9c – e); aedeagus with U-shaped dorsal plate; endosomal membrane not spinulate (Figure 3.9f – h); paired endosomal sclerites greatly reduced, not spinulate (Figure 3.9f – h).

Female

Macropterous; 3.19 mm ± 0.63 mm (n = 10) (Table 3.1). COLOURATION. Mostly as in male. Discoidal area of hemelytra with more pronounced dark brown mottling than in male; costal area veins dark brown, with costal margin banded stramineous and dark brown. VESTITURE. As in male. STRUCTURE. Discoidal area increasing from one to nine areolae wide; sutural area one to ten areolae wide. Otherwise as in male.

Host plants

Recorded from two families and two genera. Myrtaceae: *Leptospermum* sp., 1 specimen. Proteaceae: *Hakea microcarpa*, 24 specimens.

Distribution

Known from Mt. Barrow State reserve, near the southern end of the Central Plateau Conservation Area, and near Bronte Park in the Top Marshes Conservation Area, Tasmania, Australia (Figure 3.7).

Remarks

This species is transferred from *Tingis* to *Cercotingis* based on the following characters: the shape of the paranota anterior to the pronotal disc, the spination of the head, the shape of the peritreme of the metathoracic gland, and the host association with Proteaceae. This species is similar to *C. croajingolong* and *C. namadgi*, but can be distinguished by its long, erect occipital and medial spines and greatly exaggerated medial carina.

***Cercotingis namadgi* sp. nov.**

(Figures 3.4, 3.7, 3.10)

Type material

HOLOTYPE: AUSTRALIA: Australian Capital Territory: Namadgi National Park, 2 km N of Glendale Depot on Boboyan Rd, 35.67207°S 148.99905°E, 862 m, 13 Dec 2013, G. Cassis and J. Karras, *Hakea microcarpa* R.Br. (Proteaceae), det. Neville Walsh RBGV, 1 ♂ (UNSW_ENT 00046235) (ANIC).

PARATYPES: AUSTRALIA: Australian Capital Territory: Namadgi National Park, 2 km N of Glendale Depot on Boboyan Rd, 35.67207°S 148.99905°E, 862 m, 13 Dec 2013, G. Cassis and J. Karras, *Hakea microcarpa* R.Br. (Proteaceae), det. Neville Walsh RBGV, 5 ♂ (UNSW_ENT 00046232-UNSW_ENT 00046234, UNSW_ENT 00046236,

UNSW_ENT 00046237), 3 ♀ (UNSW_ENT 00046238-UNSW_ENT 00046240) (UNSW). Namadgi National Park, 5.2 km N of jnct of Yaouk Rd & Boboyan Rd on Boboyan Rd, 35.88703°S 148.9857°E, 1206 m, 09 Dec 2013, G. Cassis and J. Karras, *Hakea microcarpa* R.Br. (Proteaceae), det. Neville Walsh RBGV, 4 ♂ (UNSW_ENT 00046243-UNSW_ENT 00046246), 8 ♀ (UNSW_ENT 00046247-UNSW_ENT 00046254) (UNSW). Namadgi National Park, ca. 5 km W of Orroral Gate on Cotter Hut Rd, 35.61382°S 148.91842°E, 1151 m, 10 Dec 2013, G. Cassis and J. Karras, *Hakea microcarpa* R.Br. (Proteaceae), det. Neville Walsh RBGV, 1 ♂ (UNSW_ENT 00046241), 1 ♀ (UNSW_ENT 00046242) (UNSW).

Diagnosis

Cercotingis namadgi is recognised by the following combination of characters: anterior margin of collum straight or slightly curved posteriorly; lateral margin of paranota adpressed to pronotal disc, paranotal areolae laterad to pronotal disc obscured and not visible from dorsal view; anterior portion of costal margin uniseriate or biseriate; metasternal carinae straight, parallel, width equal to mesosternal carinae.

Male

Macropterous; 3.59 mm ± 0.13 mm (n = 10) (Table 3.1). COLOURATION. Brown to dark brown. *Head*: reddish brown; medial spine reddish brown, frontal and occipital spines golden brown to brown; bucculae stramineous, clypeus dark reddish brown, genae dark reddish brown; eyes black to reddish-black. *Antennae*: AI-AII dark brown, AIII dark brown proximally, lightening to golden brown distally, AIV dark brown to black. *Labium*: golden brown, LIV black. *Pronotum*: disc dark brown, blackish laterally at the humeral angles, stramineous on posterior projection; calli dark reddish brown; collum brown, paranota brown, darkening to dark brown adjacent to the humeral angles, cells translucent; lateral carinae stramineous to brown anteriorly, brown across disc,

stramineous posteriorly; medial carina brown, with black macula at apex of disc, stramineous on the posterior projection. *Thoracic pleura and sterna*: proepisternum golden brown anteriorly, dark reddish brown posteriorly, proepimeron and supracoxal lobes golden brown; mesepisternum mostly dark reddish brown, mesepimeron and supracoxal lobes golden brown; metepisternum golden brown; peritreme of metathoracic gland golden brown; prosternum and mesosternum dark reddish brown, metasternum golden brown; sternal carinae stramineous. *Hemelytra*: discoidal area stramineous anteriorly, light brown to brown posteriorly; costal and subcostal areas light brown to brown; cubitus vein with two dark brown bands; R+M vein light brown to brown, with occasional dark brown bands. *Legs*: tarsi dark brown, tarsal claws golden brown; tibiae golden brown, occasionally dark brown proximally; femora dark brown; trochanter golden brown; coxae black. *Abdominal venter*: golden brown; abdominal sterna mostly golden brown, darkening dorsally, sternites IV-VII with brown band medially, posterior edge of sternite VIII dark brown across length; spiracles dark brown; pygophore golden brown darkening to dark brown posteriorly. VESTITURE. *Head*: white arcuate decumbent setae in bands from antennal tubercles to occipital spines and from frontal spines along either side of medial spine to back of head; bucculae with short white setae; dense globules of wax covering bucculae, gena, frons, encircling eye and from frons to apex. Occipital and medial spines with white decumbent setae. *Antennae*: AI-AIII with white to stramineous decumbent setae, AIV with stramineous semi-erect to erect aciculate setae; distal end of AII and AIII with dense ring of microtrichia. *Pronotum*: anterior margin glabrous, rarely with short setae; paranotal margins, medial and lateral carinae, and disc with short setae; disc with numerous punctures with 6-8 triangular tuberculate processes distributed evenly around internal rim; calli with short white to golden brown setae, globules of wax often covering calli. *Thoracic pleura and sterna*: anterior portion

of proepisternum, proepimeron, posterior portion of mesepisternum, mesepimeron, and metepisternum with moderate distribution of short white setae and tubercle-lined punctures as on pronotal disc; anterior portion of pro- and mesepisternum glabrous; sternal carinae with sparse distribution of arcuate setae; all surfaces covered with small globules of wax, propluron heavily coated with wax. *Legs*: coxae to tibiae with white short setae; ventral surface of tarsi with semi-erect aciculate setae; coxae covered with wax. *Hemelytra*: costal margins glabrous or rarely sparsely covered with short setae; subcostal, discoidal, and sutural area veins glabrous; cuboidal and R+M veins with sparse distribution of white to stramineous short setae. *Abdominal venter*: moderate distribution of decumbent arcuate setae, with white wax coating entire abdomen. STRUCTURE. *Head*: spines rounded apically; frontal spines upright, parallel or convergent distally, less than half the length of AI; medial spine conical, stout, length slightly exceeding that of frontal spines, width about 1/2 of length; occipital spines straight, entirely protruding beyond collum or with only base of spine hidden. *Antennae*: AI and AII short, AI 2x longer than AII; AIII longer than the pronotal width across humeral angles, AIV weakly clavate. *Labium*: moderate length, exceeding anterior margin of metasternum. *Pronotum*: strongly convex; collum apex inflated to subglobose, height 1/2 of disc; medial and lateral carinae raised, uniseriate; medial and lateral carinae equal width, lateral carinae slightly divaricating; paranota curved, adpressed to disc medially, upturned and erect posteriorly, two to three areolae wide, exceeding height of hemelytra, 1/2 height of disc. *Thoracic sterna*: mesosternal and metasternal carinae elevated, uniseriate, areolae rectangular; mesosternal carinae straight, parallel, metasternal carinae curved, convergent posteriorly. *Legs*: legs thin; femora tapered proximally. *Thoracic pleura*: peritreme large, loop-like, strongly depressed medially, with dorsal extension reaching hemelytral margin. *Hemelytra*: areolae small and uniform size in discoidal and subcostal areas; sutural area

areolae similar to discoidal area proximally, increasing in size 4x to 5x distally; costal areolae large, rectangular; costal area uniseriate, subcostal area mostly biseriate, discoidal increasing from one to six areolae wide, sutural area one to eight areolae wide. *Male genitalia*: pygophore (Figure 3.10a, b); parameres (Figure 3.10c - e); aedeagus with U-shaped dorsal plate (Figure 3.10f); endosomal membrane mostly lacking spinules, very minute when present (Figure 3.10f – h); pair of elongate, medium-sized, spinulate endosomal lobal sclerites (Figure 3.10f – h).

Female

Macropterous; 3.92 mm ± 0.11 (n = 10) (Table 3.1). COLOURATION. Overall lighter than male with more pronounced patterning, stramineous to golden brown. VESTITURE. As in male. STRUCTURE. As in male.

Host plants

Recorded from *Hakea microcarpa*, 23 specimens (Proteaceae).

Distribution

Known from Namadgi National Park in the Australian Capital Territory (Figure 3.7).

Etymology

Named for Namadgi National Park, the only location where this species is currently known.

Remarks

Cercotingis namadgi is closely related to *C. croajingolong*, and shares many characters; but are distinguishable by the adpressed paranota on *C. namadgi* (vs. free on *C. croajingolong*). This species may be an altitudinal variant or may be restricted to montane habitats.

Cercotingis tasmaniensis sp. nov.

(Figures 3.5, 3.7)

Type material

HOLOTYPE: AUSTRALIA: Tasmania: Riparian shrubland on bank of New River, 28.3 km W of Ida Bay, 43.40882°S 146.55627°E, 19 m, 08 Feb 2016, R. Shofner, *Orites diversifolius* R. Br. (Proteaceae), det. Miguel de Salas TMAG, 1 ♂ (UNSW_ENT 00046471) (TMAG).

PARATYPES: AUSTRALIA: Tasmania: Reservoir Lakes nr Mt La Perouse, 43.48327°S 146.73057°E, 800 m, 16 Feb 1988, P. B. McQuillan, 1 ♀ (UNSW_ENT 00046472) (TDAH). Riparian shrubland on bank of New River, 28.3 km W of Ida Bay, 43.40882°S 146.55627°E, 19 m, 08 Feb 2016, R. Shofner, *Orites diversifolius* R. Br. (Proteaceae), det. Miguel de Salas TMAG, 1 ♀ (UNSW_ENT 00027448) (UNSW).

Diagnosis

Cercotingis tasmaniensis can be recognised by the following combination of characters: posterior half of medial carina golden brown, brown, or stramineous; areolae of pronotal carinae small, obscure, carinae nearly contiguous with pronotal disc; paranota areolate along entire length, areolae easily visible and well-defined; anterior portion of costal margin biseriate; metasternal carinae straight, parallel, width equal to mesosternal carinae.

Male

Macropterous; 3.43 mm (n = 1) (Table 3.1). COLOURATION. Brown to stramineous. *Head*: brown to dark brown; spines golden brown to stramineous; bucculae stramineous; eyes red. *Antennae*: AI-AIII golden brown, AIV golden brown, darkening apically. *Rostrum*: golden brown with dark brown to black band proximally on second segment, dark brown to black apex. *Pronotum*: disc brown; calli dark brown; collum and paranota

brown to golden brown; lateral and medial carinae stramineous anteriorly, dark brown medially, black posteriorly. *Thoracic pleura and sterna*: proepisternum golden brown anteriorly, mostly dark brown posteriorly, proepimeron and supracoxal lobes golden brown to stramineous; mesepisternum mostly dark brown, mesepimeron and supracoxal lobes golden brown to stramineous; metepisternum dark brown anteriorly, golden brown posteriorly; peritreme of metathoracic gland stramineous; pro-, meso-, and metasternum golden brown to brown; prosternal carinae dark brown, mesosternal and metasternal carinae stramineous. *Hemelytra*: discoidal area stramineous proximally, darkening to golden brown distally, with dark brown to black blotch on cubitus vein; subcostal area stramineous proximally, darkening to dark brown distally, costal margin stramineous with dark brown costal veins; sutural area stramineous along interior margin, remainder brown; apex of hemelytra golden brown, with inverted cordate dark brown field covering distal end of sutural area, with smaller cordate pale blotch incised into distal end of dark blotch. *Legs*: mostly golden brown, coxae dark brown; tarsi dark brown to black distally. *Abdominal venter*: golden brown, posterior margin of abdominal sternites III-IX dark brown; AII dark brown. VESTITURE. *Head*: distribution of golden brown aciculate setae in bands from base of AI to occipital spines and from frontal spines along either side of medial spine, to back of head; frons and gena with stramineous aciculate setae; medial spine with stramineous short aciculate to hooked setae; vertex with large globules of wax; bucculae with arcuate aciculate setae and ciliate punctures. *Antennae*: AI-AII with stramineous sparse, aciculate arcuate setae; AIII with stramineous aciculate decumbent setae, AIV with stramineous aciculate setae; distal end of AII and AIII with dense ring of microtrichia. *Pronotum*: anterior margin mostly glabrous, with occasional arcuate aciculate setae; paranotal margins with arcuate aciculate setae; medial and lateral carinae mostly glabrous, with occasional arcuate aciculate setae; disc with minute setae and

numerous punctures with 6-8 cilia distributed evenly around internal rim of punctures; calli often with globules of wax. *Thoracic pleura and sterna*: proepisternum with arcuate aciculate setae and ciliate punctures anteriorly as on pronotal disc, lacking ciliate punctures posteriorly, proepimeron and supracoxal lobes with arcuate aciculate setae and ciliate punctures; mesepisternum with arcuate aciculate setae, mesepimeron and supracoxal lobes with arcuate aciculate setae and ciliate punctures posteriorly; metepisternum with arcuate aciculate setae and ciliate punctures; pro-, meso-, and metapluron covered with small wax globules. *Legs*: trochanter to tarsus with golden brown aciculate setae; coxae with single row of arcuate aciculate setae. *Hemelytra*: glabrous, rarely with short aciculate setae on veins. *Abdominal venter*: aciculate setae and wax distributed throughout. STRUCTURE. *Head*: frontal spines slightly conical, convergent, approximately 1/3 length of AI; medial spine stout, conical, height approximately 1/2 of AI; occipital spines straight, cylindrical to weakly clavate, exceeding length of medial spine, easily exceeding anterior edge of collum. *Antennae*: AI and AII short, AII 1/2 length of AI; AIV weakly clavate. *Labium*: moderate length, extending to posterior margin of metasternum. *Pronotum*: strongly convex; collum apex inflated to subglobose, height 1/2 of disc; carinae decumbent on disc, slightly elevated posteriorly; medial and lateral carinae equal width, lateral carinae strongly divaricating anteriorly; paranota curved, following disc, upturned, nearly adpressed to disc, biseriate to triseriate, areolae irregular. *Thoracic sterna*: mesosternal and metasternal carinae elevated, uniseriate, areolae rectangular; mesosternal carinae straight, parallel, metasternal carinae straight to slightly curved. *Hemelytra*: areolae small, irregular, and nearly uniform size in discoidal and subcostal areas; sutural area areolae similar to discoidal area proximally, increasing in size to 10x distally; costal areolae irregular proximally, large, rectangular distally; costal area biseriate proximally to uniseriate

distally, subcostal area biseriate, discoidal increasing from one to eight areolae wide, sutural area increasing from two to nine areolae wide. *Male genitalia*: not examined.

Females

Macropterous; 3.38 – 3.49 mm (n = 2) (Table 3.1). COLOURATION. As in male. VESTITURE. As in male. STRUCTURE. Noticeably broader than males; otherwise as in male.

Host plants

Recorded from *Orites diversifolius*, 2 specimens (Proteaceae).

Distribution

Known from Southwest National Park near Ida Bay, and Reservoir Lakes near Mt. Peruse, Tasmania (Figure 3.7).

Remarks

This species is similar to *C. decoris*, but can be distinguished by the shape of the metasternal carinae.

***Proteatingis* gen. nov.**

(Figures 3.2a, b, 3.5, 3.11 – 3.20)

Type species

Tingis mjobergi Horváth, 1925 by original designation.

Diagnosis

The genus *Proteatingis* is recognised by the following combination of characters: body elongate and almost parallel-sided to slightly rounded; five cephalic spines; bucculae narrow, areolate; antennae long, slender, AI – AIII with short setae, AIV with aciculate setae; AI and AII short, AIII long, length subequal to exceeding distance between humeral angles, AIV weakly clavate; body elongate, oblong to parallel-sided, hemelytra exceeding

abdomen; collum raised, slightly inflated, projecting slightly forward over head to form hood; pronotum convex, tricarinate, with numerous punctures, these with 6-8 triangular tuberculate processes distributed evenly around internal rim; paranota areolate across collum and pronotal disc with deeply impressed calli, uniseriate posterior to calli; costal area uniseriate, subcostal area biseriate; peritreme of metathoracic gland large, loop-like.

Male

Macropterous, 2.5 mm – 3.5 mm (Table 3.1). COLOURATION. Ground colour stramineous, brown, golden brown, dark brown; calli brown, dark brown, or black; head brown, reddish brown, dark brown, or black; thoracic sternites usually same colour as head; abdomen similar to ground colour but usually darker. VESTITURE. *Head*: setae in bands from antennal tubercles to frontal spines, and from frontal spines along either side of medial spine to back of head, and from antennal tubercles along dorsal margin of eye; bucculae with arcuate or aciculate setae and ciliate punctures; waxy deposits often encircling eye and from frons to antennal tubercles to apex. *Antennae*: AI-AIII with white to stramineous decumbent setae, AIV with stramineous semi-erect to erect aciculate setae; distal end of AII and AIII with dense ring of microtrichia. *Pronotum*: disc with sparse distribution of minute setae; waxy exudate deposited in calli. *Thoracic pleura and sterna*: proepisternum with anterior minute setae and numerous punctures, these with 6-8 triangular tuberculate processes distributed evenly around internal rim, lacking these punctures posteriorly; proepimeron and supracoxal lobes with minute setae and tuberculate punctures; mesepisternum with minute setae; mesepimeron and supracoxal lobes with minute setae and tuberculate punctures posteriorly; metepisternum with minute setae and tuberculate punctures. *Legs*: sparse distribution of minute setae on femora and tibiae; distal end of tibiae with slightly longer setae and denser distribution. *Hemelytra*: glabrous, except R+M and cubitus veins with sparse distribution of minute

setae. *Abdominal venter*: sparse to moderate distribution of minute setae, usually pruinose. STRUCTURE. *Head*: five cephalic spines present, unbranched; frontal spines parallel or convergent. *Antennae*: AI and AII short, AII 1/2 to subequal length of AI; AIII usually longer than distance between humeral angles; AIV weakly clavate, length roughly equal to AI + AII. *Labium*: moderate length, extending to anterior or posterior end of metasternum. *Paranota*: paranota areolate across collum and disc with deeply impressed calli, uniseriate posterior to calli. *Pronotum*: strongly convex, collum slightly raised, slightly inflated posteriorly; dorsal surface of disc with numerous punctures, these with 6-8 triangular tuberculate processes distributed evenly around internal rim; tricarinate, these extending from posterior margin of collum to posterior projection of pronotum; medial and lateral carinae equal width; lateral carinae slightly to moderately divaricating anteriorly; paranota extending from anterior margin of collum to posterior edge of disc, curved, following shape of disc; paranota areolate across collum, carina-like to areolate across disc. *Thoracic pleura and sterna*: peritreme of the metathoracic gland loop-like, often with dorsal extension reaching margin of hemelytra. Sternal carinae elevated, uniseriate, areolae rectangular to slightly rounded; prosternal carinae straight, parallel; mesosternal carinae straight to slightly divaricating anteriorly and slightly converging posteriorly; metasternal carinae vary from straight and parallel, equal in width to mesosternal carinae, to divaricating, wider than width of mesosternal carinae. *Hemelytra*: areolae small, irregular, nearly uniform in size in discoidal and subcostal areas; sutural area areolae anteriorly similar in size to discoidal areolae, increasing in size posteriorly; subcostal area biseriate with regular arrangement of areolae; costal area uniseriate. *Male genitalia*: pygophore boxlike, with lateral margins tumose, sometimes with pair of basal spurs near posterior margin of genital margin; parameres C-shaped with apophysis strongly tapered distally; aedeagus with Y-shaped dorsal plate; endosomal membrane

usually heavily spinulate; pair of sclerotised, hooklike lobal sclerites rarely with elongate spinulate endosomal lobal sclerites.

Female

Macropterous. Body 2.6 mm – 3.8 mm (Table 3.1), usually slightly larger and wider than male. COLOURATION. As in male. VESTITURE. As in male. STRUCTURE. As in male.

Distribution

Australia (Drake and Ruhoff 1965, Cassis and Gross 1995, Péricart and Golub 1996, Dang et al. 2014): ACT, NSW, NT, QLD, VIC, and WA.

Etymology

This genus is named for its host affiliation with members of the Proteaceae.

Remarks

Like *Cercotingis*, *Proteatingis* is morphologically similar to several other genera; there is no single character that distinguishes it. It is defined polythetically by a combination of characters (as in Diagnosis, above). *Proteatingis* can be distinguished from *Perissonemia* by the presence of lateral carinae on the pronotum (*Perissonemia* either lacks these carinae or they are weakly developed) and the well-developed paranota (lacking in *Perissonemia*). The uniseriate paranota and entirely uniseriate costal area sets *Proteatingis* apart from *Cercotingis*. Additionally, the hood of *Proteatingis* differentiates the genus from *Cercotingis*, *Ulonemia*, as well as other similar genera such as *Eritingis* and *Nethersia*.

Checklist of Proteatingis

P. astibosetes sp. nov. ..... New South Wales, Queensland

P. burckhardti (Péricart, 1992) ..... Australian Capital Territory, New South Wales, Victoria

P. howardi sp. nov. ..... New South Wales, Queensland

P. minuta sp. nov. .....Tasmania

P. mjobergi (Horváth, 1925)..... Northern Territory, Queensland

P. plesia (Drake & Ruhoff, 1961)..... Western Australia

Key to the species of Proteatingis

1. Total length excluding antennae less than 2.8 mm; Tasmania..... ..... *P. minuta* sp. nov.

1'. Total length excluding antennae greater than 2.9 mm; Tasmania, mainland Australia 2

2. Costal areolae irregular, reticulated, biseriate more than half the length of costal area; dorsal surface with prominent pattern of dark brown reticulations..... ..... *P. howardi* sp. nov.

2'. Costal areolae square to rectangular, uniseriate; if reticulate or biseriate, these confined to anterior third of costal margin, transitioning to square or rectangular areolae posteriorly; dorsal pattern variable, never with prominent reticulations 3

3. Paranota carina-like across pronotal disc .....*P. astibosetes* sp. nov.

3'. Paranota areolate along entire length, areolae easily visible and well-defined..... 4

4. Antennal segment I black; Pilbara and southwest WA .... *P. plesia* (Drake & Ruhoff, 1961)

4’. Antennal segment I brown, golden brown, reddish brown, or dark brown, never black; Tasmania, mainland Australia except Pilbara and southwest WA 5

5. Metasternal carinae straight, parallel, width equal to mesosternal carinae; areolae of lateral carinae small, obscure; eyes black; head black ....*P. burckhardti* (Péricart, 1992)

5’. Metasternal carinae curved, obovate, width greater than mesosternal carinae; areolae of lateral carinae large, easily seen; eyes red; head brown to dark brown .... *P. mjobergi* (Horváth, 1925)

***Proteatingis astibosetes* sp. nov.**

(Figures 3.5, 3.11, 3.12)

Type material

HOLOTYPE: AUSTRALIA: Queensland: Bochow Park picnic area, Natural Bridge, 28.19902°S 153.2298°E, 173 m, 05 Oct 2017, R. Shofner, *Grevillea robusta* A. Cunn. ex R. Br. (Proteaceae), det. R. Shofner, 1 ♂ (UNSW_ENT 00046590) (QM). **PARATYPES:** AUSTRALIA: New South Wales: Bogan River, 33.0068°S 148.03461°E, J. Armstrong, 6 ♀ (UNSW_ENT 00046511) (AM). Queensland: 91 km N of Quilpie, 25.99847°S 144.4098°E, 300 m, 02 Nov 1998, Schuh, Cassis, Silveira, *Amyema quandang* (Lindley) Tieghem *var. quandang* (Loranthaceae), det. Det: Royal Bot Gard. NSW NSW427341, 1 ♀ (UNSW_ENT 00046514) *Hakea leucoptera* R. Br. (Proteaceae) NSW 427661, 1 ♀ (UNSW_ENT 00046512), 1 ♂ (UNSW_ENT 00046513) (AM). Bochow Park picnic area, Natural Bridge, 28.19902°S 153.2298°E, 173 m, 05 Oct 2017, R. Shofner, *Grevillea robusta* A. Cunn. ex R. Br. (Proteaceae), det. R. Shofner, 1 ♀ (UNSW_ENT 00046589) (UNSW). Mt Glorious, Basset site,

27.31666°S 152.75°E, 700 m, Nov 1987, Y. Basset, *Argyrodendron actinophyllum* (Malvaceae), 1 ♀ (AMNH_PBI 00037422) (QM).

Diagnosis

Proteatingis astibosetes is recognised by the following combination of characters: occipital spines extending to midpoint of eyes; paranota with large areola laterad to pronotal disc, 3x size of other paranotal areolae; paranota carina-like across pronotal disc; medial and lateral carinae slightly raised, uniseriate; hemelytra width subequal to width across humeral angles; discoidal area 5 – 6 areolae wide; metasternal carinae divaricating, convergent posteriorly.

Male

Body 3.33 mm ± 0.08 mm (n = 2) (Table 3.1). COLOURATION. Brown to stramineous. *Head*: dark brown to black; medial spine brown, frontal and occipital spines golden brown to stramineous; antennal tubercles reddish brown; bucculae stramineous, clypeus dark reddish brown, genae black; eyes red in fresh specimens, black in older material. *Antennae*: AI-AII brown, AIII golden brown, AIV brown. *Labium*: golden brown, LIV black. *Pronotum*: disc brown to stramineous; calli black; collum brown to stramineous, paranota brown to stramineous, cells translucent; lateral carinae stramineous; medial carina brown to stramineous. *Thoracic pleura and sterna*: proepisternum golden brown anteriorly, black posteriorly, proepimeron black anteriorly, becoming golden brown posteriorly, stramineous along posterior edge, supracoxal lobes golden brown; mesepisternum mostly black, mesepimeron golden brown dorsally, supracoxal lobes golden brown; metepisternum black anteriorly, becoming golden brown posteriorly, stramineous along posterior edge, supracoxal lobes golden brown; peritreme of metathoracic gland stramineous; prosternum and mesosternum dark reddish brown, metasternum golden brown; sternal carinae stramineous. *Hemelytra*: brown to

stramineous, discoidal area occasionally darker than the rest of the hemelytra; cubitus vein occasionally with dark brown band. *Legs*: tarsi golden brown proximally to dark brown distally, tarsal claws golden brown; tibiae golden brown, occasionally dark brown proximally; femora dark brown; trochanter golden brown; coxae black. *Abdominal venter*: golden brown; abdominal sterna mostly golden brown, darkening dorsally, sternites IV-VII with brown band medially, posterior edge of sternite VIII dark brown across length; spiracles dark brown; pygophore golden brown darkening to dark brown posteriorly. VESTITURE. *Head*: apex pruinose; bucculae with short white setae. Frontal, occipital, and medial spines pruinose, occasionally with globules of wax. *Antennae*: AI pruinose; AI-AIII with white to stramineous decumbent setae, AIV with stramineous semi-erect to erect aciculate setae; distal end of AII and AIII with dense ring of microtrichia. *Pronotum*: anterior margin glabrous to slightly pruinose; paranotal margins, medial and lateral carinae, and disc with short setae; disc and collum pruinose; disc with numerous punctures with 6-8 triangular tuberculate processes distributed evenly around internal rim; calli glabrous but with globules of wax. *Thoracic pleura and sterna*: anterior portion of proepisternum, proepimeron, posterior portion of mesepisternum, mesepimeron, and metepisternum with moderate distribution of short white setae and tubercle-lined punctures as on pronotal disc; anterior portion of pro- and mesepisternum glabrous; sternal carinae with sparse distribution of arcuate setae; all surfaces covered with small globules of wax, propluron heavily coated with wax. *Legs*: coxae to tibiae with white short setae; ventral surface of tarsi with semi-erect aciculate setae; coxae covered with wax. *Hemelytra*: costal margins glabrous; subcostal veins pruinose; discoidal area veins lightly pruinose to glabrous; sutural area veins glabrous; cuboidal and R+M veins with sparse distribution of white to stramineous short setae. *Abdominal venter*: moderate distribution of decumbent arcuate setae, with white wax coating entire abdomen.

STRUCTURE. *Head*: frontal spines upright, oblong to slightly conical, convergent distally, approximately 1/3 length of AI; medial spine conical, length 2x that of frontal spines, width about 1/4 of length; occipital spines straight, rounded apically, extending to midpoint of eyes. *Antennae*: AI and AII short, AII 3/4 length of AI; AIII longer than the pronotal width across humeral angles, AIV weakly clavate. *Labium*: moderate length, exceeding anterior margin of metasternum. *Pronotum*: strongly convex; collum apex slightly inflated, height 1/2 of disc; medial and lateral carinae slightly raised, uniseriate, increasing in height on posterior projection of pronotum; medial and lateral carinae equal width, lateral carinae divaricating; paranota curved, following disc, upturned anteriorly, two areolae wide, a single areola 3x larger than surrounding areolae laterad to collum; paranota becoming carina-like posteriorly, barely exceeding height of hemelytra. *Thoracic sterna*: pro-, meso-, and metasternal carinae elevated, uniseriate, areolae rectangular; prosternal carinae straight, parallel; mesosternal carinae straight to slightly divaricating anteriorly and slightly converging posteriorly; metasternal carinae wider than mesosternal carinae, parallel or slightly horseshoe-shaped, slightly convergent posteriorly. *Legs*: legs thin; femora tapered proximally. *Thoracic pleura and sterna*: peritreme large, loop-like, strongly depressed medially, with dorsal extension reaching hemelytral margin. *Hemelytra*: areolae small and uniform size in discoidal and subcostal areas; sutural area areolae similar to discoidal area proximally, increasing in size 3x to 4x distally; costal areolae large, rectangular; costal area uniseriate; subcostal area biseriate; discoidal increasing from one to five or six areolae wide; sutural area one to eight areolae wide; hemelytra width subequal to width across humeral angles. *Male genitalia*: pygophore (Figure 3.11a, b); parameres (Figure 3.11c – e); dorsal plate Y-shaped (Figure 3.11f); aedeagus with paired large endosomal lobal sclerites (Figure 3.11f – h); endosomal spinulation variable in size, with some spinules enlarged (Figure 3.11f – h).

Female

Body 3.62 mm ± 0.15 mm (n = 6) (Table 3.1). COLOURATION. Overall lighter than male with more pronounced patterning, stramineous to golden brown. VESTITURE. As in male. STRUCTURE. As in male.

Host plants

Recorded from 3 families and 4 genera. Loranthaceae: *Amyema quandang* var. *quandang*, 1 specimen. Malvaceae: *Argyrodendron actinophyllum*, 1 specimen. Proteaceae: *Grevillea robusta*, 2 specimens; *Hakea leucoptera*, 2 specimens.

Distribution

Found in scattered localities from the Channel Country of central Queensland and northern New South Wales, as well as the Border Ranges and the vicinity of Mt. Glorious, Queensland (Figure 3.12).

Etymology

From the Greek astibos, meaning “desert” or a “pathless place,” and –etes, meaning “to dwell.” This name refers to the geographic distribution and habitat of this species, which is the only *Proteatingis* to inhabit the vast and arid interior of Australia. Noun in apposition.

Remarks

Proteatingis astibosetes has a narrower body form than most other *Proteatingis* and lacks the distinctive “waist” that other narrow-body species possess. In addition, the areolae of the paranota are unique in that there is a single large areola present that is approximately 3x larger than the other paranotal areolae (vs. all other *Proteatingis*, which have paranotal areolae all of subequal size).

Proteatingis burckhardti (Péricart, 1992), comb. nov.

(Figures 3.12 – 3.14)

Ulonemia burckhardti Péricart, 1992: 83 (original description); Cassis and Gross (1995: 437) (Australian catalogue); Dang et al. (2014: 49).

Proteatingis burckhardti: new combination, this work.

Material examined

AUSTRALIA: Australian Capital Territory: Black Mountain, 35.26387°S 149.10051°E, 26 Nov 1959, G. F. Gross, 1 unknown sex (UNSW_ENT 00046466) (SAMA). Black Mtn., 35.16°S 149.06°E, 1 Dec 1960, C. N. Smithers, 1 ♀ (UNSW_ENT 00046408), 1 ♂ (UNSW_ENT 00046409) (AM); 19 Nov 1985, G. Cassis, *Acacia decurrens* Willd. (Fabaceae), 1 ♂ (UNSW_ENT 00046411) (AM); 3 Oct 1988, G. Cassis, parrot pea, 1 ♀ (UNSW_ENT 00046410) (AM). Namadgi National Park, Honeysuckle Creek Campground, 35.58357°S 148.97598°E, 1126 m, 11 Dec 2013, G. Cassis and J. Karras, *Grevillea rosmarinifolia* A. Cunn. (Proteaceae), det. Neville Walsh RBGV, 43 ♂ (UNSW_ENT 00046112-UNSW_ENT 00046131, UNSW_ENT 00046166-UNSW_ENT 00046185, UNSW_ENT 00046187, UNSW_ENT 00046186, UNSW_ENT 00046193), 117 ♀ (UNSW_ENT 00046132-AMNH_IZC 00046141, UNSW_ENT 00046133-UNSW_ENT 00046165, UNSW_ENT 00046195, UNSW_ENT 00046196), 1 unknown sex (UNSW_ENT 00046188), 4 unknown sex (UNSW_ENT 00046189-UNSW_ENT 00046192) *Grevillea lanigera* A. Cunn. ex R.Br. (Proteaceae), det. Neville Walsh RBGV, 4 ♀ (UNSW_ENT 00046197-UNSW_ENT 00046200), 1 unknown sex (UNSW_ENT 00046201) (UNSW). Namadgi National Park, ca. 5 km W of Orroral Gate on Cotter Hut Rd, 35.61382°S 148.91842°E, 1,151 m, 10 Dec 2013, G. Cassis and J. Karras, *Grevillea lanigera* A. Cunn. ex R.Br. (Proteaceae), det. Neville Walsh RBGV, 13 ♂ (UNSW_ENT 00046202-UNSW_ENT 00046214), 17 ♀

(UNSW_ENT 00046215-UNSW_ENT 00046231) (UNSW). New South Wales: 0.7 km N of jn. Darkes Forest Rd on Old Princes Hwy, 34.23285°S 150.94483°E, 360 m, 11 Sep 2000, G. Cassis and R. Silveira, 6 ♂ (UNSW_ENT 00046368-UNSW_ENT 00046373), 5 ♀ (UNSW_ENT 00046374-UNSW_ENT 00046378), 1; (UNSW_ENT 00046379) (UNSW). Cheltenham, 33.7568°S 151.0846°E, 13 Nov 1960, C. E. Chadwick, *Leptospermum flavescens* Sm. (Myrtaceae), 1 ♀ (UNSW_ENT 00046426) (ASCU). Fullers Bridge, 33.799°S 151.151°E, Unknown, 1 ♀ (AMNH_PBI 00011743) (AM). Fullers Bridge, Lane Cove River, 33.79269°S 151.15705°E, 6 m, Oct 1934, K. K. Spence, 1 ♀ (UNSW_ENT 00046415) (AM). Narrabeen, 33.71666°S 151.3°E, 10 Nov 1902, W. B. G., 1 ♂ (UNSW_ENT 00046425) (ASCU). Royal National Park, 34.072°S 151.05789°E, 20 m, 2002, Schwartz and Silveira, *Allocasuarina* sp. (Casuarinaceae), det. Field ID, 1 ♀ (UNSW_ENT 00046407) *Angophora hispida* (Sm.) Blaxell (Myrtaceae), det. Field ID, 2 ♀ (UNSW_ENT 00046396, UNSW_ENT 00046397) *Grevillea buxifolia* (Sm.) R. Br. (Proteaceae), det. Field ID, 5 ♂ (UNSW_ENT 00046398-UNSW_ENT 00046402), 4 ♀ (UNSW_ENT 00046403-UNSW_ENT 00046406) *Grevillea* sp. (Proteaceae), det. Field ID, 1 ♂ (UNSW_ENT 00046389), 6 ♀ (UNSW_ENT 00046390-UNSW_ENT 00046395) (AM). Royal National Park, Audley tip, 34.04°S 151.03°E, 06 Dec 2006, Reid & Dungelhoef, 1 ♀ (UNSW_ENT 00046465) (UNSW). Royal National Park, Coast Track, Wattamolla – Curracurrang, 34.1377°S 151.11335°E, 29 m, 04 Oct 2000, R. Silveira and M. Elliott, 5 ♂ (UNSW_ENT 00046360-UNSW_ENT 00046364), 3 ♀ (UNSW_ENT 00046365-UNSW_ENT 00046367) (UNSW). Royal National Park, The Coast Walk – Bundeena, 34.09172°S 151.15722°E, 77 m, 26 Nov 2001, Cassis, Schuh, and Schwartz, *Grevillea buxifolia* (Sm.) R. Br. (Proteaceae), det. Field ID, 3 ♂ (UNSW_ENT 00046381-UNSW_ENT

00046383), 5 ♀ (UNSW_ENT 00046384-UNSW_ENT 00046388) (AM). Springwood [Gully], Sassafras Gully, 33.7152°S 150.5512°E, 09 Dec 1966, C. Smithers, 1 ♀ (UNSW_ENT 00046418) (AM). Sydney, 33.8652°S 151.20959°E, no date provided, Unknown, 3 ♀ (UNSW_ENT 00046413, UNSW_ENT 00046414, UNSW_ENT 00046416), 1 ♂ (UNSW_ENT 00046417) (AM). Wedderburn, 34.1485°S 150.8179°E, 18 Oct 1959, C. E. Chadwick, *Grevillea* sp. (Proteaceae), 6 mixed sexes (UNSW_ENT 00046427, UNSW_ENT 00046428) (ASCU). Woronora Dam district, 34.1163°S 150.94901°E, 259 m, 11 Sep 2000, G. Cassis and R. Silveira, 1 ♀ (UNSW_ENT 00046380) (UNSW). Nr. McMahon's Pt. King's Tableland Rd. Wentworth Falls, 33.88745°S 150.38481°E, 19 Jan 1990, G. Cassis, *Eucalyptus* sp. (Myrtaceae), 1 ♂ (UNSW_ENT 00046419), 5 ♀ (UNSW_ENT 00046420-UNSW_ENT 00046424) (AM). Victoria: Grampians nr peak Mt. William, 37.29277°S 142.60114°E, 1167 m, 05 May 1978, J. J. H. Szent-Ivany, 1 ♂ (UNSW_ENT 00046412) (SAMA). Lake Condah Mission, 38.07646°S 141.788°E, 25 Mar 2011, M. Cheng & A. Namyatova, *Grevillea rosmarinifolia* A. Cunn. (Proteaceae), det. V. Stajsic, 4 ♀ (UNSW_ENT 00046356-UNSW_ENT 00046359) (UNSW).

Diagnosis

Proteatingis burckhardti can be recognised by the following combination of characters: head black; eyes black; anterior margin of collum curved, projecting forward; collum moderately inflated, forming a hood; costal area uniseriate; metasternal carinae straight, parallel, width equal to mesosternal carinae.

Male

Macropterous; large morph 3.27 mm ± 0.1 mm (n = 10); small morph 3.02 mm ± 0.08 mm (n = 10) (Table 3.1). COLOURATION. Golden brown to stramineous. *Head*: black;

spines stramineous, unicolorous; bucculae stramineous, darkening to black proximally; eyes black. *Antennae*: AI-AIII golden brown, AIII marginally lighter; AIV brown distally, transitioning to golden brown proximally. *Rostrum*: golden brown with dark brown to black apex. *Pronotum*: disc golden brown to stramineous; calli dark brown to black; collum and paranota golden brown to stramineous; lateral and medial carinae stramineous. *Thoracic pleura and sterna*: proepisternum golden brown anteriorly, mostly black posteriorly, proepimeron and supracoxal lobes golden brown to stramineous; mesepisternum mostly black, mesepimeron and supracoxal lobes golden brown to stramineous; metepisternum black anteriorly, golden brown posteriorly; peritreme of metathoracic gland stramineous; pro-, meso-, and metasternum black; sternal carinae stramineous. *Hemelytra*: discoidal area brown medially, fading to stramineous at edges, interrupted by white streaks or blotches; costal margin stramineous with brown costal veins; sutural area golden brown to stramineous with brown veins distally. *Legs*: mostly golden brown, coxae black; tarsi black distally. *Abdominal venter*: golden brown; AII dark brown to black. VESTITURE. *Head*: sparse distribution of stramineous aciculate setae in band from base of AI to occipital spines, and from medial spine to frontal spines; occipital and medial spines with stramineous short aciculate to hooked setae; vertex with large globules of wax; bucculae with arcuate aciculate setae and ciliate punctures, covered with large globules of wax. *Antennae*: AI-AII with stramineous sparse, aciculate arcuate setae; AIII with stramineous aciculate decumbent setae, AIV with stramineous aciculate setae; distal end of AII and AIII with dense ring of microtrichia. *Pronotum*: paranotal and anterior margins with arcuate aciculate setae, these continuing posteriorly on medial and lateral carinae; disc with minute setae and numerous punctures with 6-8 cilia distributed evenly around internal rim of punctures; calli often with copious quantities of wax. *Thoracic pleura and sterna*: proepisternum with arcuate aciculate setae and ciliate

punctures anteriorly as on pronotal disc, mostly glabrous posteriorly, proepimeron and supracoxal lobes with arcuate aciculate setae and ciliate punctures; mesepisternum glabrous, mesepimeron and supracoxal lobes with arcuate aciculate setae and ciliate punctures posteriorly; mesepisternum glabrous; pro-, meso-, and metapluron covered with small wax globules. *Legs*: trochanter to tarsus with golden brown aciculate setae; coxae glabrous. *Hemelytra*: costal margins sparsely covered with arcuate aciculate setae, extending onto veins. *Abdominal venter*: aciculate setae and wax distributed throughout. STRUCTURE. *Head*: frontal spines slightly conical, convergent, approximately 1/3 length of AI; medial spine straight, conical apically, height approximately equal to AI, approximately 5x longer than wide; occipital spines straight, cylindrical, exceeding length of medial spine, easily exceeding anterior edge of collum. *Antennae*: AI and AII short, AII ½ length of AI; AIV lanceolate. *Labium*: moderate length, extending to anterior margin of metasternum. *Pronotum*: strongly convex; collum apex inflated to subglobose, height subequal to disc, appearing as extension of medial carina, reaching anterior margin of collum; carinae elevated from disc uniseriate, medial and lateral carinae equal width, lateral carinae strongly divaricating anteriorly; paranota curved, following disc, upturned obliquely, uniseriate, areolae rectangular. *Thoracic sterna*: mesosternal and metasternal carinae elevated, uniseriate, areolae rectangular; mesosternal carinae straight, parallel, metasternal carinae straight to slightly curved. *Hemelytra*: areolae small and uniform size in discoidal and subcostal areas; sutural area areolae similar to discoidal area proximally, increasing in size to 10x distally; costal areolae large, rectangular; costal area uniseriate, subcostal area biseriate, discoidal increasing from one to seven areolae wide, sutural area increasing from one to nine areolae wide. *Male genitalia*: pygophore (Figure 3.14a, b); parameres (Figure 3.14c – e); dorsal plate Y-shaped (Figure 3.14f); aedeagus with paired

enlarged endosomal lobal sclerites (Figure 3.14f – h); endosomal membrane spinulate (Figure 3.14f – h).

Female

Macropterous; large morph 3.41 mm ± 0.09 mm (n = 10); small morph 3.15 mm ± 0.11 mm (n = 10) (Table 3.1). COLOURATION. As in male. VESTITURE. As in male. STRUCTURE. Females broader across hemelytra than males.

Host plants

Known from six genera in four families. Casuarinaceae: *Allocasuarina* sp., 1 specimen. Fabaceae: *Acacia decurrens*, 1 specimen. Myrtaceae: *Angophora hispida*, 2 specimens; *Eucalyptus* sp., 6 specimens; *Leptospermum flavescens*, 1 specimen. Proteaceae: *Grevillea buxifolia*, 17 specimens; *G. lanigera*, 35 specimens; *G. rosmarinifolia*, 169 specimens; *Grevillea* sp., 13 specimens. The records from *Allocasuarina* and Myrtaceae spp. should be considered sitting records.

Distribution

From Royal National Park in New South Wales, south through the Australian Capital Territory; also known from the Grampians in southwest Victoria (Figure 3.12).

Remarks

Proteatingis burckhardti is similar to *P. mjobergi* and *P. plesia*; it can be distinguished from the latter two species by the straight and parallel metasternal carinae. Additionally, *P. mjobergi* has red eyes (vs. black); *P. plesia* has black AI (vs. golden brown).

***Proteatingis howardi* sp. nov.**

(Figures 3.12, 3.15, 3.16)

Type material

HOLOTYPE: AUSTRALIA: New South Wales: Victoria Park Nature Reserve, 7.2 km SSW of Alstonville, 28.90116°S 153.41002°E, 163 m, 07 Sep 2017, S. Cullerton & R. Shofner, *Macadamia tetraphylla* L.A.S. Johnson (Proteaceae), det. R. Shofner, 1 ♂ (UNSW_ENT 00046544) (AM).

PARATYPES: AUSTRALIA: New South Wales: Victoria Park Nature Reserve, 7.2 km SSW of Alstonville, 28.90116°S 153.41002°E, 163 m, 07 Sep 2017, S. Cullerton & R. Shofner, *Macadamia tetraphylla* L.A.S. Johnson (Proteaceae), det. R. Shofner, 27 ♂ (UNSW_ENT 00046541-UNSW_ENT 00046543, UNSW_ENT 00046545-UNSW_ENT 00046568), 20 ♀ (UNSW_ENT 00046569-UNSW_ENT 00046588) (UNSW).

Other material examined

AUSTRALIA: New South Wales: Crooks Valley Road, 1.5 km S Crystal Creek, 28.32451°S 153.32056°E, 68 m, 05 Oct 2017, R. Shofner, *Macadamia tetraphylla* L.A.S. Johnson (Proteaceae), det. R. Shofner, 2 ♂ (UNSW_ENT 00046616, UNSW_ENT 00046617), 2 ♀ (UNSW_ENT 00046618, UNSW_ENT 00046619) (UNSW). Old Byron Bay Road, 1.6 km SE Newrybar, 28.73009°S 153.54454°E, 132 m, 14 Apr 2015, R. Shofner, G. Cassis, & W. Sherwin, *Macadamia* sp. (Proteaceae), det. G. Cassis, 22 ♂ (UNSW_ENT 00046620-UNSW_ENT 00046627, UNSW_ENT 00046640-UNSW_ENT 00046653), 14 ♀ (UNSW_ENT 00046628-UNSW_ENT 00046636, UNSW_ENT 00046654-UNSW_ENT 00046658) (UNSW). Old Byron Bay Road, 1.8 km SE of Newrybar, 28.73213°S 153.54451°E, 130 m, 02 Oct 2017, R.

Shofner, *Macadamia* sp. (Proteaceae), det. R. Shofner, 5 ♂ (UNSW_ENT 00046609-UNSW_ENT 00046612, UNSW_ENT 00046615), 2 ♀ (UNSW_ENT 00046613, UNSW_ENT 00046614) (UNSW). Queensland: Australia Zoo, 2.25 km N of Beerwah, 26.83752°S 152.96146°E, 55 m, 04 Oct 2017, R. Shofner, *Macadamia* sp. (Proteaceae), det. R. Shofner, 1 ♂ (UNSW_ENT 00046595), 1 ♀ (UNSW_ENT 00046596) (UNSW). Blackall Range, 26.7°S 152.883°E, 25 May 1966, D. A. I., *Macadamia integrifolia* Maiden & Betche (Proteaceae), 2 ♀ (UNSW_ENT 00046516, UNSW_ENT 00046517), 1 ♂ (UNSW_ENT 00046518), 1 unknown sex (UNSW_ENT 00046519) (QDPI). Maleny, 26.767°S 152.85°E, 29 Mar 1966, D. A. I., *Macadamia integrifolia* Maiden & Betche (Proteaceae), 2 ♂ (UNSW_ENT 00046520, UNSW_ENT 00046521) (QDPI). Mapleton, 26.6248°S 152.86662°E, 28 Aug 1966, D. A. I., *Macadamia* sp. (Proteaceae), 1 ♀ (UNSW_ENT 00046522) (QDPI). Montville, 26.69°S 152.893°E, 09 May 1967, D. A. I., *Macadamia integrifolia* Maiden & Betche (Proteaceae), 1 ♀ (UNSW_ENT 00046515) (QDPI).

Diagnosis

Proteatingis howardi can be recognised by the following combination of characters: dorsal surface with prominent pattern of dark brown reticulations; costal areolae irregular, reticulated, biseriate more than half the length of costal area.

Male

Macropterous; males 2.99 mm ± 0.05 mm (n = 10) (Table 3.1). COLOURATION. Brown or golden-brown, with three dark brown lines medially on pronotal disc, with dark brown reticulate pattern covering hemelytra, with alternating light and dark bands on costal area of hemelytra and paranota, with pale maculae at juncture of cubitus and R+M veins. *Head*: dark brown; spines dark brown to golden brown, lightening distally; bucculae dark

brown, margins stramineous; eyes reddish-black. *Antennae*: AI-AII brown; AIII golden brown; AIV brown, to golden brown proximally. *Rostrum*: brown proximally, stramineous medially, dark brown apex. *Pronotum*: disc brown medially, with three dark brown lines medially along carinae, pale on posterior projection; calli dark brown to black; collum brown; paranota with alternating light and dark bands; carinae brown, occasionally paler posteriorly. *Thoracic pleura and sterna*: propleura brown to stramineous posteriorly; proepisternum, mesepisternum, and mesepimeron brown to stramineous along coxae; metepisternum brown, stramineous posteriorly; peritreme of metathoracic gland stramineous; pro-, meso-, and metasternum brown; sternal ridges stramineous. *Hemelytra*: brown or golden-brown, with dark brown reticulate pattern covering costal and sutural areas; alternating light and dark bands on costal area; pale maculae at juncture of cubitus and R+M veins. *Legs*: coxae brown; trochanters golden brown; femora brown medially, golden brown proximally and distally; tibiae and tarsi golden brown. *Abdominal venter*: brown medially, darkening laterally. VESTITURE. *Head*: sparse distribution of golden brown aciculate setae along either side of medial spine; occipital, medial, and frontal spines with short golden-brown slightly arcuate aciculate setae; waxy globules frequently present from median and occipital spines to lorum. *Antennae*: AI-AII with golden brown sparse, aciculate arcuate setae; AIII- with golden brown aciculate decumbent setae; AIV with golden-brown aciculate setae and golden-brown hairlike setae. *Pronotum*: paranotal and anterior margins with arcuate aciculate setae, continuing posteriorly on medial and lateral carinae; disc with aciculate setae and numerous punctures with 5-6 cilia distributed evenly around internal rim of punctures; anterior angle frequently with waxy globules similar to head. *Thoracic pleura and sterna*: prosternum, mesepisternum, metasternum, and mesepimeron with arcuate aciculate setae and ciliate punctures as on pronotal disc. *Legs*: coxae to tarsi with golden

brown aciculate setae. *Hemelytra*: costal margins and veins sparsely covered with arcuate aciculate setae. *Abdominal venter*: decumbent to arcuate aciculate setae, denser posteriorly than anteriorly. STRUCTURE. *Head*: spines truncate; frontal spines convergent, in contact distally, less than half length of AI; medial spine straight, stout, height equal to frontal spines, width about half of height; occipital spines straight, cylindrical, often barely protruding beyond collum. *Antennae*: AI and AII short, AII subequal in length to AI; AIV weakly clavate. *Labium*: moderate length, extending to anterior margin of metasternum. *Pronotum*: strongly convex; collum apex weakly inflated, height to 2/3 of disc; carinae minutely elevated off disc, one areola in height, medial and lateral carinae equal width, lateral carinae weakly divaricating anteriorly; paranota curved, following disc, upturned obliquely, 1-2 areolae wide. *Thoracic sterna*: mesosternal and metasternal carinae elevated, one areole wide, areolae rectangular; mesosternal carinae straight, parallel, metasternal carinae curved, truncate-ovate. *Hemelytra*: areolae small and uniform size in discoidal and subcostal areas; sutural area areolae similar to discoidal area proximally, increasing in size to 3x distally; costal areolae small, irregular to rectangular one areole wide; subcostal area two areolae wide, areolae rectangular; discoidal area increasing from six to eight areolae wide, sutural area ten to eleven areolae wide. *Male genitalia*: pygophore (Figure 3.16a, b); parameres (Figure 3.16c – e); dorsal plate Y-shaped (Figure 3.16f); aedeagus with paired elongate spinulate endosomal lobal sclerites (Figure 3.16f – h); endosomal membrane spinulate (Figure 3.16f – h).

Female

Macropterous; 3.22 mm ± 0.07 mm (n = 10) (Table 3.1). COLOURATION. As in male, occasionally ground colour slightly lighter than male. VESTITURE. As in male. STRUCTURE. As in male.

Host plants

Recorded from one genus and one family. Proteaceae: *Macadamia integrifolia*, 7 specimens; *M. tetraphylla*, 52 specimens; and *Macadamia*. sp., 46 specimens.

Distribution

Known from the Blackall Range and Glasshouse Mountains in Queensland, and the Border Ranges and Northern Rivers region in New South Wales (Figure 3.12).

Etymology

Named after Bob and Judy Howard, who greatly supported this research; additionally, the first specimens of this species seen during this study were collected on their property.

Remarks

Proteatingis howardi is similar to *P. plesia*, but can be distinguished by the reticulate areolae of the costal area (vs. ovorectangular in *P. plesia*). *Proteatingis howardi* is a major pest of macadamia nut crops in the same manner as *C. decoris*. It has caused significant economic losses by feeding on macadamia flowers, which wilt and fail to produce fruit.

***Proteatingis minuta* sp. nov.**

(Figures 3.12, 3.13, 3.17)

Type material

HOLOTYPE: AUSTRALIA: Tasmania: Bronte Park, 7.8 km E of Marlborough Hwy on Serpentine Rd, 42.08998°S 146.5667°E, 972 m, 23 Feb 2014, G. Cassis and J. Karras, Hakea sp. (Proteaceae), 1 ♂ (UNSW_ENT 00046255) (TMAG).

PARATYPES: AUSTRALIA: Tasmania: Bronte Park, 7.8 km E of Marlborough Hwy on Serpentine Rd, 42.08998°S 146.5667°E, 972 m, 23 Feb 2014, G. Cassis and J. Karras, Hakea sp. (Proteaceae), 3 ♂ (UNSW_ENT 00046257, UNSW_ENT 00046259, UNSW_ENT 00046261), 2 ♀ (UNSW_ENT 00046263, UNSW_ENT 00046265)

(TMAG), Hakea sp. (Proteaceae), 3 ♂ (UNSW_ENT 00046256, UNSW_ENT 00046258, UNSW_ENT 00046260), 3 ♀ (UNSW_ENT 00046262, UNSW_ENT 00046264, UNSW_ENT 00046266) (UNSW).

Other material examined

AUSTRALIA: Tasmania: Bronte Park, 7.8 km E of Marlborough Hwy on Serpentine Rd, 42.08998°S 146.5667°E, 972 m, 23 Feb 2014, G. Cassis and J. Karras, Hakea sp. (Proteaceae), 2; nymph (UNSW_ENT 00046267, UNSW_ENT 00046269) (TMAG), Hakea sp. (Proteaceae), 2; nymph (UNSW_ENT 00046268, UNSW_ENT 00046270) (UNSW).

Diagnosis

Proteatingis minuta is recognised by the following combination of characters: small body size, less than 2.8 mm; head black; eyes black; anterior margin of collum curved, projecting forward; collum moderately inflated, forming a hood, hood subequal to slightly exceeding height of pronotal disc; costal area uniseriate; metasternal carinae straight, parallel, width equal to mesosternal carinae.

Male

Macropterous; 2.66 mm ± 0.04 mm (n = 7) (Table 3.1). COLOURATION. Greenish grey, pronotal disc golden brown. *Head*: black; spines dark golden brown, black distally; bucculae stramineous, clypeus black, genae black; eyes black to reddish-black. *Antennae*: black. *Labium*: mottled brown and black, with LIV darkening to black. *Pronotum*: disc golden brown, cells darkening to dark brown on posterior projection; calli black; collum and paranota brown, cells silvery to translucent; lateral carinae brown to golden brown, stramineous posteriorly; medial carina brown anteriorly, with black macula at apex of disc, with dark brown band posterior to disc, stramineous on the posterior projection. *Thoracic pleura and sterna*: proepisternum golden brown anteriorly, black posteriorly,

proepimeron and supracoxal lobes golden brown; mesepisternum mostly black, mesepimeron and supracoxal lobes golden brown; metepisternum black to golden brown on supracoxal lobes; peritreme of metathoracic gland stramineous; pro-, meso-, and metasternum black; sternal carinae stramineous. *Hemelytra*: discoidal area either greenish grey or brown, occasionally variable; costal area dark brown to brown; proximal juncture R+M vein and cubitus vein dark brown to black; cubitus vein with dark brown band medially. *Legs*: tarsi black, tarsal claws brown; tibiae dark brown proximally, fading to golden brown distally; femora dark brown to black; coxae black. *Abdominal venter*: golden brown; abdominal sterna mostly golden brown, darkening to black dorsally, posterior edge of sternites II-VIII dark brown across length; spiracles dark brown to black; pygophore brown darkening to black posteriorly. VESTITURE. *Head*: stramineous arcuate setae in bands from antennal tubercles to occipital spines and from frontal spines along either side of medial spine to back of head; bucculae with arcuate setae; dense globules of wax encircling eye, and from frons to apex. Occipital and medial spines with golden brown decumbent setae, erect distally. *Antennae*: AI-AIII with white sparse, decumbent setae, AIV with white semi-erect to erect aciculate setae; distal end of AII and AIII with dense ring of microtrichia. *Pronotum*: anterior margin glabrous, rarely with short setae; paranotal margins, medial and lateral carinae, and disc with arcuate setae; disc with numerous punctures with 6-8 triangular tuberculate processes distributed evenly around internal rim; calli with short golden brown setae, globules of wax often covering calli. *Thoracic pleura and sterna*: anterior portion of proepisternum, proepimeron, posterior portion of mesepisternum, mesepimeron, and metepisternum with arcuate setae and tubercle-lined punctures as on pronotal disc; anterior portion of pro- and mesepisternum glabrous; sternal carinae with sparse distribution of arcuate setae; all surfaces covered with small globules of wax, propluron heavily coated with wax. *Legs*:

coxae to tibiae with white to stramineous arcuate setae; ventral surface of tarsi with semi-erect aciculate setae. *Hemelytra*: costal margins sparsely covered with arcuate setae; discoidal area veins with sparse distribution of arcuate setae; sutural area veins glabrous or occasionally with very sparse distribution of arcuate setae. *Abdominal venter*: moderate distribution of arcuate setae, with white wax coating entire abdomen. STRUCTURE. *Head*: spines rounded apically; frontal spines upright, parallel or convergent distally, less than half the length of AI; medial spine straight, stout, height 2x that of frontal spines, width about 1/4 to 1/3 of height; occipital spines straight, up to half their length protruding beyond collum. *Antennae*: AI and AII short, AI 2x longer than AII; AIII longer than the pronotal width across humeral angles, AIV weakly clavate. *Labium*: moderate length, exceeding anterior margin of metasternum. *Pronotum*: strongly convex; collum apex inflated to subglobose, height equal to disc; medial and lateral carinae appearing decurrent to disc but weakly areolate, carinae areolate over posterior third, uniseriate; medial and lateral carinae equal width, lateral carinae divaricating; paranota curved, following disc, hardly upturned, mostly one areole wide, two areolae wide anteriorly, not exceeding height of hemelytra. *Thoracic sterna*: mesosternal and metasternal carinae elevated, uniseriate, areolae rectangular; mesosternal carinae straight, parallel, metasternal carinae curved, slightly ovate, convergent posteriorly. *Legs*: legs thin; femora tapered proximally. *Thoracic pleura*: peritreme large, loop-like, strongly depressed medially, with dorsal extension reaching hemelytral margin. *Hemelytra*: areolae small and uniform size in discoidal and subcostal areas, increasing in size in subcostal area posterior from juncture of R+M and cubitus veins; sutural area areolae similar to discoidal area proximally, increasing in size to 5x distally; costal areolae large, rectangular; costal area uniseriate, subcostal area mostly biseriate, discoidal increasing from one to six areolae wide, sutural area one to eight areolae wide. *Male genitalia*:

pygophore (Figure 3.17a, b); parameres (Figure 3.17c – e); dorsal plate Y-shaped (Figure 3.17f); aedeagus with paired mid-size endosomal lobal sclerites (Figure 3.17f – h).

Female

Macropterous; 2.67 mm ± 0.03 mm (n = 5) (Table 3.1). COLOURATION. Mostly as in male. Discoidal area of hemelytra with more pronounced dark brown mottling than in male; costal area veins dark brown, with costal margin banded stramineous and dark brown. VESTATURE. As in male. STRUCTURE. As in male.

Host plants

Recorded from *Hakea* sp., 16 specimens (Proteaceae).

Distribution

Known from near Bronte Park in the Top Marshes Conservation Area, Tasmania, Australia (Figure 3.12).

Etymology

Named for its diminutive size in relation to all other species of this genus.

Remarks

This species is diminutive compared to all other *Proteatingis*, however, this species is extremely similar both genetically and morphologically to *P. burckhardti* and can only be reliably differentiated via its body size and geographic location. This species may eventually be recognised as a subspecies of *P. burckhardti*.

***Proteatingis mjobergi* (Horváth, 1925) comb. nov.**

(Figures 3.15, 3.18, 3.19)

Tingis (*Tingis*) *mjobergi* Horváth, 1925: 5 (original description); Drake (1947: 114) (incorrect subsequent spelling; *Tingis myobergi*).

Ulonemia mjobergi: Drake and Ruhoff (1960a: 29) (*nov. comb.* as *Ulonemia mjöbergi*); Drake and Ruhoff (1961a: 139) (redescription); Drake and Ruhoff (1961a: 112) (redescription); Drake and Ruhoff (1965: 421) (world catalogue); Cassis and Gross (1995: 438) (Australian catalogue).

Proteatingis mjobergi: new combination, this work.

Material examined

AUSTRALIA: Northern Territory: 30 km SSE Nathan River, 15.83333°S 135.5°E, 27 Aug 1987, Anne & Les Dollin, 1 ♀ (UNSW_ENT 00046469) (ANIC). 60 km SW Borroloola, 16.25°S 135.83333°E, 27 Aug 1987, Anne & Les Dollin, 1 ♂ (UNSW_ENT 00046470) (ANIC). 85 km W Borroloola, 16.16667°S 135.66667°E, 27 Aug 1987, Anne & Les Dollin, 1 ♂ (UNSW_ENT 00046468) (ANIC). 100 km W Borroloola, 16.08333°S 135.58333°E, 27 Aug 1987, Anne & Les Dollin, 1 ♂ (UNSW_ENT 00046467) (ANIC). Fish River Station, transect M, 14.2273°S 131.02757°E, 127 m, 29 Apr 2012, C. Symonds, *Grevillea* sp. (Proteaceae), det. Ben Wirf (NTH) - Field ID, 2 ♂ (UNSW_ENT 00026279, UNSW_ENT 00026280) (UNSW). Hayes Creek ca. 70 km S of Adelaide River, 13.62731°S 131.54447°E, 07 VII 1998, W.G. Ullrich, 2 ♀ (UNSW_ENT 00046324, UNSW_ENT 00046325), 1 ♂ (UNSW_ENT 00046462) (USNM). Queensland: 10 km EbS of The Quinkan and Regional Cultural Centre, 15.58387°S 144.53961°E, 196 m, 09 Mar 2017, R. Shofner, *Grevillea pteridifolia* Knight (Proteaceae), det. P. Forster & K. McDonald (QLD Herbarium), 2 ♀ (UNSW_ENT 00028999, UNSW_ENT 00029000) (UNSW). 10 km W of Petford, 17.365°S 144.818°E, 22 Jul 1982, J. F. Donaldson, J. W. Turner, 12 ♂ (UNSW_ENT 00046333-UNSW_ENT 00046344), 11 ♀ (UNSW_ENT 00046345-UNSW_ENT 00046355) (QDPI). Lakefield Ranger Station, 14.54065°S 144.3305°E, 19 Jun 2002, A. Postle, *Mangifera indica* L.

(Anacardiaceae), 1 ♂ (UNSW_ENT 00046330) (UNSW). 2 km E of Dimbulah, 40 km W of Mareeba, 17.15°S 145.11666°E, 03 Sep 1990, T. J. Henry, 1 ♂ (AMNH_PBI 00191446) (USNM). 57.6km WSW of Killarney Station, on sandbar in Alice River, 15.6252°S 143.00009°E, 80 m, 14 Jul 2015, R. Shofner, *Grevillea pteridifolia* Knight (Proteaceae), det. R. Shofner, 4 ♀ (UNSW_ENT 00046014-UNSW_ENT 00046017), 7 ♂ (UNSW_ENT 00046018-UNSW_ENT 00046024) (UNSW). Granite Gorge Nature Reserve, 17.05108°S 145.35575°E, 506 m, 23 May 2006, Cassis, Barrow, Finlay, and Symonds, *Jacksonia thesioides* A. Cunn. ex Benth. (Fabaceae), det. RBG staff, 1 ♂ (UNSW_ENT 00046328), 1 ♀ (UNSW_ENT 00046329) (UNSW). Jct. of Flinders Hwy & Cann Camp Creek Road, White Mountains National Park, 20.73105°S 145.18108°E, 567 m, 19 May 2006, Cassis, Barrow, Finlay, and Symonds, *Grevillea decora* Domin *subsp. decora* (Proteaceae), det. RBG staff, 1 ♂ (UNSW_ENT 00046327) (UNSW). Mareeba, Jul 1978, Unknown, *Grevillea parallela* Knight (Proteaceae), 1 ♀ (UNSW_ENT 00046332) (QDPI). Murphys Road, Glasshouse Mountains National Park, 6.3 km SW of Beerwah, 26.89994°S 152.9157°E, 92 m, 04 Oct 2017, R. Shofner, *Grevillea* sp. (Proteaceae), det. R. Shofner, 1 ♂ (UNSW_ENT 00046591) (UNSW). Walsonville Range, 21 Aug 1970, J. H. Barrett, *Grevillea parallela* Knight (Proteaceae), 1 ♀ (UNSW_ENT 00046331) (QDPI). ca. 30km SE of Chillagoe, on Burke Developmental Rd, 17.36519°S 144.71405°E, 547 m, 01 Jun 2006, Cassis, Barrow, Finlay, and Symonds, *Crotalaria aridicola* Domin (Fabaceae), det. RBG staff, 1 ♂ (UNSW_ENT 00046326) (UNSW). Western Australia: 28km W of Home Valley Station on Gibb River Rd, 15.78218°S 127.64028°E, 239 m, 31 May 2014, G. Cassis, J. Karras & P. Jackson, *Grevillea agrifolia* A. Cunn. ex R. Br. (Proteaceae), det. WAH, 1 ♀ (UNSW_ENT 00046299) (UNSW). 70.8 km W of Home Valley Station on Gibb River

Rd, 15.89943°S 127.31872°E, 318 m, 31 May 2014, G. Cassis, J. Karras & P. Jackson, *Grevillea teretifolia* Meisn. (Proteaceae), det. WAH, 6 ♂ (UNSW_ENT 00046300, UNSW_ENT 00046303-UNSW_ENT 00046307), 2 ♀ (UNSW_ENT 00046301, UNSW_ENT 00046302) *Hakea arborescens* R. Br. (Proteaceae), det. WAH, 3 ♂ (UNSW_ENT 00046308-UNSW_ENT 00046310), 7 ♀ (UNSW_ENT 00046311-UNSW_ENT 00046317), 6; (UNSW_ENT 00046318-UNSW_ENT 00046323) (UNSW). Kimberley Dist., Kalumburu Rd, 148.2 km N of Gibb River Rd., 15.02056°S 126.20639°E, 440 m, 21 May 1999, G. Cassis, R. Silveira, *Grevillea agrifolia* A. Cunn. ex R. Br. (Proteaceae), det. PERTH staff PERTH5635829, 1 ♀ (UNSW_ENT 00026425) *Grevillea agrifolia* A. Cunn. ex R.Br. (Proteaceae), det. PERTH staff PERTH5635829, 9 ♀ (UNSW_ENT 00026416-UNSW_ENT 00026424), 3 ♂ (UNSW_ENT 00026426-UNSW_ENT 00026428) (AM).

Diagnosis

Proteatingis mjobergi can be recognised by the following combination of characters: anterior margin of collum curved medially, projecting forward; anterior portion of costal area uniseriate; paranota areolate along entire length, areolae easily visible and well-defined; metasternal carinae curved, obovate, width greater than mesosternal carinae; areolae of lateral carinae large, easily seen.

Male

Macropterous; 3.19 mm ± 0.08 mm (n = 10) (Table 3.1). COLOURATION. Stramineous. *Head*: dark brown; spines stramineous; bucculae stramineous; eyes red. *Antennae*: AI-AIII golden brown, AIV brown. *Rostrum*: golden brown with dark brown to black band distally on first segment to proximally on second segment, dark brown to black apex. *Pronotum*: disc stramineous; calli dark brown; collum and paranota stramineous; lateral carinae stramineous, medial carina golden brown. *Thoracic pleura and sterna*:

proepisternum stramineous anteriorly, mostly brown posteriorly, proepimeron and supracoxal lobes stramineous; mesepisternum mostly dark brown to black, mesepimeron and supracoxal lobes golden brown to stramineous; metepisternum brown anteriorly, stramineous posteriorly; peritreme of metathoracic gland stramineous; prosternum brown, mesosternum dark brown, metasternum golden brown to brown; pro-, meso-, and metasternal carinae stramineous. *Hemelytra*: stramineous; costal veins brown; R+M vein with dark brown blotch distally; cubitus vein with two dark brown blotches. *Legs*: mostly stramineous, coxae dark brown; tarsi stramineous to brown. *Abdominal venter*: brown. VESTITURE. *Head*: distribution of stramineous aciculate setae in bands from base of AI to occipital spines and from frontal spines along either side of medial spine, to back of head; frons and gena with stramineous aciculate setae; medial spine with stramineous short aciculate to hooked setae; vertex with large globules of wax; bucculae with arcuate aciculate setae, ciliate punctures, and large globules of wax. *Antennae*: AI-AII with stramineous sparse, aciculate arcuate setae; AIII with stramineous aciculate decumbent setae, AIV with stramineous aciculate setae; distal end of AII and AIII with dense ring of microtrichia. *Pronotum*: anterior and paranotal margins with sparse arcuate aciculate setae, continuing onto medial and lateral carinae; disc glabrous with numerous punctures with 6-8 cilia distributed evenly around internal rim of punctures; calli with short stramineous cilia, often with globules of wax. *Thoracic pleura and sterna*: proepisternum with arcuate aciculate setae and ciliate punctures anteriorly as on pronotal disc, lacking ciliate punctures posteriorly, proepimeron and supracoxal lobes with arcuate aciculate setae and ciliate punctures; mesepisternum with arcuate aciculate setae, mesepimeron and supracoxal lobes with arcuate aciculate setae and ciliate punctures posteriorly; metepisternum with arcuate aciculate setae and ciliate punctures; pro-, meso-, and metapluron covered with small wax globules. *Legs*: coxa to femur glabrous, tibia and

tarsus with stramineous aciculate setae. *Hemelytra*: glabrous, rarely with short aciculate setae on veins. *Abdominal venter*: aciculate setae and wax distributed throughout. STRUCTURE. *Head*: frontal spines slightly conical, convergent, approximately 1/3 length of AI; medial spine straight, conical apically, height approximately equal to AI, approximately 5x longer than wide; occipital spines straight, cylindrical, approximately equal to medial spine, easily exceeding anterior edge of collum. *Antennae*: AI and AII short, AII 1/2 length of AI; AIV weakly clavate. *Labium*: moderate length, extending to posterior margin of mesosternum. *Pronotum*: strongly convex; collum apex produced, height subequal to disc; carinae greatly elevated from disc, uniseriate, areolae rectangular; medial and lateral carinae equal width, lateral carinae mostly parallel, divaricating slightly anteriorly; paranota curved, following disc, upturned obliquely, uniseriate, areolae rectangular. *Thoracic sterna*: prosternal and mesosternal carinae minimally elevated, areolae barely visible on mesosternal carina; metasternal carinae slightly elevated, uniseriate, areolae rectangular; prosternal and mesosternal carinae straight, parallel, metasternal carinae slightly obovate. *Hemelytra*: areolae small, irregular, of varying size in discoidal and subcostal areas; sutural area areolae similar to discoidal area proximally, increasing in size to 3x distally; costal areolae large, rectangular; costal area uniseriate, subcostal area biseriate, discoidal increasing from one to five or six areolae wide, sutural area increasing from one to nine areolae wide. *Male genitalia*: pygophore (Figure 3.18a, b); parameres (Figure 3.18c – e); dorsal plate Y-shaped (Figure 3.18f); aedeagus with paired large endosomal lobal sclerites (Figure 3.18f – h); endosomal spinulation variable in size, with some spinules enlarged (Figure 3.18f – h).

Female

Macropterous; 3.23 mm ± 0.11 mm (n = 10) (Table 3.1). COLOURATION. As in male. VESTITURE. As in male. STRUCTURE. As in male.

Host plants

Recorded from three families and five genera. Anacardiaceae: *Mangifera indica*, 1 specimen. Fabaceae: *Crotalaria aridicola*, 1 specimen; *Jacksonia thesioides*, 2 specimens. Proteaceae: *Grevillea agrifolia*, 14 specimens; *G. decora*, 1 specimen; *G. parallela*, 2 specimens; *G. pteridifolia*, 13 specimens; *G. teretifolia*, 8 specimens; *Grevillea* sp., 3 specimens; *Hakea arborescens*, 16 specimens.

Distribution

Occurs across northern Australia from Broome, Western Australia (Horváth, 1925) to the Wet Tropics in Far North Queensland; isolated records in White Mountains National Park and Glasshouse Mountains National Park, Queensland (Figure 3.19).

Remarks

Proteatingis mjobergi is similar to *P. astibosetes*, *P. burckhardti*, and *P. plesia*. It can be distinguished from these species by the large areolae on the paranota, costal margin, and medial carina, as well as the broad paranota. The known range of *P. mjobergi* is larger than any other species of *Proteatingis*. It occurs in a wide variety of habitats over its extensive distribution.

***Proteatingis plesia* (Drake and Ruhoff, 1961), comb. nov.**

(Figures 3.15, 3.19, 3.20)

Ulonemia plesia Drake and Ruhoff, 1961: 138 (original description); Drake and Ruhoff (1965: 425) (world catalogue); Cassis and Gross (1995: 438) (Australian catalogue).

Proteatingis plesia: new combination, this work.

Type material

HOLOTYPE: ♀, AUSTRALIA: Western Australia: Swan River, L. J. Newman (Hacker Collection (C. J. Drake Collection 1956)). Photograph of type examined.

Material examined

AUSTRALIA: Western Australia: 15 km N of Millstream-Roebourne Rd on Karratha - Tom Price Rd, 21.07402°S 116.97158°E, 96 m, 30 Aug 2005, G. Cassis, S. Lassau, S. and G. Carter, *Stemodia grossa* Benth. (Scrophulariaceae), det. Perth staff PERTH 7273126, 1 ♀ (UNSW_ENT 00046459) (AM). 4 km SW of Poison Creek Beach, Cape Arid National Park, 33.92254°S 123.3181°E, 70 m, 25 Nov 1999, R.T. Schuh, G. Cassis, and R. Silveira, *Hakea obliqua* R. Br *subsp. obliqua* (Proteaceae), det. PERTH staff PERTH 05671825, 4 ♀ (AMNH_PBI 00011749-AMNH_PBI 00011752) (AM), *Conospermum distichum* R. Br. (Proteaceae), det. PERTH staff PERTH05670403, 1 ♀ (UNSW_ENT 00046461) (UNSW). 7.5 km E of Balladonia Road on Fisheries Road, 33.74644°S 123.1687°E, 120 m, 25 Nov 1999, R.T. Schuh, G. Cassis, and R. Silveira, *Hakea preissii* Meisn. (Proteaceae), det. PERTH staff PERTH 05670926, 6 ♀ (AMNH_PBI 00011753, AMNH_PBI 00011754, AMNH_PBI 00011756, AMNH_PBI 00011758, AMNH_PBI 00011761, AMNH_PBI 00011763), 1 unknown sex (AMNH_PBI 00011755), 4 ♂ (AMNH_PBI 00011757, AMNH_PBI 00011759, AMNH_PBI 00011760, AMNH_PBI 00011762) (AM). 39 km E of Lake King, 33.07796°S 120.0936°E, 400 m, 21 Nov 1999, R.T. Schuh, G. Cassis, and R. Silveira, *Hakea pandanicarpa* R. Br. (Proteaceae), det. Perth Staff 05671620, 1 unknown sex (AMNH_PBI 00011776), 11 ♀ (AMNH_PBI 00011777-AMNH_PBI 00011779, AMNH_PBI 00011781, AMNH_PBI 00011782, AMNH_PBI 00011784-AMNH_PBI 00011786, AMNH_PBI 00011788, AMNH_PBI 00011790, AMNH_PBI 00011791), 4 ♂ (AMNH_PBI 00011780, AMNH_PBI 00011783, AMNH_PBI 00011787, AMNH_PBI 00011789) *Hakea horrida* R.M. Barker (Proteaceae), det. PERTH staff PERTH 05671221, 1 ♂ (UNSW_ENT 00046445), 4 ♀ (UNSW_ENT 00046446-

UNSW_ENT 00046449) (AM). 135 km W of Coolgardie on Great Eastern Hiway, 31.27202°S 120.0059°E, 489 m, 17 Nov 1999, R.T. Schuh, G. Cassis, and R. Silveira, *Grevillea hookeriana* Meisn. *subsp. apiciloba* (Proteaceae), det. PERTH staff PERTH 05670187, 1 ♀ (AMNH_PBI 00179348) (AMNH). Mosman Park, Perth, 32°S 115.75°E, 30 m, 06 Sep 2001, G. Cassis, *Hakea* sp. (Proteaceae), 4 ♂ (UNSW_ENT 00046473-UNSW_ENT 00046476), 15 ♀ (UNSW_ENT 00046477-UNSW_ENT 00046491) (UNSW). Yalgorup National Park, 32.83472°S 115.6524°E, 80 m, 04 Dec 1999, R.T. Schuh, G. Cassis, and R. Silveira, *Hakea trifurcata* (Sm.) R. Br. (Proteaceae), det. PERTH staff PERTH 05670330, 4 ♀ (AMNH_PBI 00011744-AMNH_PBI 00011747), 1 ♂ (AMNH_PBI 00011748) *Hakea prostrata* R. Br. (Proteaceae), det. PERTH staff PERTH 05671728, 5 ♂ (UNSW_ENT 00046450-UNSW_ENT 00046454), 4 ♀ (UNSW_ENT 00046455-UNSW_ENT 00046458) (AM). Yalgorup National Park, 32.83583°S 115.65111°E, 27 Nov 1998, G. Cassis, *Dryandra sessilis* (Knight) Domin *var. cygnorum* (Proteaceae) PERTH 05227623, 1 ♂ (UNSW_ENT 00046444) (AM). Yalgorup National Park, near Martins Tank Campground, 32.84222°S 115.66222°E, 15 m, 14 Dec 1997, Schuh, Cassis, Brailovsky, *Dryandra sessilis* (Knight) Domin (Proteaceae), det. PERTH staff PERTH 05055083, 1 ♂ (UNSW_ENT 00046460) (AM). ca 13 km E of Denmark on South Coast Hiway, 34.99397°S 117.5086°E, 80 m, 01 Dec 1999, R.T. Schuh, G. Cassis, and R. Silveira, *Hakea prostrata* R. Br. (Proteaceae), det. PERTH staff PERTH 05672236, 1; (AMNH_PBI 00011764), 6 ♀ (AMNH_PBI 00011765, AMNH_PBI 00011769, AMNH_PBI 00011772-AMNH_PBI 00011775), 5 ♂ (AMNH_PBI 00011766-AMNH_PBI 00011768, AMNH_PBI 00011770, AMNH_PBI 00011771) (AM).

Diagnosis

Proteatingis plesia is recognised by the following combination of characters: antennal segment I black; collum elevated, forming short hood; anterior margin of collum projecting forward; paranota areolate along entire length, areolae easily visible and well-defined; metasternal carinae truncate-obovate.

Male

Macropterous; 3.36 mm ± 0.13 mm (n = 10) (Table 3.1). COLOURATION. Stramineous to reddish brown. *Head*: black; spines stramineous; bucculae stramineous; eyes red in nymphs and teneral imagos, fading to black with age. *Antennae*: AI black, AII-AIII golden brown, AIV golden brown proximally, quickly darkening to dark brown or black distally. *Rostrum*: golden brown with dark brown to black apex. *Pronotum*: disc stramineous to brown; calli black; collum and paranota stramineous to golden brown; lateral and medial carinae stramineous, medial carina reddish brown to brown posteriorly, lateral carina white posteriorly. *Thoracic pleura and sterna*: proepisternum stramineous to golden brown anteriorly, mostly black posteriorly, proepimeron stramineous to golden brown, supracoxal lobes golden brown; mesepisternum mostly black, mesepimeron and supracoxal lobes golden brown; metepisternum black ventrally, golden brown dorsally; peritreme of metathoracic gland stramineous; prosternum and mesosternum black, metasternum brown; pro-, meso-, and metasternal carinae stramineous. *Hemelytra*: discoidal area stramineous medially, stramineous to brown proximally and distally; subcostal area stramineous to reddish brown to brown; costal margin stramineous to golden brown with brown costal veins; sutural area stramineous. *Legs*: mostly golden brown, coxae dark brown to black; tarsi dark brown to black distally. *Abdominal venter*: golden brown. VESTITURE. *Head*: distribution of golden brown aciculate setae in bands from base of AI to occipital spines and from frontal spines along either side of medial

spine, to back of head; frons and gena with stramineous aciculate setae; medial spine with stramineous short aciculate to hooked setae; vertex with large globules of wax; bucculae with arcuate aciculate setae and ciliate punctures. *Antennae*: AI-AII with stramineous sparse, aciculate arcuate setae; AIII with stramineous aciculate decumbent setae, AIV with stramineous aciculate setae; distal end of AII and AIII with dense ring of microtrichia. *Pronotum*: anterior and paranotal margins with sparse distribution of arcuate aciculate setae; medial and lateral carinae with sparse distribution of arcuate aciculate setae; disc with minute setae and numerous punctures with 6-8 cilia distributed evenly around internal rim of punctures; calli often with globules of wax. *Thoracic pleura and sterna*: proepisternum with arcuate aciculate setae and ciliate punctures anteriorly as on pronotal disc, lacking ciliate punctures posteriorly, proepimeron and supracoxal lobes with arcuate aciculate setae and ciliate punctures; mesepisternum with arcuate aciculate setae, mesepimeron and supracoxal lobes with arcuate aciculate setae and ciliate punctures posteriorly; metepisternum with arcuate aciculate setae and ciliate punctures; pro-, meso-, and metapluron covered with small wax globules. *Legs*: coxae to femur glabrous, tibia with golden brown aciculate setae, setae very short proximally, increasing in length distally; coxae with single row of arcuate aciculate setae. *Hemelytra*: sparse distribution of short aciculate setae on veins. *Abdominal venter*: aciculate setae and wax distributed throughout. STRUCTURE. *Head*: frontal spines slightly conical, strongly convergent to crossed, approximately 1/2 length of AI; medial spine stout, conical, height subequal to AI; occipital spines straight, cylindrical, exceeding length of medial spine, easily exceeding anterior edge of collum. *Antennae*: AI and AII short, AII 1/2 length of AI; AIV lanceolate. *Labium*: moderate length, extending to anterior margin of metasternum. *Pronotum*: strongly convex; collum apex inflated, forming short hood, height equal to disc; anterior margin of collum projecting forward; carinae slightly

elevated from disc, uniseriate, cells very small; medial and lateral carinae equal width, lateral carinae divaricating anteriorly; paranota curved, following disc, upturned obliquely, uniseriate to biseriate, areolae rectangular. *Thoracic sterna*: pro-, meso-, and metasternal carinae elevated, uniseriate, areolae small, rectangular; prosternal and mesosternal carinae straight, parallel, metasternal carinae truncate-obovate. *Hemelytra*: areolae small, irregular, and nearly uniform size in discoidal and subcostal areas; sutural area areolae similar to discoidal area proximally, increasing in size to 2x distally; costal areolae rectangular; costal area uniseriate, subcostal area biseriate, discoidal increasing from one to six or seven areolae wide, sutural area increasing from two to seven areolae wide. *Male genitalia*: pygophore (Figure 3.20a, b); parameres (Figure 3.20c – e); dorsal plate Y-shaped (Figure 3.20f); aedeagus with paired large endosomal lobal sclerites (Figure 3.20f – h); endosomal spinulation present (Figure 3.20f – h).

Female

Macropterous; 3.58 mm ± 0.08 mm (n = 10) (Table 3.1). COLOURATION. As in male. VESTITURE. As in male. STRUCTURE. As in male.

Host plants

Recorded from two families and five genera. Proteaceae: *Conospermum distichum*, 1 specimen; *Dryandra sessilis*, 2 specimens; *Grevillea hookeriana*, 1 specimen; *Hakea horrida*, 5 specimens; *H. obliqua*, 4 specimens; *H. pandanicarpa*, 16 specimens; *H. preissii*, 11 specimens; *H. prostrata*, 21 specimens; *H. trifurcata*, 5 specimens; *Hakea* sp., 19 specimens. Scrophulariaceae: *Stemodia grossa*, 1 specimen.

Distribution

Found in southwestern Western Australia and near Broome, WA (Figure 3.19).

Remarks

This species is superficially similar to *P. burckhardti*, *P. howardi*, and *P. mjobergi*, but does not overlap the distribution these species. It can be distinguished from *P. burckhardti* and *P. mjobergi* by the black first antennal segment, and from *P. howardi* by the ovorectangular areolae of the costal margin (vs. reticulate in *P. howardi*).

Ulonemia Drake and Poor 1937

(Figure 3.21 – 3.23)

Perissonemia (*Ulonemia*) Drake and Poor, (1937): 3 (original description).

Ulonemia: Drake (1942: 359) (raised to genus rank); Drake and Ruhoff (1960a: 29) (taxonomy); (1960b: 87) (taxonomy); (1965: 419) (world catalogue); Jing (1981: 289) (Chinese catalogue); Péricart (1992: 83) (taxonomy); Cassis and Gross (1995: 437) (Australian catalogue); Péricart and Golub (1996: 77) (taxonomy); Dang et al. (2014: 50) (taxonomy).

Type species

Perissonemia (*Ulonemia*) *dignata* Drake and Poor, 1937, by original designation.

Diagnosis

Ulonemia is recognised by the following combination of characters: body elongate, oblong to parallel-sided, hemelytra exceeding abdomen; five cephalic spines; bucculae narrow, areolate; antennae long, slender, AI – AIII with short setae, AIV with aciculate setae; AI and AII short, AIII long, length subequal to exceeding distance between humeral angles, AIV weakly clavate; collum flattened anteriorly, anterior margin straight or slightly curved posteriorly, hood absent, collum inflated slightly posteriorly at juncture of medial carina; pronotum convex, tricarinate, with numerous punctures, these with 6-8 triangular tuberculate processes distributed evenly around internal rim; paranota areolate

across collum with deeply impressed calli, areolae reduced posteriorly, appearing carina-like across disc but with areolae still present; costal area uniseriate, subcostal area biseriate; peritreme of metathoracic gland large, loop-like.

Male

Macropterous, 3.0 mm – 3.2 mm (Table 3.1). COLOURATION. Ground colour stramineous, brown, golden brown, dark brown; calli brown, dark brown, or black; head brown, reddish brown, dark brown, or black; thoracic sternites usually same colour as head; abdomen similar to ground colour but usually darker. VESTITURE. *Head*: setae in bands from antennal tubercles to frontal spines, and from frontal spines along either side of medial spine to back of head, and from antennal tubercles along dorsal margin of eye; bucculae with arcuate or aciculate setae and ciliate punctures; waxy deposits often encircling eye and from frons to antennal tubercles to apex. *Antennae*: AI-AIII with white to stramineous decumbent setae, AIV with stramineous semi-erect to erect aciculate setae; distal end of AII and AIII with dense ring of microtrichia. *Pronotum*: disc with sparse distribution of minute setae; waxy exudate deposited in calli. *Thoracic pleura and sterna*: proepisternum with anterior minute setae and numerous punctures, these with 6-8 triangular tuberculate processes distributed evenly around internal rim, lacking these punctures posteriorly; proepimeron and supracoxal lobes with minute setae and tuberculate punctures; mesepisternum with minute setae; mesepimeron and supracoxal lobes with minute setae and tuberculate punctures posteriorly; metepisternum with minute setae and tuberculate punctures. *Legs*: sparse distribution of minute setae on femora and tibiae; distal end of tibiae with slightly longer setae and denser distribution. *Hemelytra*: glabrous, except R+M and cubitus veins with sparse distribution of minute setae. *Abdominal venter*: sparse to moderate distribution of minute setae, usually pruinose. STRUCTURE. *Head*: five cephalic spines present, unbranched; frontal spines

parallel or convergent. *Antennae*: AI and AII short, AII 1/2 to subequal length of AI; AIII usually longer than distance between humeral angles; AIV weakly clavate, length roughly equal to AI + AII. *Labium*: moderate length, extending to anterior or posterior end of metasternum. *Pronotum*: strongly convex, collum flattened, slightly raised, or greatly inflated and globose; dorsal surface of disc with numerous punctures, these with 6-8 triangular tuberculate processes distributed evenly around internal rim; tricarinate, these extending from posterior margin of collum to posterior projection of pronotum; medial and lateral carinae equal width; lateral carinae slightly to moderately divaricating anteriorly; paranota extending from anterior margin of collum to posterior edge of disc, curved, following shape of disc; paranota areolate across collum, carina-like to areolate across disc. *Thoracic pleura and sterna*: peritreme of the metathoracic gland loop-like, often with dorsal extension reaching margin of hemelytra. Sternal carinae elevated, uniseriate, areolae rectangular to slightly rounded; prosternal carinae straight, parallel; mesosternal carinae straight to slightly divaricating anteriorly and slightly converging posteriorly; metasternal carinae vary from straight and parallel, equal in width to mesosternal carinae, to divaricating, wider than width of mesosternal carinae. *Hemelytra*: areolae small, irregular, nearly uniform in size in discoidal and subcostal areas; sutural area areolae anteriorly similar in size to discoidal areolae, increasing in size posteriorly; subcostal area biseriate with regular arrangement of areolae; costal area uniseriate, biseriate, or biseriate anteriorly to uniseriate posteriorly. *Male genitalia*: pygophore boxlike, with lateral margins only slightly curved, sometimes with pair of basal spurs near posterior margin of genital margin; parameres C-shaped with apophysis strongly tapered distally; aedeagus with Y-shaped dorsal plate; endosomal membrane lacking spinules; pair of sclerotised, endosomal lobal sclerites present but highly reduced in form.

Female

Macropterous. Body 3.3 mm – 3.5 mm, usually slightly larger and wider than male (Table 3.1). COLOURATION. As in male. VESTITURE. As in male. STRUCTURE. As in male.

Distribution

Australia, Borneo, China, India, Malaysia, New Guinea, Philippines, Taiwan, Vietnam (Drake and Ruhoff 1965, Cassis and Gross 1995, Péricart and Golub 1996, Dang et al. 2014).

Remarks

The male genitalia are based on those of *U. leai*, as they are not known for any other species of the genus.

Ulonemia is a difficult genus to diagnose. The original description of the genus by Drake and Poor (1937) distinguishes it from *Perissonemia* by the presence of long lateral carinae, and "differently formed paranota and collar," features that can be found in a plethora of genera that are otherwise similar to *Perissonemia*. The description of *Ulonemia* also states that the hood is either present or absent, and the paranota are either areolate or carina-like, which is a wide range of variability seen in many tingid taxa and does little to aid identification of the genus. Comparison to the type species *U. dignata* offers some insight to the diagnosis of the genus, though the holotype is badly damaged. The collum of *U. dignata* is raised and produced posteriorly, forming a weak hood, the paranota are reduced across the pronotal disc, appearing carina-like but remaining unicarinate, and the costal margin is uniseriate for the entire length. As was demonstrated in the previous chapter, these characters are fairly uniform within genetic clusters, and *Ulonemia* as currently defined has much variety in these characters between species. A

key to the species of *Ulonemia* is not provided, as most species are extralimital to Australia, with *U. leai* as the sole representative of the genus on the continent.

Checklist of Ulonemia

U. angusta Dang et al., 2014.....China

U. aota Drake & Ruhoff, 1965 .....New Guinea

U. aptata Drake, 1960.....New Guinea

U. assamensis (Distant, 1903) .....Borneo, China, India, Taiwan, Vietnam

U. dignata (Drake & Poor, 1937) .....Philippines

U. electa (Drake & Poor, 1937).....Philippines

U. ermaea Drake & Ruhoff, 1965 .....New Guinea

U. jingae Dang et al., 2014 .....China

U. leai Drake, 1942.....Queensland

U. magna Dang et al., 2014 .....China

U. malaccae (Drake, 1942).....Malaysia

***Ulonemia leai* Drake 1942**

(Figures 3.21 – 3.23)

Ulonemia leai Drake, 1942: 360 (original description); Drake and Ruhoff (1965: 421) (world catalogue); Cassis and Gross (1995: 438) (Australian catalogue); Dang et al. (2014: 50) (taxonomy).

Type material

HOLOTYPE: AUSTRALIA: Queensland: Cairns district, A. M. Lea (Hacker Collection (C. J. Drake Collection 1956)), ♀. Photograph of type examined.

Other material examined

AUSTRALIA: Queensland: Tully Falls, 17.78333°S 145.56667°E, 10 Mar 1956, J. L. Gressitt, Light Trap, 1 ♂ (UNSW_ENT 00046439) (BPBM). ?Mareeba (sic) area, 16.99708°S 145.42306°E, 13 Jun 1997, K. Lewis, *Macadamia* sp. (Proteaceae), 1 ♂ (UNSW_ENT 00046440), 1 ♀ (UNSW_ENT 00046441), 1 unknown sex (UNSW_ENT 00046463) (QDPI). Beantree Rd. nr. Tolga, 17.23537°S 145.51378°E, 2015, Unknown, *Macadamia* sp. (Proteaceae), 2 ♀ (UNSW_ENT 00046442, UNSW_ENT 00046443), 1 ♂ (UNSW_ENT 00046529) (UNSW).

Diagnosis

Ulonemia leai can be recognised by the following characters: paranota carina-like across pronotal disc; paranotal areolae all roughly equal size; discoidal area with 8 areolae at widest point; occipital spines not reaching midpoint of eye; collum inflated posteriorly on either side of medial carina, broad, with concave anterior margin.

Male

Macropterous; 3.18 mm ± 0.00 mm (n = 2) (Table 3.1). COLOURATION. Stramineous to reddish brown or golden brown to brown. *Head*: golden brown to brown; spines stramineous; bucculae stramineous; eyes red. *Antennae*: AI-AIII golden brown, AIV golden brown proximally, quickly darkening to black distally. *Rostrum*: golden brown with dark brown to black apex. *Pronotum*: disc stramineous to golden brown; calli black; collum and paranota stramineous to golden brown; lateral and medial carinae stramineous, medial carina occasionally brown posteriorly. *Thoracic pleura and sterna*: proepisternum stramineous anteriorly, mostly golden brown to brown posteriorly, proepimeron stramineous, supracoxal lobes stramineous; mesepisternum mostly golden brown to brown, mesepimeron and supracoxal lobes stramineous; metepisternum golden brown to brown ventrally, stramineous dorsally; peritreme of metathoracic gland

stramineous; prosternum and mesosternum golden brown to brown, metasternum golden brown; pro-, meso-, and metasternal carinae stramineous. *Hemelytra*: discoidal area reddish brown to brown, with stramineous to golden brown field medially; subcostal area stramineous to golden brown; costal margin stramineous to golden brown; sutural area reddish brown to brown. *Legs*: mostly golden brown; tarsi dark brown to black distally. *Abdominal venter*: golden brown. VESTITURE. *Head*: distribution of golden brown aciculate setae in bands from base of AI to occipital spines and from frontal spines along either side of medial spine, to back of head; frons and gena with stramineous aciculate setae; medial spine with stramineous short aciculate to hooked setae; vertex with large globules of wax; bucculae with minute setae and ciliate punctures. *Antennae*: AI-AII with stramineous sparse, arcuate setae; AIII with stramineous decumbent setae, AIV with stramineous aciculate setae. *Pronotum*: anterior margin glabrous, rarely with short setae; pronotal margins with sparse distribution of arcuate aciculate setae; medial and lateral carinae with sparse distribution of arcuate aciculate setae; disc with minute setae and numerous punctures with 6-8 triangular tuberculate processes distributed evenly around internal rim of punctures; calli with dense short black setae, globules of wax often covering calli. *Thoracic pleura and sterna*: proepisternum with minute setae and tubercle-lined punctures anteriorly as on pronotal disc, lacking ciliate punctures posteriorly, proepimeron and supracoxal lobes with minute setae and tubercle-lined punctures; mesepisternum with minute setae, mesepimeron and supracoxal lobes with minute setae and tubercle-lined punctures posteriorly; metepisternum with minute setae and tubercle-lined punctures; propluron covered with small wax globules. *Legs*: coxae to femur with minute setae, tibia with minute setae proximally to aciculate setae distally. *Hemelytra*: sparse distribution of short aciculate setae on R+M and cubitus veins. *Abdominal venter*: minute setae and wax distributed throughout. STRUCTURE. *Head*: frontal spines slightly

conical, parallel to convergent, approximately 1/3 length of AI; medial spine stout, conical, height 1/2 of AI; occipital spines straight, mostly cylindrical, conical at apex, length subequal to medial spine, hardly protruding from anterior edge of collum. *Antennae*: AI and AII short, AII 1/3 length of AI; AIV linear to lanceolate. *Labium*: moderate length, extending beyond anterior margin of metasternum. *Pronotum*: strongly convex; collum mostly flattened, inflated posteriorly on either side of medial carina, height to 1/2 of disc; carinae minutely elevated from disc, height increasing posteriorly, uniseriate, cells very small; medial and lateral carinae equal width, lateral carinae divaricating slightly at apex of disc; paranota curved, following disc, upturned obliquely, biseriate, becoming carina-like posteriorly, areolae rectangular. *Thoracic sterna*: pro-, meso-, and metasternal carinae elevated, uniseriate, areolae small, rectangular; prosternal and mesosternal carinae straight, parallel, metasternal carinae truncate-obovate. *Hemelytra*: areolae small, irregular, and nearly uniform size in discoidal and subcostal areas; sutural area areolae similar to discoidal area proximally, increasing in size to 5x distally; costal areolae rectangular; costal area uniseriate, subcostal area biseriate, discoidal increasing from one to eight areolae wide, sutural area increasing from two to eleven areolae wide. *Male genitalia*: pygophore boxlike, with lateral margins only slightly curved, sometimes with pair of basal spurs near posterior margin of genital margin (Figure 3.22a, b); parameres C-shaped with apophysis strongly tapered distally (Figure 3.22c – e); aedeagus with Y-shaped dorsal plate (Figure 3.22f); endosomal membrane lacking spinules (Figure 3.22f – h); pair of sclerotised, endosomal lobal sclerites present but highly reduced in form (Figure 3.22f – h).

Female

Macropterous; 3.41 mm ± 0.05 mm (n = 2) (Table 3.1). COLOURATION. As in male. VESTITURE. As in male. STRUCTURE. As in male.

Host plants

Recorded from *Macadamia* sp., 6 specimens (Proteaceae).

Distribution

Drake (1942) recorded the type from “Corns District.”, which is a typographical error, as the tag on the holotype (visible in photos) says “Cairns dist.” Drake and Ruhoff (1965) corrected the error and list the type locality as “Cairns District.” Also known from near Mareeba and the Atherton Tablelands and Tully Gorge National Park south of Cairns, Queensland (Figure 3.23).

Remarks

This species superficially resembles *U. dignata*, and due to its unique morphological character combinations and genetic differentiation from other Australian *Ulonemia* sensu lato, it is the only species from Australia to be retained in the genus.

Uncertain taxonomic placement

***Ulonemia concava* Drake, 1942, incertae sedis**

(Figures 3.21, 3.23, 3.24)

Ulonemia concava Drake, 1942: 359 (original description); Drake and Ruhoff (1965: 420) (world catalogue); Cassis and Gross (1995: 437) (Australian catalogue); Dang et al. (2014: 50) (taxonomy).

Type material

HOLOTYPE: AUSTRALIA: Queensland: Cedar Creek, Jan 25 1931, Hacker Collection (C. J. Drake Collection 1956), ♂. Photograph of type examined.

Other material examined

AUSTRALIA: Queensland: Maleny, 26.767°S 152.85°E, 13 Oct 1967, D. A. I., *Macadamia tetraphylla* L.A.S. Johnson (Proteaceae), 4 mixed sexes (UNSW_ENT 00046437, UNSW_ENT 00046438) (QDPI).

Diagnosis

Ulonemia concava can be recognised by the following combination of characters: occipital spines exceeding mid-point of eye; paranota carina-like across pronotal disc; paranota areolae anterior to pronotal disc of uniform or near-uniform size; pronotal carinae ridge-like, lacking areolae; collum flattened, lacking hood; costal area biseriate anteriorly, uniseriate posteriorly, distinct constriction of hemelytra at posterior edge of discoidal area.

Male

Macropterous; 3.46 mm (n = 1) (Table 3.1). COLOURATION. Golden brown to stramineous. *Head*: reddish brown; frontal and occipital spines stramineous, medial spine reddish brown to stramineous; bucculae stramineous; eyes black. *Antennae*: AI-AIII golden brown, AIV golden brown proximally, darkening to dark brown distally. *Rostrum*: golden brown with dark brown to black apex. *Pronotum*: disc golden brown; calli dark reddish brown; collum and paranota stramineous to golden brown; lateral and medial carinae stramineous. *Thoracic pleura and sterna*: proepisternum stramineous anteriorly, mostly reddish brown to brown posteriorly, proepimeron reddish brown to brown, supracoxal lobes golden brown; mesepisternum mostly reddish brown to brown, mesepimeron and supracoxal lobes reddish brown to golden brown; metepisternum reddish brown ventrally, golden brown dorsally; peritreme of metathoracic gland golden brown; prosternum and mesosternum golden brown to brown, metasternum golden brown; pro-, meso-, and metasternal carinae stramineous. *Hemelytra*: discoidal area reddish brown to stramineous; subcostal, costal, and sutural areas stramineous to golden

brown; R+M and cubitus veins each with brown bar distally. *Legs*: mostly golden brown; coxae reddish brown. *Abdominal venter*: reddish brown to golden brown. VESTITURE. *Head*: distribution of golden brown aciculate setae from base of medial spine anteriorly to posterior margin of head; frons and gena with stramineous aciculate setae; medial spine with stramineous short aciculate setae; vertex with large globules of wax; bucculae with minute setae and ciliate punctures. *Antennae*: AI-AII with stramineous aciculate arcuate setae; AIII with stramineous aciculate decumbent setae, AIV with dense stramineous aciculate setae; distal end of AII and AIII with dense ring of microtrichia. *Pronotum*: anterior and paranotal margins with sparse distribution of minute setae; medial and lateral carinae with sparse distribution of minute setae; disc with minute setae and numerous punctures with 6-8 cilia distributed evenly around internal rim of punctures; calli with stramineous setae, globules of wax often covering calli. *Thoracic pleura and sterna*: proepisternum with minute setae and ciliate punctures anteriorly as on pronotal disc, lacking ciliate punctures posteriorly, proepimeron and supracoxal lobes with minute setae and ciliate punctures; mesepisternum with minute setae, mesepimeron and supracoxal lobes with minute setae and ciliate punctures posteriorly; metepisternum with minute setae and ciliate punctures; propluron covered with small wax globules. *Legs*: coxae to femur with minute setae, tibia with minute setae proximally to aciculate setae distally. *Hemelytra*: sparse distribution of short aciculate setae on R+M and cubitus veins; discoidal area with sparse distribution of minute setae on veins; sutural and subcostal areas glabrous; costal margin with sparse distribution of minute setae. *Abdominal venter*: minute setae and wax distributed throughout. STRUCTURE. *Head*: frontal spines conical, strongly convergent, approximately 1/5 length of AI; medial spine stout, subglobose to conical, height equal to frontal spines; occipital spines straight, mostly cylindrical, length 2x medial spine, strongly protruding from anterior edge of collum.

Antennae: AI and AII short, AII 1/3 length of AI; AIV linear to weakly clavate. *Labium*: moderate length, extending beyond anterior margin of metasternum. *Pronotum*: strongly convex; collum flattened, lacking hood, anterior margin straight to slightly projecting anteriorly; medial and lateral carinae decumbent on disc, becoming uniseriate posteriorly, cells very small; medial and lateral carinae equal width, lateral carinae divaricating slightly anterior to apex of disc; paranota curved, following disc, biseriate, becoming carina-like posteriorly, areolae rectangular. *Thoracic sterna*: pro-, meso-, and metasternal carinae elevated, uniseriate, areolae small, rectangular; prosternal and mesosternal carinae straight, parallel, metasternal carinae truncate-obovate. *Hemelytra*: areolae small, irregular, and nearly uniform size in discoidal, subcostal, and costal areas; sutural area areolae similar to discoidal area proximally, increasing in size to 8-10x distally; costal areolae rectangular; costal area uniseriate, subcostal area biseriate, discoidal increasing from one to eight areolae wide, sutural area increasing from two to eleven areolae wide. *Male genitalia*: pygophore boxlike, with lateral margins only slightly curved, with pair of basal spurs near posterior margin of genital margin (Figure 3.24a, b); parameres C-shaped with apophysis tapered distally (Figure 3.24c – e); aedeagus with Y-shaped dorsal plate (Figure 3.24f); endosomal membrane spinulate (Figure 3.24f – h); pair of sclerotised, endosomal lobal sclerites present (Figure 3.24f – h).

Female

Macropterous; 3.87 mm (n = 1) (Table 3.1). COLOURATION. As in male. VESTITURE. As in male. STRUCTURE. Larger body size than males; otherwise as in male.

Host plants

Recorded from *Macadamia tetraphylla*, 4 specimens (Proteaceae).

Distribution

Drake (1942) recorded this species from Cedar Creek, Queensland; also known from the vicinity of Maleny, Queensland (Figure 3.23).

Remarks

No records of this species after 1967 are known. Collection notes accompanying the QDPI specimens indicate that there were large outbreaks of this species in macadamia orchards at the time. Recent efforts to locate this species have failed. The current status of this species is unknown.

Morphological character combinations present in this species place it intermediate to *Cercotingis*, *Proteatingis*, and *Ulonemia*. The paranota are similar to other species of *Ulonemia*, though in *U. concava* incertae sedis the areolae are lacking entirely on the posterior portion of the pronotal disc (vs. highly reduced in *Ulonemia*). The biseriate costal margin is similar to *Cercotingis*, and excludes *U. concava* incertae sedis from both *Proteatingis* and *Ulonemia*. The male genitalia are most similar to *Proteatingis*, with the Y-shaped dorsal plate, sclerites on the endosoma, and hook-like lobal sclerites unique to that genus. The placement of *U. concava* incertae sedis therefore remains unresolved until further specimens and DNA can be obtained and analysed.

DISCUSSION

The three genera documented in this chapter, *Cercotingis*, *Proteatingis,* and *Ulonemia*, plus *U. concava* incertae sedis, are very similar in their morphology. In addition, they all have an affinity for host taxa within the Proteaceae. The phylogenetic analysis in chapter 2, however, clearly indicates that these genera are paraphyletic in their original status as *Ulonemia*, with respect to other morphologically conserved genera (e.g. *Eritingis*, *Ischnotingis*, and *Nethersia*). Also, while the morphology of species within *Ulonemia* sensu lato is similar, no single character, or combination of characters, unified the genus. As such, *Ulonemia* was reclassified, including the erection of two new genera and restricted definition of *Ulonemia*, in alignment with the phylogenetic arrangement of the constituent species.

Morphological character combinations were established in this chapter that support each new genus and the re-defined *Ulonemia*. *Cercotingis* possesses triseriate paranota and a biseriate costal area anterior to the midline of the discoidal area, and lacks a hood. *Proteatingis* possesses uniseriate paranota, an entirely uniseriate costal area, and a raised collum that projects forward over the posterior margin of the head to form a small hood. *Ulonemia* possesses a raised collum that is somewhat produced posteriorly, forming a slight hood, the paranota are reduced across the pronotal disc, appearing carina-like but remaining unicarinate, and the costal margin is uniseriate for the entire length. *Ulonemia* remains difficult to diagnose, and these characters are based on habitus photographs of the holotype and specimens of *U. leai*. A thorough analysis of the remaining species in the genus may reveal the need for further taxonomic changes, with potential broader impacts on other Australasian tingid lineages with simplified morphologies.

All three genera covered in this work have species that have become pestiferous on *Macadamia*. One species, *U. leai*, is not known to occur in the native range of any *Macadamia* species, and has only been found in association with plantations in the Atherton Tableland. This suggests that *U. leai* likely has an alternative native proteaceous host and has shifted to *Macadamia* in this region via its introduction as an orchard crop.

Two species of *Proteatingis*, *P. astibosetes* and *P. mjobergi*, have been collected near *Macadamia* growing areas. While they have yet to be collected from *Macadamia*, the presence of multiple lineages of tingid on *Macadamia*, including a documented novel infestation, point towards these two species as potential threats to the macadamia nut industry. Continual monitoring of the tingid species present in *Macadamia* orchards is crucial in identifying potentially problematic new invasions.

Table 3.1. Measurements of *Cercotingis, Proteatingis,* and *Ulonemia* external characters. All measurements in millimetres. Mean, standard deviation (SD), range, minimum (min), and maximum (max) values are provided for each species. Abbreviations: Pron = pronotum; Hmlt = hemelytra; Disc = discoidal area; Strl = sutural area; Intr = interoculardistance; AI = antennal segment I; AII = antennal segment II; AIII = antennal segment III; AIV = antennal segment IV.

		Length -	-	-	-	-	Width -						
Cercotingis		Body	Head	Pron	Hmlt	Disc	Strl	Head	Pron	Intr	AI	AII	AIII	AIV
croajingolong														
Male (n = 6)	Mean	3.51	0.28	1.43	2.59	1.35	1.80	0.47	0.91	0.23	0.15	0.13	1.22	0.30
	SD	0.19	0.02	0.10	0.14	0.08	0.09	0.02	0.06	0.01	0.02	0.01	0.07	0.02
	Range	0.60	0.07	0.31	0.44	0.25	0.28	0.05	0.17	0.03	0.05	0.03	0.18	0.06
	Min	3.14	0.23	1.24	2.31	1.18	1.62	0.45	0.80	0.21	0.13	0.12	1.08	0.28
	Max	3.74	0.30	1.54	2.76	1.43	1.91	0.49	0.98	0.24	0.18	0.15	1.27	0.34
Female (n = 8)														
	Mean	3.60	0.28	1.53	2.65	1.44	1.79	0.50	0.98	0.25	0.16	0.13	1.11	0.30
	SD	0.18	0.03	0.10	0.14	0.07	0.09	0.02	0.05	0.02	0.01	0.01	0.06	0.03
	Range	0.69	0.09	0.32	0.51	0.22	0.33	0.07	0.16	0.07	0.03	0.03	0.22	0.09
	Min	3.23	0.24	1.33	2.38	1.30	1.61	0.46	0.88	0.21	0.15	0.11	0.98	0.24
	Max	3.92	0.33	1.65	2.89	1.52	1.94	0.53	1.04	0.28	0.18	0.14	1.20	0.33

Table 3.1 continued, next page

Table 3.1. (continued)

Cercotingis		Length Body	- Head	- Pron	- Hmlt	- Disc	- Strl	Width Head	- Pron	Intr	AI	AII	AIII	AIV
decoris														
Male (n = 10)	Mean	3.27	0.27	1.32	2.39	1.23	1.68	0.45	0.81	0.21	0.17	0.13	1.03	0.32
	SD	0.08	0.01	0.04	0.06	0.04	0.04	0.01	0.03	0.02	0.01	0.01	0.06	0.03
	Range	0.27	0.05	0.13	0.20	0.14	0.14	0.03	0.10	0.08	0.03	0.03	0.19	0.10
	Min	3.13	0.25	1.25	2.30	1.18	1.63	0.44	0.75	0.17	0.15	0.11	0.91	0.26
	Max	3.40	0.29	1.38	2.49	1.32	1.77	0.47	0.85	0.26	0.18	0.14	1.10	0.36
Female (n = 10)	Mean	3.51	0.28	1.44	2.58	1.37	1.79	0.47	0.89	0.23	0.17	0.13	1.03	0.33
	SD	0.09	0.01	0.04	0.07	0.04	0.05	0.01	0.03	0.02	0.01	0.01	0.04	0.02
	Range	0.26	0.03	0.14	0.24	0.12	0.15	0.03	0.10	0.05	0.02	0.03	0.14	0.06
	Min	3.35	0.26	1.36	2.45	1.31	1.71	0.46	0.83	0.20	0.16	0.12	0.97	0.31
	Max	3.62	0.29	1.50	2.70	1.43	1.86	0.49	0.93	0.25	0.18	0.14	1.11	0.37
impensa														
Male (n = 2)	Mean	2.66	0.28	1.05	1.91	1.01	1.33	0.38	0.73	0.18	0.25	0.16	1.94	0.51
	SD	0.03	0.01	0.02	0.02	0.02	0.02	0.00	0.01	0.01	0.00	0.02	0.16	0.02
	Range	0.06	0.02	0.05	0.05	0.04	0.03	0.01	0.02	0.03	0.00	0.03	0.33	0.04
	Min	2.62	0.27	1.02	1.88	0.99	1.32	0.38	0.72	0.17	0.25	0.15	1.78	0.50
	Max	2.69	0.29	1.07	1.93	1.04	1.35	0.39	0.74	0.20	0.25	0.18	2.10	0.53
Female (n = 10)														
	Mean	3.19	0.32	1.29	2.31	1.29	1.59	0.45	0.88	0.22	0.22	0.15	1.60	0.39
	SD	0.63	0.07	0.26	0.45	0.24	0.31	0.09	0.17	0.05	0.04	0.03	0.27	0.08
	Range	1.43	0.19	0.63	0.98	0.55	0.70	0.20	0.43	0.14	0.11	0.10	0.79	0.26
	Min	2.63	0.25	1.04	1.93	1.07	1.30	0.36	0.71	0.17	0.16	0.10	1.18	0.27
	Max	4.07	0.43	1.67	2.91	1.62	2.00	0.57	1.14	0.30	0.27	0.21	1.97	0.53

Table 3.1 continued, next page

Table 3.1. (continued)

Cercotingis		Length Body	- Head	- Pron	- Hmlt	- Disc	- Strl	Width Head	- Pron	Intr	AI	AII	AIII	AIV
namadgi														
Male (n = 10)	Mean	3.59	0.31	1.50	2.59	1.38	1.78	0.52	0.98	0.24	0.17	0.14	1.35	0.33
	SD	0.13	0.02	0.05	0.10	0.06	0.09	0.02	0.04	0.01	0.01	0.01	0.08	0.02
	Range	0.46	0.05	0.18	0.33	0.22	0.27	0.05	0.14	0.04	0.04	0.03	0.31	0.08
	Min	3.31	0.30	1.38	2.40	1.27	1.63	0.50	0.92	0.22	0.14	0.13	1.14	0.28
	Max	3.77	0.34	1.57	2.73	1.49	1.90	0.55	1.06	0.26	0.18	0.15	1.46	0.36
Female (n = 10)														
	Mean	3.92	0.33	1.68	2.80	1.58	1.91	0.55	1.09	0.28	0.18	0.14	1.27	0.31
	SD	0.11	0.02	0.05	0.09	0.06	0.06	0.01	0.05	0.01	0.01	0.01	0.06	0.03
	Range	0.39	0.07	0.18	0.30	0.24	0.20	0.04	0.14	0.04	0.04	0.02	0.21	0.08
	Min	3.78	0.28	1.59	2.69	1.47	1.83	0.53	1.01	0.26	0.15	0.13	1.13	0.27
	Max	4.17	0.36	1.77	2.99	1.71	2.04	0.58	1.15	0.30	0.19	0.15	1.34	0.35
tasmaniensis														
Male (n = 1)	Mean	3.43	0.26	1.43	2.53	1.29	1.74	0.47	0.90	0.23	0.14	0.12	1.13	0.35
	SD	0.00	0.00	0.00	0.00	0.00	0.00	0.00	0.00	0.00	0.00	0.00	0.00	0.00
	Range	0.00	0.00	0.00	0.00	0.00	0.00	0.00	0.00	0.00	0.00	0.00	0.00	0.00
	Min	3.43	0.26	1.43	2.53	1.29	1.74	0.47	0.90	0.23	0.14	0.12	1.13	0.35
	Max	3.43	0.26	1.43	2.53	1.29	1.74	0.47	0.90	0.23	0.14	0.12	1.13	0.35
Female (n = 2)	Mean	3.44	0.30	1.45	2.51	1.33	1.69	0.48	0.90	0.24	0.13	0.11	0.92	0.30
	SD	0.05	0.01	0.01	0.04	0.02	0.03	0.01	0.02	0.00	0.01	0.01	0.03	0.00
	Range	0.11	0.02	0.03	0.08	0.03	0.06	0.01	0.03	0.00	0.03	0.02	0.07	0.01
	Min	3.38	0.29	1.44	2.47	1.32	1.66	0.48	0.88	0.24	0.12	0.10	0.89	0.29
	Max	3.49	0.31	1.47	2.55	1.35	1.72	0.49	0.91	0.24	0.15	0.11	0.96	0.30

Table 3.1 continued, next page

Table 3.1. (continued)

Proteatingis		Length Body	- Head	- Pron	- Hmlt	- Disc	- Strl	Width Head	- Pron	Intr	AI	AII	AIII	AIV
astibosetes														
Male (n = 2)	Mean	3.33	0.25	1.61	2.33	1.31	1.47	0.52	0.92	0.24	0.18	0.13	1.05	0.40
	SD	0.08	0.00	0.07	0.05	0.00	0.02	0.02	0.01	0.00	0.01	0.01	0.04	0.02
	Range	0.17	0.00	0.14	0.10	0.01	0.04	0.04	0.02	0.00	0.01	0.02	0.08	0.04
	Min	3.25	0.24	1.55	2.28	1.31	1.46	0.50	0.91	0.24	0.18	0.12	1.01	0.38
	Max	3.42	0.25	1.68	2.38	1.32	1.49	0.54	0.93	0.24	0.19	0.14	1.09	0.42
Female (n = 6)	Mean	3.62	0.29	1.73	2.51	1.45	1.60	0.54	1.01	0.28	0.17	0.12	1.04	0.44
	SD	0.15	0.04	0.07	0.12	0.07	0.10	0.02	0.04	0.02	0.02	0.01	0.04	0.02
	Range	0.45	0.11	0.18	0.31	0.22	0.27	0.05	0.12	0.06	0.04	0.03	0.11	0.06
	Min	3.37	0.24	1.61	2.36	1.35	1.50	0.50	0.95	0.25	0.15	0.11	0.99	0.41
	Max	3.82	0.35	1.79	2.67	1.57	1.77	0.56	1.07	0.32	0.19	0.14	1.10	0.47
burckhardti (large)														
Male (n = 10)	Mean	3.27	0.23	1.45	2.35	1.25	1.60	0.46	0.85	0.25	0.17	0.13	1.27	0.35
	SD	0.10	0.02	0.07	0.08	0.07	0.04	0.01	0.02	0.01	0.01	0.01	0.06	0.05
	Range	0.33	0.05	0.26	0.23	0.25	0.14	0.05	0.07	0.04	0.03	0.02	0.21	0.16
	Min	3.12	0.20	1.31	2.25	1.14	1.53	0.44	0.82	0.23	0.15	0.11	1.16	0.25
	Max	3.46	0.24	1.57	2.48	1.40	1.68	0.49	0.89	0.28	0.18	0.14	1.38	0.40
Female (n = 10)														
	Mean	3.41	0.24	1.57	2.43	1.34	1.60	0.48	0.92	0.28	0.18	0.12	1.24	0.32
	SD	0.09	0.02	0.05	0.07	0.05	0.06	0.01	0.04	0.01	0.01	0.01	0.04	0.03
	Range	0.26	0.05	0.17	0.20	0.15	0.18	0.04	0.12	0.05	0.05	0.03	0.15	0.08
	Min	3.27	0.22	1.47	2.32	1.27	1.51	0.46	0.86	0.24	0.15	0.11	1.18	0.29
	Max	3.53	0.27	1.64	2.52	1.42	1.69	0.50	0.98	0.30	0.20	0.14	1.32	0.37

Table 3.1 continued, next page

Table 3.1. (continued)

Proteatingis		Length Body	- Head	- Pron	- Hmlt	- Disc	- Strl	Width Head	- Pron	Intr	AI	AII	AIII	AIV
burckhardti (small)														
Male (n = 10)	Mean	3.02	0.22	1.32	2.14	1.11	1.47	0.44	0.78	0.24	0.16	0.11	1.14	0.32
	SD	0.08	0.02	0.04	0.06	0.04	0.05	0.01	0.02	0.01	0.01	0.01	0.04	0.03
	Range	0.25	0.06	0.13	0.22	0.12	0.15	0.02	0.07	0.04	0.04	0.03	0.15	0.09
	Min	2.88	0.19	1.26	2.00	1.04	1.37	0.43	0.75	0.22	0.14	0.09	1.05	0.28
	Max	3.12	0.25	1.38	2.23	1.16	1.52	0.46	0.82	0.26	0.18	0.12	1.20	0.36
Female (n = 10)	Mean	3.15	0.24	1.41	2.22	1.22	1.50	0.47	0.83	0.25	0.15	0.11	1.09	0.34
	SD	0.11	0.02	0.07	0.09	0.06	0.06	0.01	0.03	0.01	0.01	0.01	0.04	0.03
	Range	0.43	0.06	0.24	0.36	0.23	0.22	0.05	0.13	0.03	0.02	0.02	0.14	0.10
	Min	2.88	0.21	1.26	2.01	1.09	1.38	0.44	0.77	0.23	0.14	0.10	1.03	0.28
	Max	3.32	0.27	1.51	2.37	1.32	1.61	0.50	0.90	0.27	0.16	0.12	1.17	0.38
howardi														
Male (n = 10)	Mean	2.99	0.16	1.46	2.14	1.25	1.37	0.47	0.91	0.22	0.15	0.11	0.92	0.31
	SD	0.05	0.02	0.03	0.04	0.04	0.03	0.01	0.02	0.01	0.01	0.01	0.04	0.04
	Range	0.17	0.06	0.09	0.17	0.14	0.11	0.03	0.06	0.03	0.03	0.02	0.15	0.14
	Min	2.87	0.14	1.42	2.04	1.21	1.30	0.45	0.87	0.21	0.14	0.10	0.84	0.23
	Max	3.04	0.20	1.51	2.20	1.34	1.41	0.49	0.94	0.24	0.17	0.12	0.99	0.37
Female (n = 10)	Mean	3.22	0.17	1.60	2.31	1.39	1.46	0.49	0.99	0.23	0.16	0.11	0.95	0.34
	SD	0.07	0.01	0.04	0.06	0.05	0.05	0.01	0.02	0.01	0.01	0.01	0.02	0.03
	Range	0.26	0.03	0.12	0.22	0.16	0.17	0.04	0.08	0.02	0.04	0.04	0.05	0.10
	Min	3.07	0.15	1.52	2.19	1.31	1.39	0.47	0.94	0.22	0.14	0.09	0.92	0.28
	Max	3.33	0.18	1.64	2.41	1.47	1.55	0.51	1.02	0.25	0.18	0.13	0.98	0.38

Table 3.1 continued, next page

Table 3.1. (continued)

Proteatingis		Length Body	- Head	- Pron	- Hmlt	- Disc	- Strl	Width Head	- Pron	Intr	AI	AII	AIII	AIV
burckhardti minuta														
Male (n = 7)	Mean	2.66	0.26	1.17	1.84	0.99	1.23	0.45	0.73	0.25	0.33	0.23	1.83	0.49
	SD	0.04	0.02	0.03	0.04	0.07	0.04	0.01	0.01	0.01	0.11	0.08	0.26	0.01
	Range	0.14	0.05	0.09	0.13	0.23	0.12	0.04	0.02	0.03	0.36	0.27	0.57	0.03
	Min	2.56	0.23	1.12	1.75	0.87	1.16	0.42	0.72	0.23	0.15	0.11	1.61	0.48
	Max	2.70	0.28	1.21	1.88	1.10	1.28	0.47	0.74	0.26	0.51	0.38	2.19	0.50
Female (n = 5)														
	Mean	2.67	0.26	1.21	1.86	1.06	1.20	0.46	0.75	0.26	0.30	0.21	1.71	0.60
	SD	0.03	0.02	0.03	0.02	0.04	0.02	0.01	0.02	0.01	0.05	0.06	0.15	0.00
	Range	0.09	0.05	0.09	0.07	0.13	0.06	0.03	0.05	0.02	0.15	0.18	0.37	0.00
	Min	2.63	0.25	1.16	1.82	0.98	1.16	0.44	0.72	0.25	0.25	0.14	1.53	0.59
	Max	2.72	0.30	1.25	1.89	1.11	1.22	0.47	0.77	0.27	0.39	0.31	1.91	0.60
mjobergi														
Male (n = 10)	Mean	3.19	0.21	1.56	2.21	1.27	1.42	0.49	0.90	0.23	0.14	0.12	1.19	0.37
	SD	0.08	0.02	0.05	0.07	0.04	0.04	0.02	0.02	0.01	0.01	0.01	0.05	0.03
	Range	0.27	0.09	0.18	0.22	0.15	0.15	0.05	0.09	0.05	0.03	0.03	0.16	0.08
	Min	3.07	0.18	1.50	2.12	1.20	1.36	0.47	0.84	0.20	0.13	0.10	1.12	0.33
	Max	3.33	0.27	1.68	2.34	1.36	1.52	0.52	0.93	0.25	0.16	0.13	1.27	0.41
Female (n = 10)														
	Mean	3.23	0.22	1.62	2.22	1.34	1.39	0.50	0.95	0.25	0.14	0.11	1.10	0.38
	SD	0.11	0.02	0.06	0.09	0.05	0.07	0.02	0.03	0.01	0.01	0.01	0.04	0.04
	Range	0.37	0.05	0.25	0.29	0.14	0.27	0.06	0.10	0.03	0.02	0.03	0.15	0.12
	Min	3.06	0.20	1.51	2.10	1.27	1.30	0.48	0.90	0.23	0.13	0.10	1.01	0.32
	Max	3.43	0.25	1.75	2.39	1.41	1.57	0.53	1.00	0.27	0.16	0.13	1.16	0.44

Table 3.1 continued, next page

Table 3.1. (continued)

Proteatingis		Length Body	- Head	- Pron	- Hmlt	- Disc	- Strl	Width Head	- Pron	Intr	AI	AII	AIII	AIV
plesia														
Male (n = 10)	Mean	3.36	0.23	1.61	2.39	1.35	1.53	0.48	1.00	0.27	0.14	0.11	1.07	0.31
	SD	0.13	0.04	0.06	0.09	0.07	0.06	0.01	0.04	0.01	0.01	0.01	0.03	0.02
	Range	0.40	0.13	0.21	0.30	0.24	0.20	0.04	0.11	0.05	0.03	0.04	0.11	0.07
	Min	3.17	0.17	1.51	2.24	1.23	1.44	0.46	0.94	0.24	0.13	0.09	1.01	0.27
	Max	3.58	0.29	1.72	2.54	1.47	1.63	0.50	1.05	0.29	0.16	0.13	1.12	0.35
Female (n = 10)	Mean	3.58	0.25	1.77	2.52	1.51	1.56	0.51	1.09	0.27	0.16	0.11	1.08	0.28
	SD	0.08	0.02	0.05	0.06	0.04	0.05	0.01	0.02	0.02	0.01	0.01	0.04	0.03
	Range	0.24	0.05	0.19	0.21	0.14	0.16	0.02	0.08	0.07	0.04	0.04	0.13	0.07
	Min	3.44	0.23	1.68	2.40	1.43	1.45	0.50	1.03	0.24	0.14	0.10	1.02	0.24
	Max	3.68	0.28	1.87	2.61	1.57	1.62	0.52	1.12	0.31	0.18	0.14	1.16	0.31
Ulonemia leai														
Male (n = 2)	Mean	3.18	0.30	1.35	2.26	1.23	1.52	0.49	0.82	0.20	0.18	0.12	1.40	0.36
	SD	0.00	0.01	0.03	0.02	0.00	0.01	0.01	0.03	0.00	0.02	0.01	0.00	0.00
	Range	0.00	0.03	0.06	0.03	0.00	0.03	0.03	0.05	0.01	0.04	0.02	0.01	0.00
	Min	3.18	0.29	1.32	2.24	1.23	1.51	0.48	0.79	0.19	0.16	0.11	1.39	0.36
	Max	3.18	0.32	1.38	2.27	1.23	1.54	0.50	0.84	0.20	0.20	0.13	1.40	0.36
Female (n = 2)														
	Mean	3.41	0.30	1.53	2.42	1.38	1.57	0.52	0.95	0.22	0.19	0.11	1.38	0.47
	SD	0.05	0.02	0.02	0.02	0.04	0.01	0.00	0.02	0.01	0.02	0.00	0.02	0.02
	Range	0.11	0.03	0.05	0.05	0.07	0.03	0.01	0.04	0.02	0.04	0.01	0.04	0.03
	Min	3.36	0.29	1.51	2.40	1.35	1.56	0.52	0.94	0.21	0.17	0.10	1.36	0.45
	Max	3.47	0.32	1.56	2.44	1.42	1.59	0.53	0.97	0.23	0.21	0.11	1.40	0.49

Table 3.1 continued, next page

Table 3.1. (continued)

Incertae sedis		Length Body	- Head	- Pron	- Hmlt	- Disc	- Strl	Width Head	- Pron	Intr	AI	AII	AIII	AIV
concava														
Male (n = 1)	Mean	3.46	0.23	1.46	2.57	1.37	1.78	0.45	0.87	0.19	0.17	0.13	1.06	0.41
	SD	0.00	0.00	0.00	0.00	0.00	0.00	0.00	0.00	0.00	0.00	0.00	0.00	0.00
	Range	0.00	0.00	0.00	0.00	0.00	0.00	0.00	0.00	0.00	0.00	0.00	0.00	0.00
	Min	3.46	0.23	1.46	2.57	1.37	1.78	0.45	0.87	0.19	0.17	0.13	1.06	0.41
	Max	3.46	0.23	1.46	2.57	1.37	1.78	0.45	0.87	0.19	0.17	0.13	1.06	0.41
Female (n = 1)	Mean	3.87	0.26	1.60	2.92	1.58	2.01	0.47	0.96	0.22	0.19	0.14	1.08	0.40
	SD	0.00	0.00	0.00	0.00	0.00	0.00	0.00	0.00	0.00	0.00	0.00	0.00	0.00
	Range	0.00	0.00	0.00	0.00	0.00	0.00	0.00	0.00	0.00	0.00	0.00	0.00	0.00
	Min	3.87	0.26	1.60	2.92	1.58	2.01	0.47	0.96	0.22	0.19	0.14	1.08	0.40
	Max	3.87	0.26	1.60	2.92	1.58	2.01	0.47	0.96	0.22	0.19	0.14	1.08	0.40

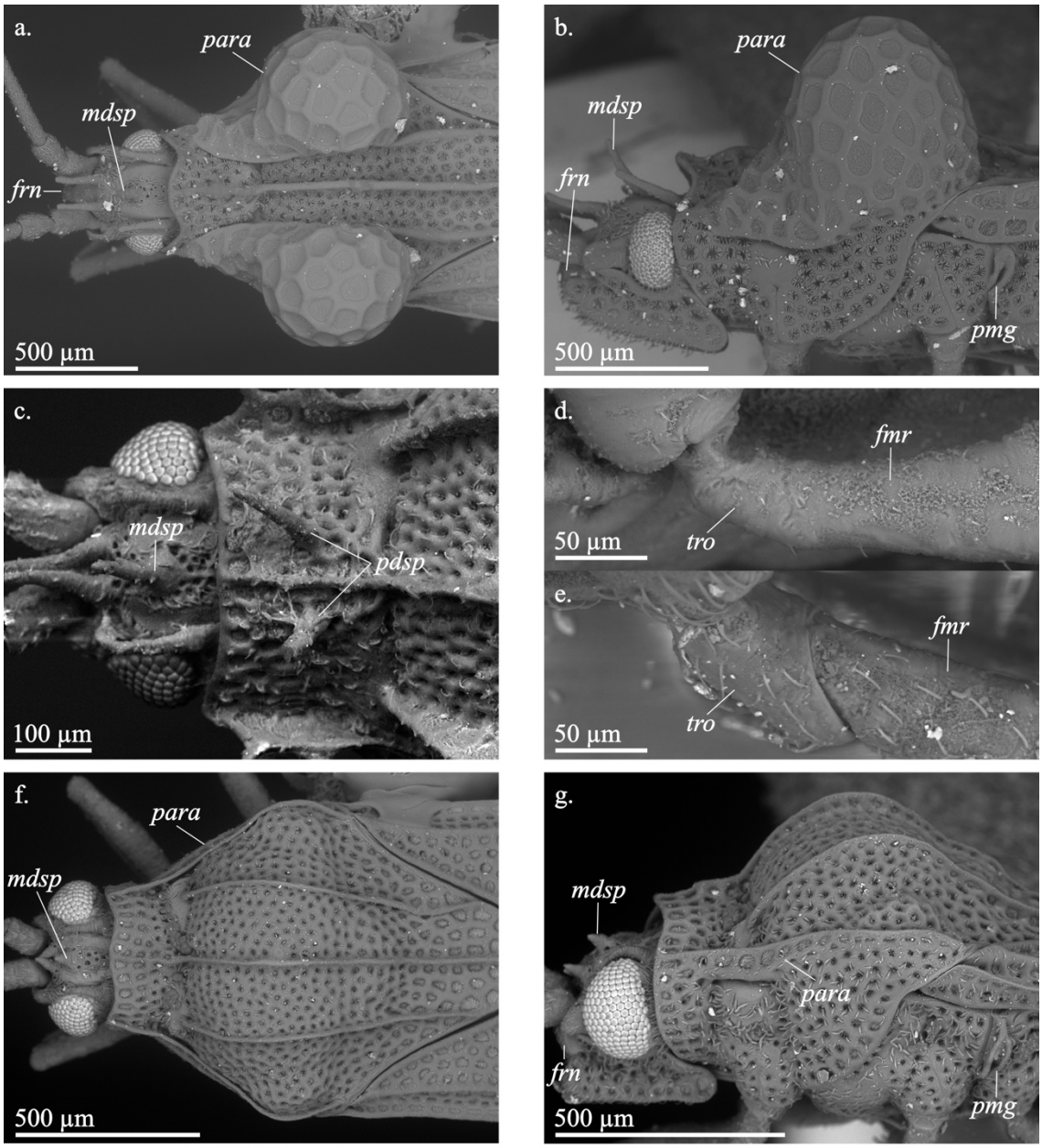

Figure 3.1. Scanning electron micrographs of *Cysteochila* sp. (a., b.), *Engynoma multispinosa* (c.), *Epimixia* sp. (d.), and *Eritingis trivirgata* (e. – g.). Abbreviations: *fmr* – femur; *frn* – frons; *mdsp* – medial spine; *para* – paranotum; *pdsp* – paired spines; *pmg* – peritreme of the metathoracic gland.

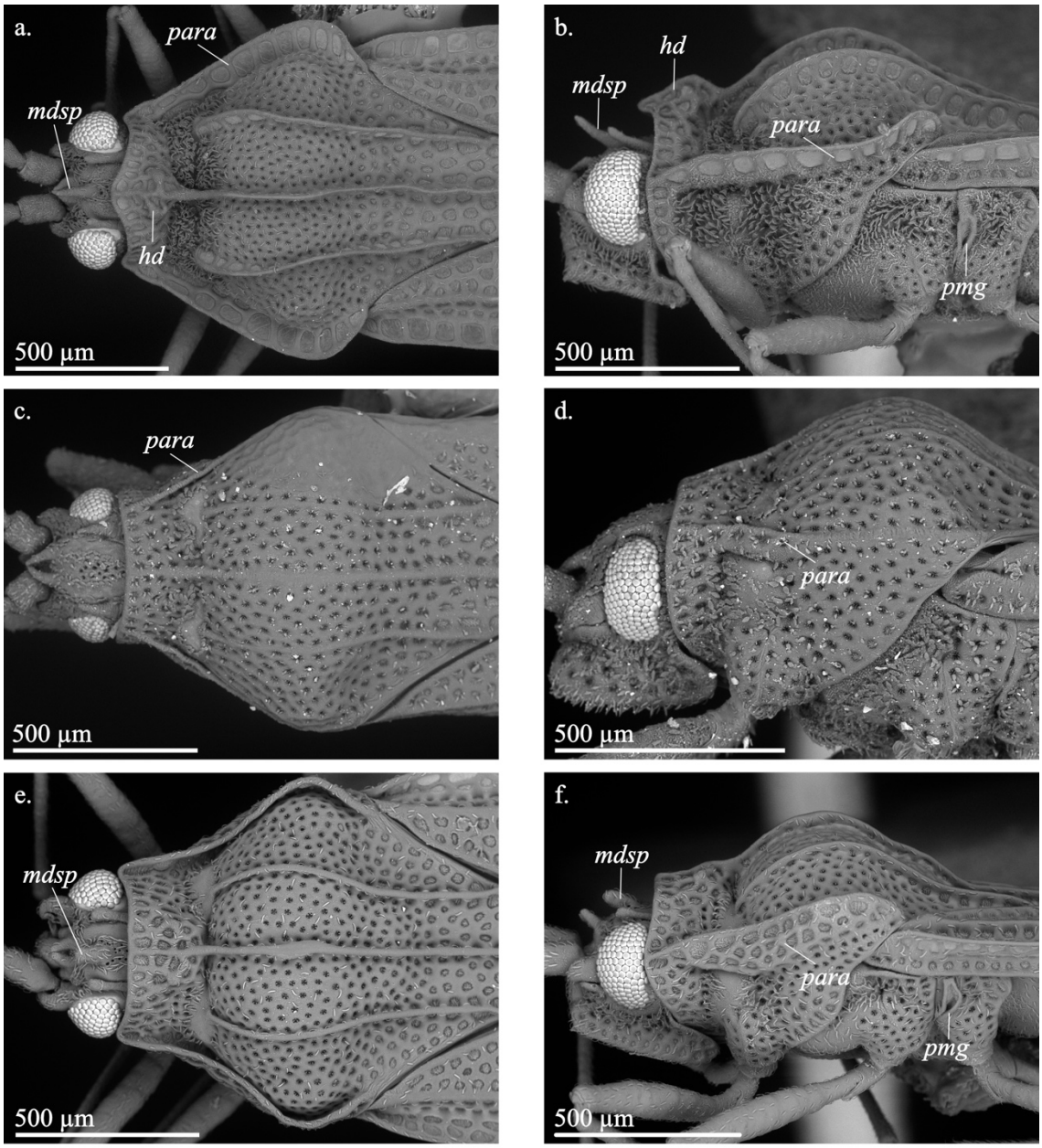

Figure 3.2. Scanning electron micrographs of *Proteatingis mjobergi* (a., b.), *Malandiola semota* (c., d.), and *Cercotingis tasmaniensis* (e., f.). Abbreviations: *hd* - hood; *mdsp* – medial spine; *para* – paranotum; *pmg* – peritreme of the metathoracic gland. NOTE: *M. semota* lacks a medial spine and peritreme.

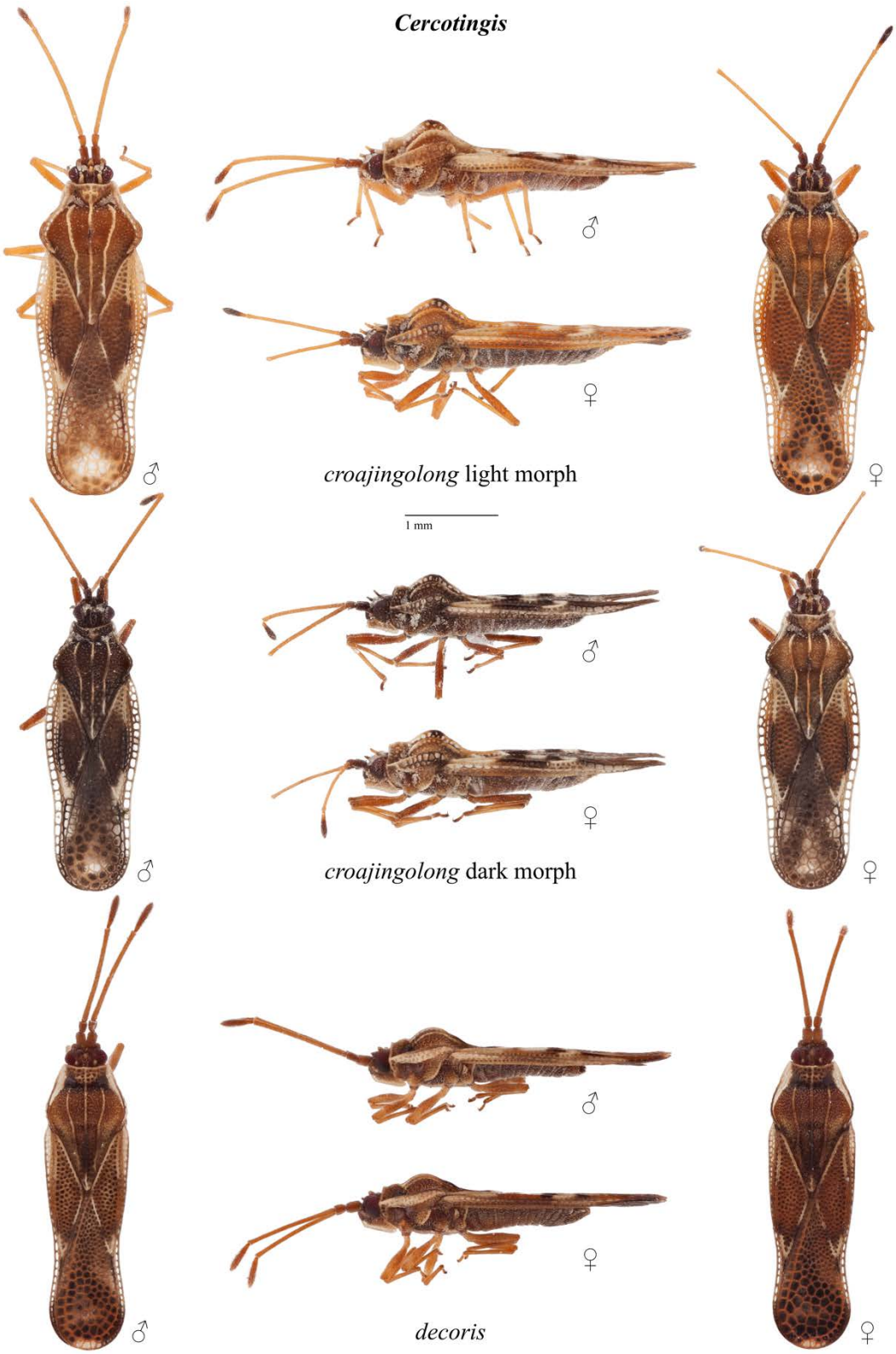

Figure 3.3. Dorsal and lateral habitus photos of *Cercotingis croajingolong* light and dark morphs and *C. decoris*. Scale bar = 1 mm.

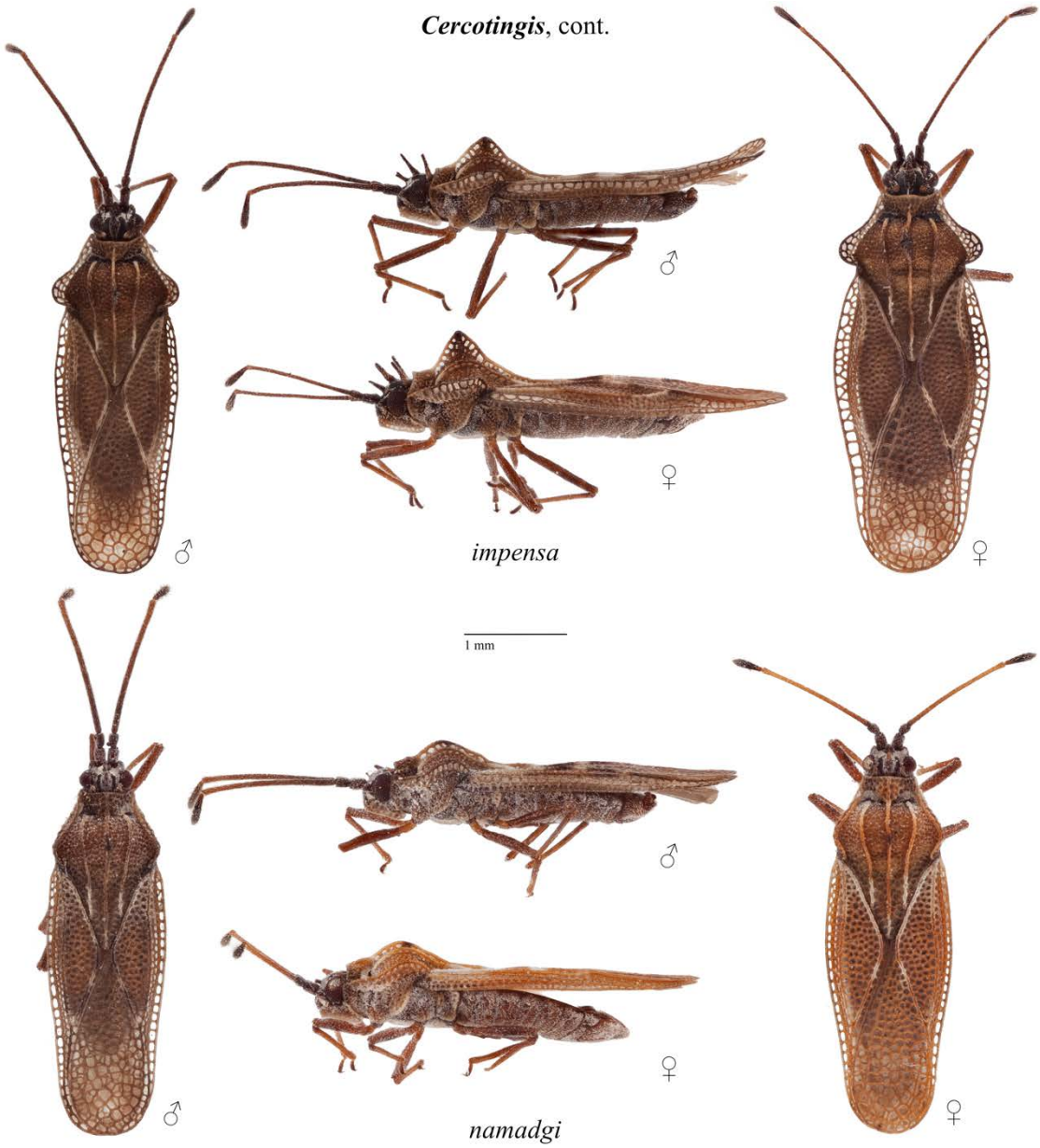

Figure 3.4. Dorsal and lateral habitus photos of *Cercotingis impensa* and *C. namadgi*. Scale bar = 1 mm.

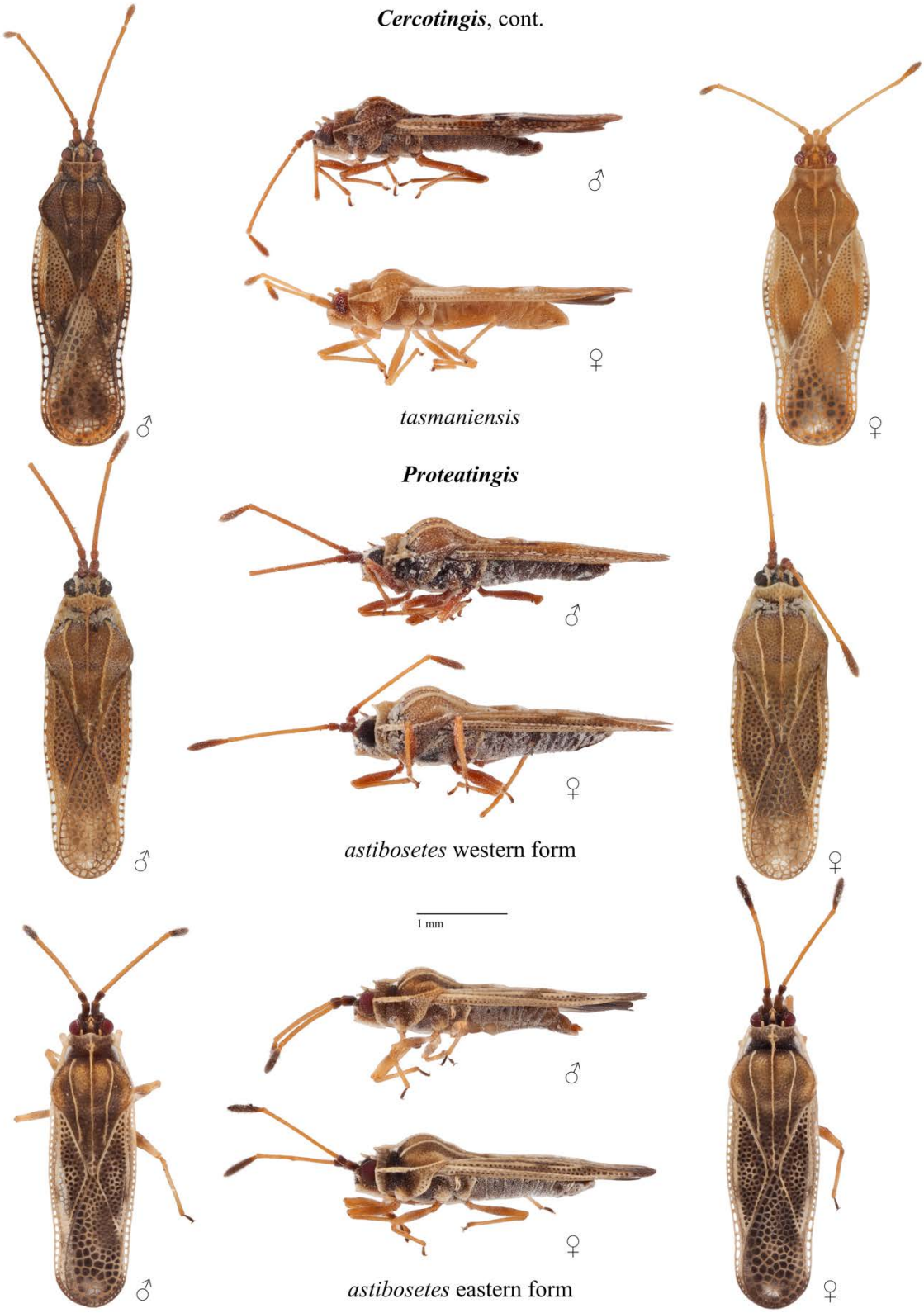

Figure 3.5. Dorsal and lateral habitus photos of *Cercotingis tasmaniensis* and *Proteatingis astibosetes* western and eastern forms. Scale bar = 1 mm.

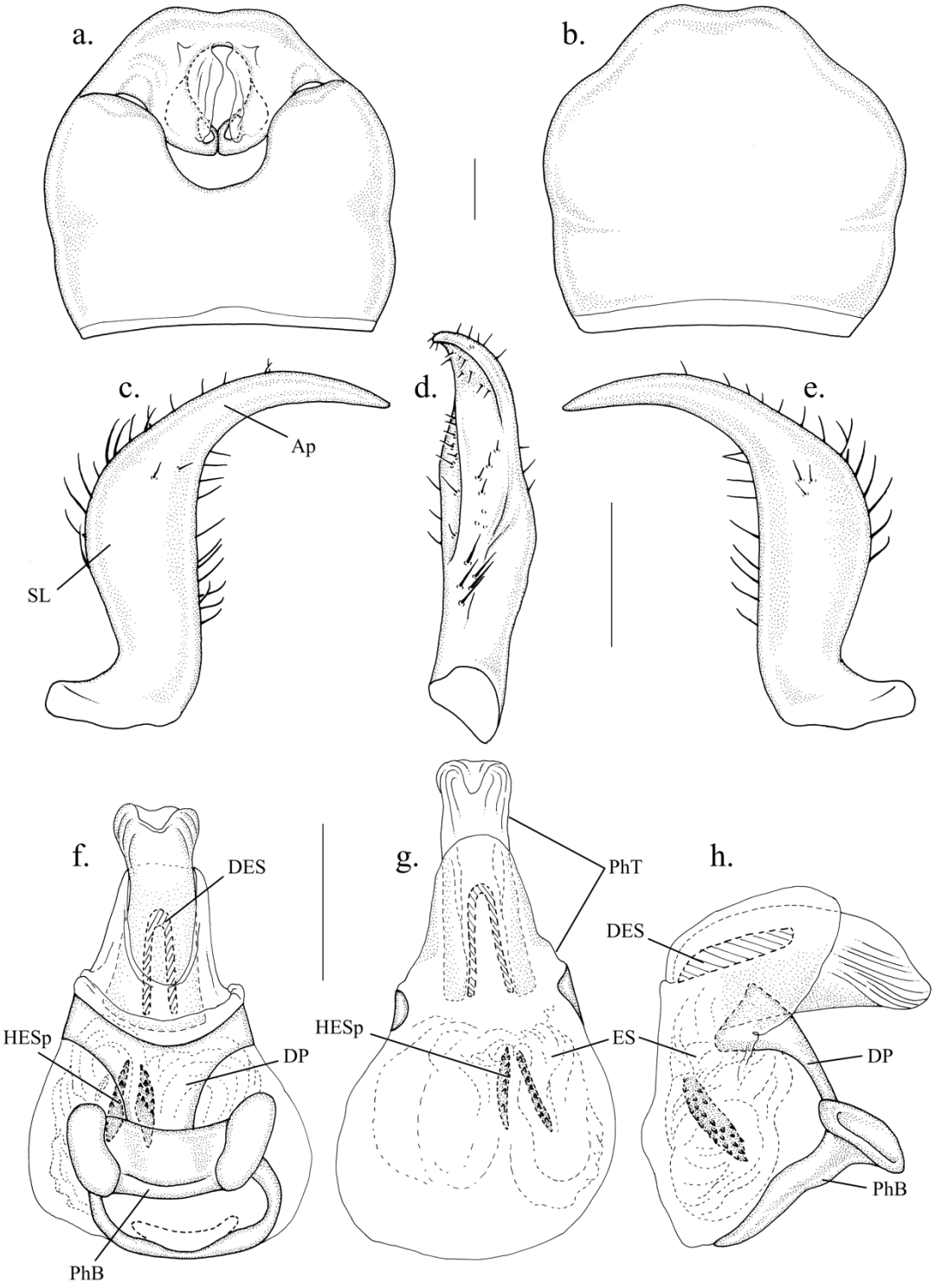

Figure 3.6. Male genitalia of *Cercotingis croajingolong*: a. pygophore, dorsal view; b. pygophore, ventral view; c. left paramere, dorsal view; d. right paramere, lateral view; e. right paramere, dorsal view; f. aedeagus, dorsal view; g. aedeagus, ventral view; h. aedeagus, right lateral view. Abbreviations: Ap – apophysis; DES – dorsal endosomal sclerite; DP – dorsal plate; ES – endosoma; HESp – hooked endosomal sclerites; PhB – phallobase; PhT – phallotheca; SL – sensory lobe. Scale bars = 0.1 mm.

Figure 3.7. Distribution map for *Cercotingis croajingolong*, *C. decoris*, *C. impensa*, *C. namadgi*, and *C. tasmaniensis*. Locality information taken from the PBI database.

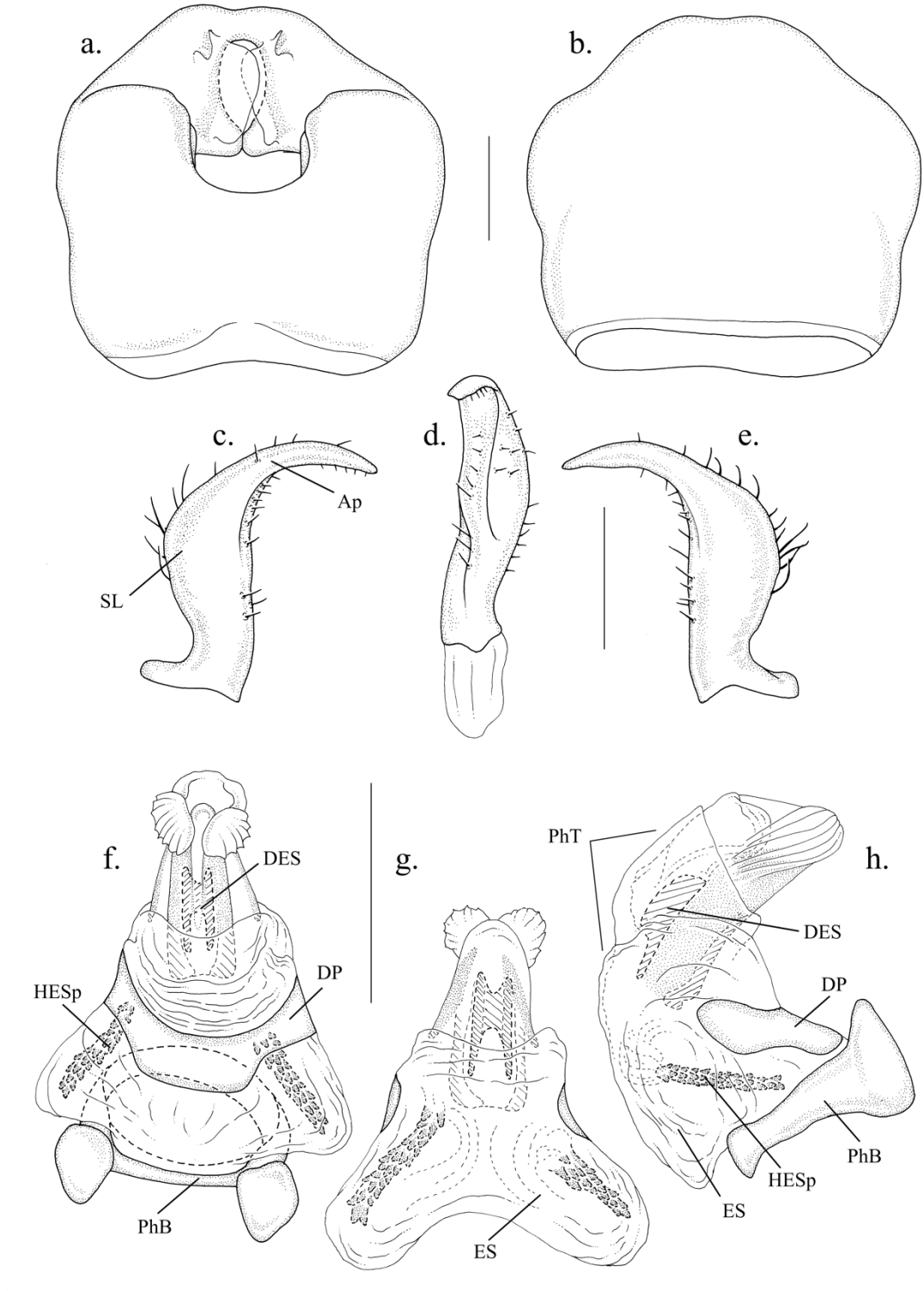

Figure 3.8. Male genitalia of *Cercotingis decoris*: a. pygophore, dorsal view; b. pygophore, ventral view; c. left paramere, dorsal view; d. right paramere, lateral view; e. right paramere, dorsal view; f. aedeagus, dorsal view; g. aedeagus, ventral view; h. aedeagus, right lateral view. Abbreviations: Ap – apophysis; DES – dorsal endosomal sclerite; DP – dorsal plate; ES – endosoma; HESp – hooked endosomal sclerites; PhB – phallobase; PhT – phallotheca; SL – sensory lobe. Scale bars = 0.1 mm.

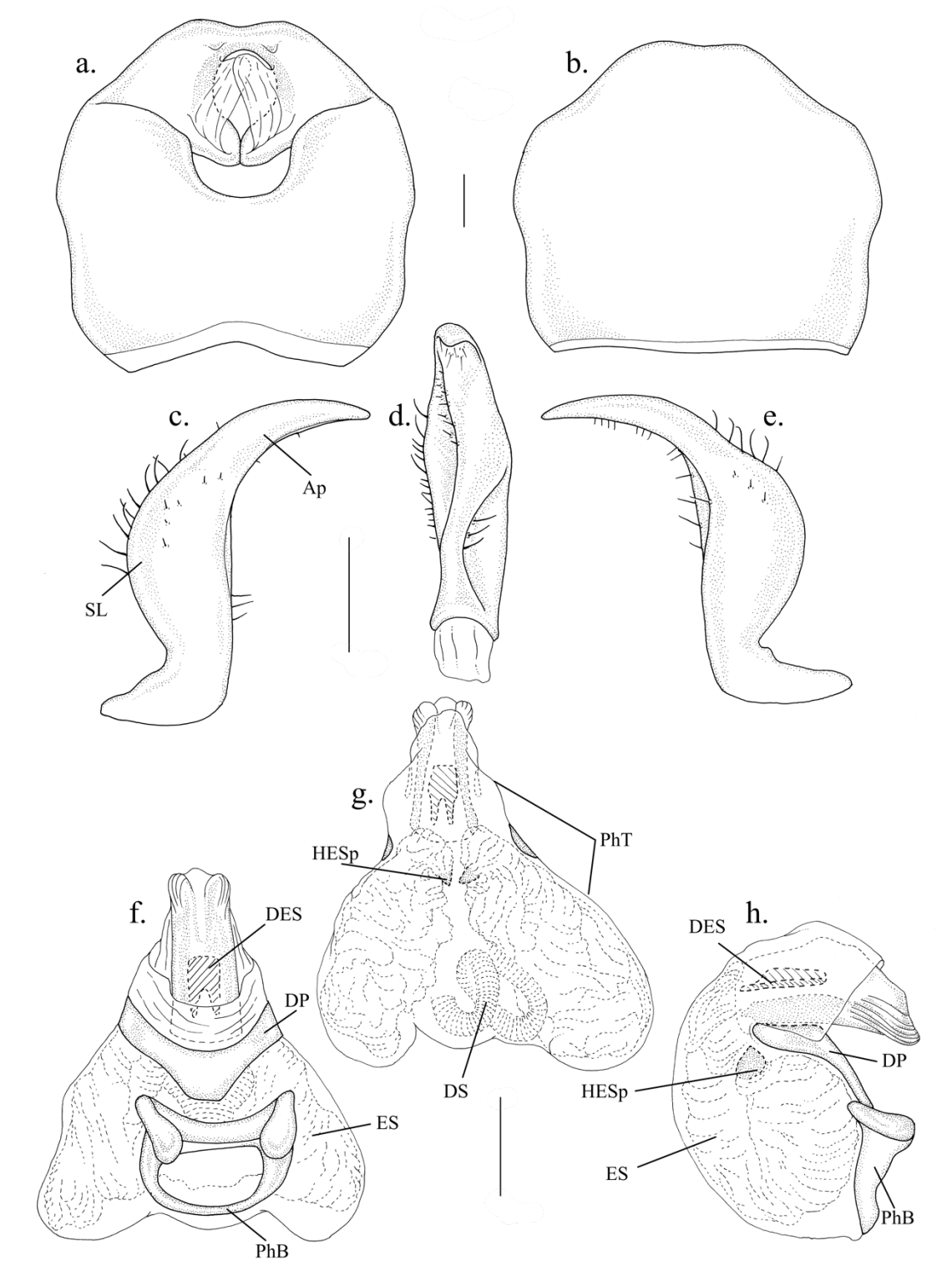

Figure 3.9. Male genitalia of *Cercotingis impensa*: a. pygophore, dorsal view; b. pygophore, ventral view; c. left paramere, dorsal view; d. right paramere, lateral view; e. right paramere, dorsal view; f. aedeagus, dorsal view; g. aedeagus, ventral view; h. aedeagus, right lateral view. Abbreviations: Ap – apophysis; DES – dorsal endosomal sclerite; DP – dorsal plate; DS – ductus seminus; ES – endosoma; HESp – hooked endosomal sclerites; PhB – phallobase; PhT – phallotheca; SL – sensory lobe. Scale bars = 0.1 mm.

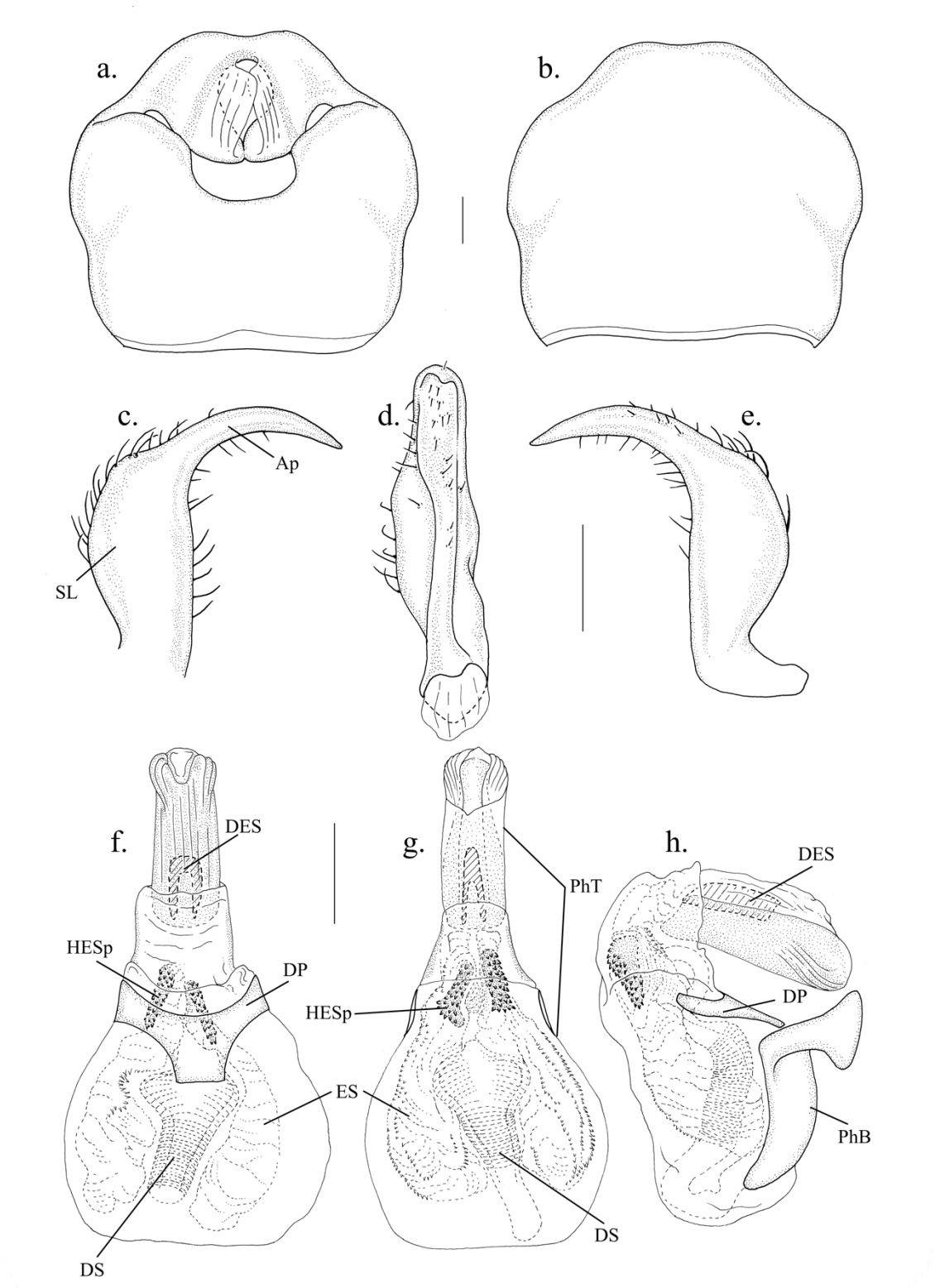

Figure 3.10. Male genitalia of *Cercotingis namadgi*: a. pygophore, dorsal view; b. pygophore, ventral view; c. left paramere, dorsal view; d. right paramere, lateral view; e. right paramere, dorsal view; f. aedeagus, dorsal view; g. aedeagus, ventral view; h. aedeagus, right lateral view. Abbreviations: Ap – apophysis; DES – dorsal endosomal sclerite; DP – dorsal plate; DS – ductus seminus; ES – endosoma; HESp – hooked endosomal sclerites; PhB – phallobase; PhT – phallotheca; SL – sensory lobe. Scale bars = 0.1 mm.

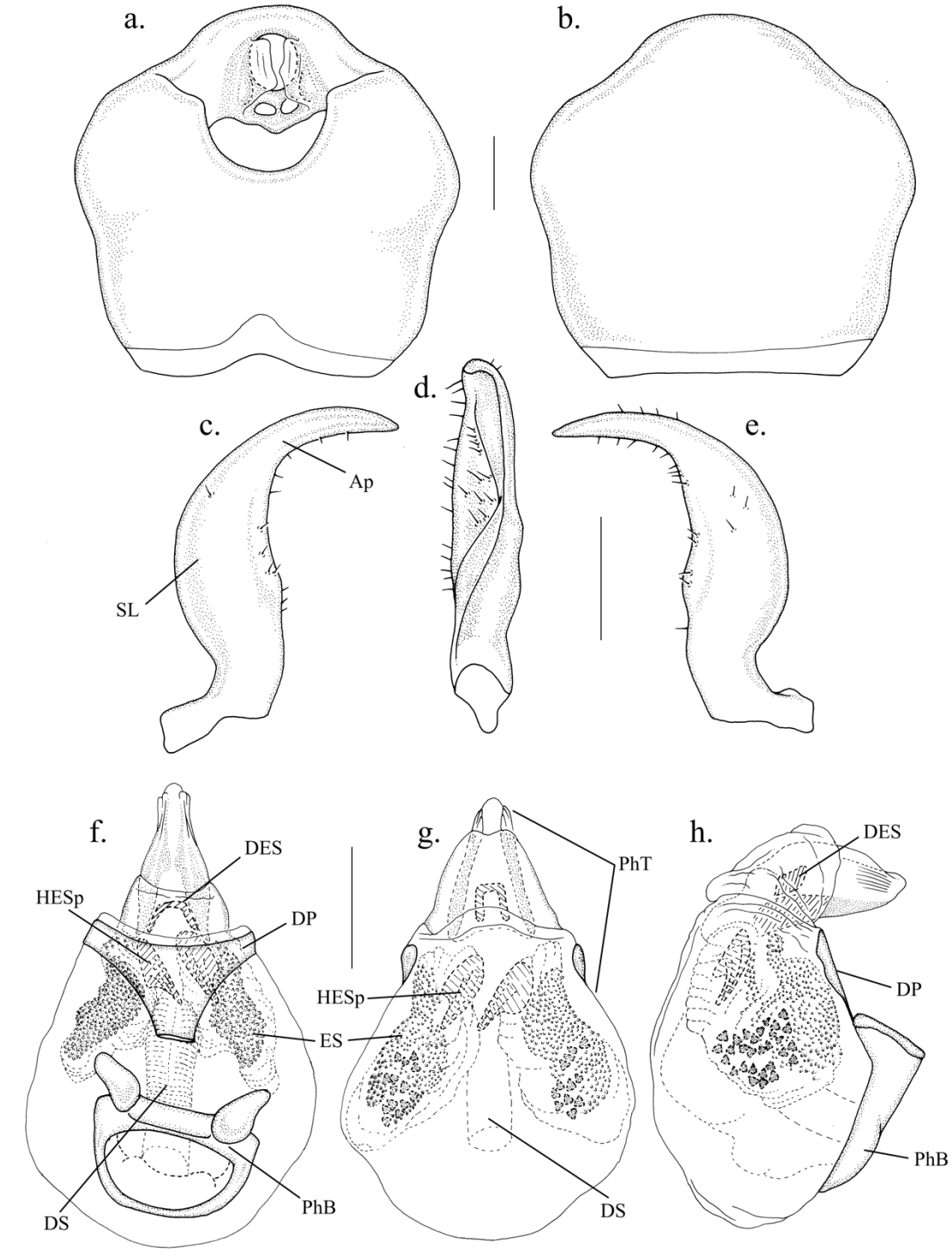

Figure 3.11. Male genitalia of *Proteatingis astibosetes*: a. pygophore, dorsal view; b. pygophore, ventral view; c. left paramere, dorsal view; d. right paramere, lateral view; e. right paramere, dorsal view; f. aedeagus, dorsal view; g. aedeagus, ventral view; h. aedeagus, right lateral view. Abbreviations: Ap – apophysis; DES – dorsal endosomal sclerite; DP – dorsal plate; DS – ductus seminus; ES – endosoma; HESp – hooked endosomal sclerites; PhB – phallobase; PhT – phallotheca; SL – sensory lobe. Scale bars = 0.1 mm.

Figure 3.12. Distribution map for *Proteatingis astibosetes*, *P. burckhardti*, *P. howardi*, and *P. minuta*. Locality information taken from the PBI database.

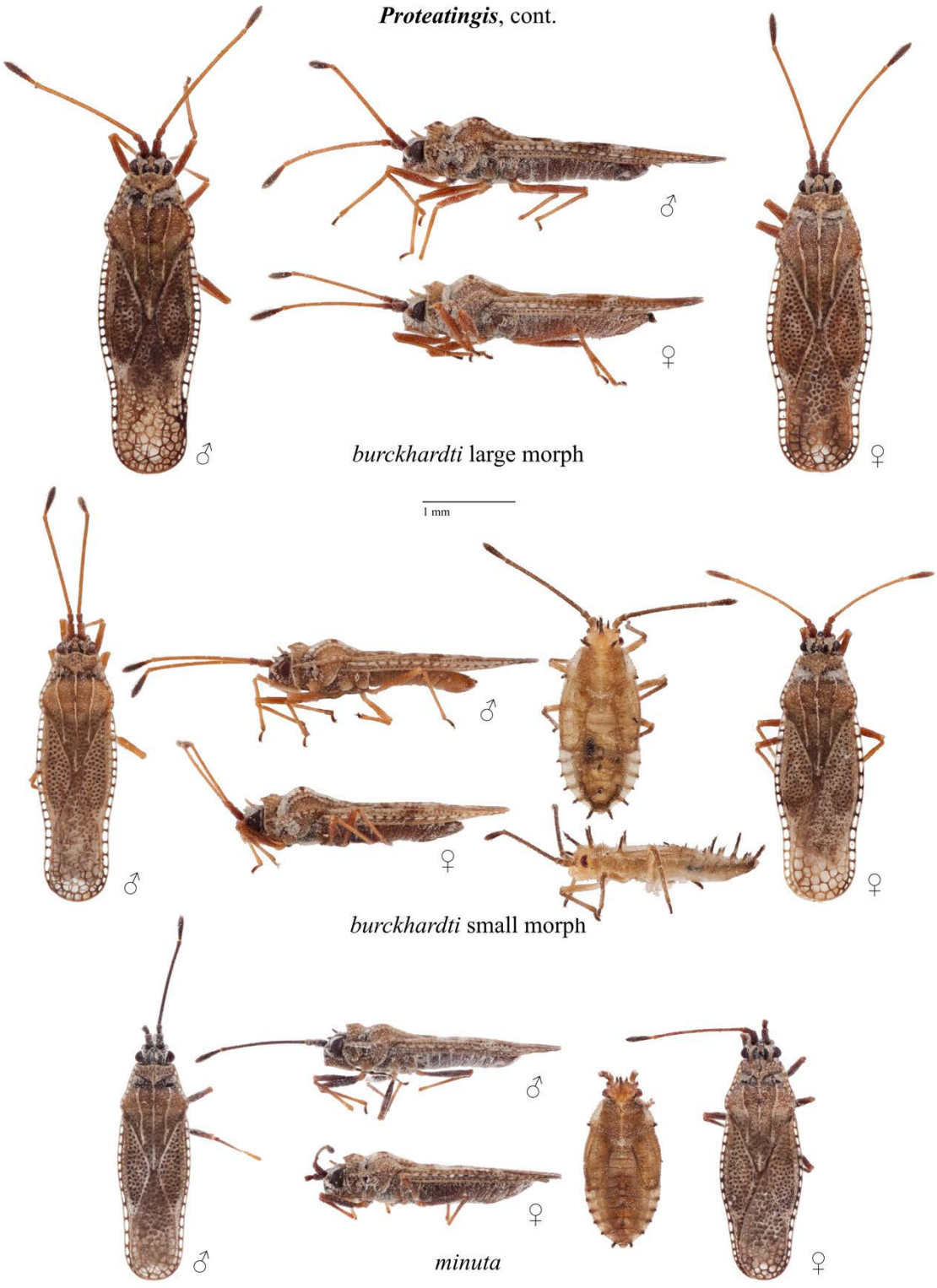

Figure 3.13. Dorsal and lateral habitus photos for *Proteatingis burckhardti* large and small morphs, and *P. minuta*. Scale bar = 1 mm.

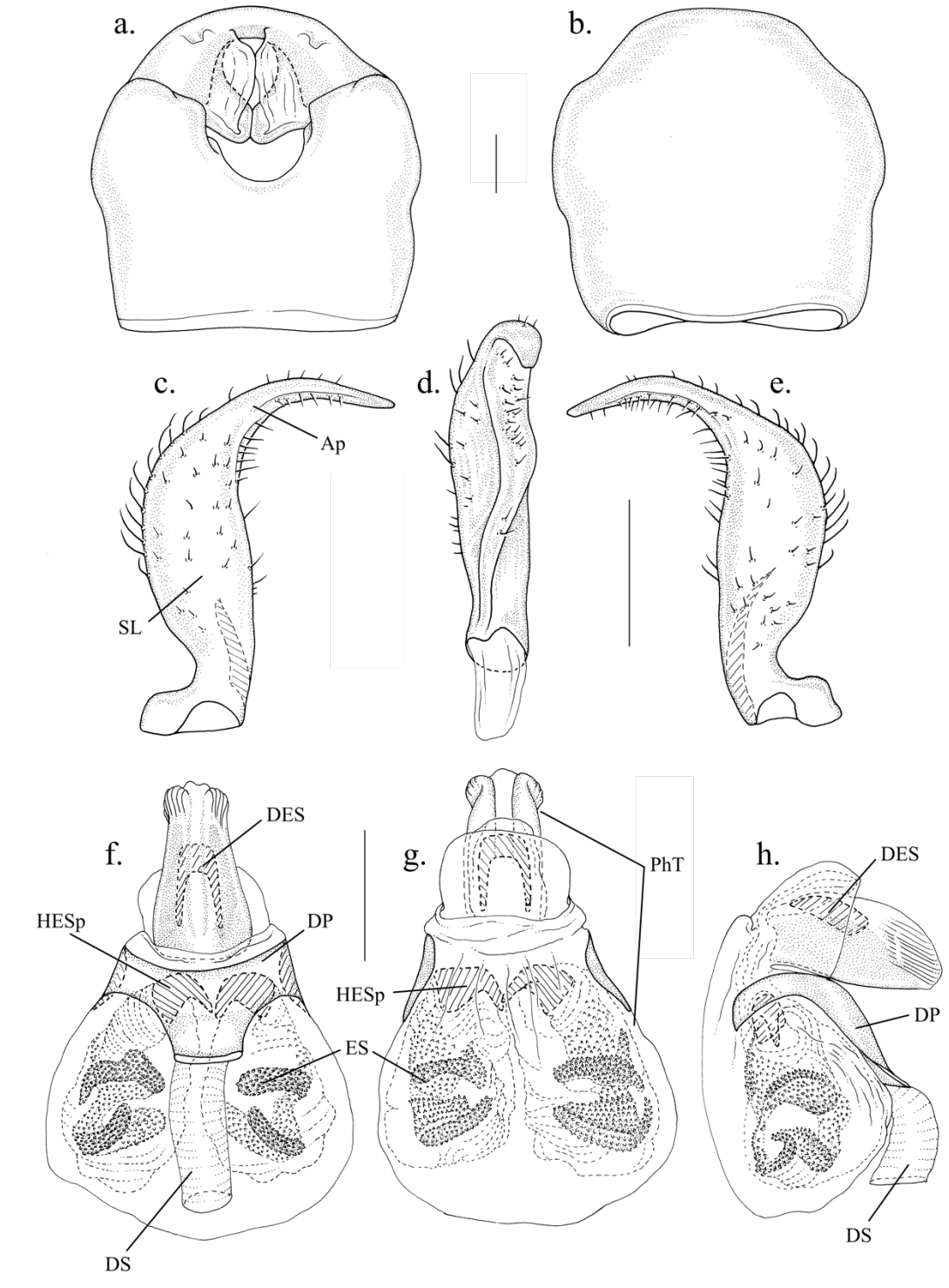

Figure 3.14. Male genitalia of *Proteatingis burckhardti*: a. pygophore, dorsal view; b. pygophore, ventral view; c. left paramere, dorsal view; d. right paramere, lateral view; e. right paramere, dorsal view; f. aedeagus, dorsal view; g. aedeagus, ventral view; h. aedeagus, right lateral view. Abbreviations: Ap – apophysis; DES – dorsal endosomal sclerite; DP – dorsal plate; DS – ductus seminus; ES – endosoma; HESp – hooked endosomal sclerites; PhT – phallotheca; SL – sensory lobe. Scale bars = 0.1 mm.

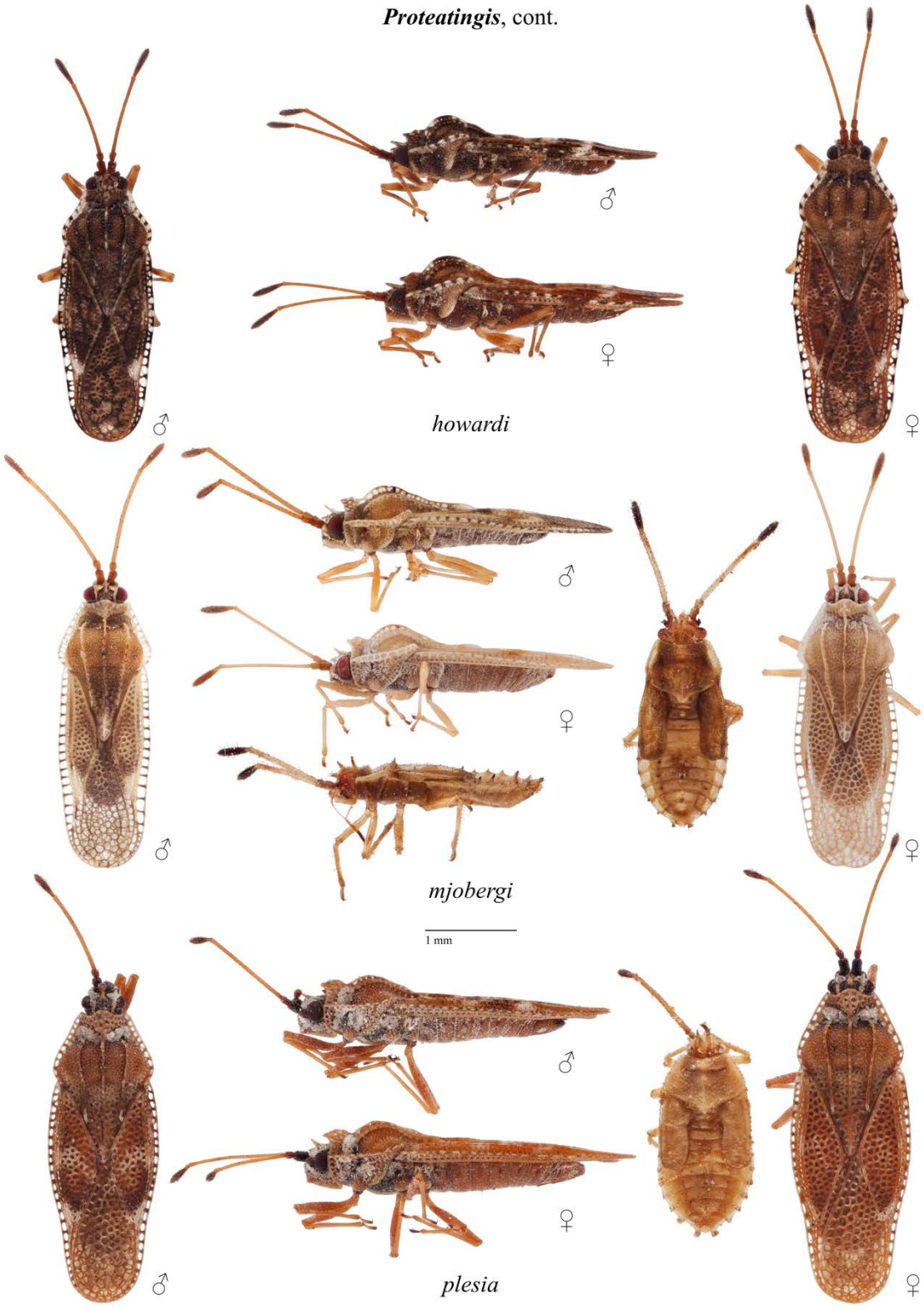

Figure 3.15. Dorsal and lateral habitus photos for *Proteatingis howardi*, *P*. *mjobergi*, and *P*. *plesia*. Scale bar = 1 mm.

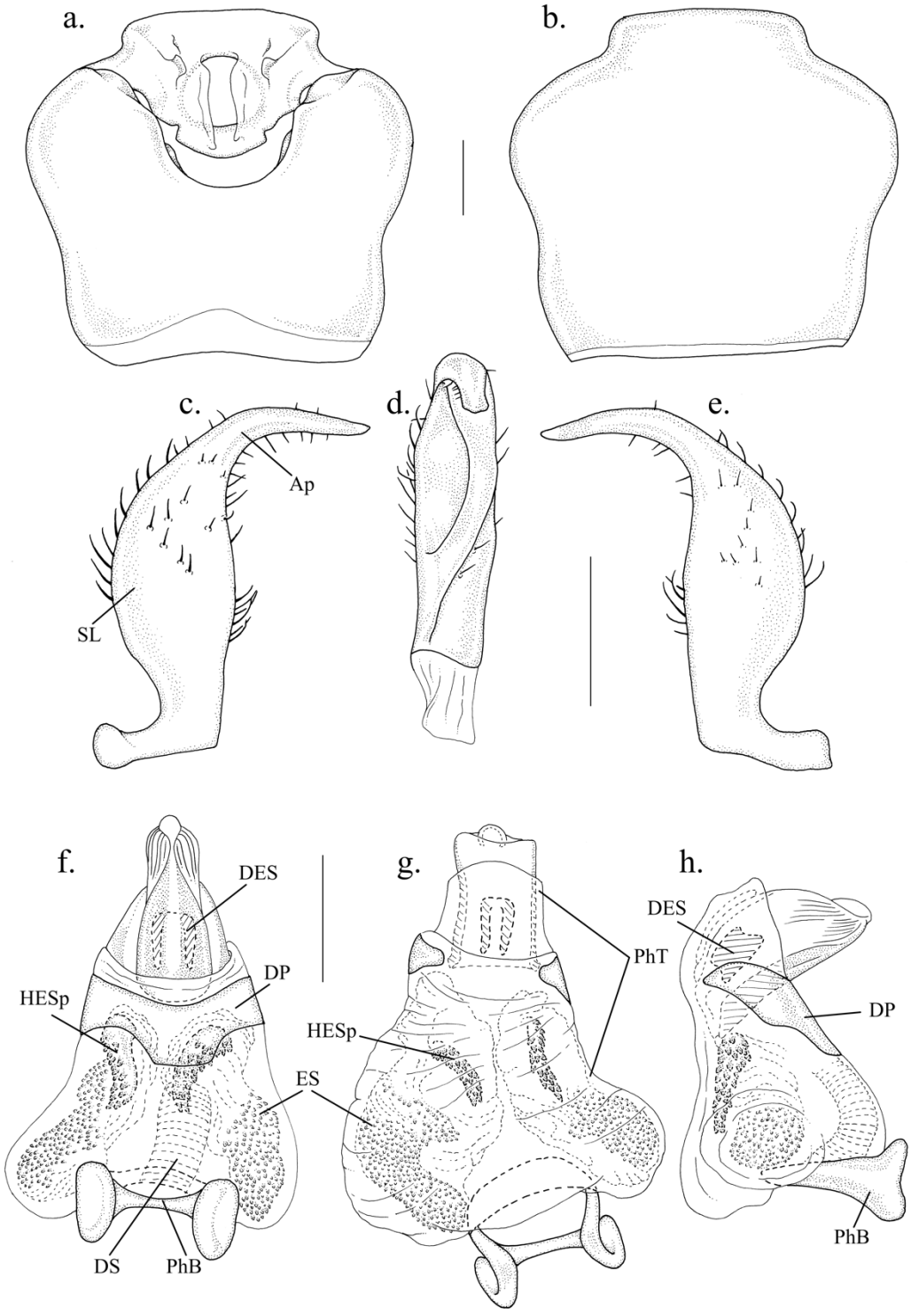

Figure 3.16. Male genitalia of *Proteatingis howardi*: a. pygophore, dorsal view; b. pygophore, ventral view; c. left paramere, dorsal view; d. right paramere, lateral view; e. right paramere, dorsal view; f. aedeagus, dorsal view; g. aedeagus, ventral view; h. aedeagus, right lateral view. Abbreviations: Ap – apophysis; DES – dorsal endosomal sclerite; DP – dorsal plate; DS – ductus seminus; ES – endosoma; HESp – hooked endosomal sclerites; PhB – phallobase; PhT – phallotheca; SL – sensory lobe. Scale bars = 0.1 mm.

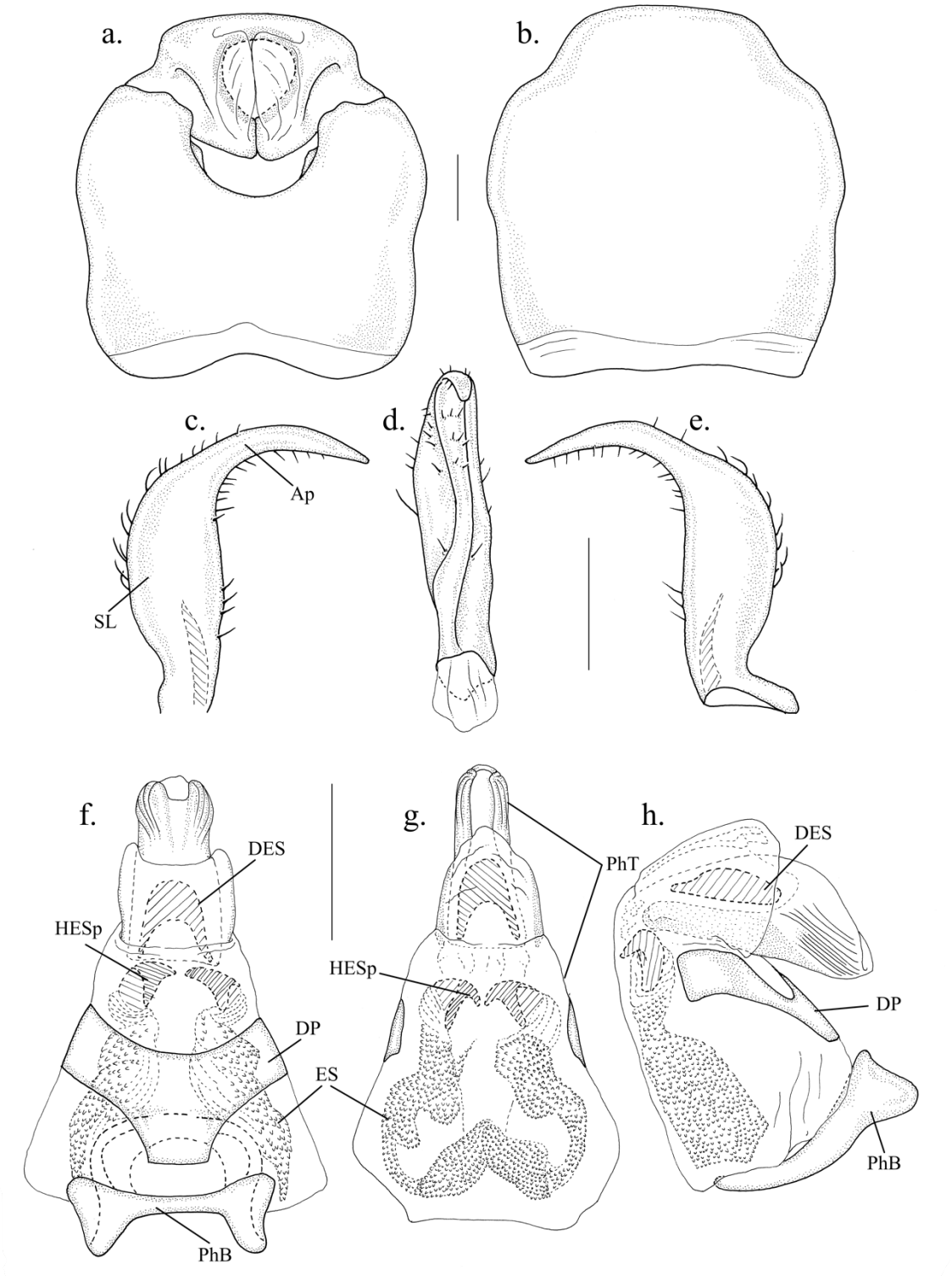

Figure 3.17. Male genitalia of *Proteatingis minuta*: a. pygophore, dorsal view; b. pygophore, ventral view; c. left paramere, dorsal view; d. right paramere, lateral view; e. right paramere, dorsal view; f. aedeagus, dorsal view; g. aedeagus, ventral view; h. aedeagus, right lateral view. Abbreviations: Ap – apophysis; DES – dorsal endosomal sclerite; DP – dorsal plate; ES – endosoma; HESp – hooked endosomal sclerites; PhB – phallobase; PhT – phallotheca; SL – sensory lobe. Scale bars = 0.1 mm.

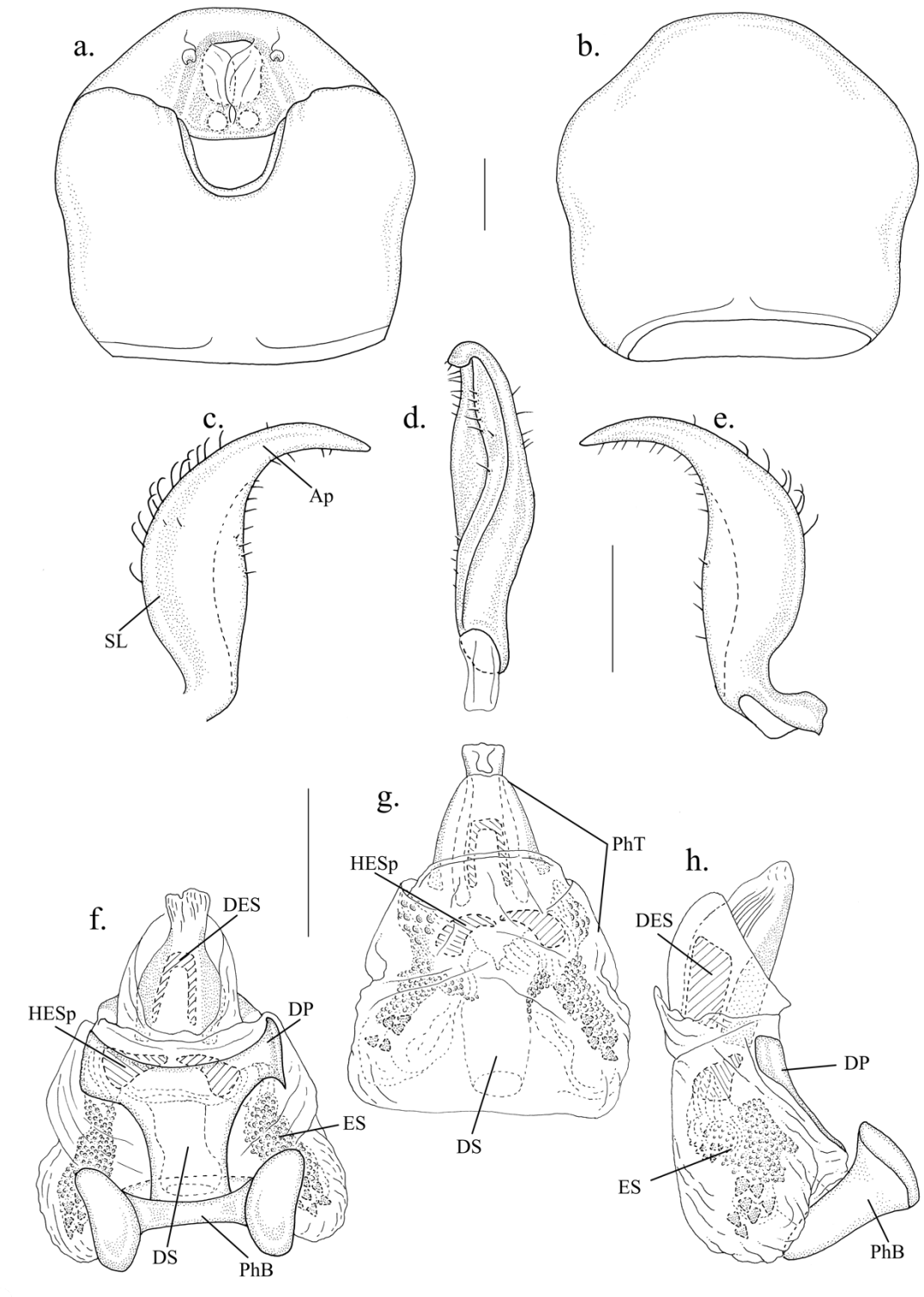

Figure 3.18. Male genitalia of *Proteatingis mjobergi*: a. pygophore, dorsal view; b. pygophore, ventral view; c. left paramere, dorsal view; d. right paramere, lateral view; e. right paramere, dorsal view; f. aedeagus, dorsal view; g. aedeagus, ventral view; h. aedeagus, right lateral view. Abbreviations: Ap – apophysis; DES – dorsal endosomal sclerite; DP – dorsal plate; DS – ductus seminus; ES – endosoma; HESp – hooked endosomal sclerites; PhB – phallobase; PhT – phallotheca; SL – sensory lobe. Scale bars = 0.1 mm.

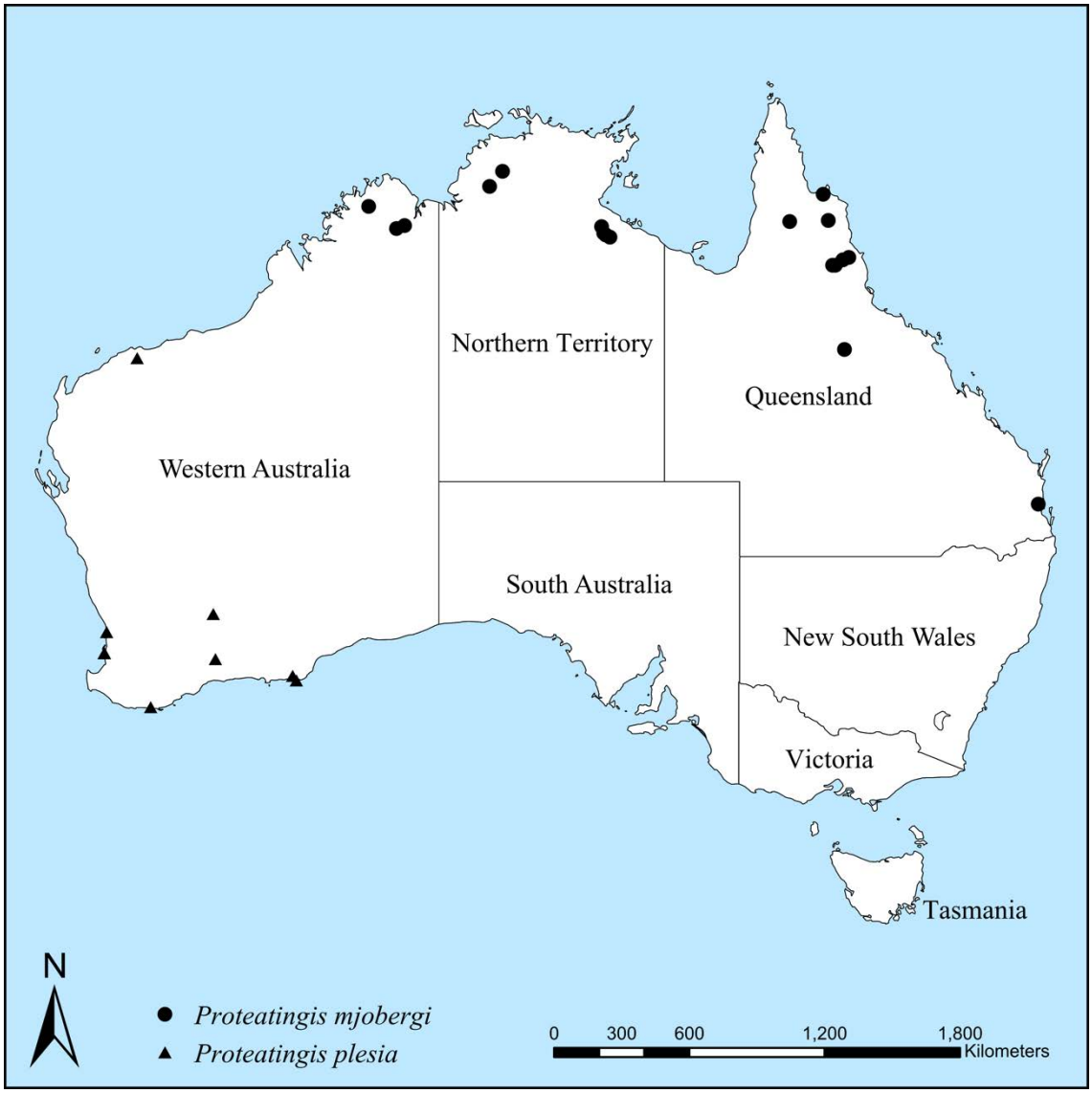

Figure 3.19. Distribution map for *Proteatingis mjobergi* and *P. plesia*. Locality information taken from the PBI database.

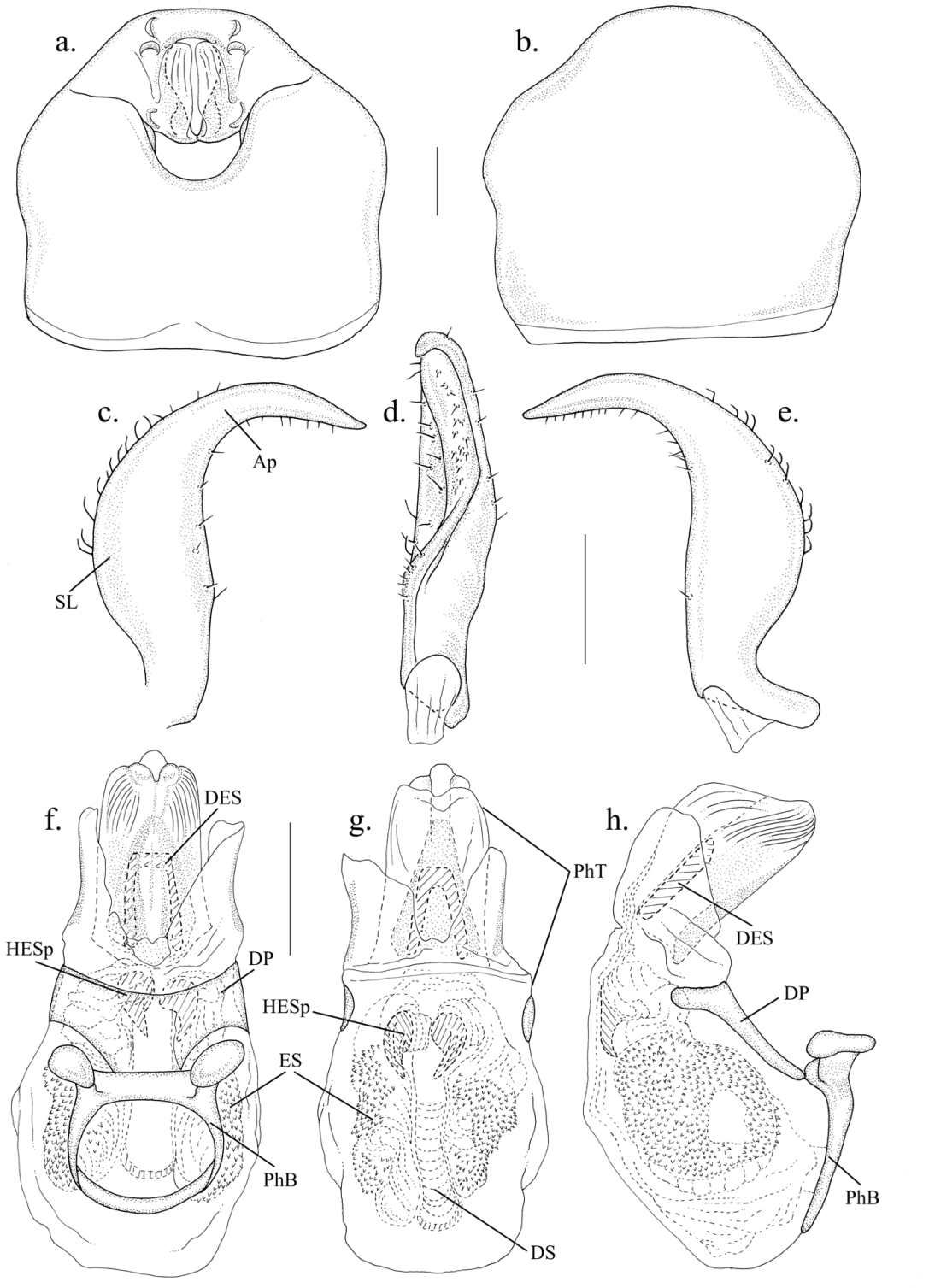

Figure 3.20. Male genitalia of *Proteatingis plesia*: a. pygophore, dorsal view; b. pygophore, ventral view; c. left paramere, dorsal view; d. right paramere, lateral view; e. right paramere, dorsal view; f. aedeagus, dorsal view; g. aedeagus, ventral view; h. aedeagus, right lateral view. Abbreviations: Ap – apophysis; DES – dorsal endosomal sclerite; DP – dorsal plate; DS – ductus seminus; ES – endosoma; HESp – hooked endosomal sclerites; PhB – phallobase; PhT – phallotheca; SL – sensory lobe. Scale bars = 0.1 mm.

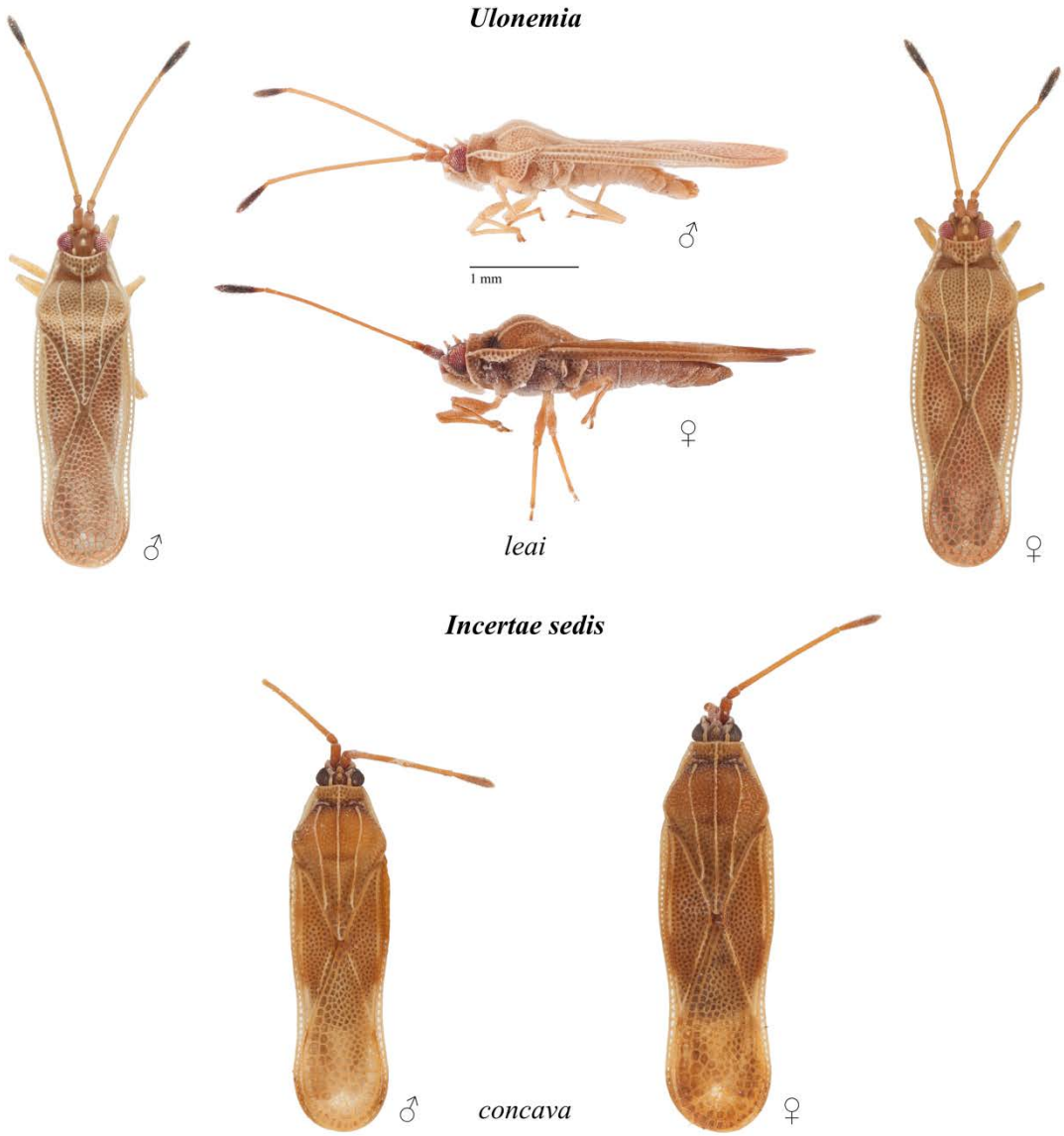

Figure 3.21. Dorsal and lateral habitus photos for *Ulonemia leai*, and dorsal habitus photos for *U. concava* incertae sedis. Scale bar = 1 mm.

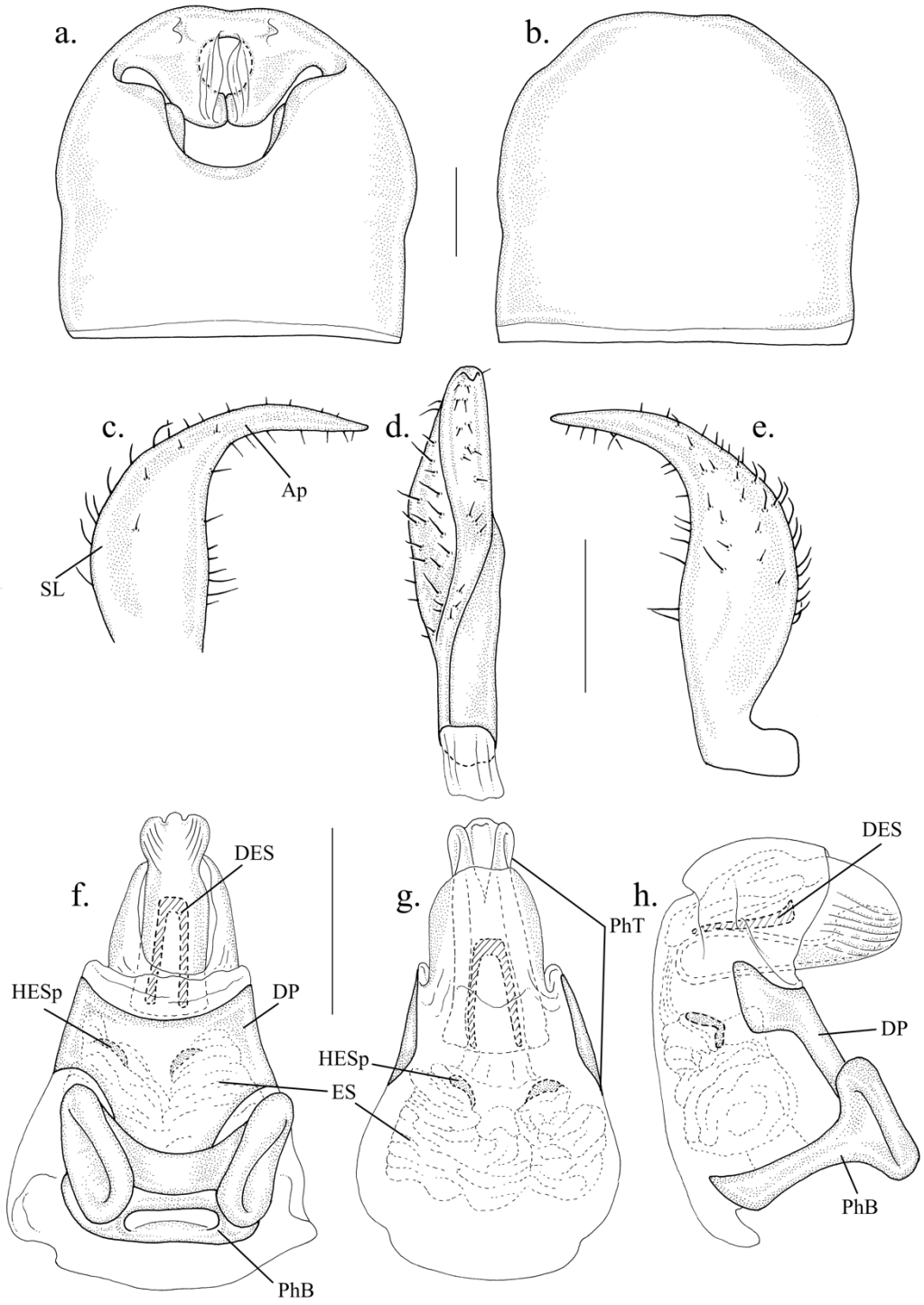

Figure 3.22. Male genitalia of *Ulonemia leai*: a. pygophore, dorsal view; b. pygophore, ventral view; c. left paramere, dorsal view; d. right paramere, lateral view; e. right paramere, dorsal view; f. aedeagus, dorsal view; g. aedeagus, ventral view; h. aedeagus, right lateral view. Abbreviations: Ap – apophysis; DES – dorsal endosomal sclerite; DP – dorsal plate; ES – endosoma; HESp – hooked endosomal sclerites; PhB – phallobase; PhT – phallotheca; SL – sensory lobe. Scale bars = 0.1 mm.

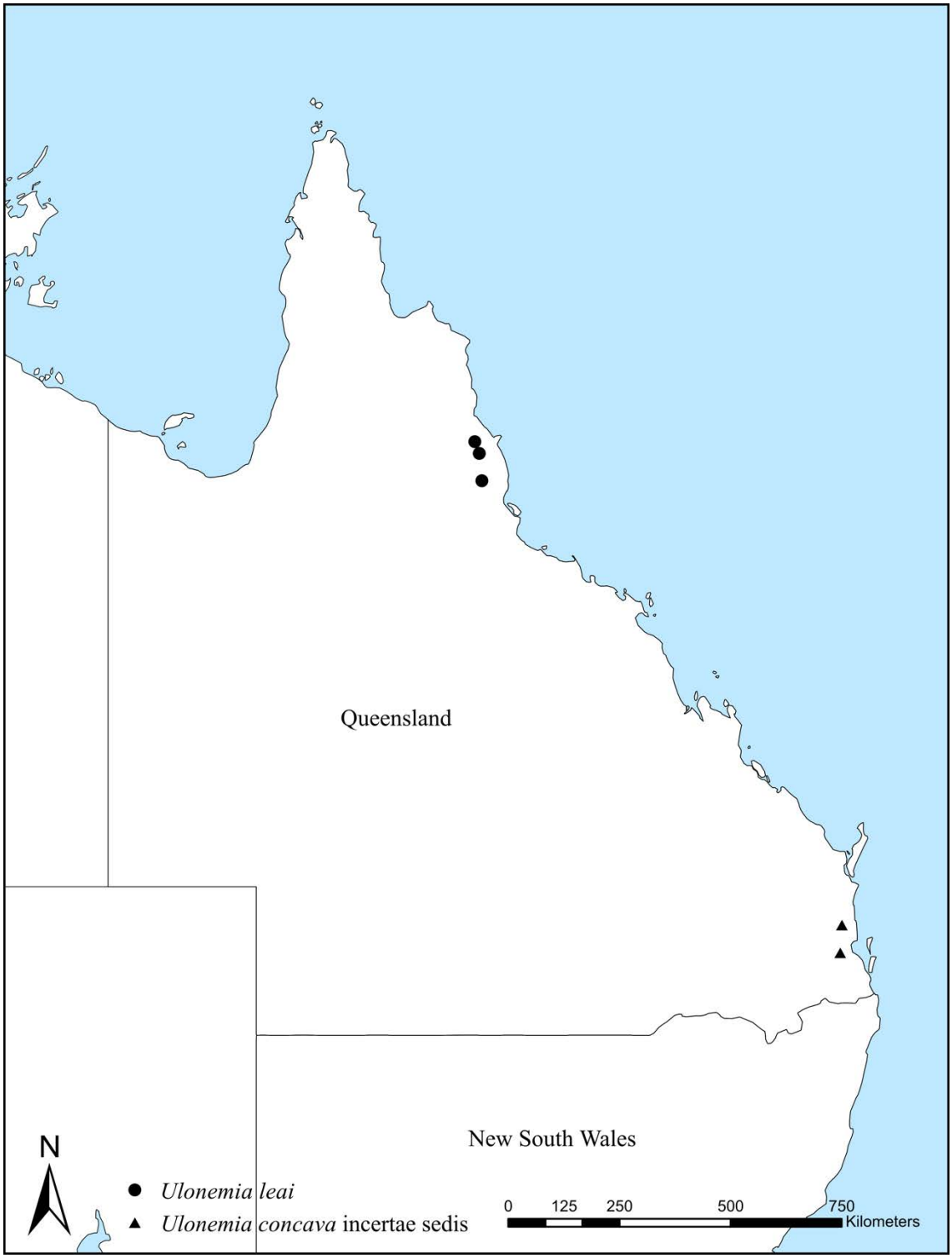

Figure 3.23. Distribution map for *Ulonemia leai* and *U. concava* incertae sedis. Locality information taken from the PBI database.

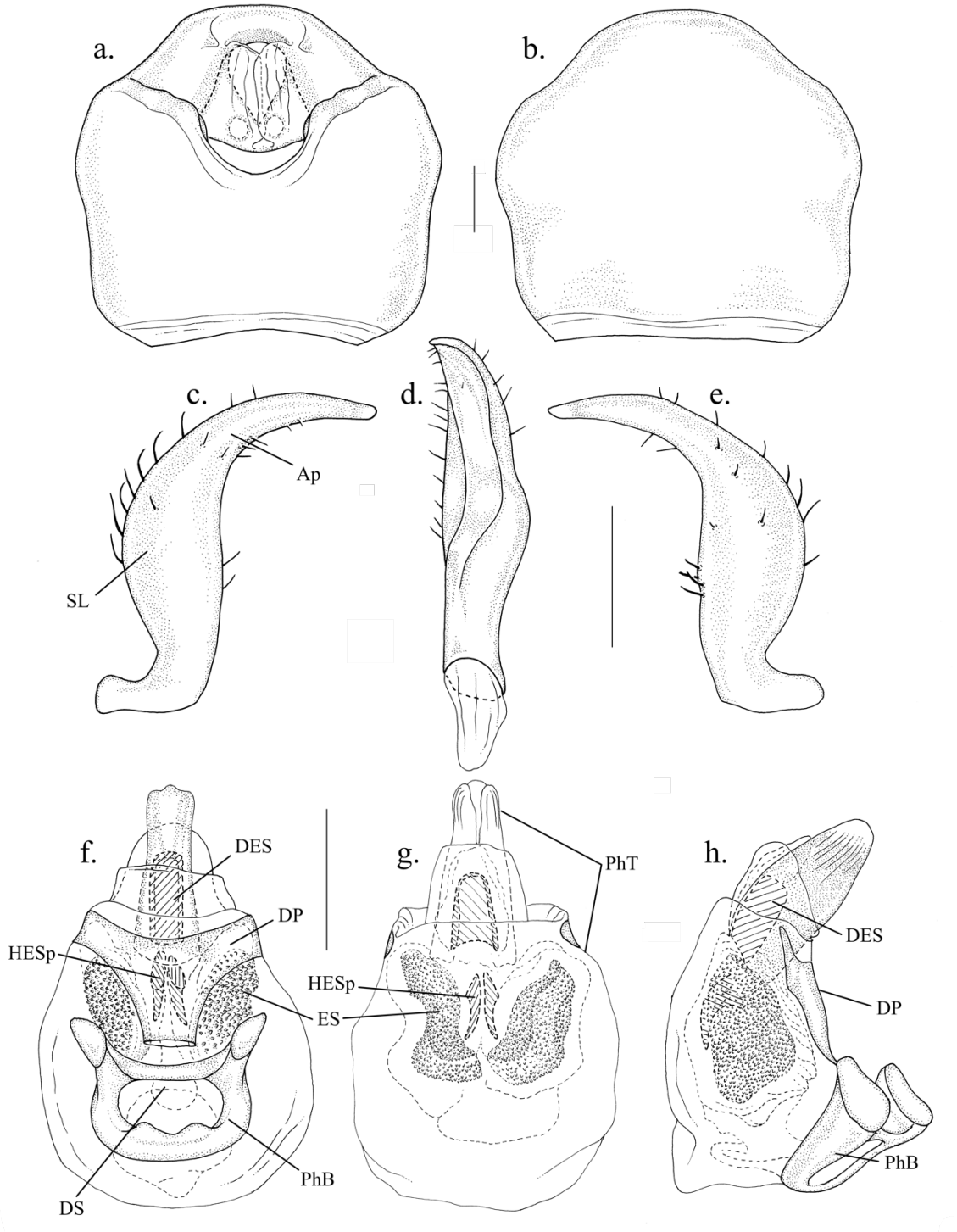

Figure 3.24. Male genitalia of *Ulonemia concava* incertae sedis: a. pygophore, dorsal view; b. pygophore, ventral view; c. left paramere, dorsal view; d. right paramere, lateral view; e. right paramere, dorsal view; f. aedeagus, dorsal view; g. aedeagus, ventral view; h. aedeagus, right lateral view. Abbreviations: Ap – apophysis; DES – dorsal endosomal sclerite; DP – dorsal plate; DS – ductus seminus; ES – endosoma; HESp – hooked endosomal sclerites; PhB – phallobase; PhT – phallotheca; SL – sensory lobe. Scale bars = 0.1 mm.

CHAPTER 4. ASSESSING CONECTEDNESS IN *CERCOTINGIS DECORIS* USING NEXT-GENERATION GENOTYPING

ABSTRACT

Recent outbreaks of the lace bug *Cercotingis decoris* in *Macadamia* orchards has caused significant economic losses to the industry. Current control methods are limited to spraying in response to detection of lace bugs in an orchard, and novel control methods are being sought. The capability of lace bugs to disperse between orchards is critical in developing better control methods, as determining dispersal ability can provide valuable information on the geographic extent over which control must be coordinated. Single-nucleotide polymorphism (SNP) data were obtained using DArT, a next-generation genotyping method, for 204 individuals over 7 localities in northern New South Wales. These data were used to determine genetic differentiation over geographic distance. Genetic differentiation between localities did not vary significantly across varying geographic distances. Clustering algorithms fastStructure and PCoA found evidence of four groups in the data, but membership between the methods differed. Population genetics analyses indicated that each sample locality had an excess of homozygous individuals, and that this was not improved in the fastStructure clusters. This evidence points to selection against heterozygotes, recent extensive mixing, non-random mating, parthenogenesis, or cryptic species within *C. decoris*. Optimal management of the species will likely require region-wide coordination.

INTRODUCTION

Many species of the family Tingidae (=lace bugs) have become economically important pests in agricultural and horticultural systems (Drake and Ruhoff 1965). The feeding mechanisms of most tingids can cause structural damage to their host plants, particularly

to the leaves; most species feed on the underside of leaves, which can turn brown and wilt (Drake and Ruhoff 1965). Tingids usually have a high degree of host specificity, and agricultural pests often attack species which are in the same family as their native hosts (Drake and Ruhoff 1965).

Within the last 10 years, a species of tingid, *Cercotingis decoris* (Drake, 1942), began invading plantations of *Macadamia* F. Muell. nut trees in northern New South Wales (NSW), Australia. The interaction between these two taxa is unusual; cultivation of *Macadamia* in Australia primarily occurs within the boundaries of the native range of the commercialised species, and *C. decoris* appears to be a native *Macadamia* specialist. Members of the genus *Cercotingis* are limited to host species within the family Proteaceae, and *C. decoris* has so far only been collected from *Macadamia*, despite efforts to locate secondary hosts (pers. obs.). These lace bugs feed on the flowers of *Macadamia*, which causes the flower to eventually wilt, turn black, and die. Enormous populations of this lace bug can develop rapidly, which can significantly impact nut production and cause severe economic losses (Huwer and Maddox 2007, Commens 2013).

To date, *Macadamia*-associated lace bugs have been controlled using applications of various pesticides. Several other control efforts have been proposed, such as biological control using parasitoid wasps or various predators, though so far none have been deemed viable. More information is necessary if control efforts are to be more fruitful. This includes 1) basic information on their biology, 2) the identity and number of potential pest lace bug species, and 3) the capability of lace bugs to disperse between orchards. Point one is outside the scope of this study. Point two is addressed in chapters 1 and 2. Point three, however, is arguably the most important, as determining dispersal ability can provide valuable information on the geographic extent over which control must be coordinated.

Dispersal can be determined through various means: mark and recapture, tagging and tracking, or genetics. Given the diminutive size of lace bugs, physical manipulation such as marking or tagging is highly impractical, therefore, a population genetics approach was the best method to determine population structure and genetic dispersal of the species. Rollins et al. (2009) demonstrated the utility of this approach in tracking invasive populations of European starlings (*Sturnus vulgaris* Linnaeus, 1758) in Western Australia (WA). They found that the supposed source population for invasions into WA, which was thought to be on the border of WA and South Australia, was not the actual source. Instead, two independent sources were identified genetically, which pointed to the east coast of Australia as the origin of the invasive starlings. In addition, these two introductions, though close geographically, were genetically distinct, and could therefore be controlled one at a time rather than simultaneously, as there was very little movement apparent between the two source populations. Similar information on the origin of pest lace bug populations and movement of individuals between *Macadamia* orchards across the region would be extremely valuable in aiding orchard managers to effectively target and reduce lace bug populations in a similar fashion.

Lace bugs are relatively sedentary (Drake and Ruhoff 1965) and are reluctant to fly, even when potential predators are encountered (pers. obs.). Given these traits, the ability of lace bugs to disperse between orchards was unknown, and the hypothesis at the start of this study was that different orchards would have noticeably differentiated gene pools due to a low dispersal rate. Under this scenario, it was predicted that this lace bug would be easy to control under current management regimes, where growers do not coordinate control times with one another, but spray their fields individually in response to emergence of lace bugs.

Therefore, the goal of this chapter was to investigate the genetic structure and dispersal of *C. decoris* in the Northern Rivers region of NSW. Single-nucleotide polymorphism (SNP) data were obtained through next-generation genotyping using restriction enzyme digestion for complexity reduction. These data were used to determine genetic differentiation over geographic distance.

MATERIALS AND METHODS

Cercotingis decoris sampling and DNA extraction

Sample localities were chosen to maximise geographic coverage, with at least two pairs of localities separated by each of 300 m, 5 km, and 20 km distances (Figure 4.1). A total of 7 localities were sampled across the *Macadamia* growing region in the Northern Rivers region of NSW. Locality codes (Table 4.1) were formed from the names of the macadamia plantation owners, with the addition of a numeral to distinguish localities that were under the same ownership. Adult and nymph *Cercotingis decoris* specimens were collected from *Macadamia* trees using a beating sheet and aspirator, then transferred to 100% undenatured ethanol. Species identifications were made in the field using a hand lens, and subsequently confirmed in the lab using a Leica M205c stereomicroscope. Specimens were transferred to 96-well plates and sent to Diversity Arrays Technology, Inc (Canberra, DArT) for DNA extraction and single-nucleotide polymorphism (SNP) sequencing via DArTseq.

SNP processing

DArT 2-row format data were imported into Rstudio running R 3.5.0 (R Core Team 2018) using dartR (Gruber and Georges 2018) and converted to an adegenet (Jombart and Ahmed 2011) genlight object. Data were filtered using dartR, in the order described here. Amplicons (strings of amplified DNA up to 64 base pairs in length) were examined for multiple SNPs based on the DArT Clone ID (a unique value assigned by DArT to each

amplicon for identification). Within each amplicon, the SNP with the highest reproducibility (proportion of replicate assay pairs for which the SNP call is consistent) and highest average polymorphism information content (avgPIC) was retained while the other SNPs were discarded to reduce the effect of linked genes. Any markers that were monomorphic across all individuals were removed. Markers below a reproducibility threshold of 100% and below a 95% call rate (the proportion of samples for which the genotype call was a 1 or 0 and not missing data) were discarded.

The filtered genlight object was exported as a dataframe using adegenet and imported to Microsoft Excel for downstream analyses with GenAlEx. The filtered genlight object was also converted in R to fastStructure format using dartR.

The following measures of within-locality diversity were calculated: observed heterozygosity (H_o) and unbiased expected heterozygosity (uH_e) in GenAlEx (Peakall and Smouse 2006, 2012), and Shannon's Information (^1H) following Sherwin et al. (2017) (calculated by a custom R script written by Alex Sentinella and William Sherwin). These measures were also calculated for a pooled dataset of all individuals.

Two measures of departure from panmixia, fit to Hardy-Weinberg equilibrium (HWE) and F_{IS} (Weir and Cockerham 1984), were calculated using GenAlEx (Peakall and Smouse 2006, 2012). Hardy-Weinberg Equilibrium was calculated per locus for each locality as well as the pooled dataset; the F_{IS} was calculated for each locality by averaging the values over all loci.

Genetic differentiation measures calculated between localities were G''_{ST} (Meirmans and Hedrick 2011) using GenAlEx, and Shannon's Mutual Information (I) following Sherwin et al. (2017) (calculated by a custom R script written by Alex Sentinella and William Sherwin). A Mantel test was run to determine whether the results of G''_{ST} and I were correlated, and therefore providing the same information. An isolation-

by-distance Mantel test was run using dartR to determine whether either G''_{ST} or I showed correlation between geographic and linearised genetic distances.

A Gower PCoA, where each axis is a locus and the individual is plotted based on its genotype, was computed using dartR (the function is a wrapper of the adegenet glPca, with default values used). Five principal components were retained. The PCoA includes ellipses that encompass at least 95% of the individuals of each sample locality.

The number of clusters in the data with minimum departure from HWE (K) was determined using fastStructure (Raj, Stephens, and Pritchard 2014). Each K between 1 and 20 was calculated to assist in determining the optimal K represented in the dataset. The optimal K was determined with the fastStructure chooseK utility. Results from fastStructure were analysed with CLUMPAK (Kopelman et al. 2015) to graphically represent the clusters for each K value. The F_{IS} for each cluster produced by the model at the K value that maximised marginal likelihood was calculated; this was done to test the ability of fastStructure to create clusters that minimise departure from HWE.

Due to unexpected results for genetic differentiation and F_{IS}, the unfiltered datasets were examined for clones using radiator (Gosselin 2017) in R. Pairwise comparisons between each individual for every locus were made to determine similarity. The individual pairwise comparisons with the highest similarity were examined to determine whether the genotypes were consistent with some form of clonality or parthenogenesis. Highly similar individuals identified by radiator were compared manually in Microsoft Excel for patterns of clonality. Patterns indicating clonality or parthenogenesis include individuals that have identical genotypes at all loci, or one individual possessing a subset of the alleles possessed by another individual.

RESULTS

The dataset received from DArT contained 204 individuals and 22,451 SNPs, with the final filtered dataset containing 204 individuals and 3,248 SNPs. The mean H_o across all localities was 0.268 ± 0.002 and the mean uH_e was 0.168 ± 0.001 (Table 4.1). The locality with the lowest H_o is WK1 (0.128 ± 0.002); the highest value (0.139 ± 0.003) occurs in three localities: BH1, CR2, and PW1. Shannon's Information (^1H) was highest at WK1 (0.291) and lowest at BH1 (0.235), with a total pooled population value of 0.272 (Table 4.1).

No localities were found to be in Hardy-Weinberg equilibrium across all loci. The locality with the highest number of non-HWE loci was GW1 (148, 4.6% of loci) and the lowest was BH2 (35, 1.1% of loci). The mean inbreeding coefficient (F_{IS}) across all localities was 0.165 ± 0.002, with the highest F_{IS} at WK1 (0.250 ± 0.006) and the lowest F_{IS} at BH1 (0.067 ± 0.006) (Table 4.1).

The highest *I* between localities is BH1 and PW1 (I = 0.039 ± 0.003 at 25,732 m) while the lowest is between BH2 and WK1 (I = 0.009 ± 0.0002 at 28,265 m) (Table 4.2). The highest G''_{ST} values between localities is BH1 and PW1 (G''_{ST} = 0.039 ± 0.001 at 25,732 m) while the lowest is between BH2 and WK1 (G''_{ST} = 0.009 ± 0.001 at 28,265 m). A Mantel test comparing G''_{ST} to I was highly significant, indicating that the two measures were correlated (r = 0.9927, p < 0.001, repetitions = 999). An isolation by distance (IBD) test indicated no significant relationship between *I* genetic differentiation and geographic distance (Mantel test, r = 0.115, p = 0.236, repetitions = 999) (Figure 4.2).

The PCoA showed very limited structure in the data: percent variation explained by the first three axes was low, at 11.9%: axis 1 was 4.9%, axis 2 was 4.1%, and axis 3 was 2.9%. However, three distinct clusters of individuals are present in the PCoA along axes 1 + 2 (Figure 4.3): a cluster consisting of most individuals from BH1 (cluster pca1,

F_{IS} = -0.310 ± 0.005), a second cluster consisting of most individuals of PW1 (cluster pca2, F_{IS} = -0.230 ± 0.005), and a third cluster consisting of the remaining individuals from all localities (cluster pca3, F_{IS} = 0.154 ± 0.002) (Table 4.3, Figure 4.3). An additional cluster is recovered on axes 1 + 3 (Figure 4.4) and 2 + 3 (Figure 4.5), consisting of 7 individuals from GW1 (cluster pca4, F_{IS} = -0.135 ± 0.009) (Table 4.3, Figures 4.4, 4.5).

The fastStructure model complexity that maximises marginal likelihood was K = 4, while the model components that explain the structure in the data was K = 9, indicating a value of K between 4 and 9 (Figure 4.6). At K = 4, BH1 and GW1 contain individuals from 3 clusters, BH2, CR1, and CR2 each contain 2 clusters; PW1 and WK1 have one cluster each (Table 4.3, Figure 4.6). Cluster str1 (F_{IS} = -0.050 ± 0.006) includes BH1 and BH2, cluster str2 (F_{IS} = 0.151 ± 0.002) includes all seven sample localities, cluster str3 (F_{IS} = 0.024 ± 0.005) includes BH1, BH2, CR1, and GW1, cluster str4 (F_{IS} = 0.116 ± 0.005) includes CR2 and GW1 (Table 4.3, Figure 4.6). The clusters returned by fastStructure have a different composition of individuals compared to the PCoA clusters (Table 4.3). Similar to the PCoA results, one fastStructure cluster at K = 4 has the majority of individuals (n = 153) spread across all sample localities. The entirety of PW1 and twelve individuals of BH1 are represented in this cluster, which is in marked contrast to the PCoA results (Table 4.3). Interestingly, despite the fact that fastStructure looks for clusters that have the smallest departure from HWE, the positive within-cluster FIS produced by fastStructure still indicate an excess of homozygous individuals in two cases: cluster str2 is still high at 0.151, as is str4 at 0.116 (Table 4.3).

The pairwise comparison for clonality in the dataset found no exact clones (Figure 4.7). The highest proportion of genome similarity was 94.2% between two females at BH1; neither individual had a multi-SNP genotype that was a subset of the other individual's genotype.

DISCUSSION

Cercotingis decoris exhibits very little genetic differentiation between sample localities, despite those localities covering a large portion of its known native range. The low values for both genetic differentiation measures indicate that *C. decoris* disperses freely across the region, which contradicts the hypothesis that this species would not be a good disperser. Pairwise comparisons of localities using *I* indicate a relatively low amount of mutual information between sites, which suggests a low degree of molecular differentiation (Table 4.2). This finding is corroborated by the differentiation measure G''_{ST}, which has a very low pooled population value of 0.063 and low pairwise comparison values (Table 4.2). Shannon's Information has been increasingly shown to handle datasets with a wide range of effective population sizes and dispersal rates with a high degree of accuracy, and has outperformed F_{ST} in simulations (Sherwin et al. 2017). Shannon's Information has a greater sensitivity to rare alleles and does not tend towards zero as within-locality diversity increases. However, pairwise *I* and G''_{ST} measures were correlated (Mantel test, $r = 0.9946$, $p < 0.001$, repetitions = 999), indicating that rare alleles did not significantly alter the interpretation of the relationships between pairs of localities. An isolation by distance plot for *I* indicates that there is no significant trend over geographic distances of at least 30 km.

Several mechanisms exist that can account for the discrepancy between the initial hypothesis—that the lace bugs would be genetically differentiated between localities—and the observed results, which indicate high dispersal rates. These mechanisms include a better-than-anticipated ability of natural dispersal and/or facilitated movement through human activities, such as transport of individuals on machinery or clothing. More samples over a greater variety of distances are needed to better quantify the relationship between geographic distance and genetic differentiation in *C. decoris*.

Consistent with the results of I and G''_{ST}, the variation explained by the PCoA axes is low, with axis 1 only explaining 4.9% of the variation within the dataset, and axes 1 through 3 combined only explaining 11.9% of the variation (Figures 4.3 – 4.5). While the clusters appear to have good separation visually, the small percent variation explained by each individual axis suggests that the differences between the clusters is extremely minor. However, three of the clusters represent a large proportion of individuals from single sample localities: BH1, GW1, and PW1. In each case, only a subset of the individuals from each locality are present in each cluster, with the rest present in a fourth cluster that encompasses the remaining individuals from the entire dataset. This is clearly illustrated by the overlap of all the ellipses around the largest cluster. The BH1, GW1, and PW1 clusters suggest some isolation between orchards, while the largest cluster suggests that there is also significant movement of individuals across the region, including some members of BH1, GW1, and PW1, plus all members of all other localities (Figures 4.1, 4.3 – 4.5).

The results for HWE and F_{IS} contrast with one another. There is no apparent trend for loci to be out of HWE for all populations; most HWE departures for a locus only occurred within one or several localities. Overall, less than 5% of all loci were out of HWE, as expected when using the 5% cutoff for significance. Rapid population growth from a small pool of individuals can decrease the Hardy-Weinberg expected heterozygosity (H_e), because the population is reflecting the diversity of a much smaller population. This is plausible, as *Cercotingis decoris* is known to increase rapidly in orchards, and populations are subsequently highly reduced by spraying. However, if the expansion happened by random mating, then a significant departure from HWE is not expected (Halliburton 2004). The HWE results indicate that the expansions have happened in a way that maintains HWE.

However, compared to the locus-by-locus HWE calculations, the F_{IS} calculations have greater power to detect departures from HWE, because they are summed over all loci. In fact, the F_{IS} values over all loci indicate an excess of homozygous individuals for each locality, with the exception of BH1 (Tables 4.1, 4.3), which suggests the assumptions for HWE are not being met. There may be selection against heterozygotes, recent extensive mixing, non-random mating, parthenogenesis, or even cryptic species.

Interestingly, despite the fact that fastStructure looks for clusters that have the smallest departure from HWE, the positive within-cluster F_{IS} produced by fastStructure still indicate an excess of homozygous individuals in two cases: cluster str2 is still high at 0.151, as is str4 at 0.116 (Table 4.3). Also, at $K = 9$, there is one cluster that comprises almost half of all individuals, including those from localities extremely far apart, by the standards of this small organism. These findings indicate that 1) in some or all localities there might be some selection against heterozygotes, recent extensive mixing, non-random mating, parthenogenesis, or even cryptic species, so that 2) the fastStructure algorithm cannot successfully create random-mating groupings. In this case, it would be better not to rely on fastStructure, but to use the *I*, G''_{ST}, and PCoA analyses of geographic differentiation, which are not dependent upon identifying random-mating groupings (although these largely agree with results of fastStructure, see Table 4.3).

The large negative F_{IS} values of the clusters produced by the PCoA indicated severe departures from HWE with a large number of excess heterozygous individuals (Table 4.3). This is in sharp contrast to the positive values for F_{IS} within localities and within fastStructure groupings. It appears to be an artefact of the clustering algorithm, which clusters individuals based on allele identity. In this case, a population at HWE would be split into two clusters, with heterozygotes split between the two, and each containing the homozygous individuals for one of the two SNP alleles. This arrangement

artificially creates a significant negative F_{IS}. In addition, the sample size for pca2 is small, which potentially impacted the calculated F_{IS} value. The F_{IS} values of the PCoA clusters should therefore be disregarded.

Heterozygote deficiencies have been observed in numerous invertebrate groups (Addison and Hart 2005, Van der Wurff et al. 2005, Costantini, Fauvelot, and Abbiati 2007, Alp et al. 2012, De Luca et al. 2016, Al-Breiki et al. 2018, Lo et al. 2018). Various explanations have been put forward for this pattern, but these are usually very tentative. Proposed explanations include null alleles (Addison and Hart 2005, Van der Wurff et al. 2005, Alp et al. 2012, Al-Breiki et al. 2018), genetic bottlenecks (De Luca et al. 2016), the Wahlund effect (Costantini, Fauvelot, and Abbiati 2007, Alp et al. 2012, Lo et al. 2018), and reproductive methods such as internal vs. external fertalisation (Addison and Hart 2005, Van der Wurff et al. 2005, Costantini, Fauvelot, and Abbiati 2007). The observed heterozygote deficiency in *C. decoris* unlikely due to null alleles, as the filtering out of SNP loci with poor scoring quality likely highly reduced their presence in the dataset. The suggestion that the observed heterozygote deficiency is due to a genetic bottleneck is generally incorrect, because a bottleneck alters gene diversity, not F_{IS}. In the case of the macadamia lace bugs, the third suggestion (Wahlund effect) seems an unlikely explanation because of the wide and frequent dispersal inferred by the observed values for G''_{ST} and *I*. Reproductive methods or other behavioural aspects of *C. decoris* biology, such as currently unobserved temporal separation of populations, are therefore the most likely candidates for the observed deficit of heterozygotes. The fact that heterozygote deficiencies are unexpected from theory but widespread in invertebrates should prompt further investigation of this pattern.

Other heteropteran pest species exhibit the same genetic patterns observed in *C. decoris*. The eucalypt pest *Thaumastocoris peregrinus* Carpintero and Dellapé, 2006 was

found to disperse over wide distances, and only exhibited moderate levels of genetic differentiation (Lo et al. 2018). *Cercotingis decoris* and *T. peregrinus* have similarities in their life history, specifically the ability to increase in population size rapidly. Both species exhibited elevated F_{IS} values over what would be expected of the populations were in panmixia. The underlying mechanisms for this departure from HWE are possibly present in a wide variety of insect species. In contrast, Chapuisat, Goudet, and Keller (1997) found populations of ants within a supercolony to have F_{IS} values of around zero, which they equate with being consistent with limited dispersal and random mating within a single nest. More research needs to be done to understand the underlying mechanisms of population genetics within invertebrates in general, and insects in particular.

CONCLUSIONS

Overall, *C. decoris* appears to have a highly homogenous gene pool across the Northern Rivers, with indications that a high number of individuals disperse between populations. This dispersal ability increases the difficulty in controlling lace bugs, as management efforts will need to be coordinated over a much wider geographic area than if the species were limited in its dispersal capabilities.

More information on the reproductive biology of this species is needed, as the high degree of similarity between genotypes and the F_{IS} results indicate that there may be some form of clonality or parthenogenesis at play. Insects have a wide variety of parthenogenetic mechanisms, with varying genetic consequences. For example, in some aphids, parthenogenesis occurs sporadically; this combines the advantages of parthenogenetic reproduction that allows rapid increases in population in response to favourable environmental conditions, and sexual reproduction that allows recombination between genomes during outcrossing (White 1973, Sunnucks et al. 1997, Haack et al. 2000). Moreover, parthenogenesis occurs frequently among pestiferous insects as an

adaptation to monocultures in agricultural systems (Hoffmann et al. 2008). In addition, most analyses conducted in this study (F_{IS}, I, ^{1}H, G''_{ST}, Mantel) assume that only a single species is present; it is possible that cryptic species may be present in our sample, or incipient species due to genetic isolation from reproductive mechanisms, which would invalidate the results of these tests. It is crucial that the genetic status of *Cercotingis decoris* be examined in further detail to resolve these uncertainties.

Table 4.1. Summary statistics for genotypic data. For each locality, top row = mean across all loci, bottom row = standard error; coordinates are in WGS84. *N* = number of samples; Lat = latitude; Lon = longitude; H_o = observed heterozygosity; uH_e = unbiased expected heterozygosity = (2*N* / (2*N*-1)) * H_e; F_{IS} = Inbreeding Coefficient = (H_e - H_o) / H_e = 1 - (H_o / H_e); ^1H = Shannon's Information.

Locality	*N*	Lat	Lon	H_o	uH_e	F_{IS}	^1H
BH1	29.805	-28.73000	153.54420	0.139	0.151	0.067	0.235
	0.014			0.003	0.003	0.006	0.063
BH2	26.401	-28.73132	153.54176	0.137	0.172	0.177	0.282
	0.015			0.002	0.003	0.005	0.046
CR1	29.649	-28.86740	153.40280	0.138	0.170	0.158	0.275
	0.014			0.003	0.003	0.006	0.051
CR2	29.429	-28.86670	153.40177	0.139	0.172	0.164	0.281
	0.015			0.003	0.003	0.005	0.049
GW1	26.553	-28.67940	153.30740	0.134	0.176	0.195	0.283
	0.016			0.003	0.003	0.006	0.051
PW1	29.650	-28.83400	153.36420	0.139	0.157	0.111	0.253
	0.015			0.003	0.003	0.006	0.055
WK1	28.554	-28.64929	153.32461	0.128	0.176	0.250	0.291
	0.023			0.002	0.003	0.006	0.046
Total	28.577			0.268	0.168	0.165	0.272
	0.011			0.002	0.001	0.002	0.052

Table 4.2. Pairwise genetic differentiation between sample localities. Top table: below diagonal = G''_{ST}; above diagonal = p. Middle table: below diagonal = I = Shannon's Mutual Information; above diagonal = variance. Bottom table: pairwise geographic distance in meters. Colour coding highlights relative values.

G''_{ST}	BH1	BH2	CR1	CR2	GW1	PW1	WK1
BH1		0.001	0.001	0.001	0.001	0.001	0.001
BH2	0.027		0.001	0.001	0.001	0.001	0.001
CR1	0.031	0.012		0.001	0.001	0.001	0.001
CR2	0.030	0.010	0.010		0.001	0.001	0.001
GW1	0.033	0.014	0.018	0.016		0.001	0.001
PW1	0.039	0.021	0.022	0.021	0.026		0.001
WK1	0.029	0.009	0.013	0.011	0.014	0.022	

I	BH1	BH2	CR1	CR2	GW1	PW1	WK1
BH1		0.001	0.001	0.001	0.001	0.001	0.001
BH2	0.019		0.000	0.000	0.000	0.001	0.000
CR1	0.023	0.010		0.000	0.000	0.001	0.000
CR2	0.022	0.008	0.008		0.000	0.000	0.000
GW1	0.025	0.012	0.015	0.014		0.001	0.000
PW1	0.027	0.016	0.016	0.015	0.019		0.001
WK1	0.021	0.007	0.011	0.009	0.011	0.016	

Meters	BH1	BH2	CR1	CR2	GW1	PW1	WK1
BH1							
BH2	343						
CR1	25164	24835					
CR2	25177	24847	155				
GW1	29149	28908	27943	27806			
PW1	25732	25389	6466	6312	22049		
WK1	28464	28265	31036	30908	4575	25505	

Table 4.3. F_{IS} values across localities, and fastStructure and PCoA clustering methods. Abbreviations: Clust – cluster; F_{IS}/Clust – pooled F_{IS} value across all individuals and loci for the given cluster; F_{IS}/Locality – pooled F_{IS} value across all individuals and loci for the given locality; fSTR – fastStructure; Mthd – cluster analysis method; SE – standard error. Clusters of each method – fSTR or PCoA – contain the individuals shown on the row marked with the cluster name, as well as the individuals on the row marked "both." The grey fields indicate that no F_{IS} value is calculated for "Both," as those individuals are included within the calculations for both methods.

		Locality								
Clust	**Mthd**	**BH1**	**BH2**	**CR1**	**CR2**	**GW1**	**PW1**	**WK1**	**F_{IS}/Clust**	**SE**
str1	fSTR	7	2						-0.050	0.006
pca1	PCoA	8							-0.310	0.005
-	Both	11								
-	fSTR								-	-
pca2	PCoA						19		-0.230	0.005
-	Both									
str2	fSTR	7				5	28		0.151	0.002
pca3	PCoA	7	7	2	12	13	9		0.154	0.002
-	Both	4	20	28	18	7	2	30		
str3	fSTR	1	4	2		2			0.024	0.005
pca4	PCoA					5			-0.135	0.009
-	Both					2				
str4	fSTR				12	7			0.116	0.005
pca4	PCoA					6			-0.135	0.009
-	Both					1				
F_{IS}/Locality		0.067	0.177	0.158	0.164	0.195	0.111	0.250		
SE		0.006	0.005	0.006	0.005	0.006	0.006	0.006		

Figure 4.1. Sample localities in the Northern Rivers region of New South Wales, Australia.

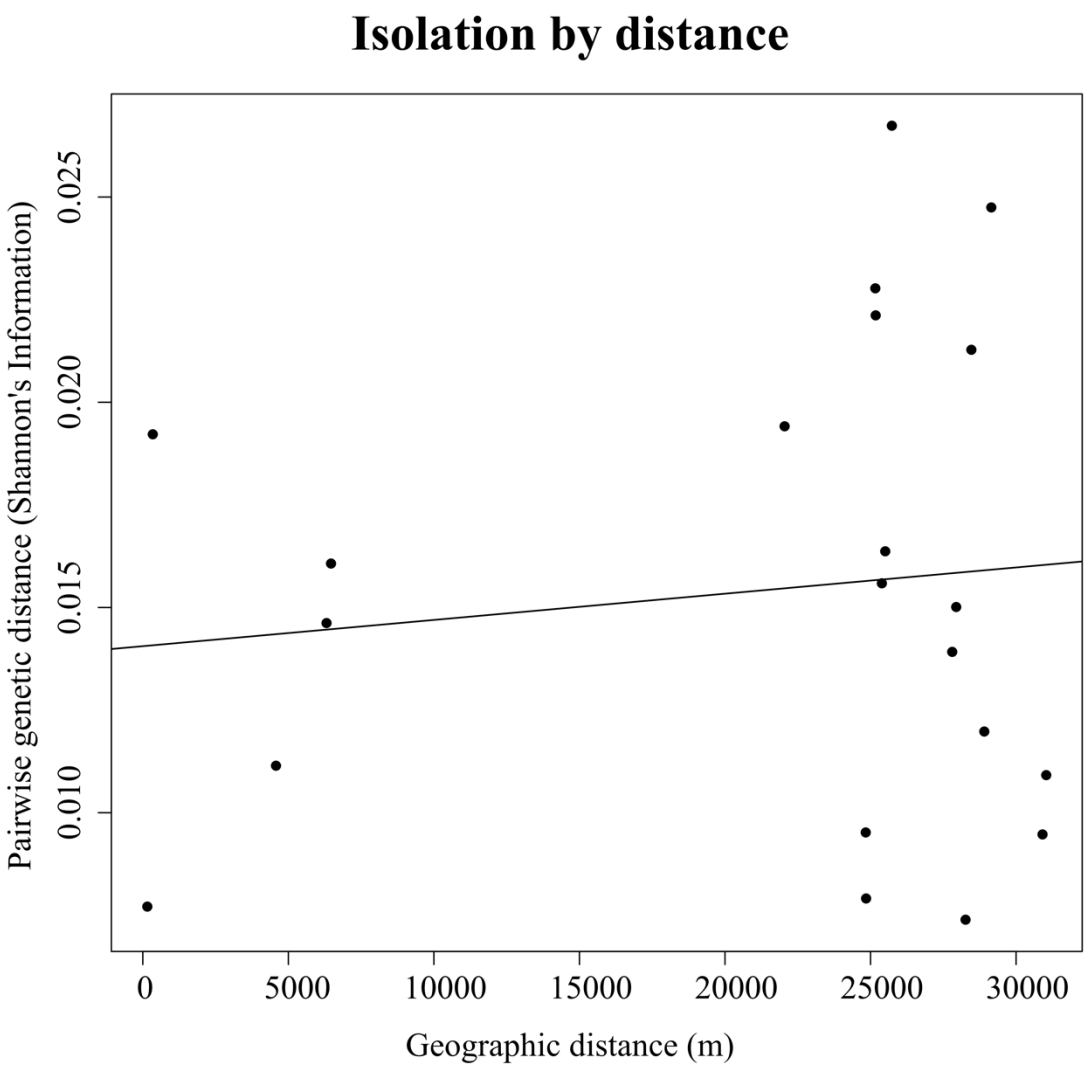

Figure 4.2. Isolation by distance plot between Shannon's Mutual Information (*I*) and meters. Mantel test: $r = 0.115$, $p = 0.236$.

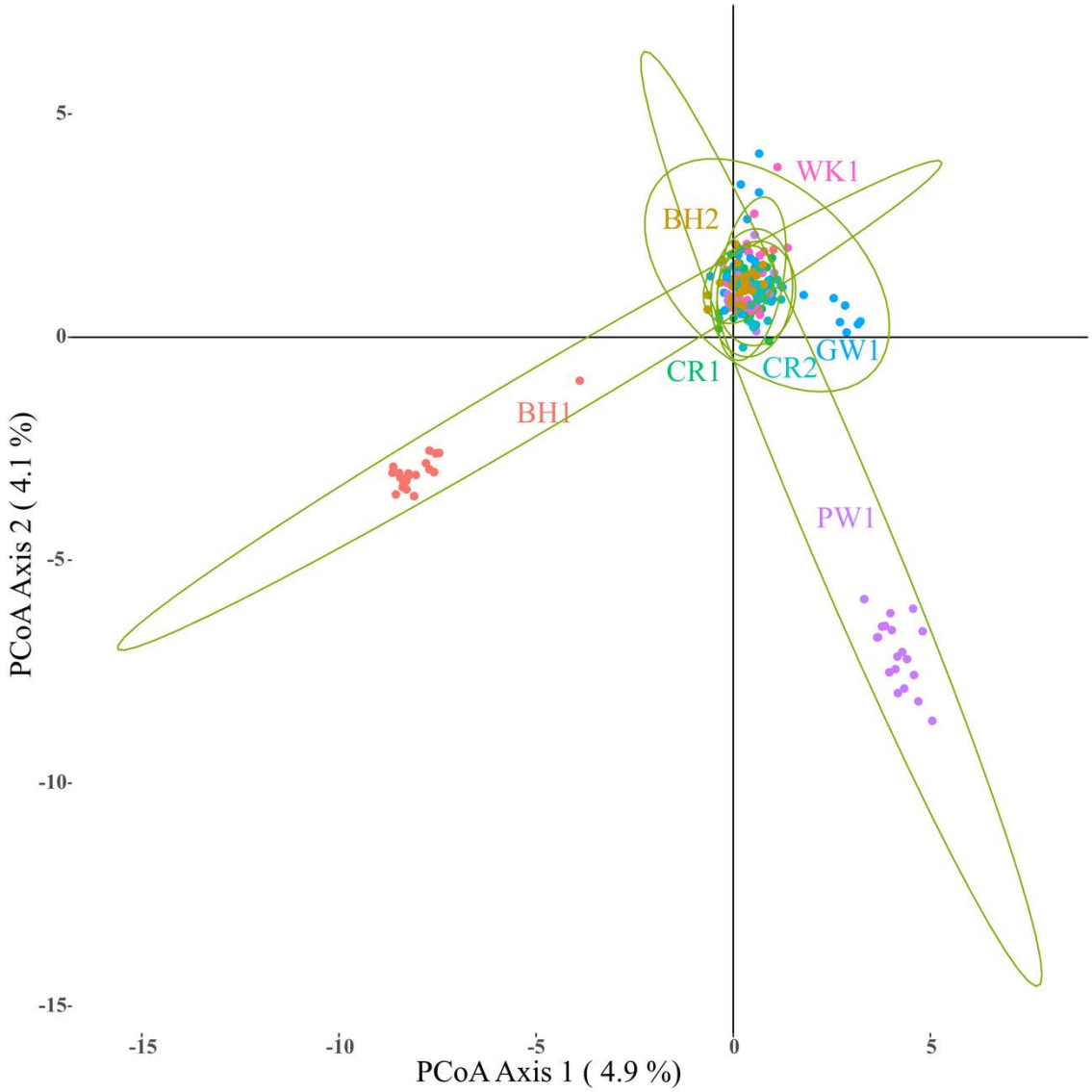

Figure 4.3. PCoA analyses of allele proportions of the filtered SNP dataset for *Cercotingis decoris*, principal component 1 vs principal component 2. Variation explained by the first three principal components: axis 1 = 4.9%, axis 2 = 4.1%, axis 3 = 2.9%. Ellipses contain 95% of the members of each sample locality.

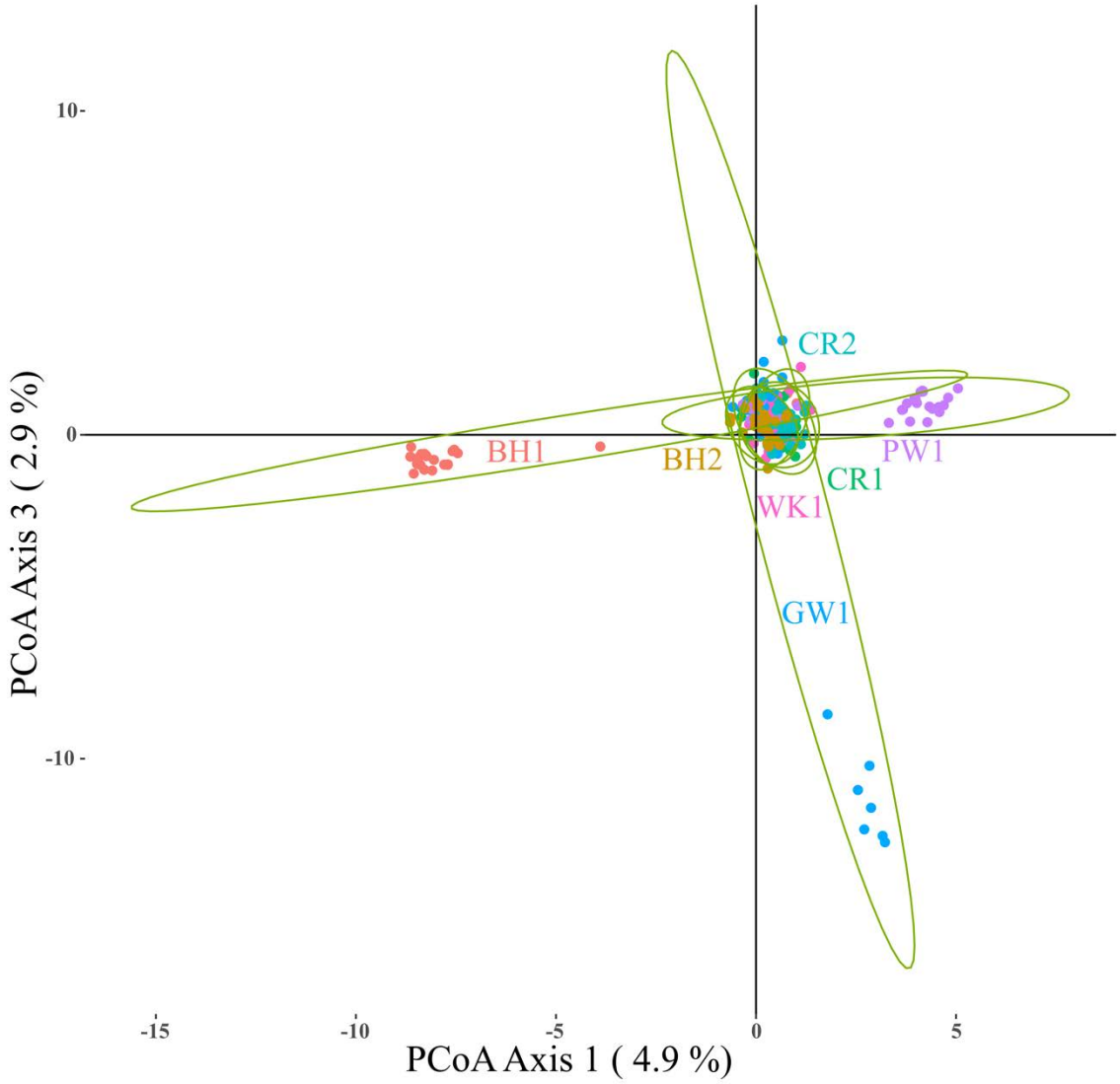

Figure 4.4. PCoA analyses of allele proportions of the filtered SNP dataset for *Cercotingis decoris*, principal component 1 vs principal component 3. Variation explained by the first three principal components: axis 1 = 4.9%, axis 2 = 4.1%, axis 3 = 2.9%. Ellipses contain 95% of the members of each sample locality.

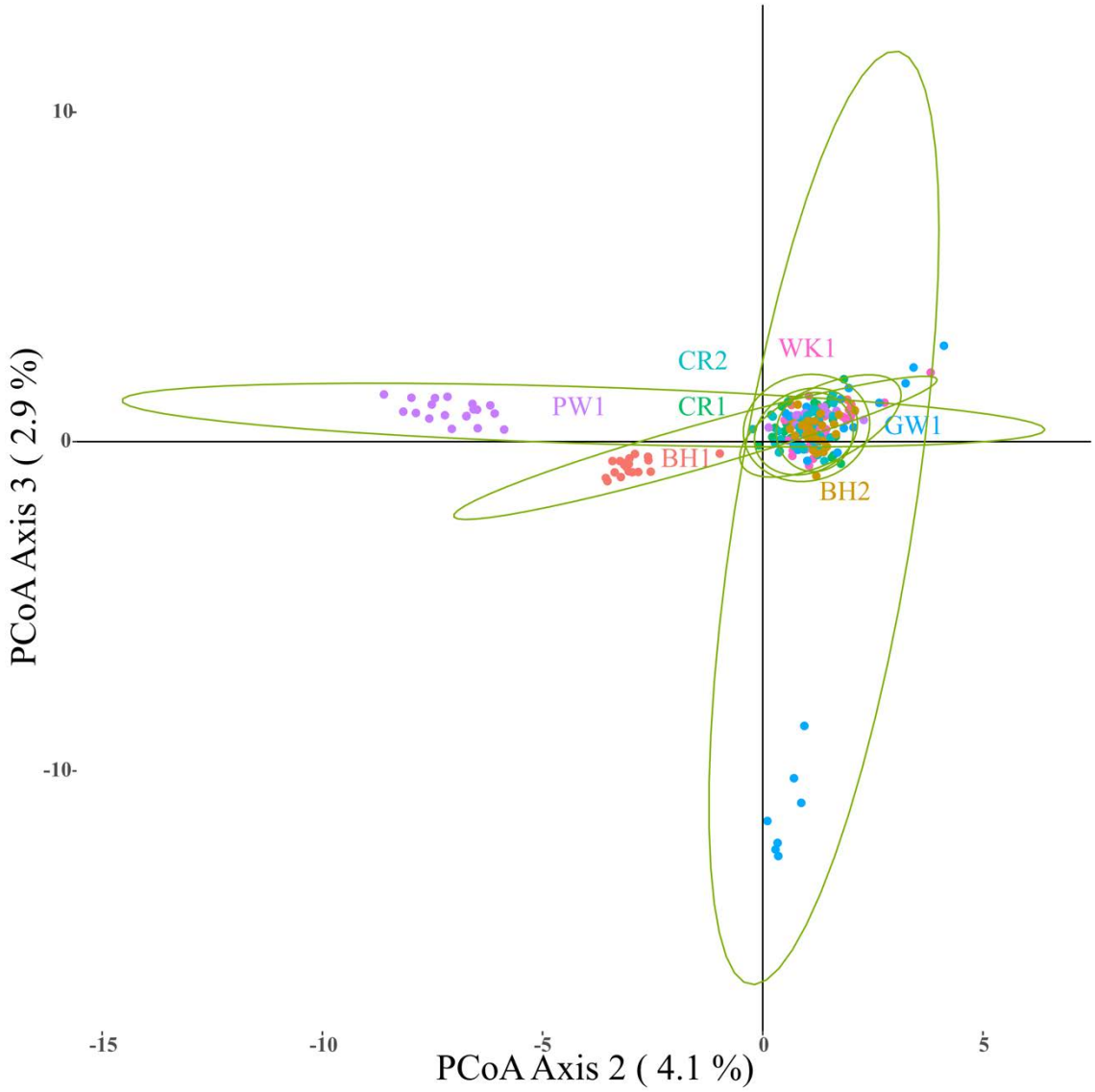

Figure 4.5. PCoA analyses of allele proportions of the filtered SNP dataset for *Cercotingis decoris*, principal component 2 vs principal component 3. Variation explained by the first three principal components: axis 1 = 4.9%, axis 2 = 4.1%, axis 3 = 2.9%. Ellipses contain 95% of the members of each sample locality.

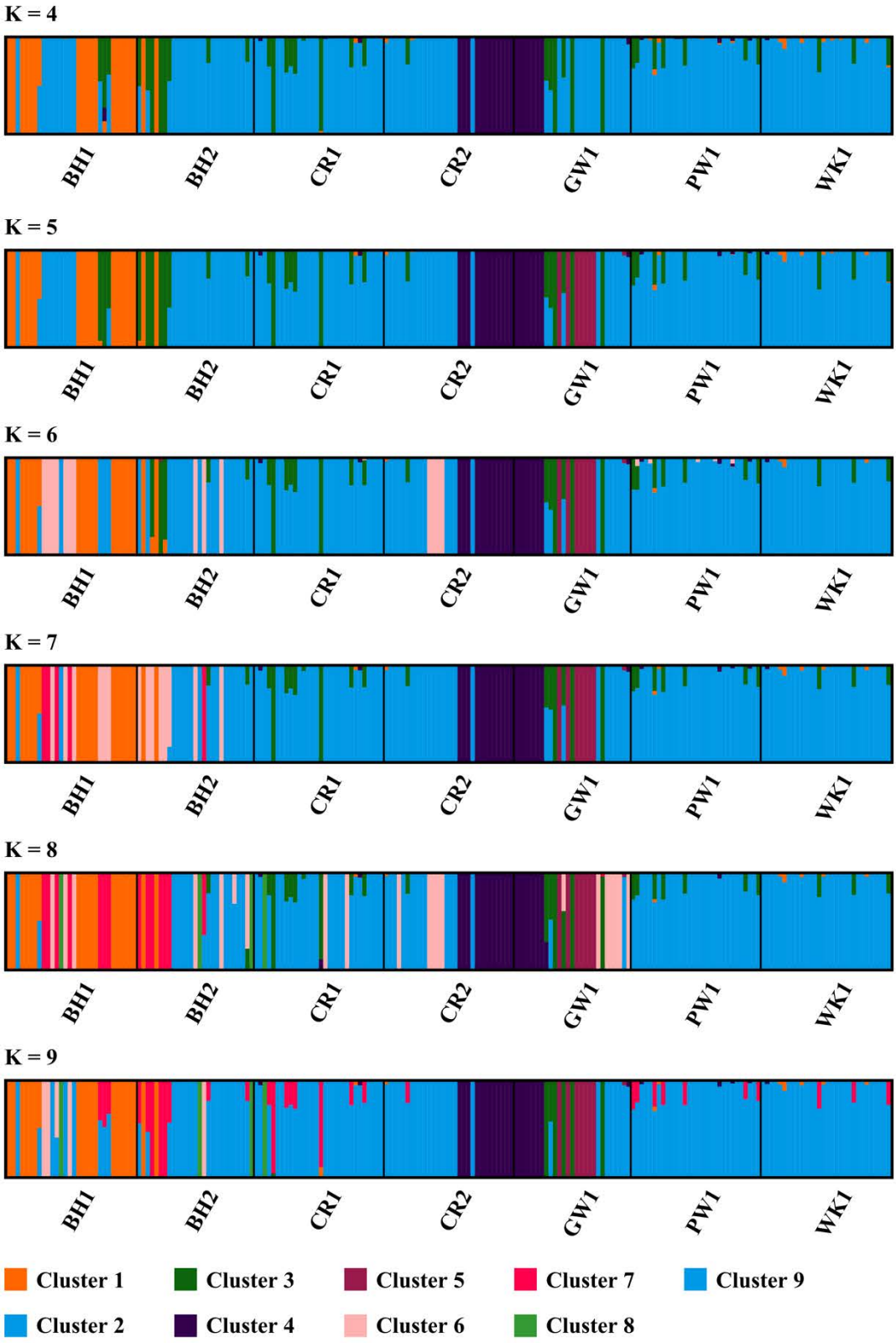

Figure 4.6. Q-probabilities for *K* = 4 through *K* = 9 produced by fastStructure. Cluster name equivalencies between this figure, the text, and Table 4.3 are as follows: Cluster 1 = str1; Cluster 2 = str2; Cluster 3 = str3; and Cluster 4 = str4.

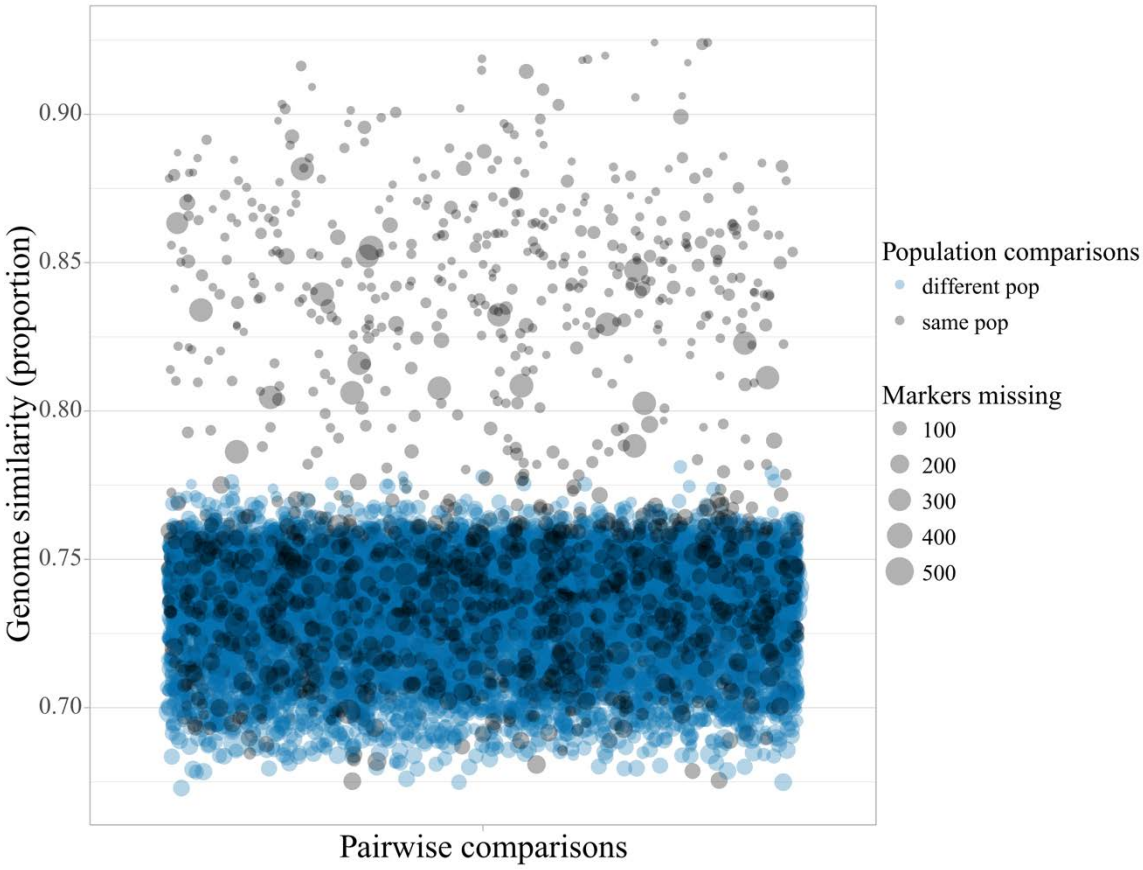

Figure 4.7. Pairwise similarity between each individual over all loci.

CHAPTER 5. GENERAL DISCUSSION

Taxonomic implications

The status of macadamia-associated lace bugs is complex. Of the four species that have been recorded from *Macadamia* thus far, three are only distantly related to each other, with the status of the fourth unknown until DNA can be acquired. The support for the classification of these species into three different genera is quite strong, based on the molecular Maximum Likelihood and Bayesian phylogenetic estimations, with *Ulonemia* sensu lato paraphyletic in both phylogenies (Figures 2.2, 2.3).

The placement of the clade containing the genera *Onchochila*, *Ischnotingis*, *Eritingis*, and *Nethersia* between two clades containing *Ulonemia* sensu lato in the Bayesian analysis has interesting implications. All *Ulonemia* sensu lato species have proteaceous hosts, whereas *Onchochila*, *Ischnotingis*, *Eritingis*, and *Nethersia* are usually confined to hosts in Fabaceae or Myrtaceae. This suggests that multiple lineages of tingids evolved on the Proteaceae, or that host specificity is more plastic than currently understood. These genera require further phylogenetic analysis with a broader sample of species to fully resolve their relationships.

Morphological characters appear to be of limited value for inferring relationships between taxa within the Tingidae. Many characters used in this study are homoplasious, which obfuscates relationships between taxa in phylogenetic analyses (Figure 2.1). However, these same characters have utility in post-hoc identification of lineages inferred from molecular analyses. Unique combinations of morphological characters should remain useful for identification of tingid genera, but further analysis across a larger selection of taxa from the family is needed to determine the full utility of morphology for tingid classification.

Pest management implications

Population genetics analyses can be highly effective at directing pest management strategies. Genetic differentiation between populations can be used to determine patterns of dispersal (Hampton et al. 2004, Rollins et al. 2009, Alp et al. 2012); gene flow between sample localities often reveals source populations or invasion pathways, which enables targeted management of those areas and provides a more efficient use of resources (Hampton et al. 2004, Rollins et al 2009, Silva-Brandão 2015). Where gene flow is extensive throughout the study area (i.e. the population is approximating panmixia), control efforts need to be applied more broadly. In either case, control efforts are informed by population genetics analyses, and their appropriate scope can be easily determined.

The original hypothesis that *C. decoris* might have very limited dispersal does not seem to be supported by the genetic data. The lack of genetic differentiation in *C. decoris* across the *Macadamia* growing region in northern New South Wales indicates that this species is highly mobile and able to disperse readily. This dispersal ability of *C. decoris* can not only hasten the spread of resistance genes (i.e., resistance to insecticides) throughout the population, but also means that control must be coordinated over a wide geographic area. Previous authors (Drake and Davis 1960) have considered tingids to be poor fliers, which would suggest a limited dispersal ability. The high dispersal of *C. decoris* between sample localities indicates that other factors may be aiding dispersal. These likely include natural means such as wind, as well as anthropogenic facilitation via hitchhiking individuals transported on machinery or clothing.

Macadamias are grown in monocultures, with tree canopies often touching (pers. obs.). Monocultures, whether managed or natural, are often more susceptible to pests than systems with higher heterogeneity (Dalin et al. 2009, Guyot et al. 2016). In addition, some aspects of the genetics of *C. decoris* in *Macadamia* orchards may point to adaptation to a

monocultural environment. This species showed a consistent excess of homozygous individuals across all sample localities (Figure 4.1, F_{IS}). Extensive selective pressure through insecticide spraying or other control methods can lead to bottleneck-like genetic signatures and loss of genetic diversity in a population (Silva-Brandão et al. 2015, De Luca et al. 2016), which can result in an excess of homozygotes in a population. In addition, excess homozygosity in the genome can be a sign of facultative or cyclical parthenogenetic reproduction (Sunnucks et al. 1997), which is a potential adaptation to agricultural monocultures where particular clones can have elevated fitness across multiple generations (Hoffmann et al. 2008). However, there are other possible explanations for this, including recent extensive mixing, other forms of non-random mating, parthenogenesis, or cryptic species.

Two *Proteatingis* species are potential sources for new lace bug outbreaks in *Macadamia* orchards, due to the potential adaptability of proteaceous-feeding tingids when presented with alternative hosts. This is evidenced by *U. leai*, which adapted to the presence of *Macadamia* orchards in the Atherton Tablelands, where *Macadamia* is not native. Both *P. astibosetes* and *P. mjobergi* occur in far south-eastern Queensland, near *Macadamia* growing areas; both species use *Grevillea* spp. as hosts, and given their close relation to *P. howardi*, could eventually exploit the resources provided by nearby *Macadamia* orchards.

To summarise control implications, control of lace bugs in macadamia nut orchards will not come easily. An increasing reliance on pesticides can drive genetic selection towards resistance, of which there are numerous pathways to achieve a pesticide resistant phenotype (Feyereisen et al. 2015). The apparently high dispersal ability of *C. decoris* might hasten the spread of resistance, and will require coordinated management on a region-wide scale. In addition, increased orchard hygiene is needed to control the

spread of lace bugs by hitchhiking individuals on clothing and equipment. There is also a need to monitor for other emergent pest species, whether they are cryptic species or otherwise. As demonstrated in chapters 2 and 3, there are multiple lace bug lineages on the Proteaceae, with three of these lineages containing verified pest species. Macadamia nut growers and orchard managers will have to adopt novel strategies—designing robust cropping systems, increased biological agents, and other integrative approaches (Barzman et al. 2015)—to effectively manage outbreaks of *C. decoris* and other pestiferous lace bug species.

REFERENCES

Addison, J. A., and M. W. Hart. 2005. Spawning, copulation and inbreeding coefficients in marine invertebrates. Biology Letters. 1: 450–453.

Al-Breiki, R. D., S. R. Kjeldsen, H. Afzal, M. S. Al Hinai, K. R. Zenger, D. R. Jerry, M. A. Al-Abri, and M. Delghandi. 2018. Genome-wide SNP analyses reveal high gene flow and signatures of local adaptation among the scalloped spiny lobster (*Panulirus homarus*) along the Omani coastline. BMC Genomics. 19: 690.

Alp, M., I. Keller, A. M. Westram, and C. T. Robinson. 2012. How river structure and biological traits influence gene flow: a population genetic study of two stream invertebrates with differing dispersal abilities. Freshwater Biology. 57: 969–981.

Barzman, M., P. Bàrberi, A. N. E. Birch, P. Boonekamp, S. Dachbrodt-Saaydeh, B. Graf, B. Hommel, J. E. Jensen, J. Kiss, P. Kudsk, J. R. Lamichhane, A. Messéan, A.-C. Moonen, A. Ratnadass, P. Ricci, J.-L. Sarah, and M. Sattin. 2015. Eight principles of integrated pest management. Agronomy for Sustainable Development. 35: 1199–1215.

Cassis, G., and C. L. Symonds. 2008. Systematics, biogeography and host associations of the lace bug genus *Inoma* (Hemiptera: Heteroptera: Tingidae). Acta Entomologica Musei Nationalis Pragae. 48: 433–484.

Cassis, G., and C. L. Symonds. 2011. Systematics, biogeography and host plant associations of the lace bug genus *Lasiacantha* Stål in Australia (Insecta: Hemiptera: Heteroptera: Tingidae). Zootaxa. 2818: 1–63.

Cassis, G., and C. L. Symonds. 2016. Plant bugs, plant interactions and the radiation of a species rich clade in south-western Australia: *Naranjakotta*, gen. nov. and

eighteen new species (Insecta : Heteroptera : Miridae : Orthotylinae). Invert. Systematics. 30: 95–186.

Cassis, G., C. L. Symonds, and L. Branson. *In press*. Systematics and species radiation of the sheoak lace bug genus *Epimixia* Kirkaldy (Insecta: Heteroptera: Tingidae) in Australia and New Caledonia. Invertebrate Systematics.

Cassis, G., and G. F. Gross. 1995. Hemiptera: Heteroptera (Coleorrhyncha to Cimicomorpha). CSIRO Australia, Melbourne.

Cassis, G., Wall, M. and Schuh, R.T. 2007. Insect Biodiversity and Industrializing the Taxonomic Process: The Plant Bug Case Study (Insecta: Heteroptera: Miridae). In: Taxonomy and Systematics of Species Rich Taxa: Towards the Tree of Life. (Hodkinson T.R., Parnell J., Waldren S., eds), pp. 193-212. CRC, Boca Raton.

Cassis, G., P. Koenig, C. L. Symonds, and R. Shofner. 2017. Systematics and host plant associations of the Australian lace bug genus *Nethersia* (Insecta: Heteroptera: Tingidae), including the description of eighteen new species. Insect Systematics & Evolution. 48: 1–95.

Chapuisat, M., J. Goudet, and L. Keller. 1997. Microsatellites reveal high population viscosity and limited dispersal in the ant *Formica paralugubris*. Evolution. 51: 475–482.

Cheng, M. 2017 Systematics study of Australian Orthotylinae (Insecta: Heteroptera: Miridae): molecular phylogeny of the subfamily, and taxonomy of *Xasmasoma* gen. nov. and *Myrtlemiris* Cheng, Mututantri and Cassis. Unpublished PhD thesis, University of New South Wales.

Commens, R. 2013. Improved control of lacebug in macadamias. Horticulture Australia Ltd.

Costantini, F., C. Fauvelot, and M. Abbiati. 2007. -Fine-scale genetic structuring in *Corallium rubrum*: evidence of inbreeding and limited effective larval dispersal. Marine Ecology Progress Series. 340: 109–119.

Crowl, T. A., T. O. Crist, R. R. Parmenter, G. Belovsky, and A. E. Lugo. 2008. The spread of invasive species and infectious disease as drivers of ecosystem change. Frontiers in Ecology and the Environment. 6: 238–246.

Dalin, P., O. Kindvall, and C. Björkman. 2009. Reduced population control of an insect pest in managed willow monocultures. PLOS ONE. 4: e5487.

Damgaard, J., and F. A. H. Sperling. 2001. Phylogeny of the water strider genus *Gerris* Fabricius (Heteroptera: Gerridae) based on COI mtDNA, EF-1α nuclear DNA and morphology. Systematic Entomology. 26: 241–254.

Dang, K., C. Li, E. Guilbert, and W. Bu. 2014. Contributions to the genus *Ulonemia* Drake and Poor (Hemiptera: Heteroptera: Tingidae) from China, with descriptions of three new species. Zootaxa. 3878: 49–60.

De Luca, D., G. Catanese, G. Procaccini, and G. Fiorito. 2016. *Octopus vulgaris* (Cuvier, 1797) in the Mediterranean Sea: Genetic Diversity and Population Structure. PLOS ONE. 11: e0149496.

Distant, W. L. 1903. Contributions to a knowledge of the Rhynchota. Annales de la Société entomologique de Belgique. 47: 43–65.

Drake, C. J. 1942. New Australian Tingitidae (Hemiptera). Journal of the Washington Academy of Sciences. 32: 359–364.

Drake, C. J. 1944. A new genus and ten new species of Serenthiines (Hemiptera: Tingitidae). Proceedings of the Entomological Society of Washington 46: 67–76.

Drake, C. J. 1945. New Tingidae. Bulletin of the Southern California Academy of Sciences. 44: 96–100.

Drake, C. J. 1960. Tingidae of New Guinea (Hemiptera). Pacific Insects. 2: 339–380.

Drake, C. J., and F. A. Ruhoff. 1960a. Lace-bug genera of the world (Hemiptera: Tingidae). Proceedings of the United States National Museum. 112: 1–105

Drake, C. J., and F. A. Ruhoff. 1960b. Tingidae: new genera, species, homonyms, and synonyms (Hemiptera). The Great Basin Naturalist. 20: 29–38.

Drake, C. J., and F. A. Ruhoff. 1961. New genera and new species of lacebugs from the Eastern Hemisphere (Hemiptera: Tingidae). Proceedings of the United States National Museum. 113: 125–183.

Drake, C. J., and F. A. Ruhoff. 1962. Synomic notes and descriptions of new Tingidae (Hemiptera). Studia Entomologica. 5: 489–506.

Drake, C. J., and F. A. Ruhoff. 1965. Lacebugs of the world. United States National Museum Bulletin. 243.

Drake, C. J., and M. E. Poor. 1937. Tingitidae from Malaysia and Madagascar (Hemiptera). The Philippine Journal of Science. 62: 1–18.

Drake, C. J., and N. T. Davis. 1960. The morphology, phylogeny, and higher classification of the family Tingidae, including the description of a new genus and species of the subfamily Vianaidinae (Hemiptera: Heteroptera). Entomologica Americana. 39: 1–100.

Fabricius, J. C. 1803. Systema rhyngotorum, secundum ordines, genera, species, adiectis synonymis, locis, observationibus, descriptionibus.

Fieber, F. X. 1844. Entomologische monographien. Leipzig. 138 pp.

Feyereisen, R., W. Dermauw, and T. Van Leeuwen. 2015. Genotype to phenotype, the molecular and physiological dimensions of resistance in arthropods. Pesticide Biochemistry and Physiology. 121: 61–77.

Froeschner, R. C. 1968. Notes on systematics and morphology of lacebug subfamily Cantacaderinae (Hemiptera: Tingidae). Proc. Ent. Soc. Wash. 70: 245–254.

Froeschner, R. C. 1996. Lace bug genera of the world, I: Introduction, subfamily Cantacaderinae (Heteroptera: Tingidae). Smithsonian Contributions to Zoology. 43 pp.

Giribet, G., S. Carranza, J. Baguñà, M. Riutort, and C. Ribera. 1996. First molecular evidence for the existence of a Tardigrada + Arthropoda clade. Molecular Biology and Evolution. 13: 76–84.

Gosselin, T. 2017. radiator - RADseq data exploration, manipulation and visualization using R. https://github.com/thierrygosselin/radiator

Gruber, Bernd, Arthur Georges, Olly Berry, and Peter Unmack. 2017. dartR: importing and analysing snp and silicodart data generated by genome-wide restriction fragment analysis. CRAN. Available from: https://cran.r-project.org/web/packages/dartR/index.html

Guilbert, E. 2001. Phylogeny and evolution of exaggerated traits among the Tingidae (Heteroptera, Cimicomorpha). Zoologica Scripta. 30: 313–324.

Guilbert, E. 2004. Do larvae evolve the same way as adults in Tingidae (Insecta: Heteroptera)? Cladistics. 20: 139–150.

Guilbert, E., and M. L. Moir. 2010. A new species of *Carldrakeana* (Insecta: Heteroptera: Tingidae) from Western Australia. Records of the Western Australian Museum. 25: 383–387.

Guilbert, E., J. Damgaard, and C. A. D'Haese. 2014. Phylogeny of the lacebugs (Insecta: Heteroptera: Tingidae) using morphological and molecular data. Systematic Entomology. 39: 431–441.

Guindon, S., J.-F. Dufayard, V. Lefort, M. Anisimova, W. Hordijk, and O. Gascuel. 2010. New algorithms and methods to estimate Maximum-Likelihood phylogenies: assessing the performance of PhyML 3.0. Systematic Biology. 59: 307–321.

Guyot, V., B. Castagneyrol, A. Vialatte, M. Deconchat, and H. Jactel. 2016. Tree diversity reduces pest damage in mature forests across Europe. Biology Letters. 12: 20151037.

Haack, L., J. C. Simon, J. P. Gauthier, M. Plantegenest, and C. A. Dedryver. 2000. Evidence for predominant clones in a cyclically parthenogenetic organism provided by combined demographic and genetic analyses. Molecular Ecology. 9: 2055–2066.

Hacker, H. 1928. New species of Australian Tingitoidea (Hemiptera). Memoirs of the Queensland Museum. 9: 174–188.

Halliburton, R. 2004. Introduction to population genetics. Pearson, Upper Saddle River, NJ, USA. 650 pp.

Hampton, J. O., P. B. S. Spencer, D. L. Alpers, L. E. Twigg, A. P. Woolnough, J. Doust, T. Higgs, and J. Pluske. 2004. Molecular techniques, wildlife management and the importance of genetic population structure and dispersal: a case study with feral pigs. Journal of Applied Ecology. 41: 735–743.

Henry, T. J. 2009. Biodiversity of Heteroptera, pp. 223–263. In Foottit, R.G., Adler, P.H. (eds.), Insect Biodiversity. Wiley-Blackwell, Oxford, UK.

Hoffmann, A. A., K. T. Reynolds, M. A. Nash, and A. R. Weeks. 2008. A high incidence of parthenogenesis in agricultural pests. Proceedings of the Royal Society of London B: Biological Sciences. 275: 2473–2481.

Horváth, G. 1925. Results of Dr. E. Mjöberg's Swedish scientific expiditions to Australia 1910-1913. 45. Tingitidae. Arkiv för Zoologi. 17A: 1–17.

Huwer, R., and C. Maddox. 2007. Lace bug – increasing incidences in NSW orchards.

Jing, X. L. 1981. Tingidae, pp. 271–368. In Hsiao, T.Y. (ed.), A handbook for the determination of the Chinese Hemiptera-Heteroptera II. Science Press, Beijing.

Jombart, T., and I. Ahmed. 2011. adegenet 1.3-1: new tools for the analysis of genome-wide SNP data. Bioinformatics. 27: 3070–3071

Kabrick, L. R., and E. A. Backus. 1990. Salivary deposits and plant damage associated with specific probing behaviors of the potato leafhopper, *Empoasca fabae*, on alfalfa stems. Entomologia Experimentalis et Applicata. 56: 287–304.

Kirkaldy, G. W. 1908. Memoir on a few heteropterous Hemiptera from eastern Australia. Proceedings of the Linnean Society of New South Wales. 32: 768–788.

Kopelman, N. M., J. Mayzel, M. Jakobsson, N. A. Rosenberg, and I. Mayrose. 2015. Clumpak: a program for identifying clustering modes and packaging population structure inferences across K. Molecular Ecology Resources. 15: 1179–1191.

Kozlov, A. M., D. Darriba, T. Flouri, B. Morel, and A. Stamatakis. 2018. RAxML-NG: A fast, scalable, and user-friendly tool for maximum likelihood phylogenetic inference. biorxiv.org.

Lanfear, R., B. Calcott, S. Y. W. Ho, and S. Guindon. 2012. PartitionFinder: combined selection of partitioning schemes and substitution models for phylogenetic analyses. Molecular Biology and Evolution. 29: 1695–1701.

Lanfear, R., P. B. Frandsen, A. M. Wright, T. Senfeld, and B. Calcott. 2017. PartitionFinder 2: new methods for selecting partitioned models of evolution for molecular and morphological phylogenetic analyses. Molecular Biology and Evolution. 34: 772–773.

Lee, C. E. 1969. Morphological and phylogenic studies on the larvae and male genitalia of the East Asiatic Tingidae (Heteroptera). Journal of the Faculty of Agriculture, Kyushu University. 15: 137–272.

Lis, B. 1999. Phylogeny and classification of Cantacaderini [=Cantacaderidae stat. nov.] (Hemiptera: Tingoidea). Annales Zoologici. 49: 157–196.

Lo, N., A. Montagu, A. Noack, H. Nahrung, H. Wei, M. Eldridge, K.-A. Gray, H. A. Rose, G. Cassis, R. N. Johnson, and S. Lawson. 2018. Population genetics of the Australian eucalypt pest *Thaumastocoris peregrinus*: evidence for a recent invasion of Sydney. Journal of Pest Science. 36: 1–12.

Maddison, W. P., and D. R. Maddison. 2017. Mesquite: a modular system for evolutionary analysis. https://www.mesquiteproject.org

Meirmans, P. G., and P. W. Hedrick. 2011. Assessing population structure: FST and related measures. Molecular Ecology Resources. 11: 5–18.

Menard, K. L., R. T. Schuh, and J. B. Woolley. 2014. Total-evidence phylogenetic analysis and reclassification of the Phylinae (Insecta: Heteroptera: Miridae), with the recognition of new tribes and subtribes and a redefinition of Phylini. Cladistics. 30: 391–427.

Moir, M. L. 2009. Two new species of the lacebug genus *Radinacantha* (Hemiptera: Heteroptera: Tingidae) from Australia. Records of the Western Australian Museum. 25: 269–275.

Moir, M. L., and B. Lis. 2012. Description of three new species of *Ceratocader* (Hemiptera: Heteroptera: Tingidae) from Western Australia. Records of the Western Australian Museum. 27: 148–155.

Moir, M. L., and E. Guilbert. 2012. *Swaustraltingis isobellae*, a new genus and new species of Australian lacebug (Insecta: Heteroptera: Tingidae), with a redescription of *Cysteochila cracentis* Drake, and notes on the lacebug fauna of south-west Australia. Australian Journal of Entomology. 51: 258–265.

Nault, L. R. 1997. Arthropod transmission of plant viruses: a new synthesis. Annals of the Entomological Society of America. 90: 521–541.

Nixon, K. C. 2002. Winclada. Ithaca, New York.

Peakall, R., and P. E. Smouse. 2006. GENALEX 6: genetic analysis in Excel. Population genetic software for teaching and research. Molecular Ecology Notes. 6: 288–295.

Peakall, R., and P. E. Smouse. 2012. GenAlEx 6.5: genetic analysis in Excel. Population genetic software for teaching and research-an update. Bioinformatics. 28: 2537–2539.

Péricart, J. 1992. Tingidae (Tinginae) d'Arabie, de la region orientale et d‘Australie, avec la description d’un genre nouveau et de 14 espèces nouvelles (Hemiptera). Entomologica Basiliensia. 15: 45–86.

Pimentel, D., S. McNair, J. Janecka, J. Wightman, C. Simmonds, C. O’Connell, E. Wong, L. Russel, J. Zern, T. Aquino, and T. Tsomondo. 2001. Economic and environmental threats of alien plant, animal, and microbe invasions. Agriculture, Ecosystems & Environment. 84: 1–20.

Pollard, D. G. 1973. Plant penetration by feeding aphids (Hemiptera, Aphidoidea): a review. Bull. Ent. Res. 62: 631–714.

R Core Team. 2018. R: A language and environment for statistical computing. R Foundation for Statistical Computing. R Foundation for Statistical Computing, Vienna, Austria.

Raj, A., M. Stephens, and J. K. Pritchard. 2014. fastSTRUCTURE: Variational Inference of Population Structure in Large SNP Datasets. Genetics. 197: 573–589.

Rollins, L. A., A. P. Woolnough, A. N. Wilton, R. Sinclair, and W. B. Sherwin. 2009. Invasive species can't cover their tracks: using microsatellites to assist management of starling (*Sturnus vulgaris*) populations in Western Australia. Molecular Ecology. 18: 1560–1573.

Schuh, R. T., G. Cassis, and E. Guilbert. 2006. Description of the first recent macropterous species of Vianaidinae (Heteroptera: Tingidae) with comments on the phylogenetic relationships of the family within the Cimicomorpha. Journal of the New York Entomological Society. 114: 38–53.

Sherwin, W. B., A. Chao, L. Jost, and P. E. Smouse. 2017. Information theory broadens the spectrum of molecular ecology and evolution. Trends in Ecology & Evolution. 32: 948–963.

Silva-Brandão, K. L., T. V. Santos, F. L. Cônsoli, and C. Omoto. 2015. Genetic Diversity and Structure of Brazilian Populations of *Diatraea saccharalis* (Lepidoptera: Crambidae): Implications for Pest Management. Journal of Economic Entomology. 108: 307–316.

Simon, C., F. Frati, A. Beckenbach, B. Crespi, H. Liu, and P. Flook. 1994. Evolution, Weighting, and Phylogenetic Utility of Mitochondrial Gene Sequences and a Compilation of Conserved Polymerase Chain Reaction Primers. Annals of the Entomological Society of America. 87: 651–701.

Smith, K. M. 1926. A comparative study of the feeding methods of certain Hemiptera and of the resulting effects upon the plant tissue, with special reference to the potato plant. Annals of Applied Biology. 13: 109–139.

Stål, C. 1873. Enumeratio Hemipterorum. Bidrag till en förteckning öfver aller hittills kända Hemiptera, jemte systematiska meddelanden. 3. Kongliga Svenska Vetenskaps-Academiens Nya Handlingar. 11: 1–163.

Stonedahl, G. M., W. R. Dolling, and G. J. duHeaume. 1992. Identification guide to common tingid pests of the world (Heteroptera: Tingidae). Tropical Pest Management. 38: 438–449.

Storey, H. H. 1939. Transmission of plant viruses by insects. The Botanical Review. 5: 240–272.

Sunnucks, P., P. J. De Barro, G. Lushai, N. MacLean, and D. Hales. 1997. Genetic structure of an aphid studied using microsatellites: cyclic parthenogenesis, differentiated lineages and host specialization. Molecular Ecology. 6: 1059–1073.

Swofford, D. L. 2003. PAUP*. Phylogenetic Analysis Using Parsimony (*and Other Methods). Version 4. Sinauer Associates, Sunderland, Massachusetts.

Symonds, C. L., and G. Cassis. 2013. New species of the lace bug genus *Lasiacantha* Stål (Insecta: Hemiptera: Heteroptera: Tingidae) from Western Australia. Austral Entomology. 52: 53–66.

Symonds, C. L., and G. Cassis. 2014. A new genus *Ittolemma* (Heteroptera: Tingidae) gen. nov. and three included species of hirsute lace bugs from temperate woodlands of southern Australia. Austral Entomology. 53: 380–390.

Symonds, C. L., and G. Cassis. 2018. Systematics and analysis of the radiation of Orthotylini plant bugs associated with callitroid conifers in Australia. Bulletin of the American Museum of Natural History. 226 pp.

Tomokuni, M. 2007. A small collection of Tingidae (Insecta: Heteroptera) from Taiwan, with a checklist of the known species. Memoirs of the National Science Museum. 44: 59–69.

Van Der Wurff, A. W. G., J. A. Isaaks, G. Ernsting, and N. M. Van Straalen. 2003. Population substructures in the soil invertebrate *Orchesella cincta*, as revealed by microsatellite and TE-AFLP markers. Molecular Ecology. 12: 1349–1359.

Webber, B. L., and J. K. Scott. 2012. Rapid global change: implications for defining natives and aliens. Global Ecology and Biogeography. 21: 305–311.

Weir, B. S., and C. C. Cockerham. 1984. Estimating F-statistics for the analysis of population structure. Evolution. 38: 1358–1370.

White, M. J. D. 1973. Animal cytology and evolution. Cambridge University Press, London. 961 pp.

APPENDIX A

Genera of Proteaceae with associated lace bug genera. Number of records indicate number of individual records for each taxon, with the sum of tingid specimens for each proteaceous genus indicated.

GENUS	NUMBER OF RECORDS
Adenanthos	2
Malandiola	2
Banksia	171
Chorotingis	56
Eritingis	1
Euaulana	74
Inoma	3
Malandiola	28
Tingis	9
Conospermum	70
Epimixia	2
Oncophysa	67
Ulonemia	1
Dryandra	2
Ulonemia	2
Grevillea	604
Aconchus	2
Agramma	1
Cysteochila	18
Engynoma	4
Epimixia	8
Eritingis	2
Leptoypha	2
Malandiola	2
Nethersia	1
Oncophysa	355
Paracopium	1
Stephanitis	3
Teleonemia	2
Ulonemia	203
Hakea	456
Eritingis	2
Inoma	1
Inonemia	1
Lasiacantha	3
Malandiola	24
Nethersia	1
Oncophysa	243
Swaustraltingis	2
Ulonemia	179

Isopogon	2
Epimixia	1
Malandiola	1
Macadamia	154
Eritingis	2
Ulonemia	152
Orites	2
Ulonemia	2
Persoonia	1
Inoma	1
Stenocarpus	2
Codotingis	2
Grand Total	**1466**